P-258

NASA CR 174992

release August, 1989.

NASA

LARGE SCALE PROP-FAN STRUCTURAL DESIGN STUDY

Volume I

Initial Concepts

By: L.C. Billman et al

HAMILTON STANDARD DIVISION
UNITED TECHNOLOGIES

Prepared for
National Aeronautics and Space Administration
NASA-Lewis Research Center
Contract NAS3-22394

NASA CR 174992

NASA

LARGE SCALE PROP-FAN STRUCTURAL DESIGN STUDY

Volume I

Initial Concepts

By: L.C. Billman et al

HAMILTON STANDARD DIVISION
UNITED TECHNOLOGIES

Prepared for
National Aeronautics and Space Administration
NASA-Lewis Research Center
Contract NAS3-22394

CONTENTS

CONTENTS (Continued)

ILLUSTRATIONS

ILLUSTRATIONS (Continued)

ILLUSTRATIONS (Continued)

TABLES

1.0 SUMMARY

Hamilton Standard, under contract to NASA/Lewis, has conducted the effort to analyze, evaluate and provide structural designs for several advanced propeller configurations. In addition, aeromechanical design requirements were established, blade fabrication concepts were screened, the feasibility of designing a dynamic model was established, the adequacy of current design and fabrication techniques was assessed and a preliminary design of SR-7 established. The specific tasks which were accomplished are:

- A Design Requirements Document which contains the critical operation conditions, was generated for use in the structural design analysis and dynamic model feasibility analysis tasks;
- A Blade Design Concept Definition Document, which defines the blade fabrication concepts for use in the structural design analysis, was generated;
- A Structural Design Analysis was conducted for six blade configuration-fabrication concept combinations. The analysis evaluated stress, deflection, resonant frequency, stall and classical flutter, and FOD;
- The feasibility of designing a dynamic model of a full-size blade configuration was established;
- Based on the structural design analysis task, those items which were unproven or beyond the state-of-the-art were assessed and identified and a technology development plan was prepared;
- The preliminary design of an advanced propeller for turboprop aircraft applications with design cruise speeds of Mach 0.7 to 0.8 was established. This task included: the review of related studies, analyses, and test efforts; an industry survey; a large-scale Prop-Fan preliminary design analysis; the design analysis of a 9-foot diameter Prop-Fan blade and preliminary design of a 14-foot diameter blade.

Volume I of this report covers the effort through the preparation of the technology development plan and Volume II covers the preliminary design of an advanced propeller.

2.0 INTRODUCTION

In recent years, considerable attention has been directed toward improving aircraft fuel consumption. Studies have shown that the inherent efficiency advantage that turboprop propulsion systems have demonstrated at lower cruise speeds may now be extended to the higher speed of today's turbofan and turbojet-powered aircraft. To achieve this goal, new propeller designs which feature more blades with thin airfoils and aerodynamic sweep are required.

Since 1975, Hamilton Standard has been deeply involved with the NASA Lewis Research Center in the development of the advanced turboprop or Prop-Fan. Many aircraft system studies have been accomplished for a variety of subsonic air transport applications, and all these studies have shown significant fuel savings with Prop-Fan propulsion. The fuel savings potential of future Prop-Fan powered aircraft is generally 15-20% for commercial applications and 25-35% for military patrol aircraft compared to equal technology turbofan systems, depending upon the specific application, cruise speed, stage length and other requirements.

To date, several small-scale, 0.6223 meter (24.5 inch) diameter models have been designed, manufactured and subjected to a number of tests. Tests have been conducted in both UTRC and NASA wind tunnels and on a modified NASA airplane. These tests have shown that propellers with 8-10 swept blades, high tip speeds and high power loadings can offer increased fuel efficiencies at speeds up to 0.8 Mn.

The purpose of this program was to establish full size structural concepts for such blades; to define their structural properties; to identify any new design, analysis, or fabrication techniques which would be required; to determine the structural trade-offs involved with several blade shapes; to establish the feasibility of fabricating dynamically scaled models of blades for aeroelastic testing and to establish the preliminary design of an advanced propeller for turboprop aircraft applications with design cruise speeds of 0.7 to 0.8 Mn.

The blade configurations for which large-scale designs would be developed in this study were specified at the onset to be SR-2 (8-way), SR-3 (8-way), a 10-way version of SR-3 (same geometry with the chord reduced by the ratio 8/10), and SR-5. A comparison of planforms for these configurations is shown in Figure 2.1. The SR-2, SR-3 (8-way), and SR-5 configurations had all been designed and built as models for wind tunnel testing.

Later, the preliminary design of a new configuration, designated SR-7, was developed utilizing the initial results of this study along with other related test and analysis efforts to date. It was intended that the SR-7 design would be built in large-scale (9 ft. diameter) for later ground and flight research tests. The results of the initial design study of the SR-2, SR-3, and SR-5 configurations are covered in Volume I (CR174992) of this report and the preliminary design of SR-7 is covered in Volume II (CR174993).

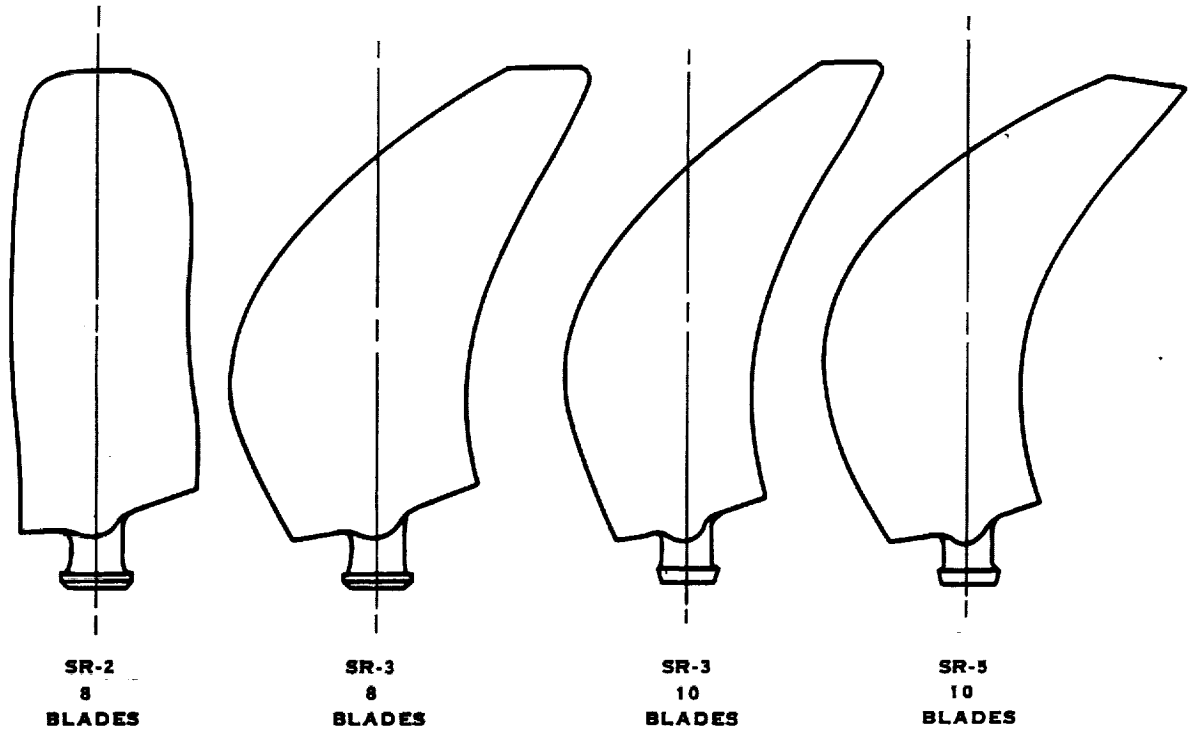

FIGURE 2.1 BLADE CONFIGURATIONS PLANFORM COMPARISON

3.0 TASK I - DEFINITION OF PROP-FAN DESIGN REQUIREMENTS

3.1 INTRODUCTION

Each time that a rotating blade is designed by Hamilton Standard, the requirements for that design are delineated in a specification. This is true for conventional propeller blades as well as Prop-Fan, turbofan, helicopter, or wind turbine blades. The requirements address structural considerations such as vibratory excitations, steady and transient loads, foreign object impacts, overspeed capacity, and many others. Additionally, the design input should include life, reliability, repairability, and others.

3.2 OBJECT

Establish the design requirements for the blade configurations to be evaluated in the Structural Design Analysis task (reference Section 4.0).

3.3 METHOD

Based upon the requirements set forth in the contract and on Hamilton Standard's years of propeller and fan blade experience, the design requirements covering aerodynamic loads, mechanical loads, critical speeds, aerodynamic excitation, response, flutter and foreign object damage were established.

The results of this effort, together with a description of the analysis procedures which would be used during the Structural Design Analysis task (reference Section 5.0) were incorporated into a Design Requirements Document which is included in Appendix A of this report.

4.0 TASK II - DEFINITION OF FABRICATION CONCEPTS

4.1 INTRODUCTION

Hamilton Standard's blade fabrication experience covers a time span of over 50 years. Over that time blades have been built using fabrication concepts and methods ranging from solid blade designs to various hollow types using both metal and composite. New blade fabrication concepts, such as super plastic formed/diffusion bonded (SPF/DB) blade structures, are under investigation for application in advanced blade designs. Many of these fabrication concepts are illustrated in Figure 4.1. This figure also illustrates some of the many different design concepts that were considered during this task.

Table 4.1 summarizes Hamilton Standard's blade design experience, from service-proven production designs to advanced designs. Experimental designs, produced and tested but not yet in service, represent Hamilton Standard's efforts to incorporate state-of-the-art technology into production blade applications. The advanced design concepts represent new methods being investigated in blade and blade component manufacturing, resulting in increased structural capacity, lighter weight, and simplified manufacturing.

4.2 OBJECT

Establish the fabrication concepts for the blade configurations to be evaluated in the Structural Design Analysis task (reference Section 5.0).

4.3 METHOD

First, the design philosophy, which addressed such goals as stress, stability, foreign object damage, distortion, material distribution and effectiveness, and special considerations for Prop-Fan blades was established. Then the various appropriate materials were reviewed and evaluated. Next, the various fabrication concepts shown in Figure 4.1 were evaluated. Based on these tasks, the recommended fabrication concepts for the blade configurations to be studied in the Structural Design Analysis task (reference Section 5.0) were selected.

The results of this effort, together with a blade retention concept, were documented in a Blade Design Concept Definition Document. Also included in this document were descriptions of the structural analysis methods to be used in the Structural Design Analysis task.

The Blade Design Concept Definition Document is included in Appendix B of this report.

TABLE 4.1. BLADE DESIGN EXPERIENCE

- Production Designs - Service Proven

  Solid Aluminum (many large and small installations)
  Hollow Steel Spar/Fiberglass Shell (P-2, E-2/C-2)
  Solid Aluminum Spar/Fiberglass Shell (DHC-7, OV-10D)
  Hollow Steel Spar/Hollow Steel Shell (B-377, KC/C-97)

- Limited Production Designs - Produced and with Limited Service

  Lightened Steel Spar/Polyimide Shell (C4 Wind Tunnel Blade)
  Monocoque Aluminum (L-1644)

- Experimental Designs - Produced and Tested

  Hollow Steel Spar/Boron Epoxy Shell (JT9D Fan)
  Solid Titanium Spar/Boron Aluminum Shell (F100 Fan)
  Hollow Composite Boron/Al Spar (AVLABS)
  Monocoque Steel (C-132)

- Advanced Deigns - Studies

  Super-Plastic Formed/Diffusion Bonded (SPF/DB) Structures:

  Integral Sheath
  Spar
  Monocoque Design
  Monocoque Design with Reinforcing Ribs

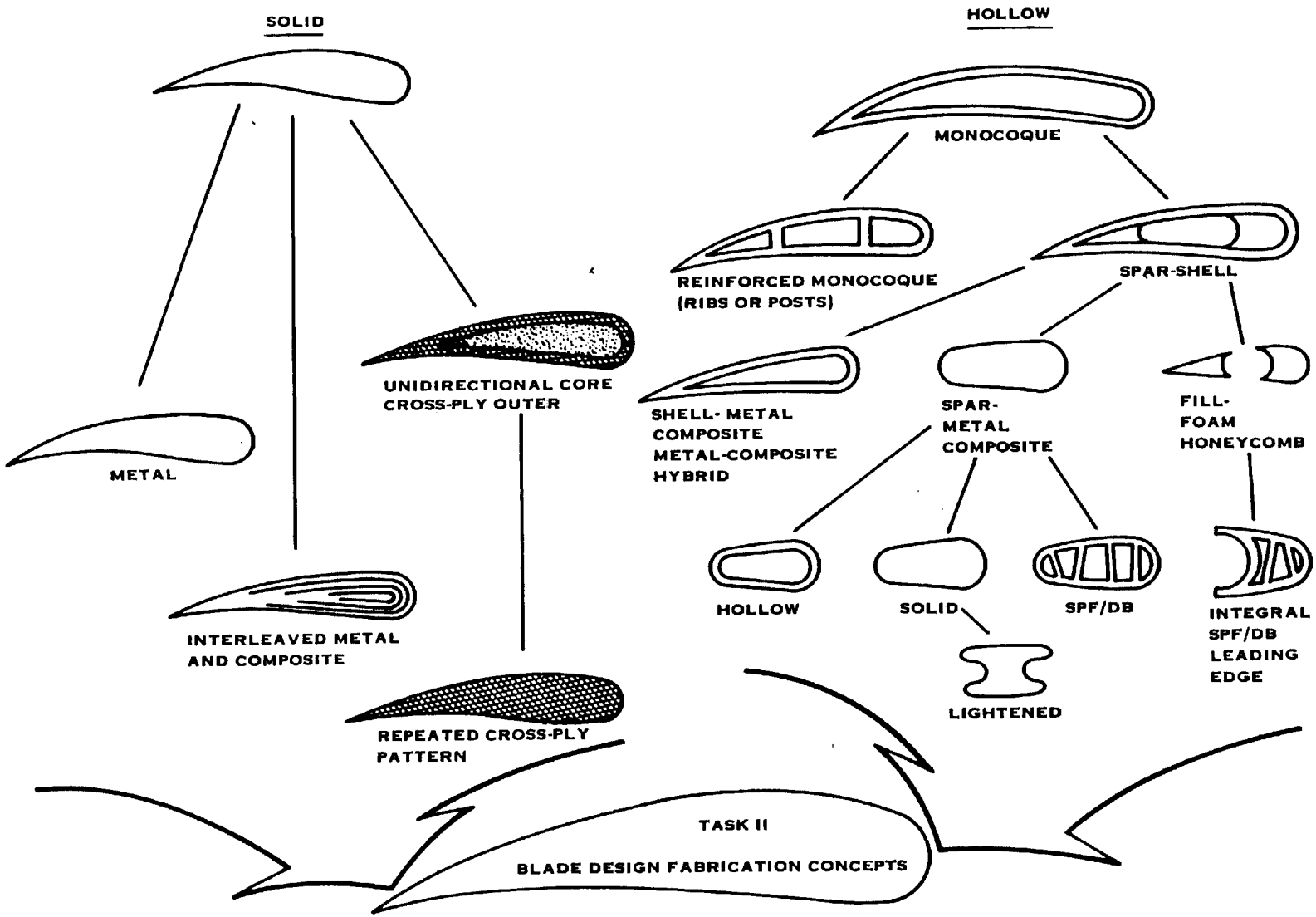

FIGURE 4.1. BLADE FABRICATION CONCEPTS

5.0 TASK III - STRUCTURAL DESIGN ANALYSIS

5.1 INTRODUCTION

Upon completion of the "Design Requirements Document" and "Fabrication Concepts Document", a study was initiated to assess the structural adequacy of the five blade design concepts which had been defined in the "Fabrication Concepts Document". These concepts were:

SR-2 8 way	Metal spar	Composite shell (referred to as SR-2)
SR-3 8 way	Metal spar	Composite shell (referred to as SR-3 (8))
SR-3 10 way	Metal spar	Composite shell (referred to as SR-3 (10))
SR-5 10 way	Metal spar	Composite shell (referred to as SR-5A)
SR-5 10 way	Composite spar	Composite shell (referred to as SR-5B)

As the study progressed, a sixth concept (SR-3C (10), composite spar and composite shell) was added, and one concept (SR-5B) was modified, based on the results of the study as it progressed.

Each of the concepts was studied for structural analysis, resonant frequency placement, foreign object impact capacity, and stability. For the structural analysis and resonant frequency calculation, a beam element analysis was used for the design with no aerodynamic sweep and a three-dimensional finite element analysis was used for those designs with sweep. Steady and cyclic stress results from the structural analysis were compared to the allowable stress limits for the various materials. Resonant frequencies were plotted to determine their proximity to integer-order excitation line intersections at the operating speed. A foreign object impact analysis was used to determine the impact capacity of each blade concept. The stability boundary for each concept was predicted by analysis and compared to the desired flight profile.

The comparisons of these results to the previously established design criteria showed that each concept would need modification in order to meet all of the design requirements.

5.2 BLADE DESIGN CONCEPTS

For this study, the outer blade shapes for the concepts were specified in the contract and were to remain unchanged. All the concepts are 3.53 m (11.0 ft.) in diameter. The design concept specifications are listed in Table 5.1. All of the concepts are spar/shell design, since this design will allow a wide variation in blade component stiffness and internal geometry. The selected materials and construction of the individual concepts are discussed below.

5.2.1 SR-2

The SR-2 concept, shown in Figure 5.1, has a hollow, formed steel spar. The shell is 181 style woven Kevlar cloth with epoxy resin, oriented at $\pm 45°$ to the blade span.

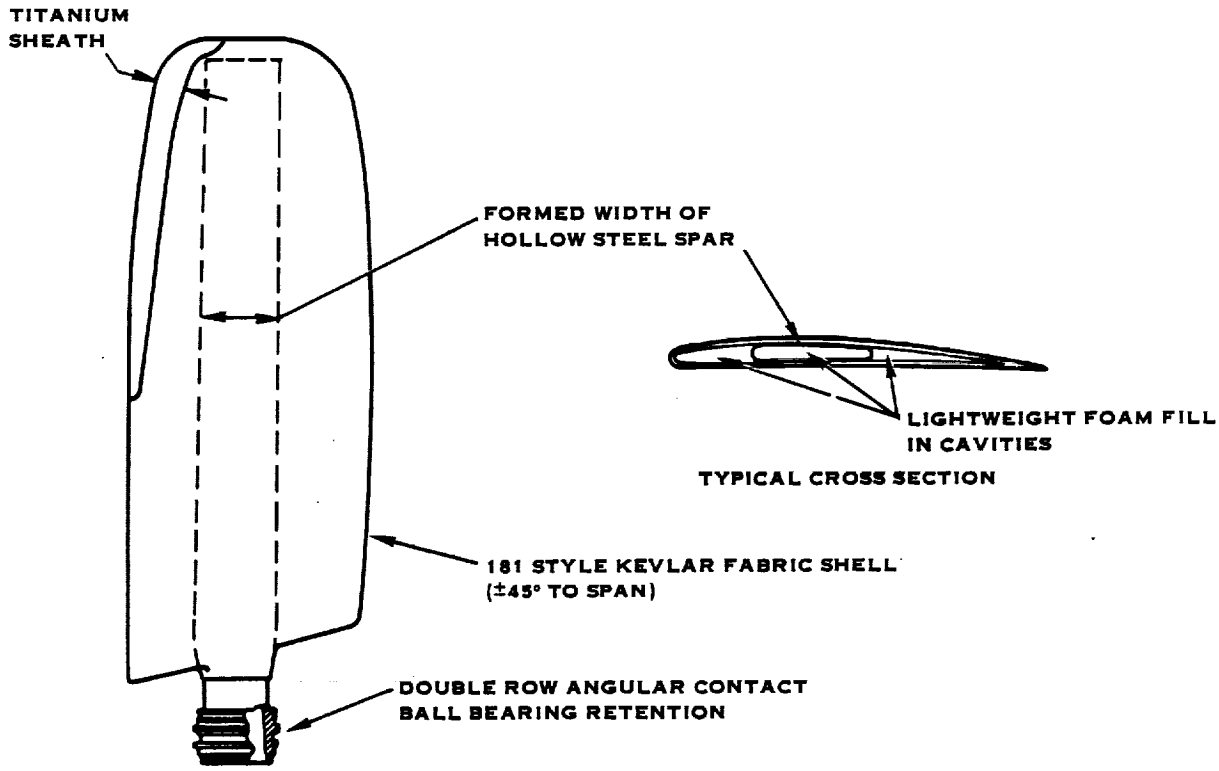

FIGURE 5.1 SR-2 FABRICATION CONCEPT HOLLOW STEEL SPAR/KEVLAR SHELL

TABLE 5.1. DESIGN CONCEPT SPECIFICATIONS

	SR-2	SR-3 (8)	SR-3 (10)	SR-5
Tip speed, m/sec (ft/sec)	244 (800)	244 (800)	244 (800)	244 (800)
Tip diameter, m (ft)	3.53 (11.0)	3.53 (11.0)	3.53 (11.0)	3.53 (11.0)
Number of blades	8	8	10	10
Power loading,* kw/m^2 (Shp/ft^2)	271.5 (37.5)	271.5 (37.5)	271.5 (37.5)	271.5 (37.5)
Tip sweep (deg)	0	34	34	48
Activity factor	203	234	187	210

*Based on blade tip diameter

5.2.2 SR-3 (8)

The SR-3 (8) is illustrated in Figure 5.2. The spar is solid forged aluminum. A 181 style glass fabric with epoxy resin, oriented at ±45° to the blade span, is used for the shell.

5.2.3 SR-3 (10)

This design, the SR-3 (10), is shown in Figure 5.3. The spar is solid forged aluminum. The shell is a 181 style Kevlar fabric cloth with epoxy resin, with 40% of the layers at 0°/90° and 60% of the layers at ±45° to the blade spar.

5.2.4 SR-3C (10)

The SR-3C (10) is a second fabrication concept using the SR-3 (10) outer airfoil geometry, and is shown in Figure 5.4. This design has a diffusion-bonded boron/aluminum composite spar, with 50% of the layers at 0° and 50% of the layers at ±15° to the blade span. The shell is 181 style glass fabric cloth with epoxy resin, oriented at ±45° to the blade span.

5.2.5 SR-5A

The SR-5A, shown in Figure 5.5, has a solid forged aluminum spar. The shell is a 121 style glass fabric cloth with epoxy resin, oriented at ±45° to the blade span.

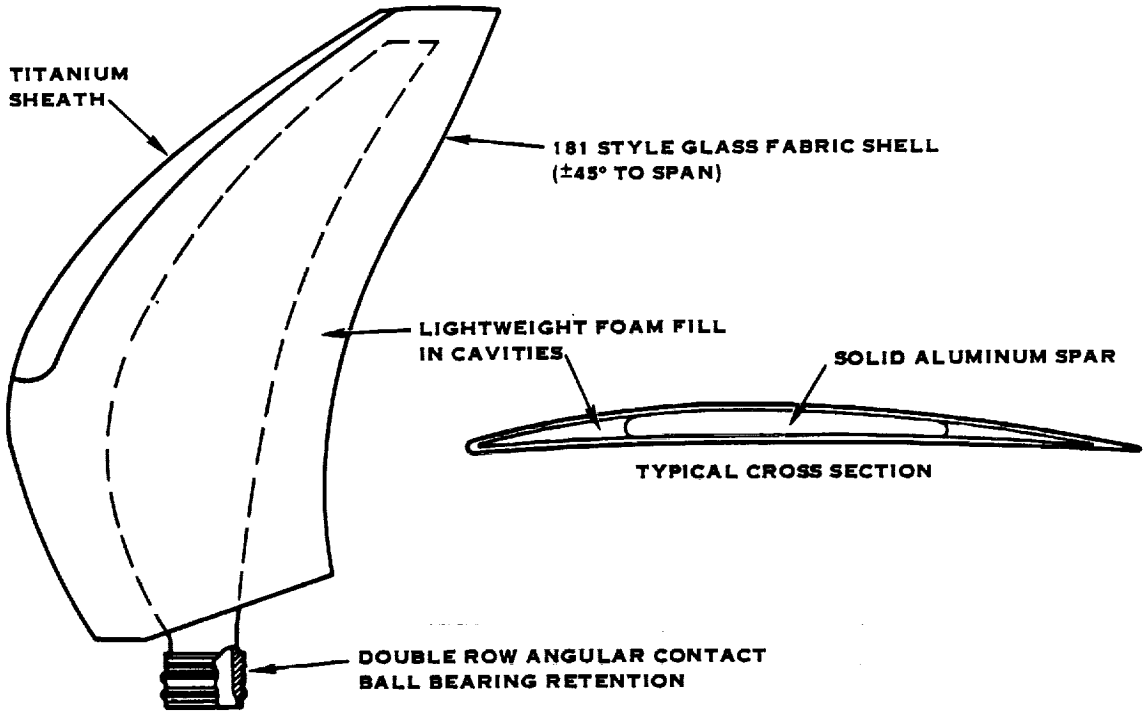

FIGURE 5.2 SR-3 (8) FABRICATION CONCEPT SOLID ALUMINUM SPAR/ FIBERGLASS SHELL

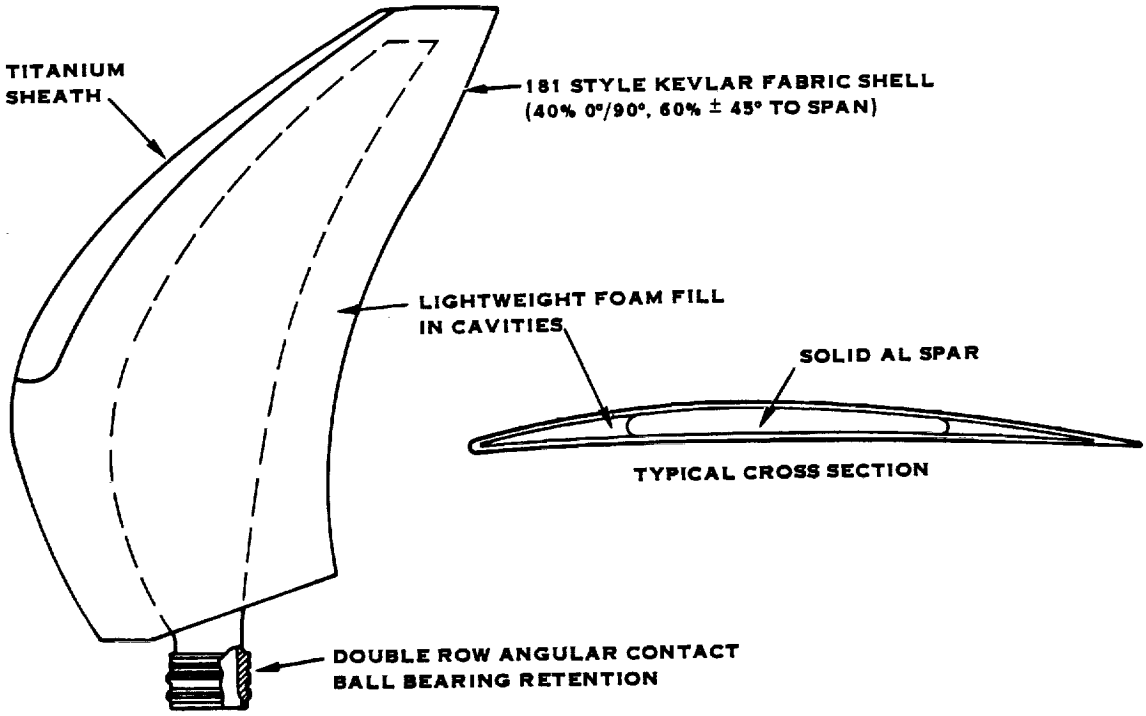

FIGURE 5-3 SR-3 (10) FABRICATION CONCEPT SOLID ALUMINUM SPAR/KEVLAR SHELL

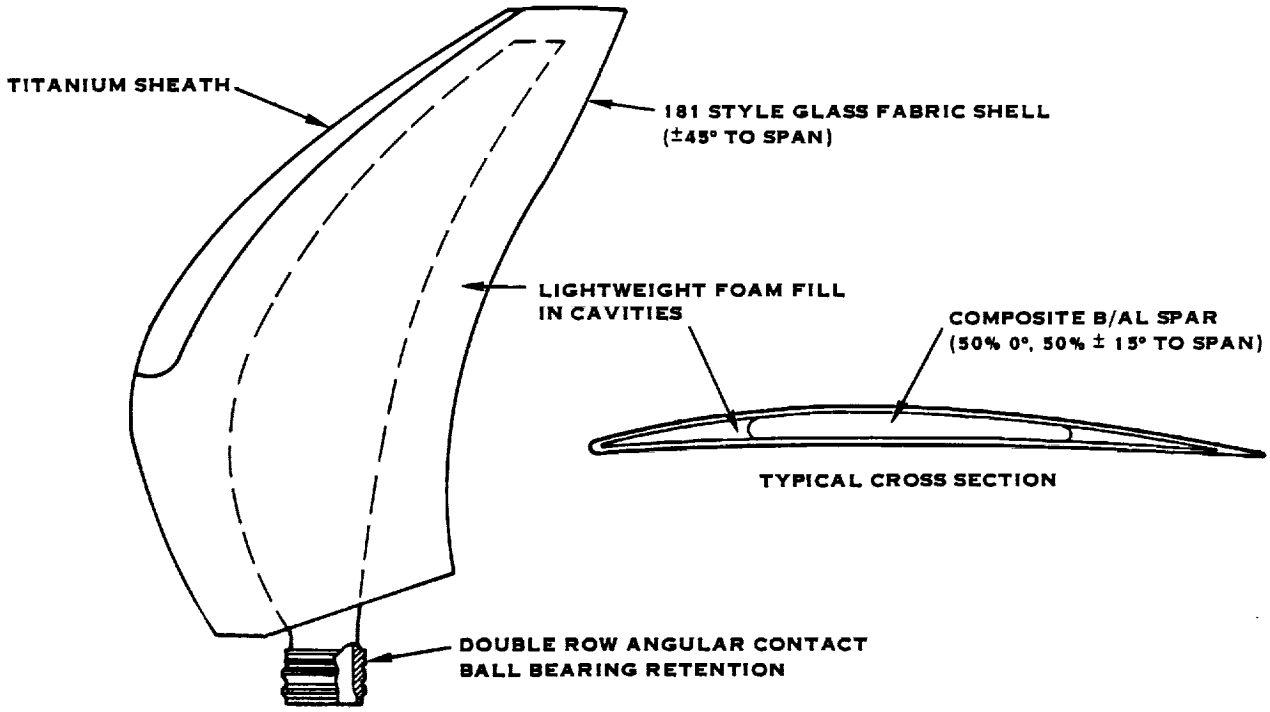

FIGURE 5.4 SR-3C (10) FABRICATION CONCEPT COMPOSITE BORON/ALUMINUM SPAR/FIBERGLASS SHELL

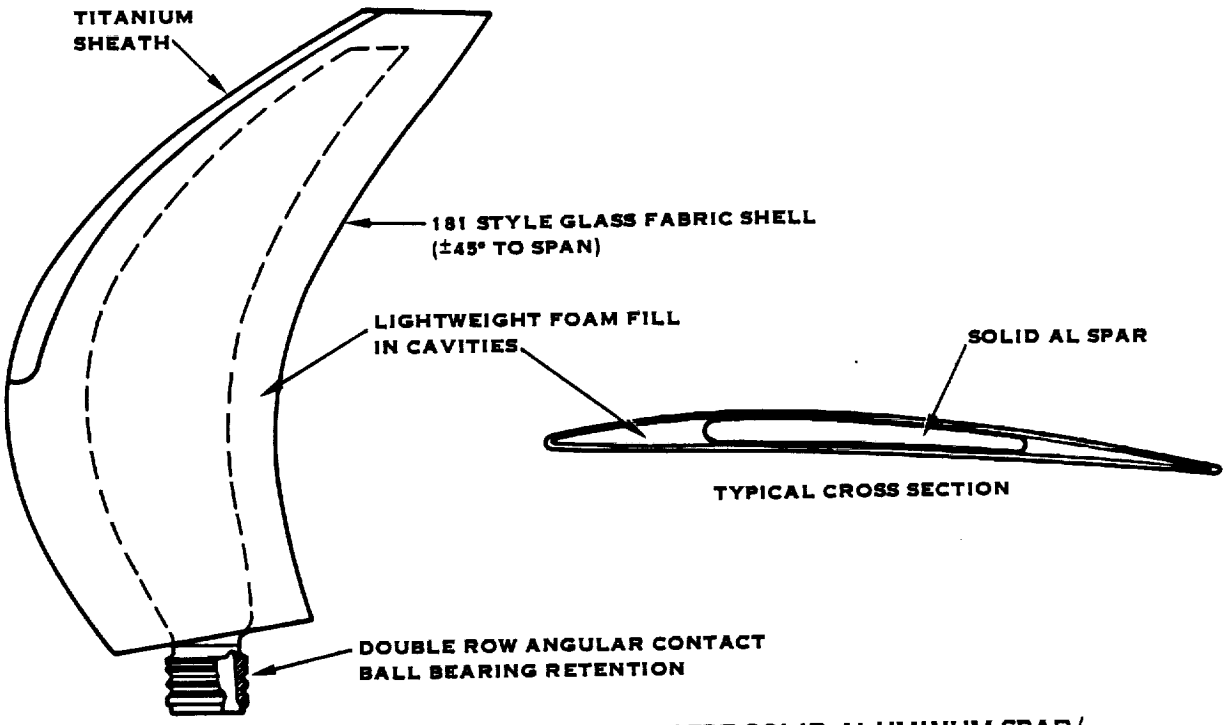

FIGURE 5.5 SR-5A FABRICATION CONCEPT SOLID ALUMINUM SPAR/ FIBERGLASS SHELL

5.2.6 SR-5B

The SR-5B, shown in Figure 5.6, has a solid forged aluminum spar. Boron/aluminum reinforcing pads (with 50% of the layers oriented at 0° and 50% oriented at 15° to the blade span) have been diffusion-bonded to its face and camber sides to provide additional stiffness and strength. The shell is 181 style glass fabric cloth, oriented at ±45° to the blade span.

5.2.7 Common Blade Design Features

All of the blade design concepts include the following:

a. lightweight foam fill in all spar and shell cavities,

b. titanium leading edge sheath for leading edge foreign object impact protection,

c. integral leading edge heater in the inboard region of the shell for deicing capability,

d. double row, angular contact ball bearing retention.

5.3 HUB AND RETENTION CONCEPT

The retention concept used in this study was a double row, angular contact ball bearing design, illustrated in Figure 5.7 for the solid metal spar blade designs.

For this design, retention spring rates were calculated as a function of propeller speed. The variation of the moment spring rate with propeller speed is plotted in Figure 5.8. These spring rates were used for the blade concept resonant frequency calculation. For this study, the in-plane and out-of-plane spring rates were assumed to be equal.

For the SR-3C (10), which has a composite spar, the composite layers would flare out and be diffusion-bonded into a metal shank. The metal shank would be SiC-Al or aluminum since the composite is boron/aluminum. This scheme is illustrated in Figure 5.9 for a single row retention.

A typical Prop-Fan hub design is shown in Figure 5.10 for a ten-blade configuration. Both the in-plane and out-of-plane cross-sections are illustrated in this figure.

5.4 DESIGN OPERATING CONDITIONS

The two operating conditions that were used during the analyses are listed in Table 5.2. For this study, the stress levels and foreign object impact capacity were calculated at the takeoff/climb condition. The elastic deflections were evaluated at the cruise condition.

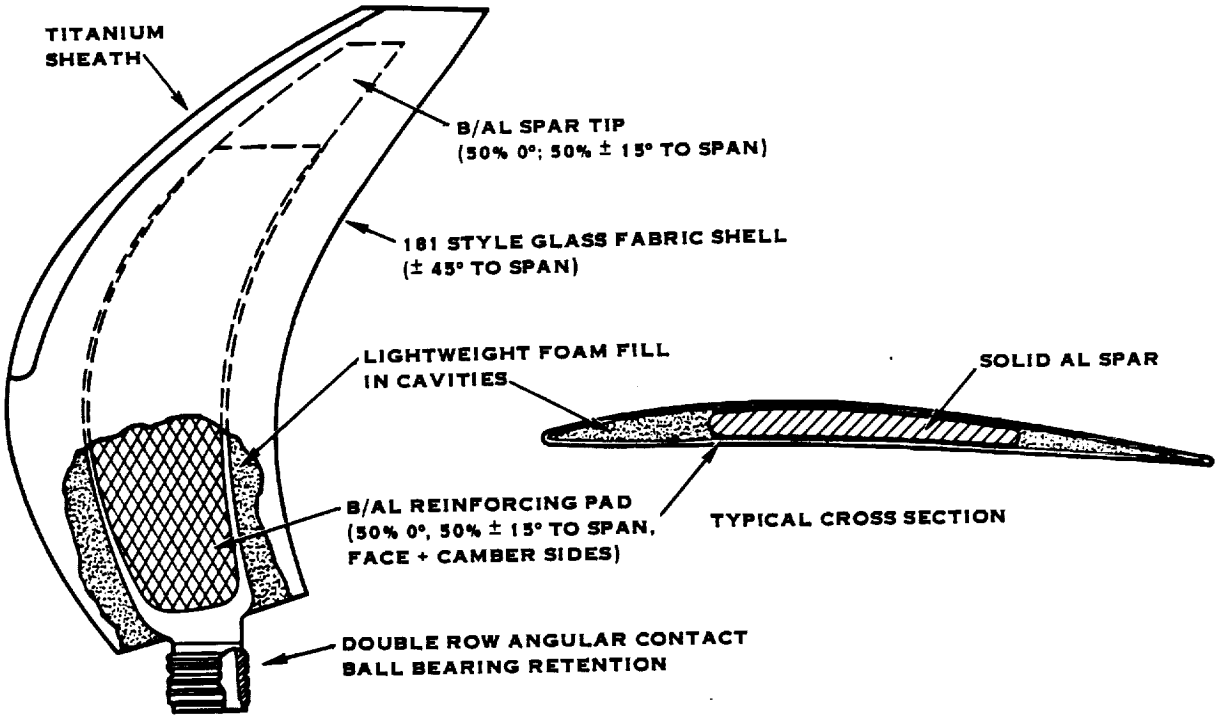

FIGURE 5.6 SR-5B FABRICATION CONCEPT SOLID ALUMINUM SPAR/BORON/ ALUMINUM REINFORCING PAD/FIBERGLASS SHELL

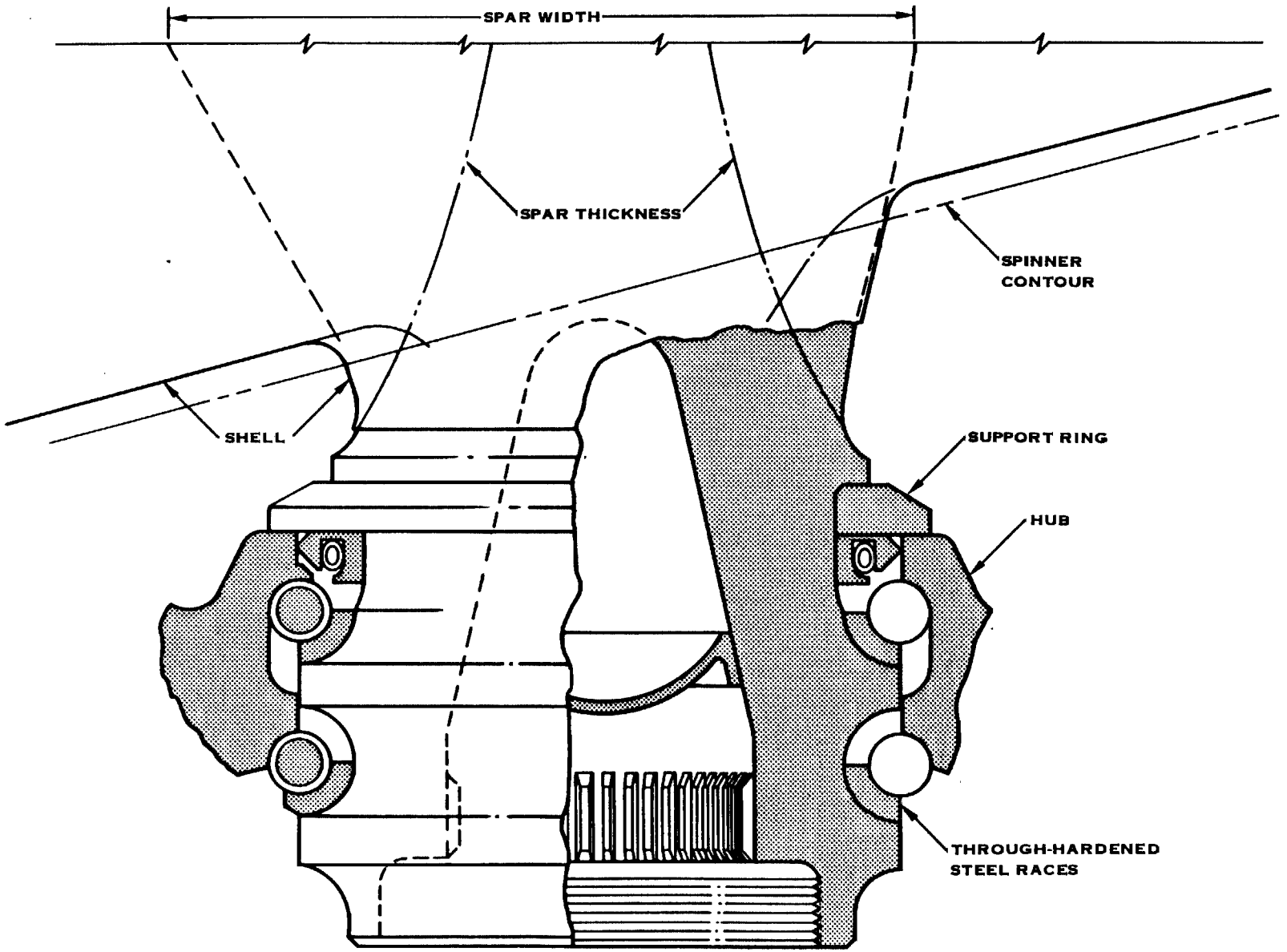

FIGURE 5-7 BLADE RETENTION - SOLID METAL SPAR DOUBLE ROW, ANGULAR CONTACT

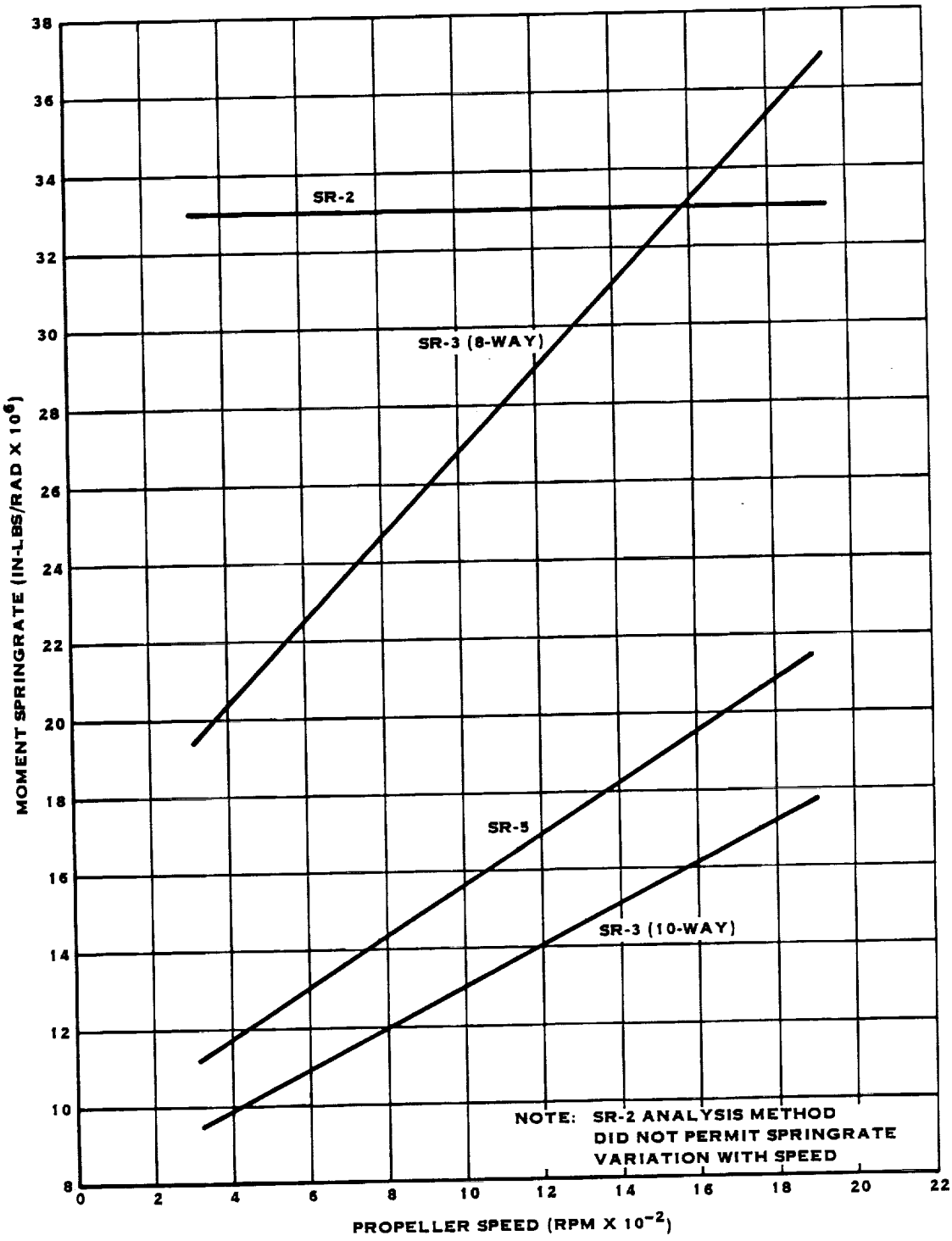

FIGURE 5-8 PROP-FAN RETENTION MOMENT SPRINGRATE VS. SPEED

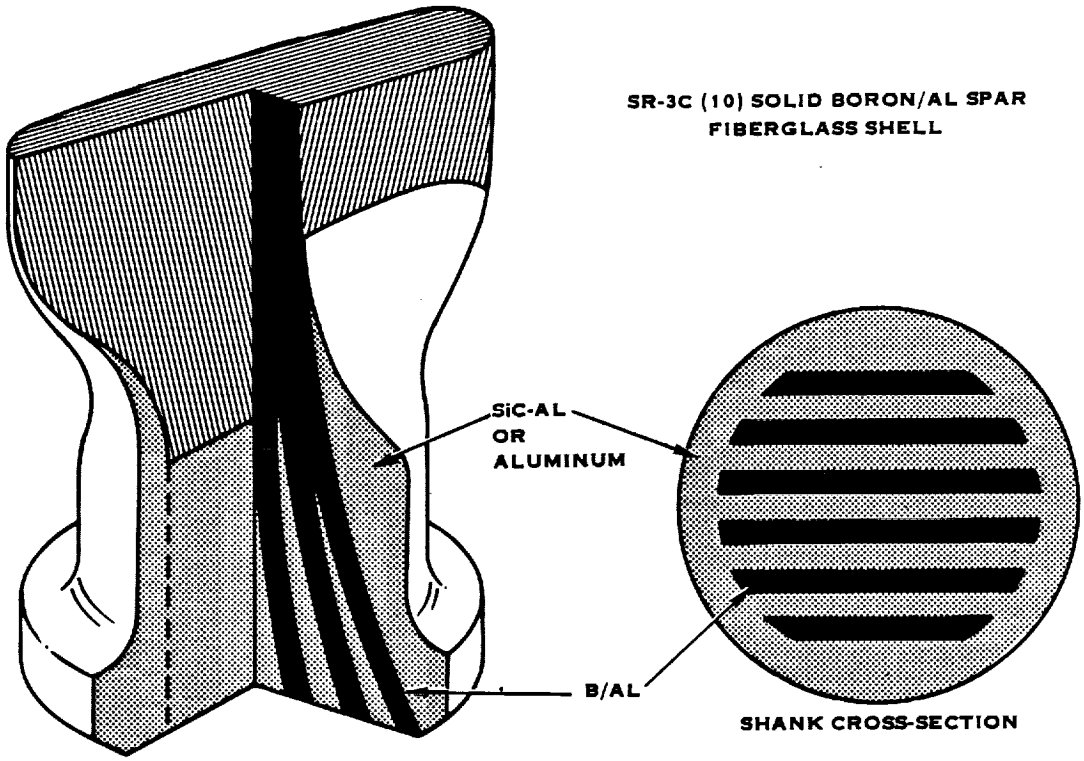

FIGURE 5.9 SHANK CONCEPT FOR COMPOSITE SPAR

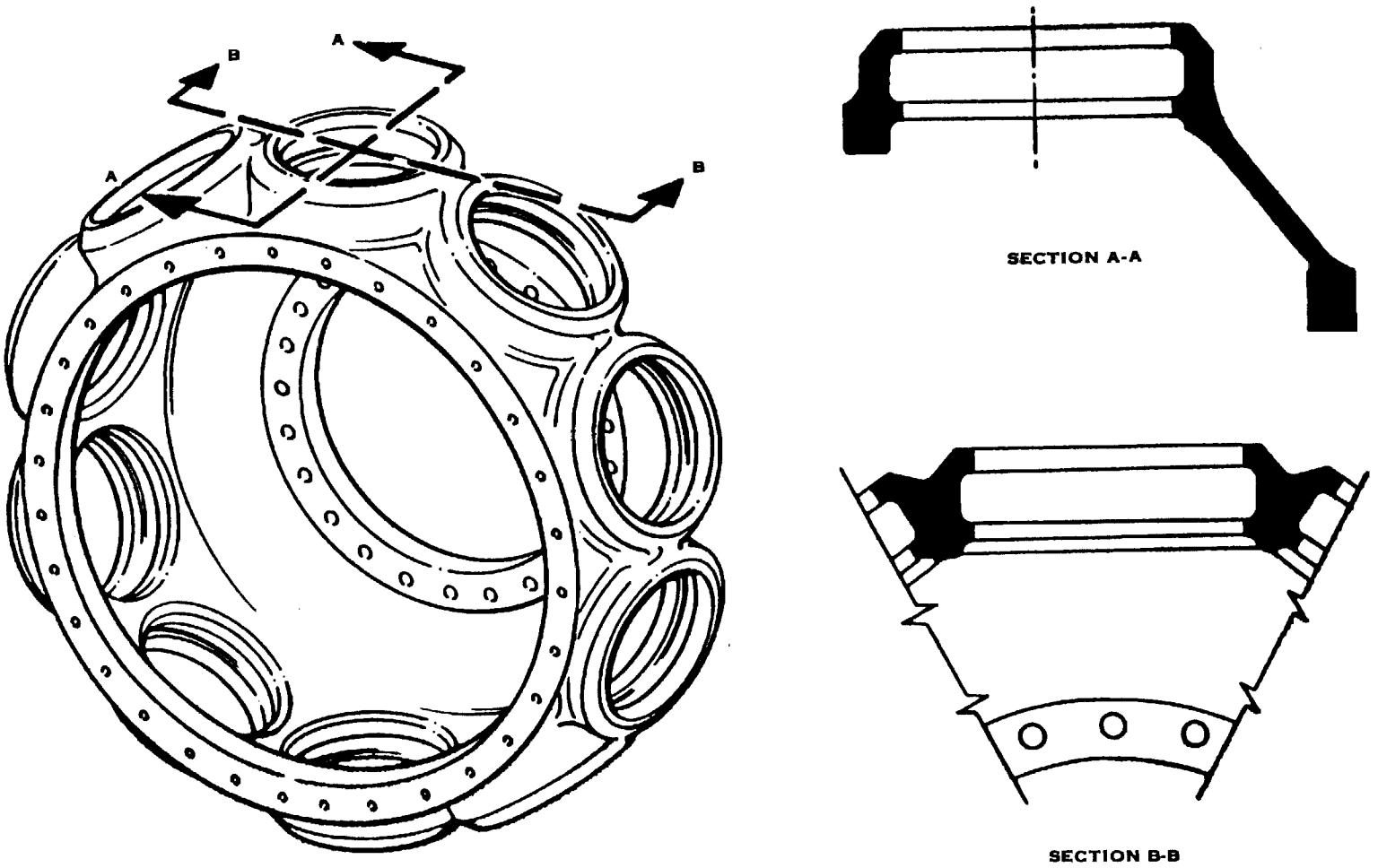

FIGURE 5.10 10-BLADE PROP-FAN DISC

TABLE 5.2. BLADE OPERATING CONDITIONS

	Cruise	Takeoff/Climb
Velocity, Mn	.8	.2
Altitude, m (ft)	10,668 (35,000)	sea level
Propeller speed, rpm	1389	1389
Power loading, kw/m^2 (HP/ft^2)	271.4 (37.5)	521.3 (72.0)
Excitation factor	4.5	4.5

5.5 DESIGN EVALUATION CRITERIA

To meet the design requirements previously established and assess design analysis data, various design evaluation criteria were used in the design process as summarized below.

Although no absolute limits were set for elastic deflections, it was generally felt that they should be minimized to maintain control of blade position during operation. These deflections include changes in diameter, sweep, offset, twist, and camber, and are illustrated in Figure 5.11. The stress requirements are shown in Figure 5.12. For each blade component, the steady and cyclic stresses will be combined and plotted on a modified Goodman diagram for that component's material. The material allowable stress limit is based on a conservative assessment of the material's strength, environment, size factors, and on full-scale material fatigue tests. The particular conditions that were evaluated against the stress criteria are:

- High-cycle fatigue - design for infinite life, i.e., 10^8 cycles.
- Low-cycle fatigue - design for 50,000 start/stop cycles, from no stress to peak stress.
- 25% overspeed - steady stress shall be below the 0.2% offset yield strength for homogeneous metal materials, or below the 5% change in elastic modulus limit for fiber reinforced resin materials.
- 40% overspeed - steady stress shall be below the ultimate tensile strength for homogeneous metal materials, or below the fracture limit for fiber reinforced resin materials.

In order to avoid dynamic magnification caused by operating too near a resonant frequency, resonance avoidance zones are specified. These zones are shown in Figure 5.13. These zones are defined as a percentage of the rotational speed and frequency at each integer-order excitation line at the operating speed. The percentage for the 2-P intersection is 20% for ground operation and 10% for flight operation. This percentage decreases to 2.5% for the 5-P intersection.

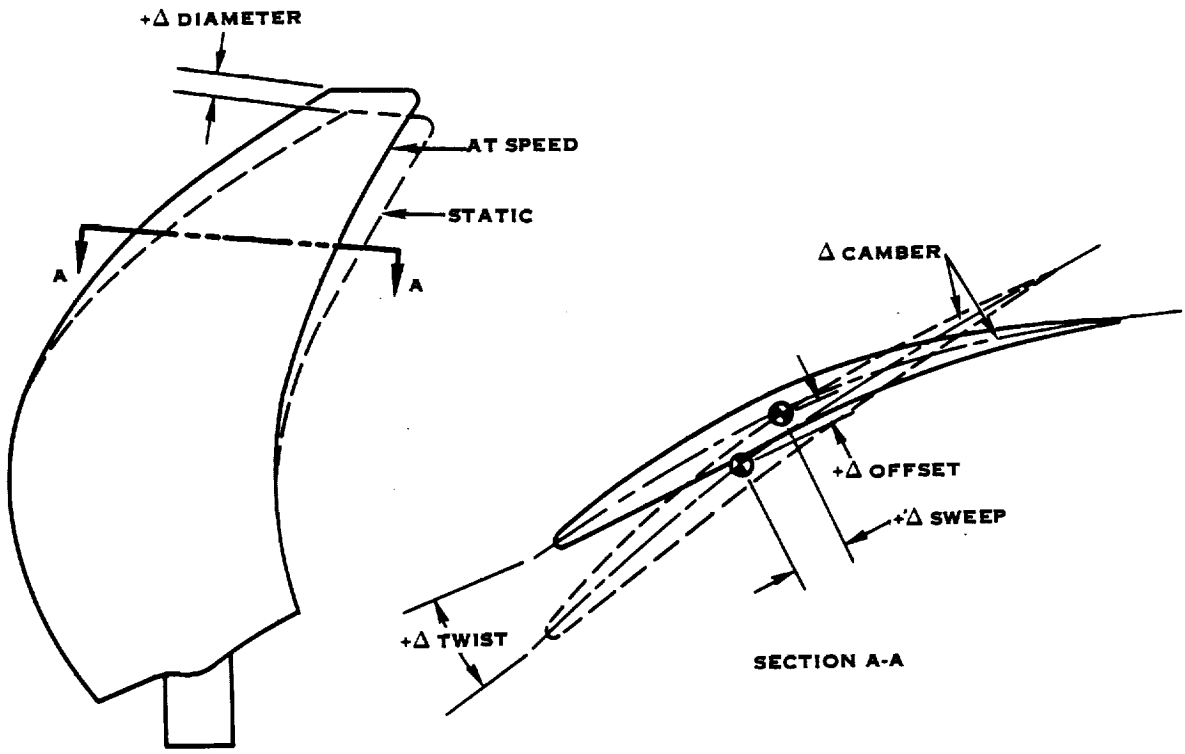

FIGURE 5.11 BLADE ELASTIC DEFLECTIONS

- DESIGN FOR INFINITE LIFE DUE TO HIGH CYCLE FATIGUE (10^8 CYCLES)
- LOW CYCLE FATIGUE IS BASED ON 50,000 START/STOP CYCLES FROM NO STRESS TO PEAK STRESS
- DESIGN LIMITS BASED ON CONSERVATIVE ASSESSMENT OF MATERIAL STRENGTHS, ENVIRONMENT, SIZE FACTORS, AND ON FULL SCALE FATIGUE TESTS
- OVERSPEED CRITERIA
  - A) 25% O.S. BELOW YIELD
  - B) 40% O.S. BELOW UTS

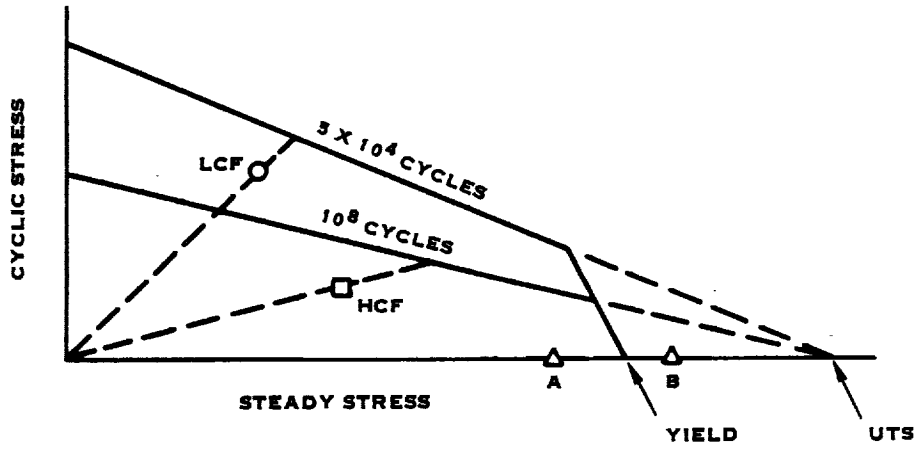

FIGURE 5.12 BLADE DESIGN STRESS CRITERIA

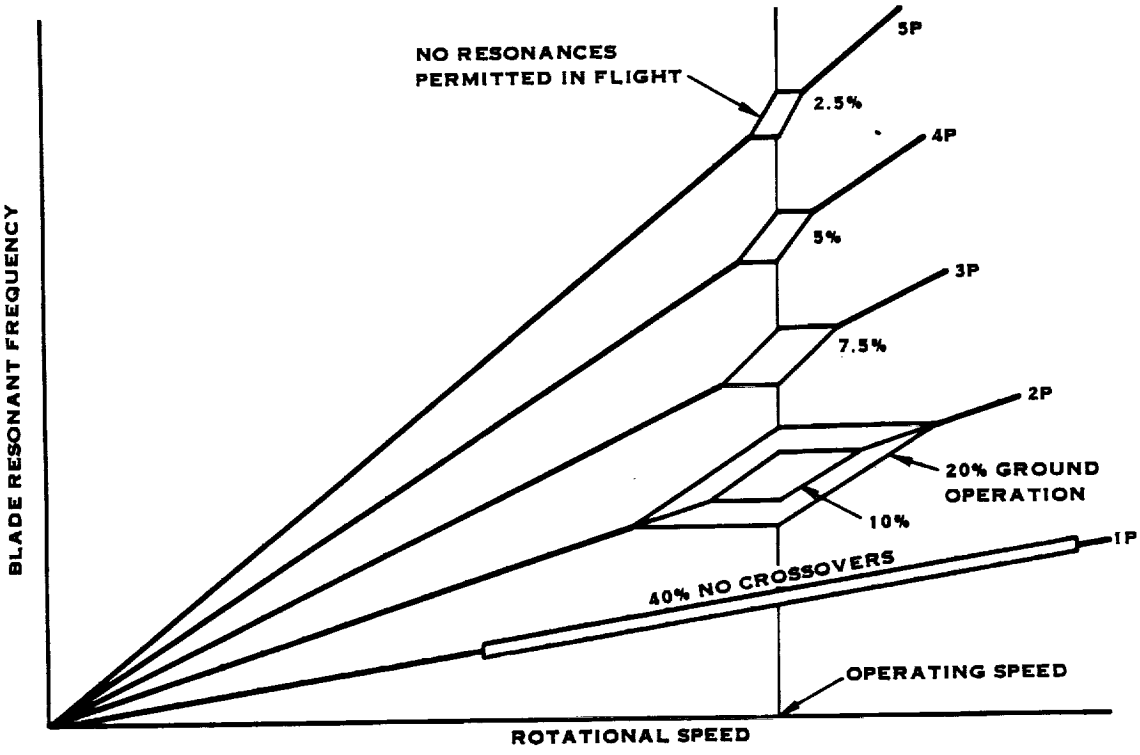

FIGURE 5.13 BLADE DESIGN FREQUENCY CRITERIA

The foreign object impact design criteria is summarized in Figure 5.14, which specifies the size of the object and the damage limit for each impact size classification. In terms of evaluating the blade concepts, the moderate impact criteria can be satisfied if the spar stress remains below the 0.2% offset yield stress, if homogeneous metal material, or below the 5% change in elastic modulus limit, if fiber reinforced resin material. The major impact criteria can be satisfied if the spar stress remains below the ultimate tensile strength, if homogeneous metal material, or below the fracture limit, if fiber reinforced resin material.

The design criteria for blade stability includes requirements for both classical and stall flutter. Classical flutter should not be encountered up to the maximum design rotational and forward speeds with the torsional frequency degraded by 15%. The propeller shall be free of stall flutter up to 120% of maximum (baseline) power at 100% rpm.

5.6 BLADE AND RETENTION COMPUTER ANALYSIS MODELING

The models used in the blade concept analysis are shown in Figures 5.15 to 5.18. Since the SR-2 concept has no sweep, a beam analysis method will yield excellent results. The beam analysis model is shown in Figure 5.15. This method places lumped mass at the individual blade and retention stations, and models the blade stiffness using a series of beam segments. The retention is simulated by beam segments whose moment of inertia gives the same bending moment stiffness as the actual retention.

The remaining concepts are all highly swept. Experience has shown that a beam method analysis will not yield acceptable results for these highly-swept blades; hence, a finite element analysis was used for the remaining concepts. The finite element models for the SR-3 (8), SR-3 (10) (both SR-3 (10) and SR-3C (10)), and the SR-5 (both the SR-5A and SR-5B) are shown in Figures 5.16 to 5.18, respectively. These models have a central layer of elements to represent the spar and foam fill, and a face side and camber side layer of elements to represent the shell. The SR-5B model had additional layers inside the face and camber side shell layers to represent the boron/aluminum reinforcing pads on the spar face and camber sides. All these outer layers are mathematically connected to the center layer by rigid link connections.

The retention was modeled by six springs connecting the butt of the blade to ground, as illustrated in Figure 5.19. Each spring acts in a different degree-of-freedom direction. For a given blade configuration analysis, the spring rates k_x, k_y, k_z and $k_{\theta z}$ remained constant with propeller speed. The other moment spring rates, $k_{\theta x}$ and $k_{\theta y}$, were assumed equal to each other, and vary with propeller speed as previously shown in Figure 5.8.

MINOR IMPACT	- SAND, SAMLL STONES, UP TO 4 OUNCE BIRDS - NO DAMAGE TO BASIC BLADE STRUCTURE - CONTINUED OPERATION
MODERATE IMPACT	- 2 INCH HAILSTONES, UP TO 2 POUND BIRDS - LOSS OF MATERIAL OR AIRFOIL DISTORTION ACCEPTABLE - OPERATION AT 75% POWER FOR 5 MINUTES - NO METAL FRAGMENTS WILL PENETRATE FUSELAGE - ROTOR UNBALANCE FORCE < 5000 POUNDS
MAJOR IMPACT	- UP TO 4 POUND BIRD - LOSS OF MATERIAL OR AIRFOIL DISTORTION ACCEPTABLE - ABILITY TO FEATHER - NO METAL FRAGMENTS WILL PENETRATE FUSELAGE - ROTOR UNBALANCE FORCE < 25,000 POUNDS

FIGURE 5.14 FOREIGN OBJECT IMPACT CRITERIA

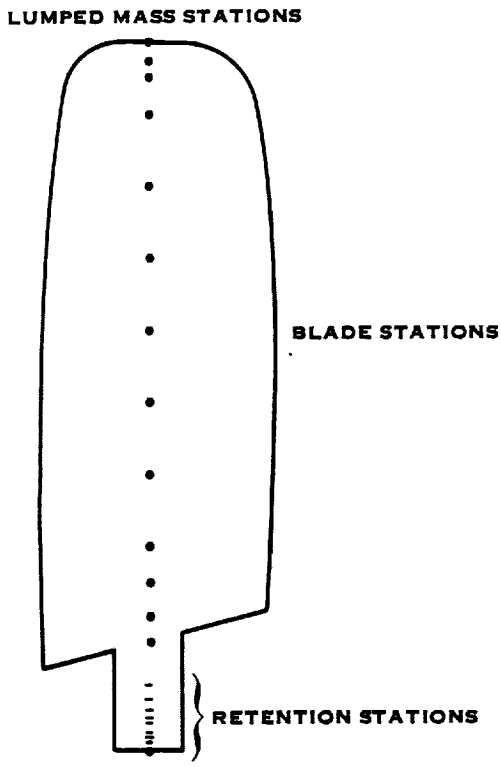

FIGURE 5-15 SR-2 BEAM ANALYSIS MODEL

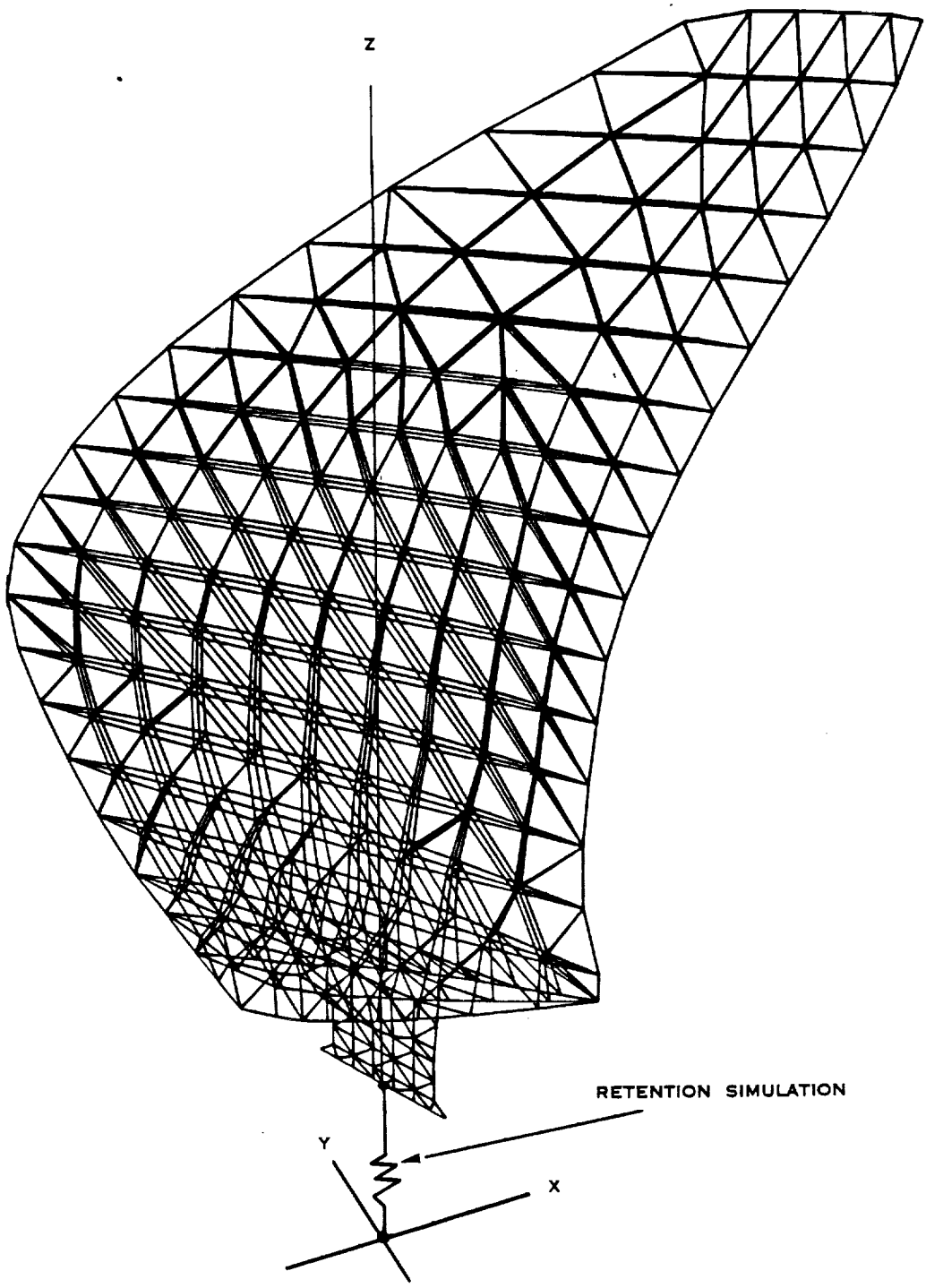

FIGURE 5.16 (8) FINITE ELEMENT MODEL

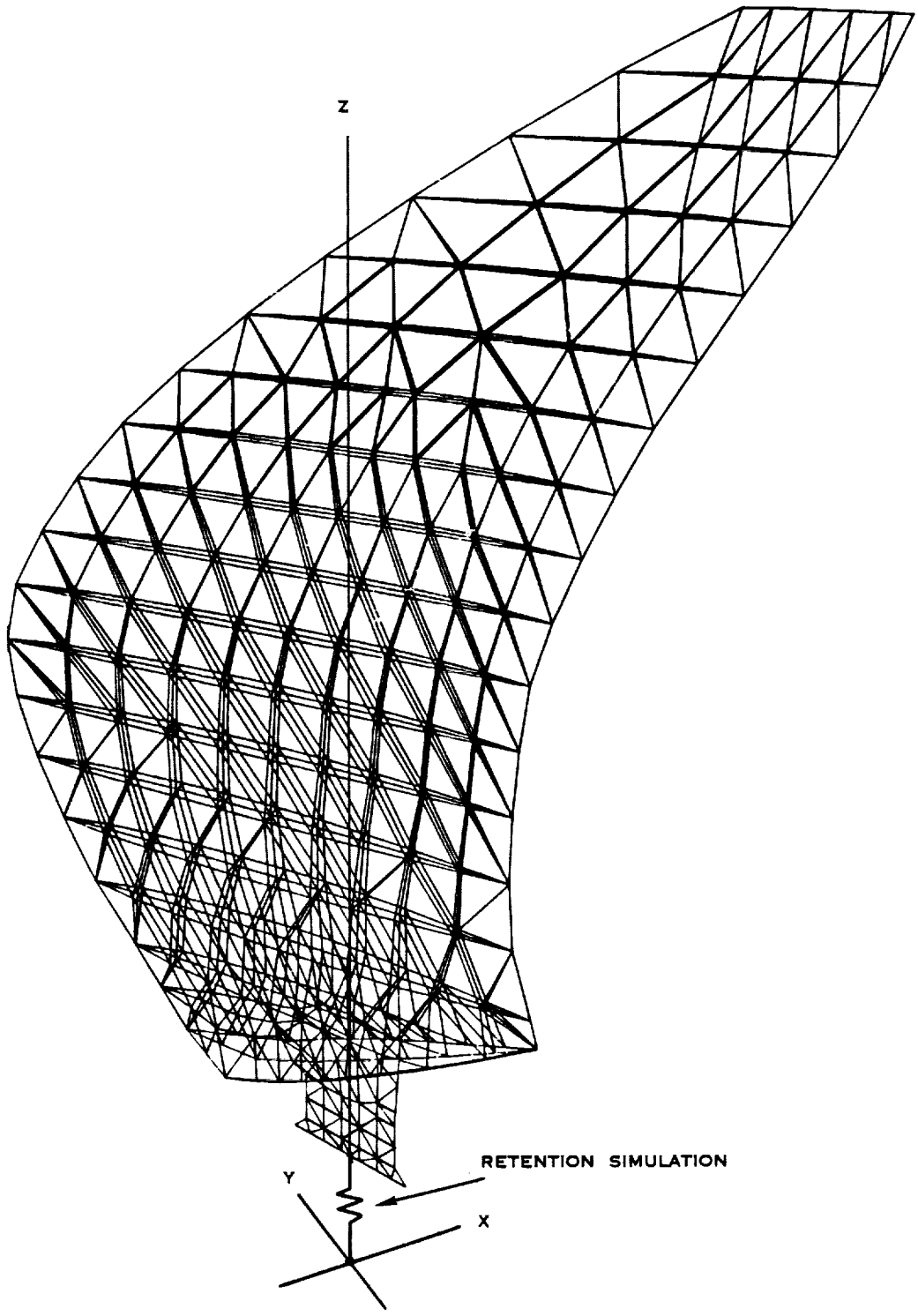

FIGURE 5.17 SR-3 (10) FINITE ELEMENT MODEL

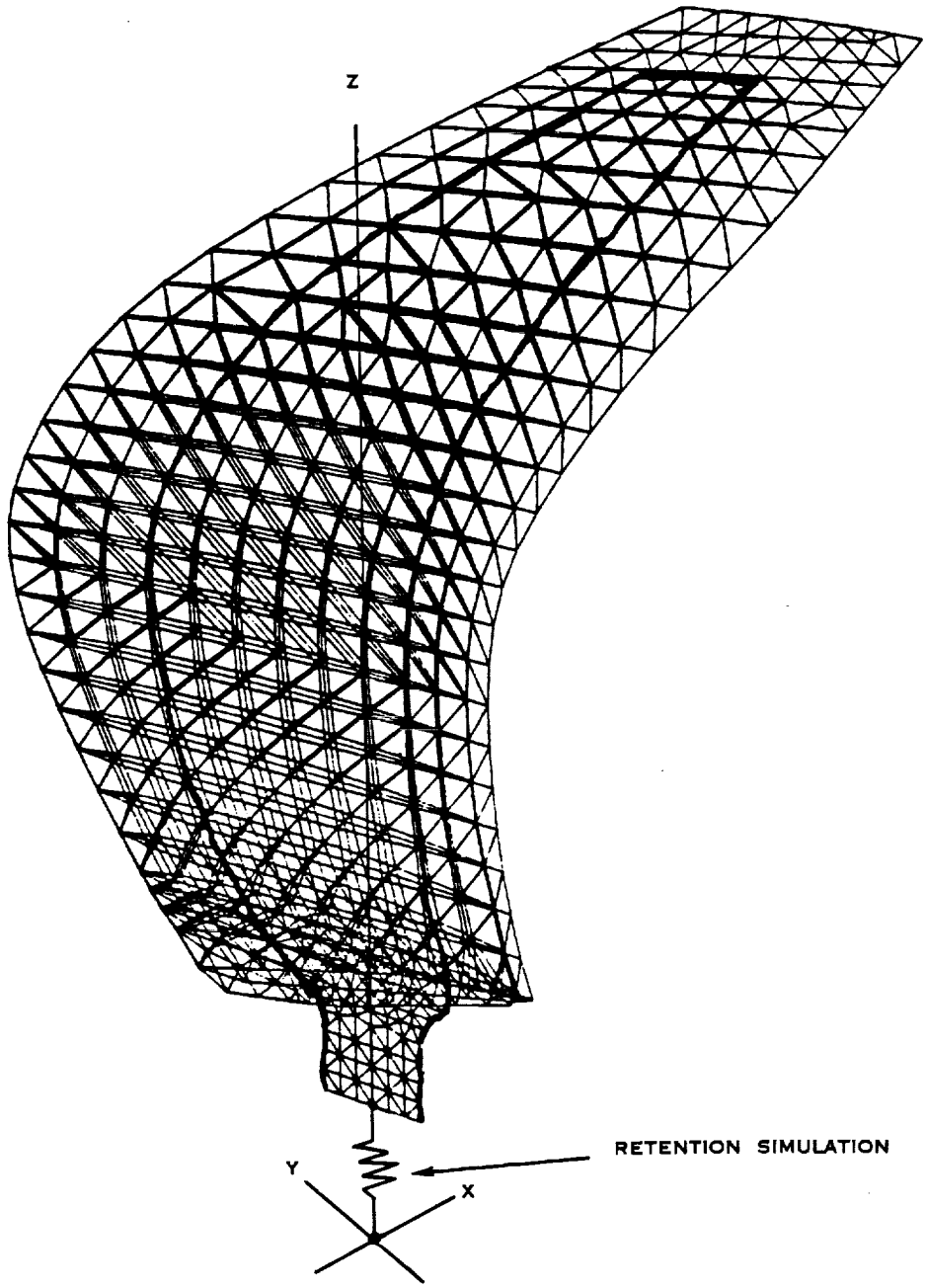

FIGURE 5.18 SR-5 (10) FINITE ELEMENT MODEL

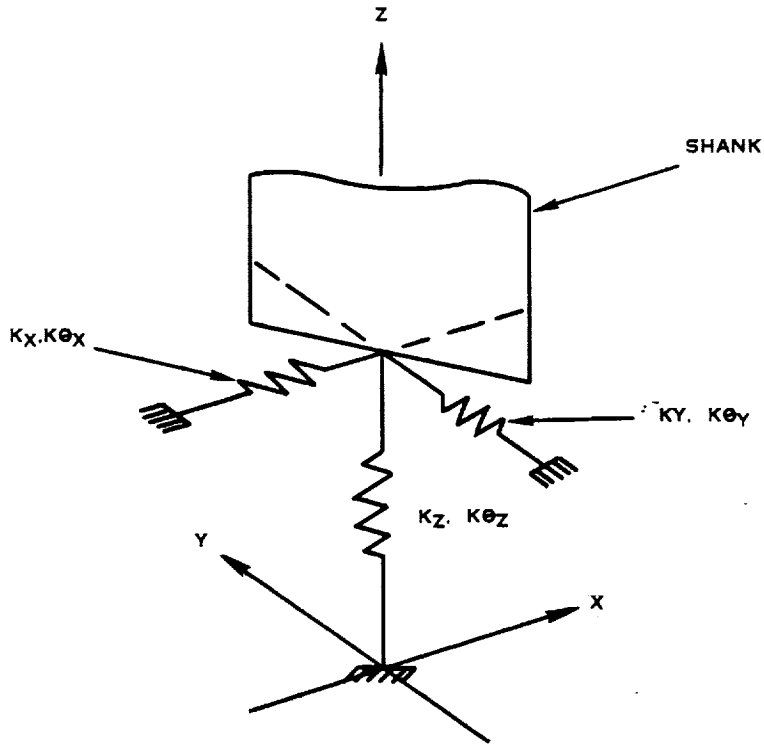

FIGURE 5.19 RETENTION MODELING

5.7 COMPUTER ANALYSIS SOLUTION REVIEW

For the steady-state operating conditions, air loads are obtained and resolved into components parallel to the coordinate directions of the computer model. These airloads are applied to the static geometry model and the analysis is performed with the blade spinning in the centrifugal field. Stiffening effects due to the centrifugal field are included in the analysis.

Vibratory excitation of a propeller blade is caused by the propeller rotation axis being at a relative angle to the direction of forward velocity. This relative angle causes the angle of attack of the blade (and thus bending loads) to vary sinusoidally during each revolution. This effect is most evident at takeoff/climb, when the relative angle is high. To account for this once-per-revolution (1P) vibratory excitation, an excitation factor is defined. Representative $0.8M_n$ commercial transport aircraft with wing mount Prop-Fans were studied in the late 1970's by the Lockheed California Company and the Boeing Commercial Airplane Company as part of the NASA technology effort to identify ways to reduce airplance fuel consumption. Hamilton Standard analysis of these single rotation Prop-Fans resulted in a 1P loading of 3.30. The high wing sweep of these configurations yeilded a significant higher-order (nP). The combination of the 1P and the nP gives an equivalent EF of 4.5. It is assumed that the nP excitations would have a magnification factor of three, and that the 1P magnification factor is unity.

A forced response analysis was used to evaluate the vibratory excitation of the blade. The vibratory airloads for a 4.5 EF at the takeoff/climb condition were resolved into the major coordinate directions and applied to the static geometry computer model. The analysis was performed with these airloads cycling at a frequency corresponding to the once-per-revolution vibration. The stiffening effects of the centrifugal field are included in the analysis.

The above procedure for the steady-state and vibratory analysis applied to both the beam analysis used on SR-2 and the finite element analysis used on all other concepts. In all cases, the airloads were applied to the static geometry.

Blade resonant frequency calculation was also performed with the blade in the static geometry, with the centrifugal stiffening effects included when applicable. The beam analysis frequency calculation gives the integer-order excitation line intersections as a function of rotational speed. These points are then plotted on a Campbell plot to determine resonant frequencies of the blade design at a specific rotational speed. The finite element analysis used a determinant cross-over method to find the resonant frequencies at a specific rotational speed. The mode shapes are also calculated by each analysis method for the blade design's resonant frequencies.

5.8 BLADE STRUCTURAL LOADS

The loads acting on a blade structure come from three sources; externally applied steady loads, vibratory loads, and body force induced loads. These loads are illustrated in Figure 5.20. The externally applied steady loads include the lift and drag airloads and foreign object loads. The vibratory loads include forced response loads and self-excited vibration (i.e., resonance). The body force induced loads are the centrifugal load and the centrifugal twisting moment. All of these loads must be accommodated by the blade structure.

5.9 BLADE WEIGHT AND RETENTION LOADS

A summary of the individual blade concept weight is given in Table 5.3. Figure 5.21 shows the loads acting on the blade retention: centrifugal load, thrust, power, bending moment and twisting moment. The twisting moments for each blade concept for steady-state cruise and steady-state takeoff operating conditions are listed in Table 5.4. Tables 5.5 through 5.7 list the centrifugal load, twisting moment and bending moment for each blade concept for the steady-state 100% speed, 25% overspeed, and 40% overspeed, respectively.

5.10 DEFLECTION RESULTS

The blade elastic deformations are illustrated in Figure 5.11. The changes in diameter, sweep, and offset were measured at the mid-chord point on the tip station. The change in twist is measured about an axis parallel to the pitch change axis. The steady-state deflections are summarized in Table 5.8. The change in camber for the SR-2 is not available since this cannot be determined using a beam method analysis.

Contour plots from individual blade configuration analyses may be found in Appendix C.

5.11 COMBINED STRESS RESULTS

Steady-state and cyclic stresses were combined and plotted directly on Goodman diagrams. This stress state was then compared to the material allowable stress limit for the specific blade component.

The high cycle fatigue stress that is plotted is the stress that has the highest percent of material allowable stress limit in the component. To determine the percent of allowable limit for a given stress point, a line is drawn on the Goodman diagram from the origin, passing through the stress point, and intersecting the material allowable limit line (see Figure 5.12). The ratio, expressed as a percent, of the steady-state stress at the given stress point to the steady state stress at the material allowable limit intersection point is the percent of material allowable stress limit for that stress point. This process is repeated for all the stress data points in the computer analysis model, and the data point with the maximum percent of allowable limit is determined.

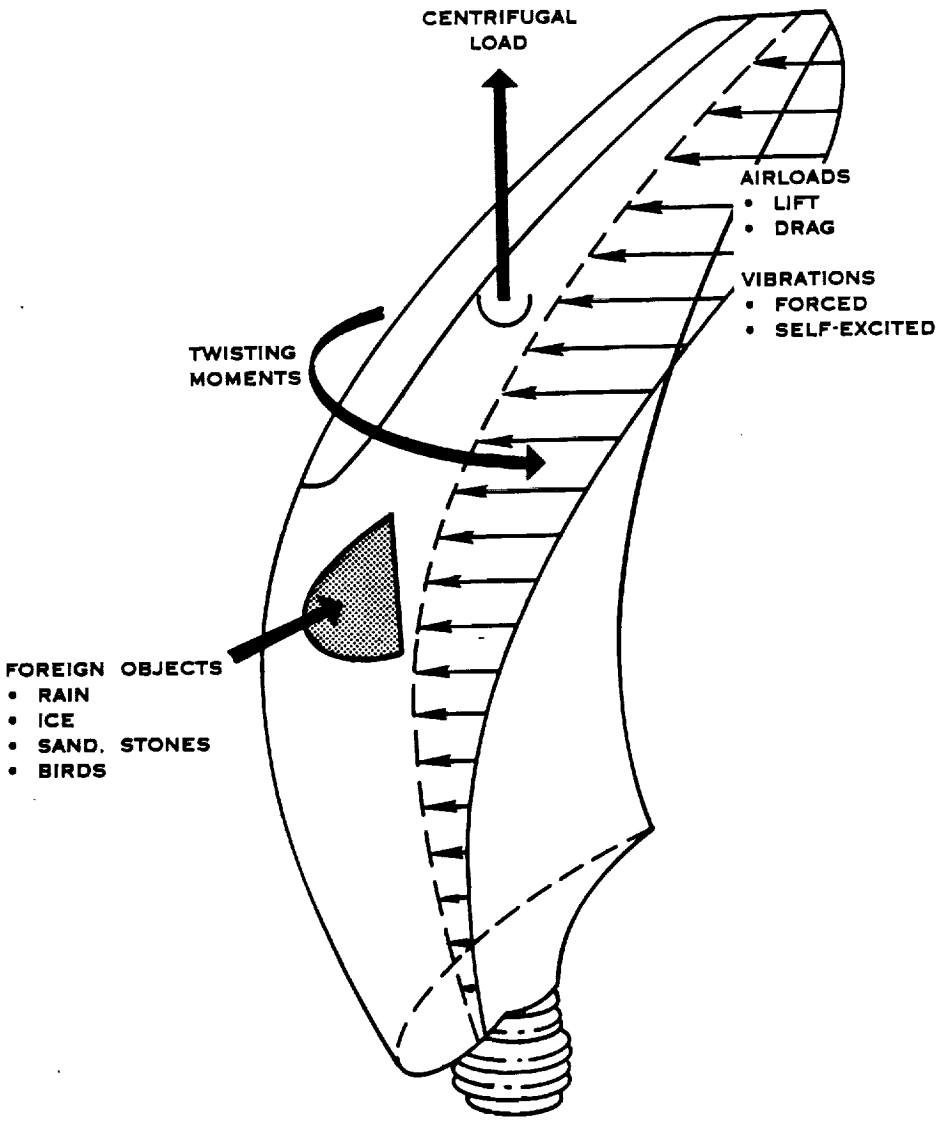

FIGURE 5.20 BLADE STRUCTURAL LOADS

	AERODYNAMICALLY INDUCED	CENTRIFUGALLY INDUCED
TENSION	(N/A)	(100%), (125%), (140%) RPM
BENDING	100% RPM ONLY	(100%), (125%), (140%) RPM
TWISTING MOMENT	100% RPM ONLY	(100%), (125%), (140%) RPM

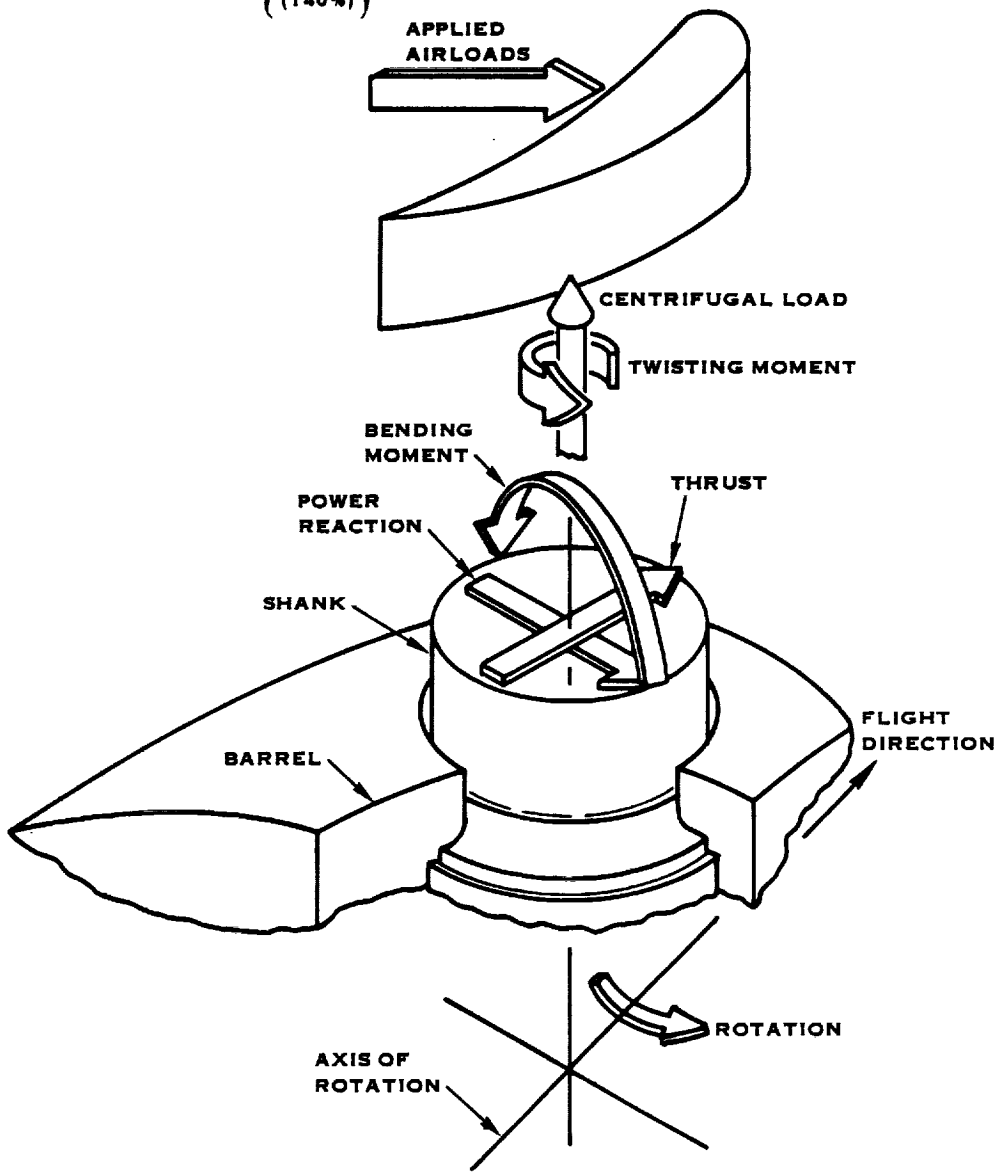

FIGURE 5.21 BLADE RETENTION LOADS

TABLE 5.3. BLADE WEIGHT SUMMARY

Blade Configuration	Per Blade Kg	(Lbs)	Per Propeller Kg	(Lbs)
SR-2	21.2	(46.7)	169.6	(373.6)
SR-3 (8)	31.9	(70.4)	255.2	(563.2)
SR-3 (10)	20.77	(45.8)	207.7	(458.0)
SR-3C (10)	21.3	(46.9)	213.0	(469.0)
SR-5A	22.4	(49.3)	224.0	(493.0)
SR-5B	24.7	(54.5)	247.0	(545.0)

Note: No retention or pitch change hardware is included.

TABLE 5.4 TWISTING MOMENT VS OPERATING CONDITION (CENTRIFUGAL AND AERODYNAMIC)

Blade Design	At Cruise N-m	(in lbs)	At Takeoff N-m	(in lbs)
SR-2	856	(7,577)	1141	(10,100)
SR-3 (8)	4711	(41,700)	5450	(48,240)
SR-3 (10)	2366	(20,940)	2772	(24,540)
SR-3C (10)	2524	(22,340)	2892	(25,600)
SR-5A	3552	(31,440)	3726	(32,980)
SR-5B	3595	(31,820)	3742	(33,120)

TABLE 5.5. STEADY-STATE SHANK LOADS AT 100% ROTOR SPEED (CRUISE CONDITION)

Blade Design	Centrifugal Load		Twisting Moment		Bending Moment	
	Kg	Lbs	N-m	(In-Lbs)	N-m	(in-Lbs)
SR-2	29,523	(65,100)	856	(7,577)	2,701	(23,905)
SR-3 (8)	53,381	(117,710)	4,711	(41,700)	6,507	(57,600)
SR-3 (10)	33,045	(72,867)	2,366	(20,940)	3,817	(33,783)
SR-3C (10)	33,187	(73,180)	2,524	(22,340)	4,512	(39,936)
SR-5A	38,572	(85,053)	3,552	(31,440)	6,321	(55,953)
SR-5B	38,419	(84,717)	3,595	(31,820)	6,223	(55,084)

TABLE 5.6. STEADY STATE SHANK LOADS AT 25% OVERSPEED

Blade Design	Centrifugal Load		Twisting Moment		Bending Moment	
	Kg	Lbs	N-m	(In-Lbs)	N-m	(in-Lbs)
SR-2	46,129	(101,718)	1,783	(15,781)	11,510	(101,886)
SR-3 (8)	83,395	(183,891)	8,515	(75,375)	12,591	(111,452)
SR-3 (10)	51,633	(113,855)	4,332	(38,344)	9,017	(79,819)
SR-3C (10)	51,839	(114,309)	4,519	(40,000)	9,975	(88,292)
SR-5A	60,268	(132,895)	5,550	(49,125)	9,877	(87,427)
SR-5B	60,030	(132,370)	5,617	(49,719)	9,724	(86,069)

Note: These values are obtained by multiplying the 100% speed takeoff condition loads by a $(1.25)^2$ factor.

TABLE 5.7. STEADY STATE SHANK LOADS AT 40% OVERSPEED

Blade Design	Centrifugal Load		Twisting Moment		Bending Moment	
	Kg	Lbs	N-m	(In-Lbs)	N-m	(in-Lbs)
SR-2	57,865	(127,596)	2,236	(19,796)	14,371	(127,206)
SR-3 (8)	104,609	(230,672)	10,682	(94,550)	15,794	(139,805)
SR-3 (10)	64,768	(142,819)	5,434	(48,098)	11,311	(100,125)
SR-3C (10)	65,027	(143,390)	5,669	(50,176)	12,512	(110,754)
SR-5A	75,600	(166,704)	6,962	(61,622)	12,390	(109,668)
SR-5B	75,301	(166,045)	7,046	(62,367)	12,197	(107,965)

Note: These values are obtained by multiplying the 100% speed takeoff condition loads by a $(1.4)^2$ factor.

In the 25% overspeed and 40% overspeed conditions, only the steady state stress is considered since the steady loads dominate the cyclic loads. The baseline steady stress value that was used was the steady stress from the stress point with the highest percent of allowable limit in high cycle fatigue. This baseline steady stress was multipled by 1.5 and 2.0 to account for the increased rotational speeds of the 25% overspeed and 40% overspeed conditions, respectively.

The high cycle fatigue, 25% overspeed condition, and 40% overspeed condition stress points are plotted in Figure 5.22 to 5.36:

Figure	Blade Configuration	Component	Stress Type
5.22	SR-2	Spar	Spanwise
5.23	SR-2	Shell	Spanwise
5.24	SR-3 (8)	Spar	Spanwise
5.25	SR-3 (8)	Shell	Spanwise
5.26	SR-3 (10)	Spar	Spanwise
5.27	SR-3 (10)	Shell	Spanwise
5.28	SR-3C (10)	Spar	Spanwise
5.29	SR-3C (10)	Spar	In-Plane Shear
5.30	SR-3C (10)	Shell	Spanwise
5.31	SR-5A	Spar	Spanwise
5.32	SR-5A	Shell	Spanwise
5.33	SR-5B	Spar	Spanwise
5.34	SR-5B	Reinforcing Pad	Spanwise
5.35	SR-5B	Reinforcing Pad	In-Plane Shear
5.36	SR-5B	Shell	Spanwise

TABLE 5-8. STEADY STATE DEFLECTION SUMMARY
(CRUISE CONDITION)

Parameter	SR-2	SR-3 (8)	SR-3 (10)	SR-3C (10)	SR-5A	SR-5B
Δ Diameter, cm (in) (+: increase)	.15 (.06)	1.22 (.482)	.85 (.333)	1.03 (.406)	2.10 (8.27)	1.33 (.524)
Δ Tip Sweep, cm (in) (+: to TE)	.18 (.07)	-1.44 (-.566)	-.167 (-.657)	-1.09 (-.431)	-.68 (-.266)	-.18 (-.072)
Δ Tip Offset, cm (in) (+: to face side)	.10 (.04)	.86 (+.338)	-1.3 (-.053)	-.10 (-.041)	-2.69 (-1.06)	-1.77 (-.697)
ST, deg: .75 r/R Tip (+: Increase Blade Angle)	0.6 0.9	-2.04 -2.19	-3.4 -3.7	-2.25 -2.8	-5.8 -9.1	-3.9 -5.4
Δ Camber, %: .75 r/R (+: Increase)	(N/A) (N/A)	-33.9% +5.5%	-42% +12%	-34.9% -6.1%	-75% +18%	-45% +14%

N/A - Not Available

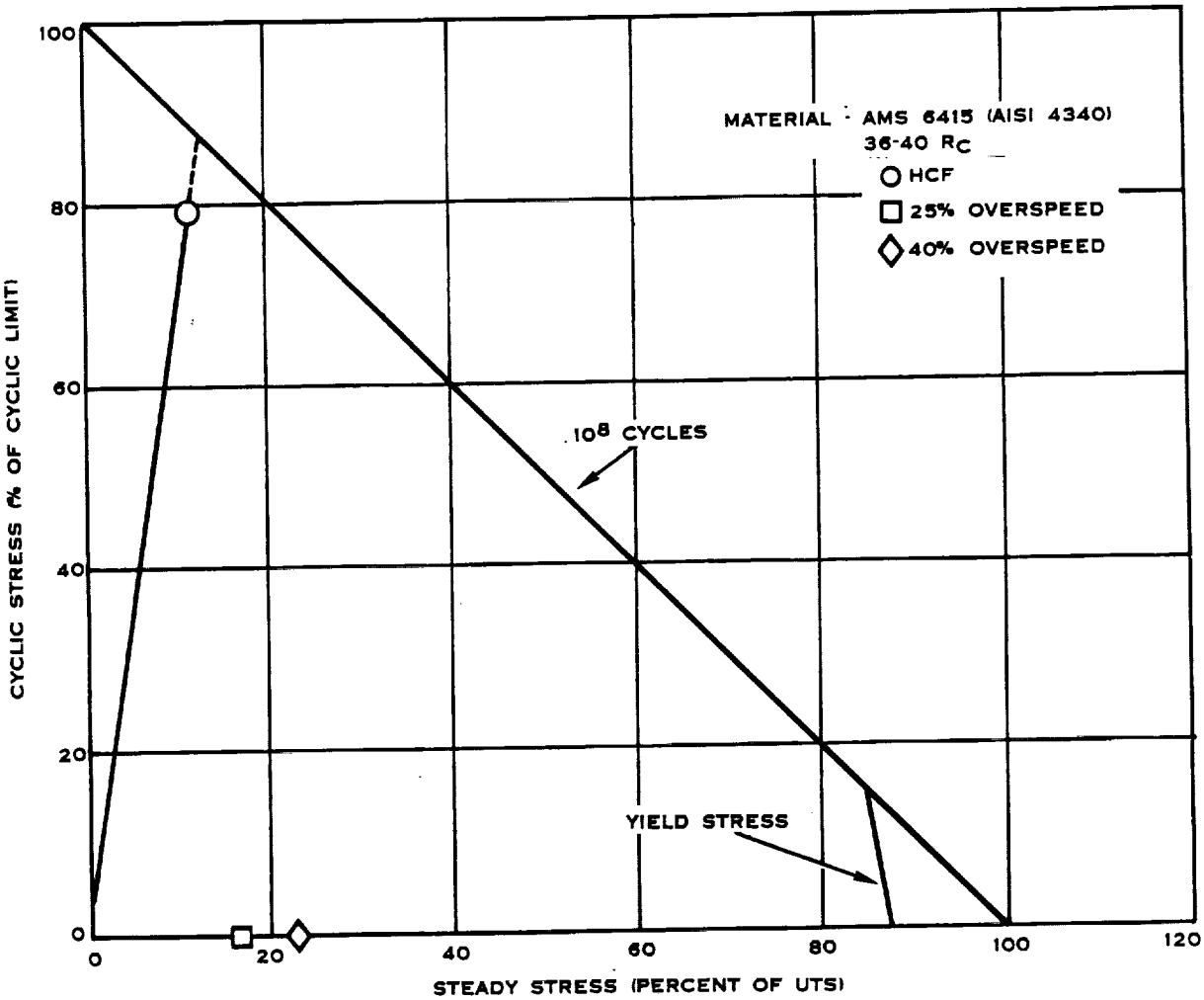

FIGURE 5.22 SR-2 SPAR SPANWISE STRESS

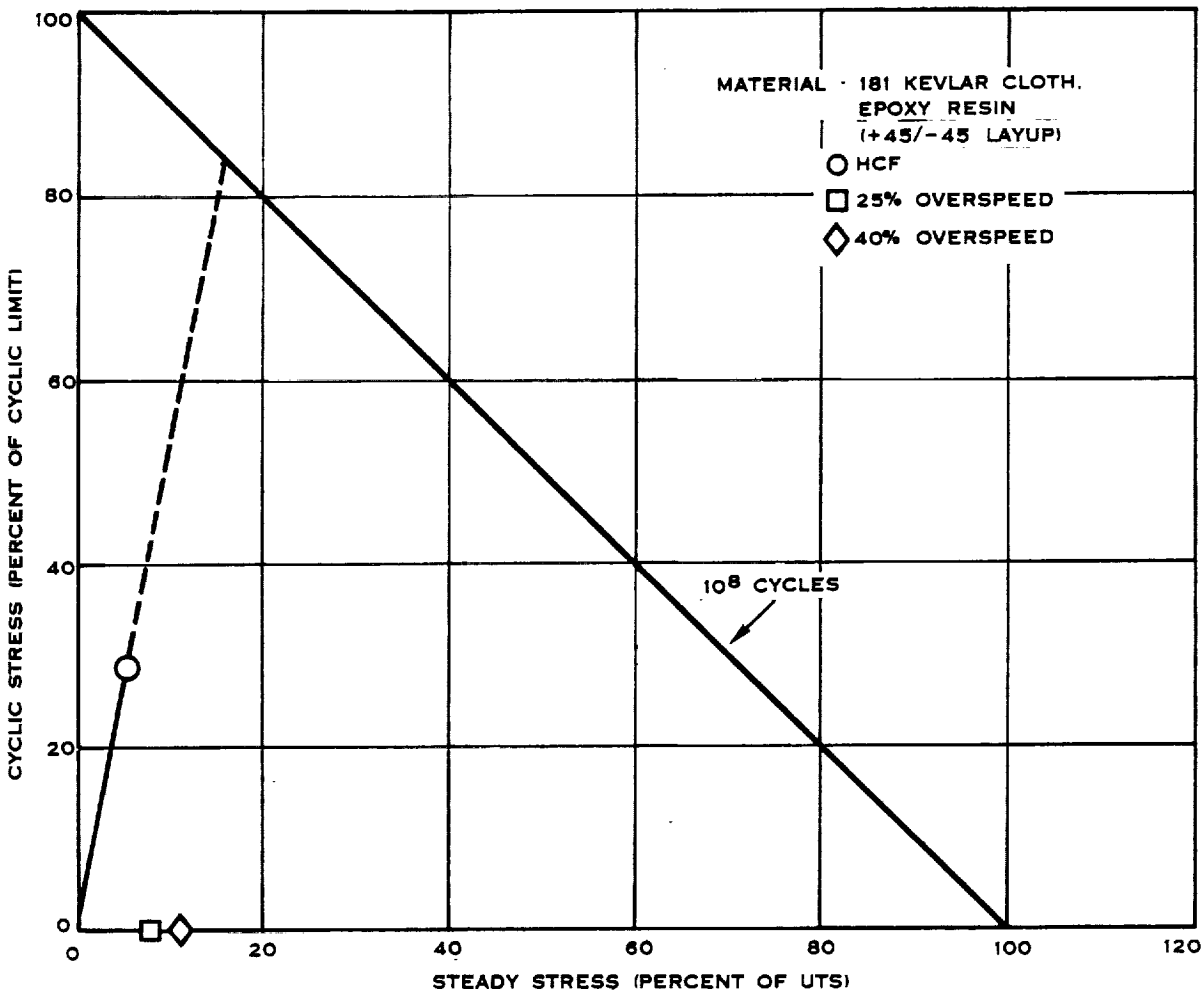

FIGURE 5-23 SR-2 SHELL SPANWISE STRESS

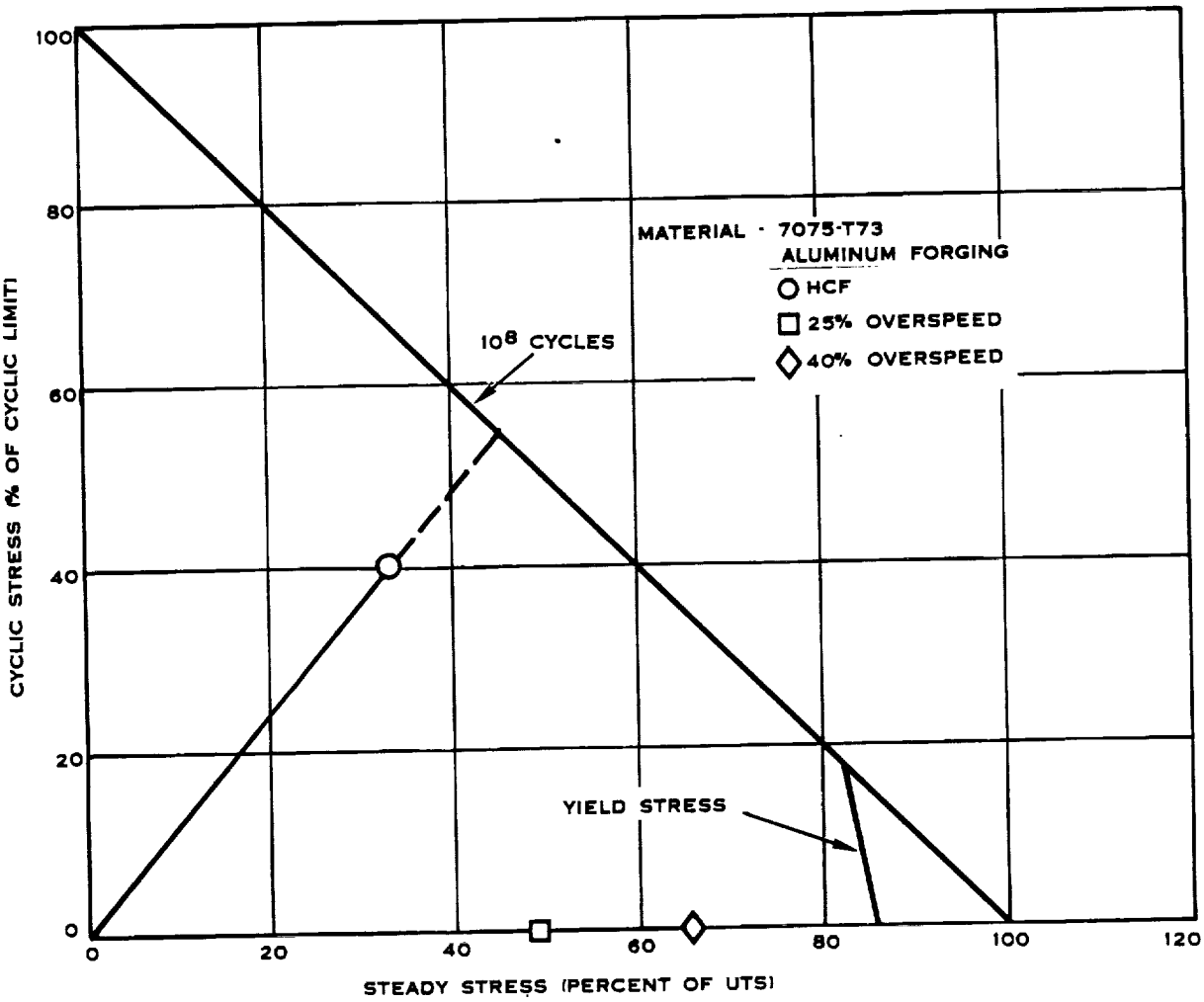

FIGURE 5.24 SR-3 (8) SPAR SPANWISE STRESS

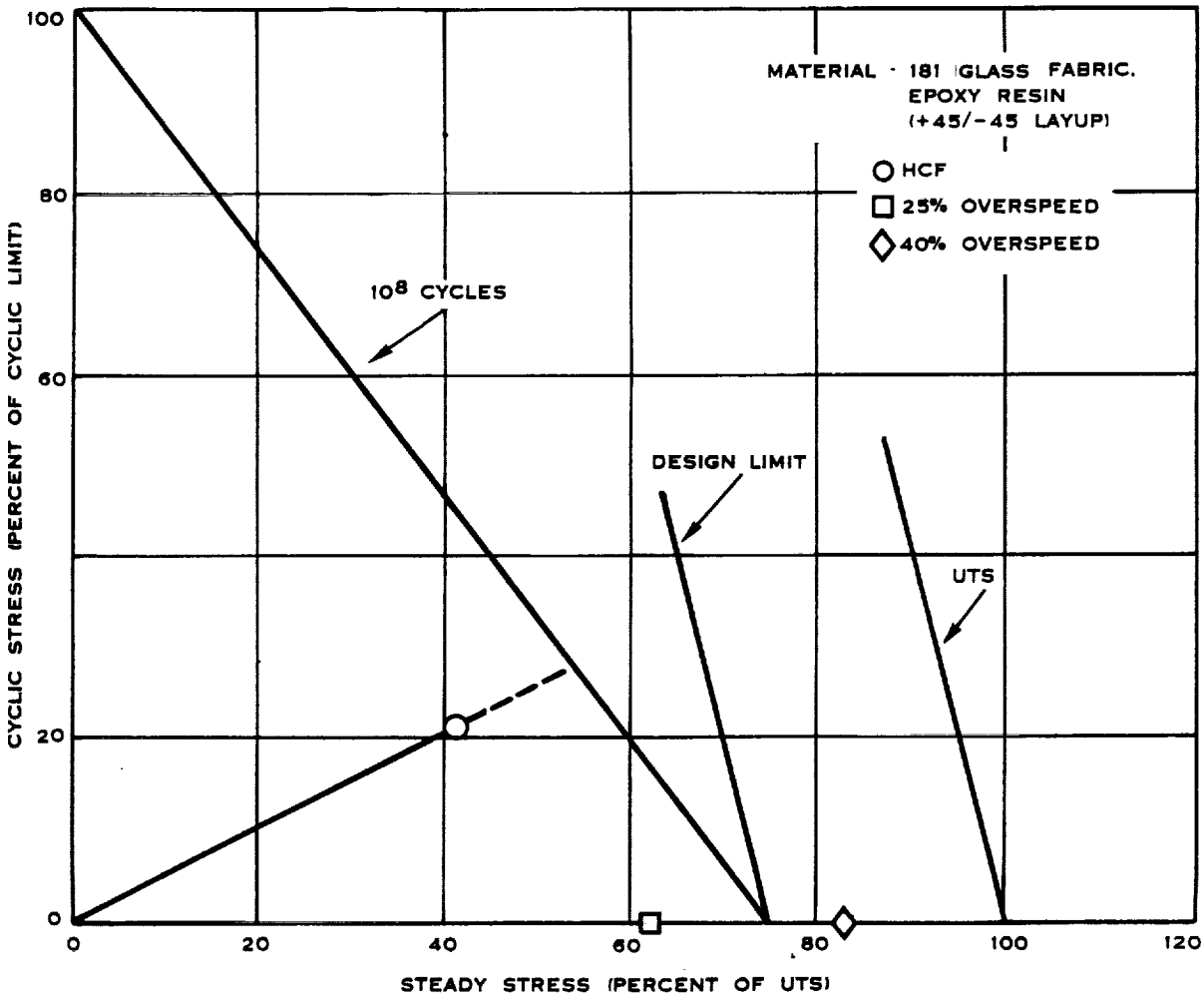

FIGURE 5.25 SR-3 (8) SHELL SPANWISE STRESS

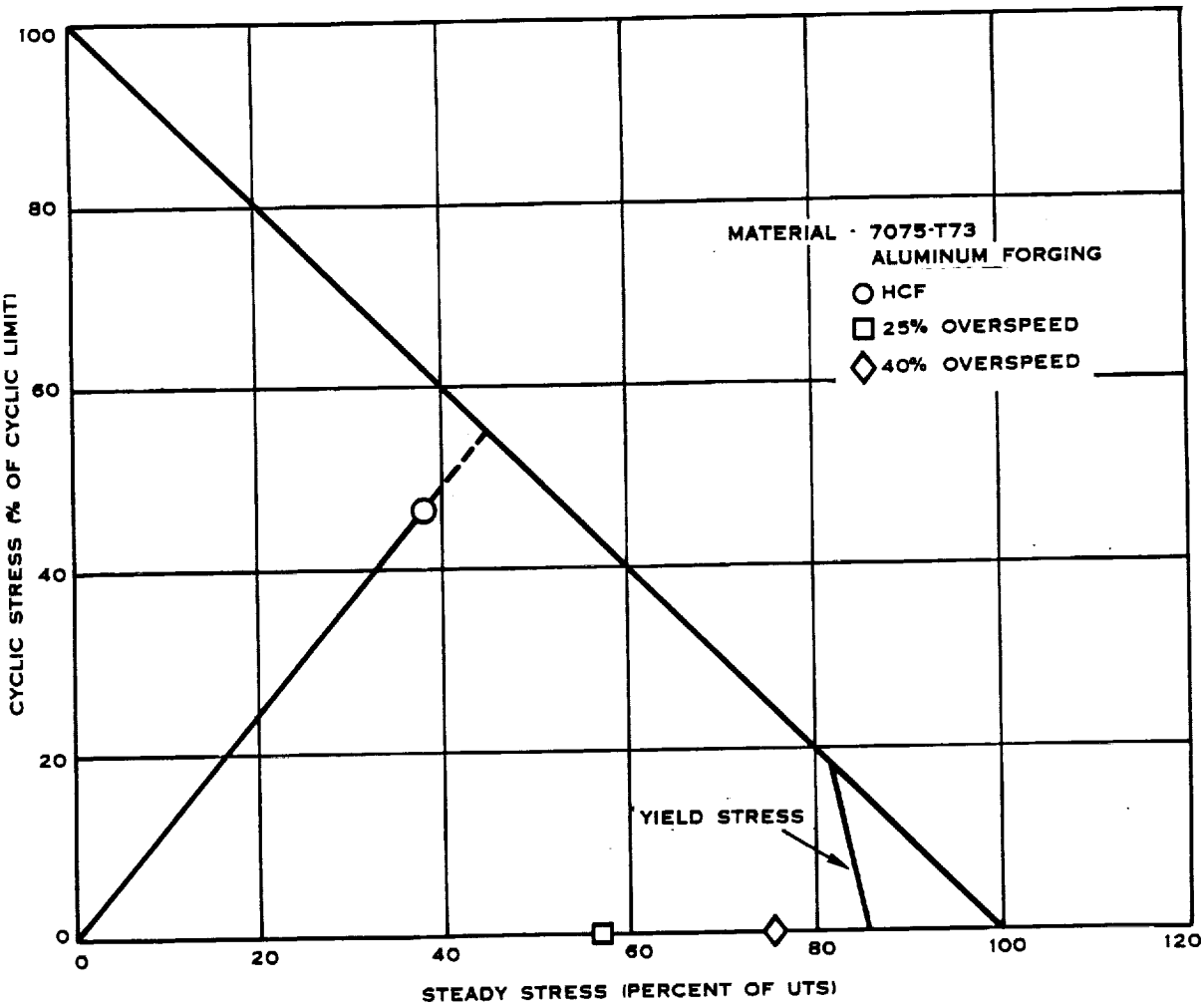

FIGURE 5.26 SR-3 (10) SPAR SPANWISE STRESS

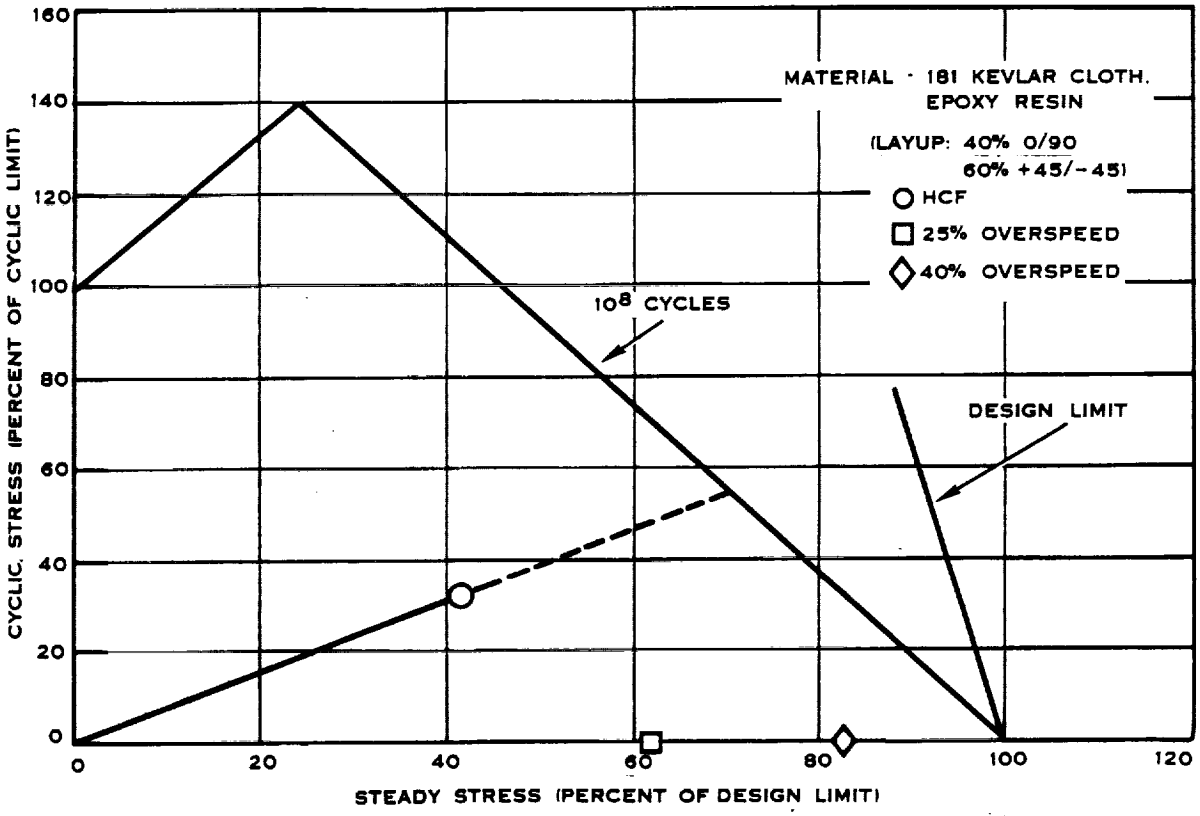

FIGURE 5.27 SR-3 (10) SHELL SPANWISE STRESS

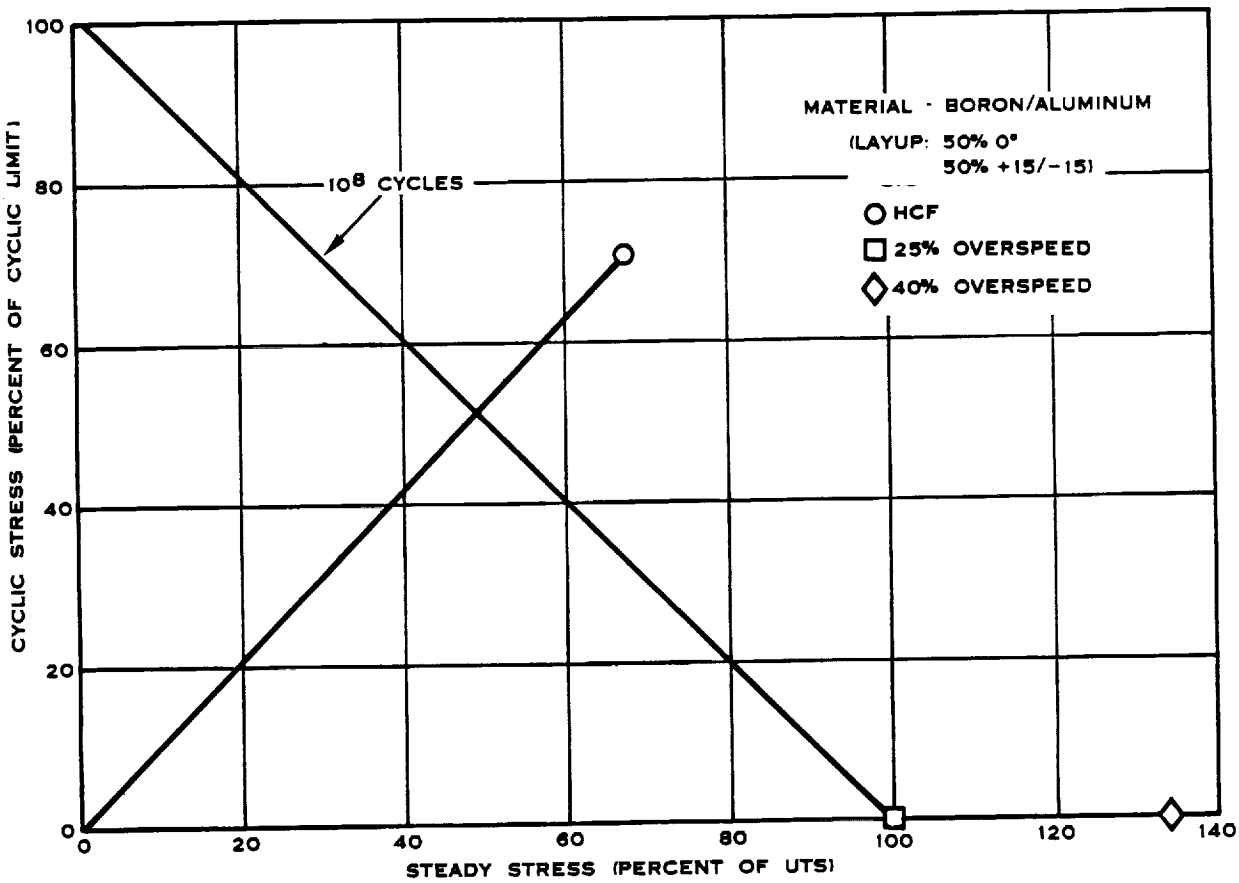

FIGURE 5.28 SR-3 C (10) SPAR SPANWISE STRESS

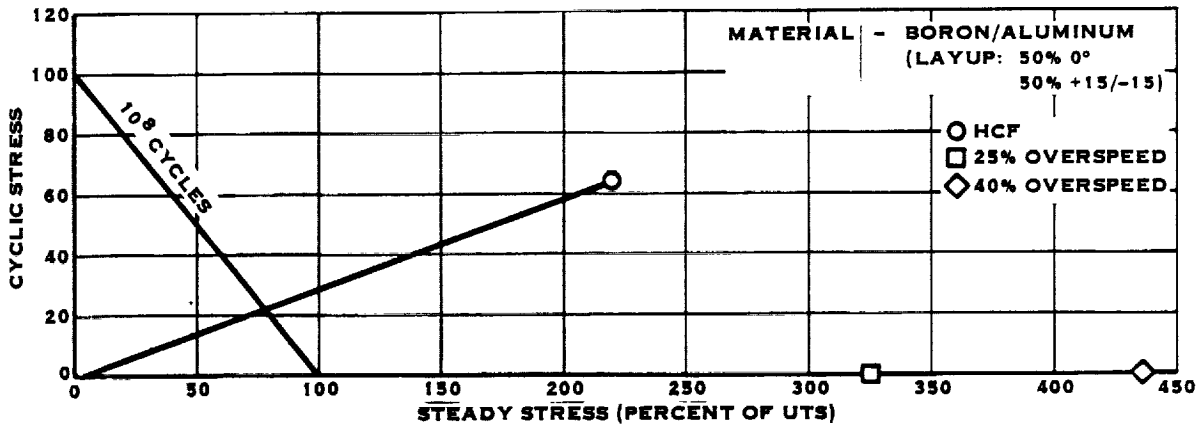

FIGURE 5-29 SR-3C (10) SPAR IN-PLANE SHEAR STRESS

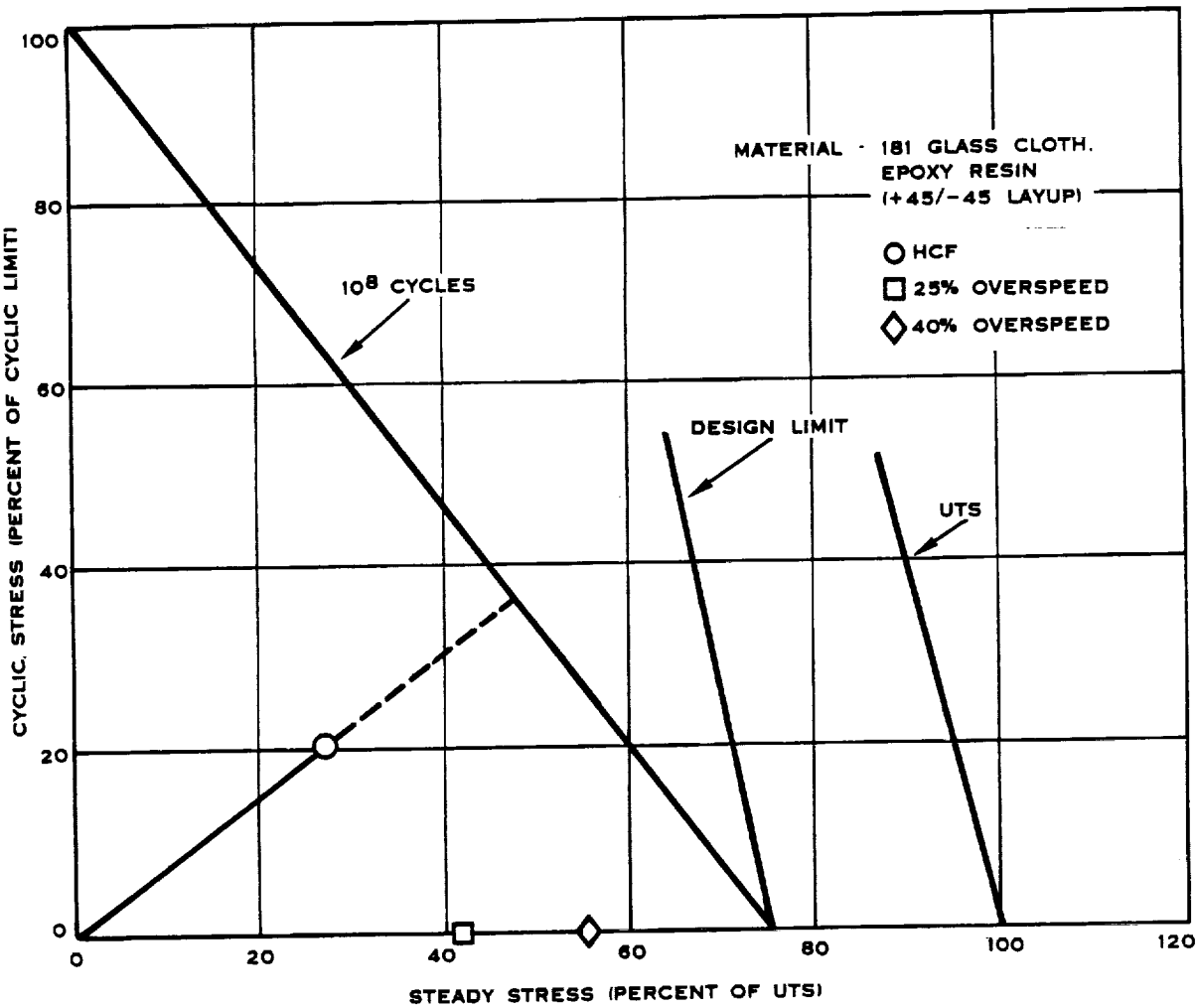

FIGURE 5.30 SR-3C (10) SHELL SPANWISE STRESS

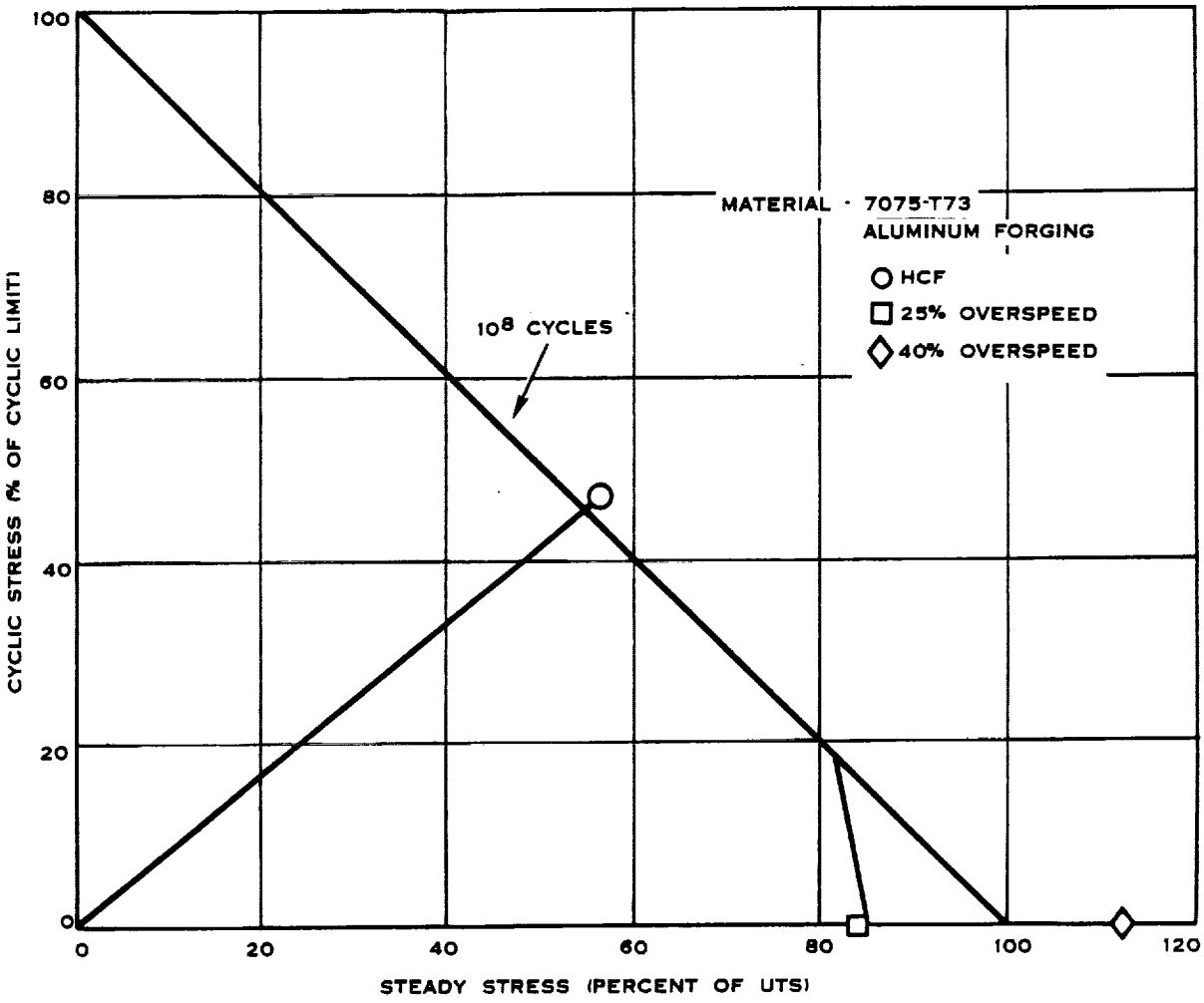

FIGURE 5.31 SR-5A SPAR SPANWISE STRESS

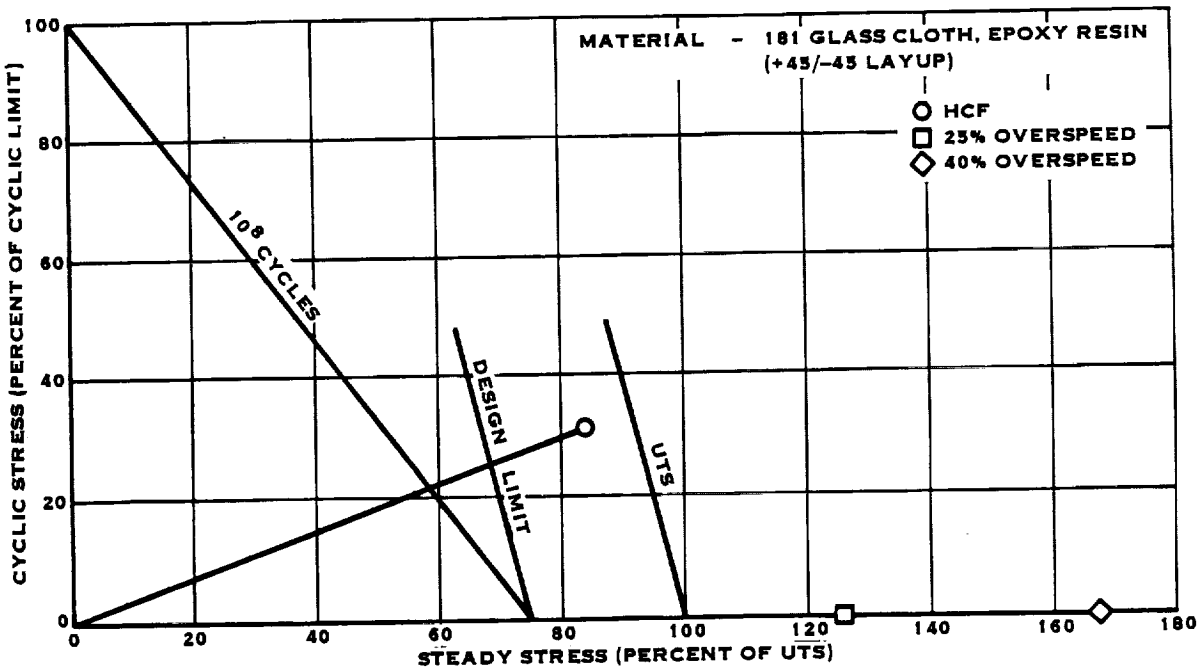

FIGURE 5-32 SR-5A SHELL SPANWISE STRESS

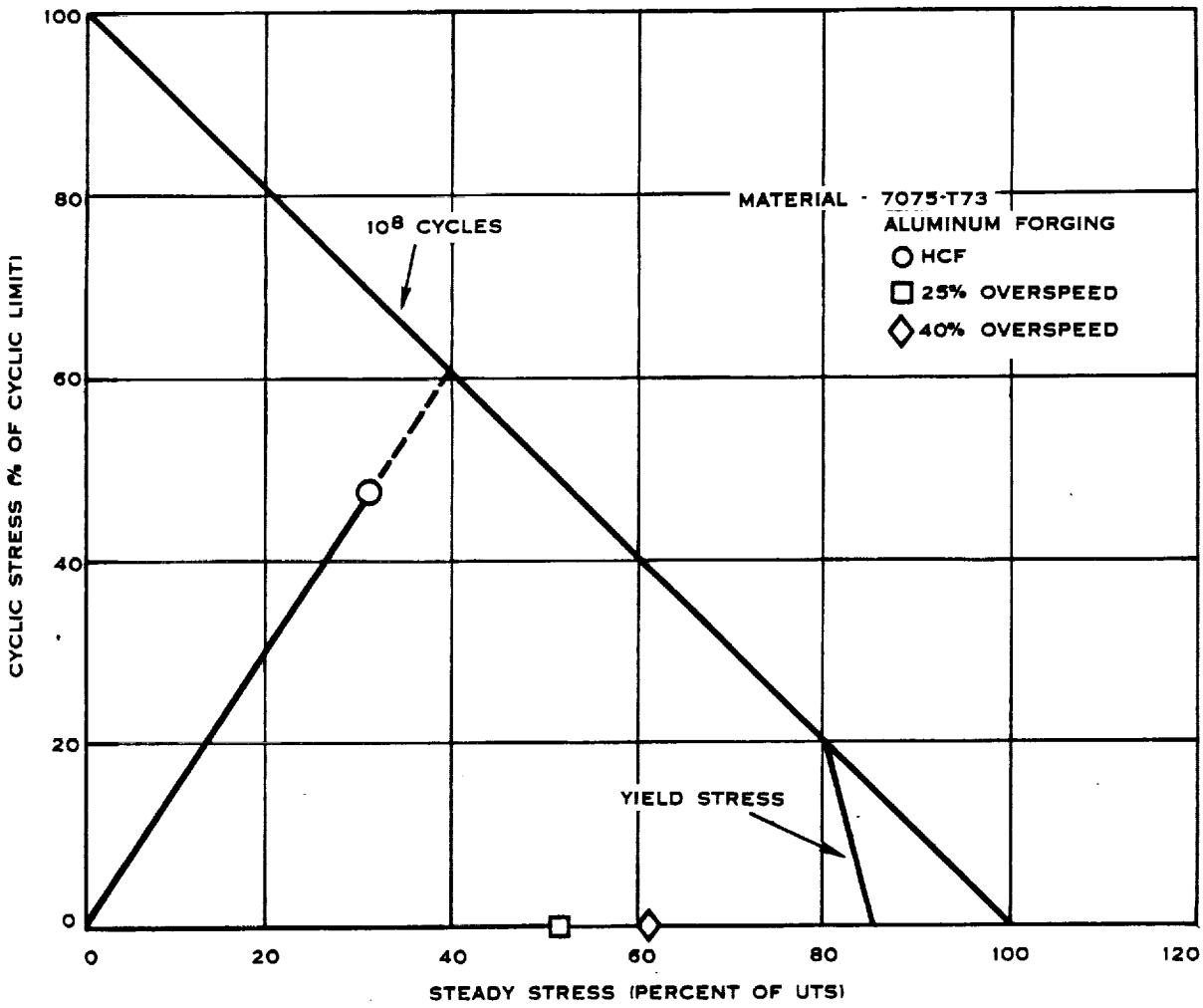

FIGURE 5-33. SR-5B SPAR SPANWISE STRESS

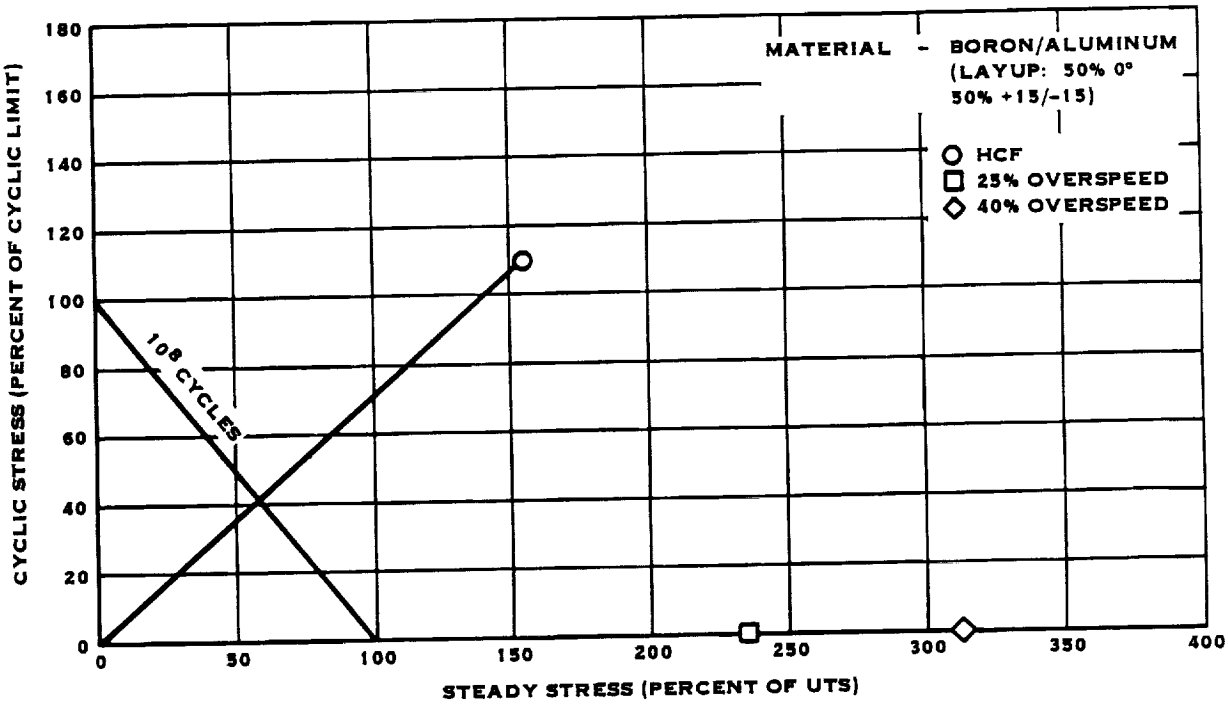

FIGURE 5-34 SR-5B SPAR-REINFORCING PAD SPANWISE STRESS

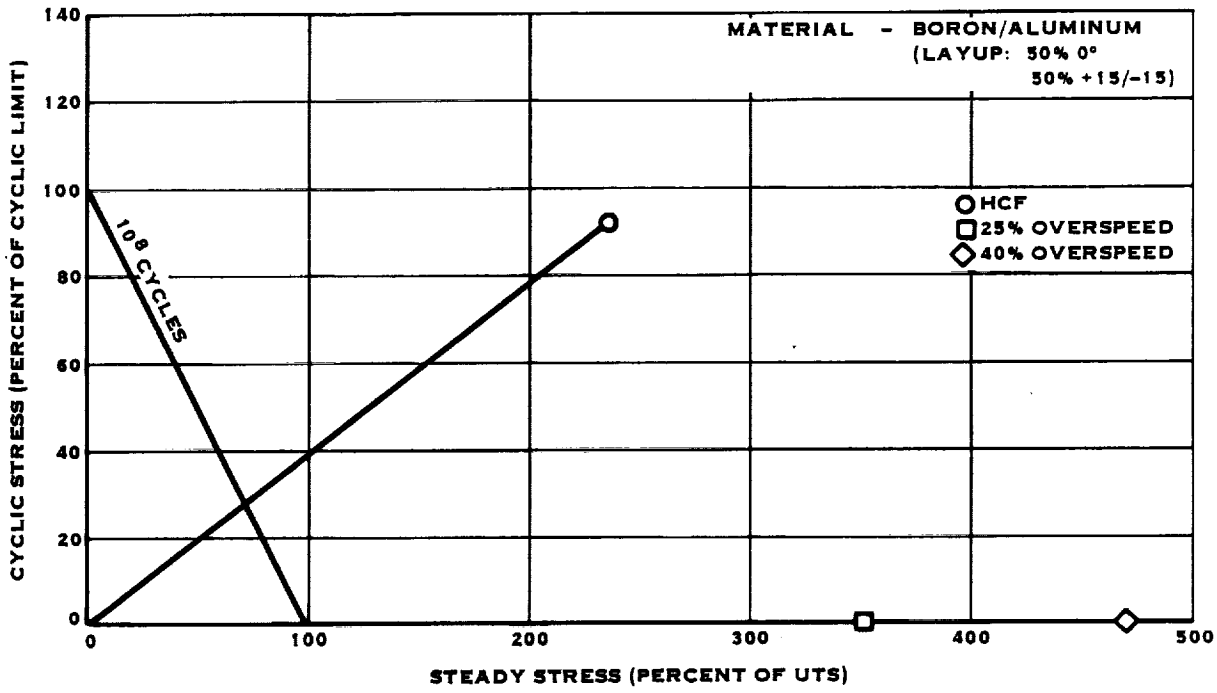

FIGURE 5-35 SR-5B SPAR REINFORCING PAD IN-PLANE SHEAR STRESS

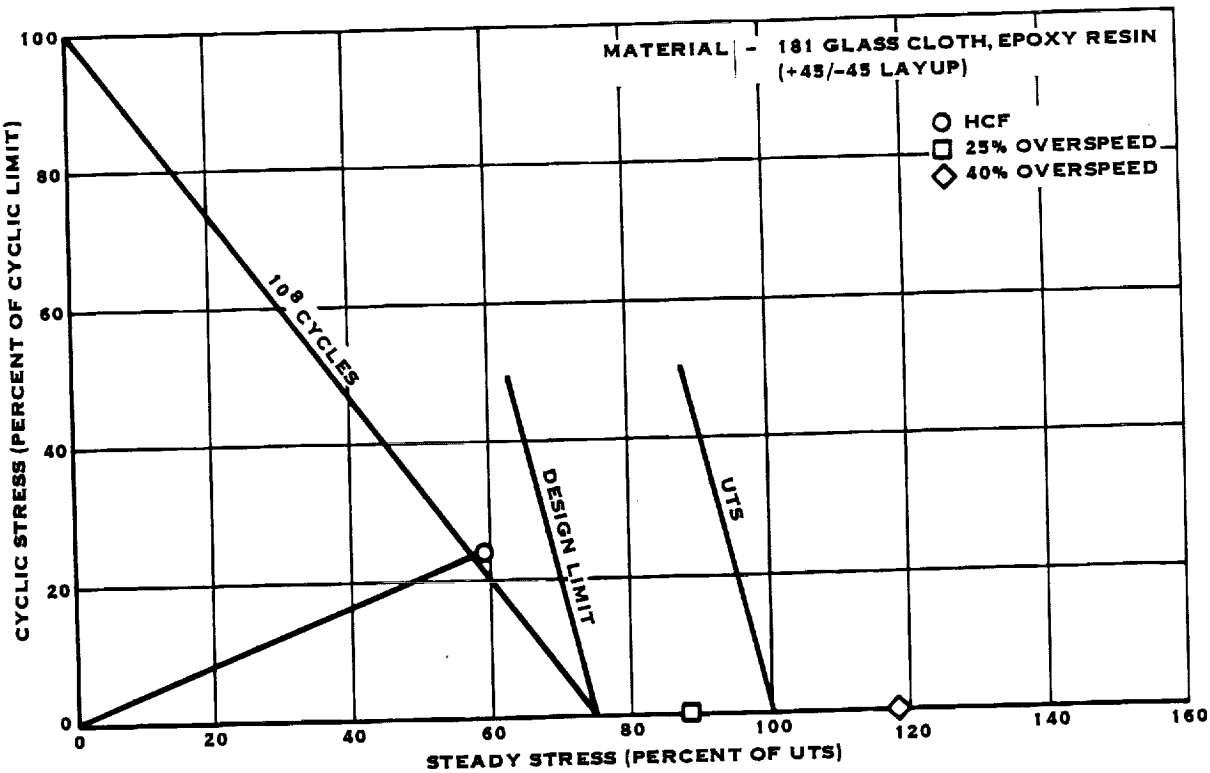

FIGURE 5-36 SR-5B SHELL SPANWISE STRESS

For the low cycle fatigue condition, the same baseline stress point was used. The low cycle fatigue steady-state and cyclic stress, which are equal by definition of low cycle fatigue, are determined by adding the absolute values of the baseline point's steady-state and cyclic stress values and dividing by two. This will result in a variation from no stress to peak stress, at that stress point.

The low cycle fatigue stress points are plotted in Figures 5.37 to 5.45.

Figure	Blade Configuration	Component	Stress Type
5.37	SR-2	Spar	Spanwise
5.38	SR-3 (8)	Shell	Spanwise
5.39	SR-3C (10)	Spar	Spanwise
5.40	SR-3C (10)	Spar	In-Plane Shear
5.41	SR-3C (10)	Shell	Spanwise
5.42	SR-5A	Shell	Spanwise
5.43	SR-5B	Reinforcing Pad	Spanwise
5.44	SR-5B	Reinforcing Pad	In-Plane Shear
5.45	SR-5B	Shell	Spanwise

Contour plots of the combined steady-state stress and cyclic stress for the blade concept components may be found in Appendix C.

5.12 FREQUENCY RESULTS

The first four resonant frequencies of each blade concept are plotted against the resonance avoidance zones in Figure 5.46. As described in Section 5.5, these resonance avoidance zones are defined to avoid dynamic magnification from operating to near a resonant frequency.

Individual blade configuration Campbell frequency diagrams and mode shapes may be found in Appendix C.

5.13 FOREIGN OBJECT IMPACT RESULTS

Five of the six blade concepts were analyzed to determine their foreign object impact capacity. This impact capacity was then compared to the previously established design criteria.

The span foreign object impact capacity at yield and failure is listed for each blade configuration in Table 5.9. The SR-2, SR-3 (8), and SR-3 (10) all have sufficient impact capacity to satisfy the design requirements for the three types of impacts. The SR-3C (10) and SR-5B blade configurations do not satisfy the major impact design criteria, due to fracturing of the boron/aluminum composite in each design concept.

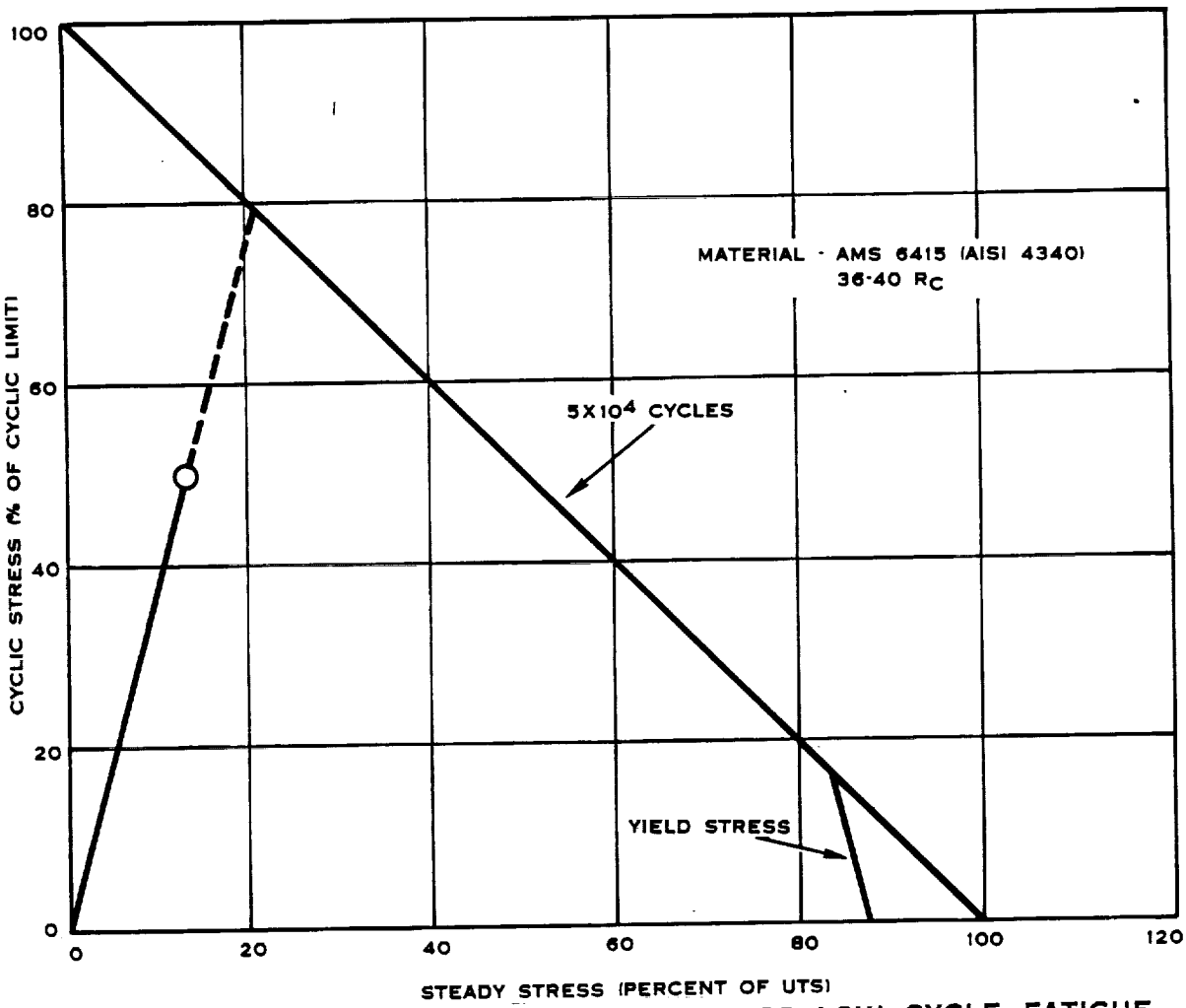

FIGURE 5-37 SR-2 SPAR SPANWISE STRESS LOW CYCLE FATIGUE

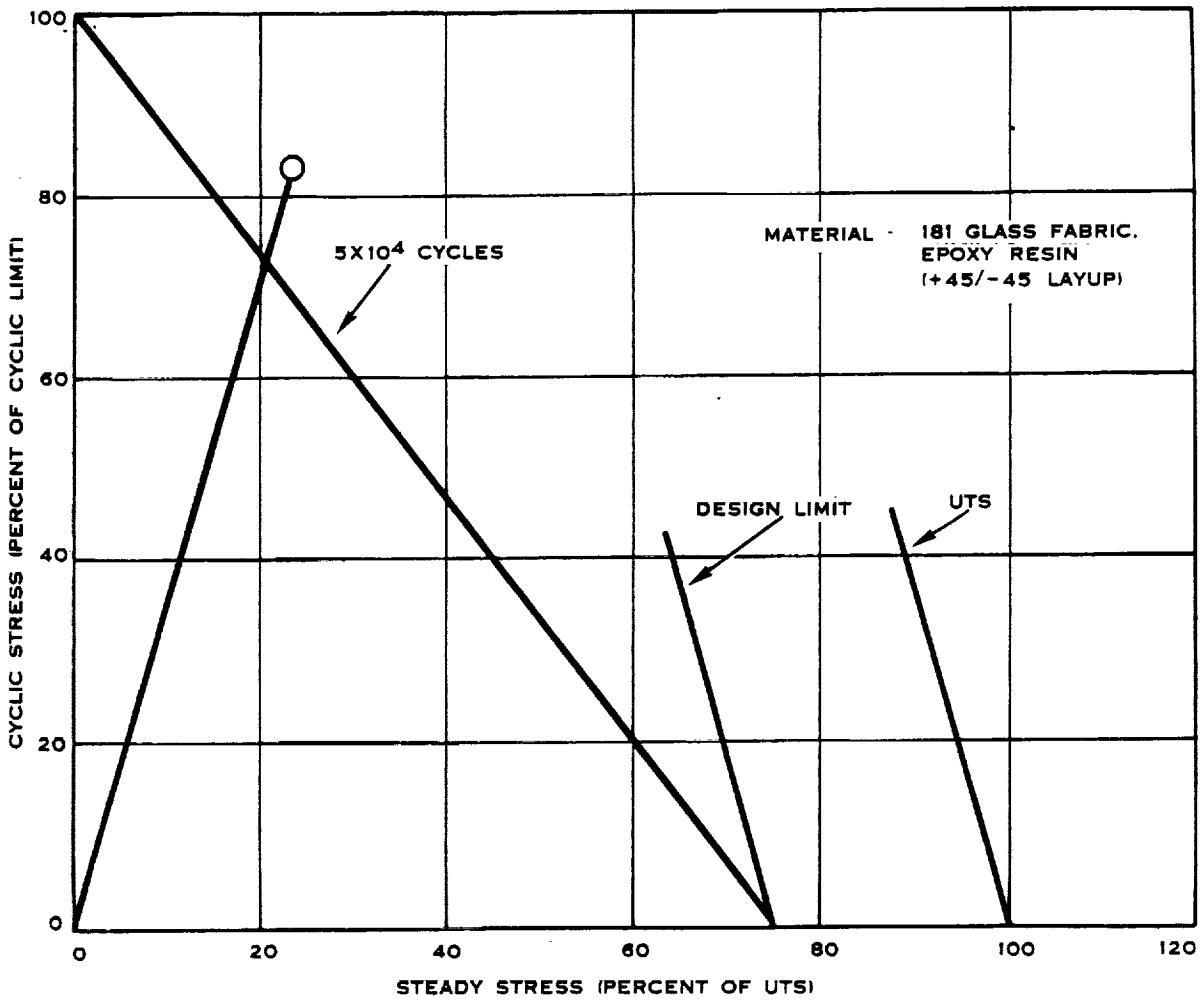

FIGURE 5-38 SR–3 (8) SHELL SPANWISE STRESS LOW CYCLE FATIGUE

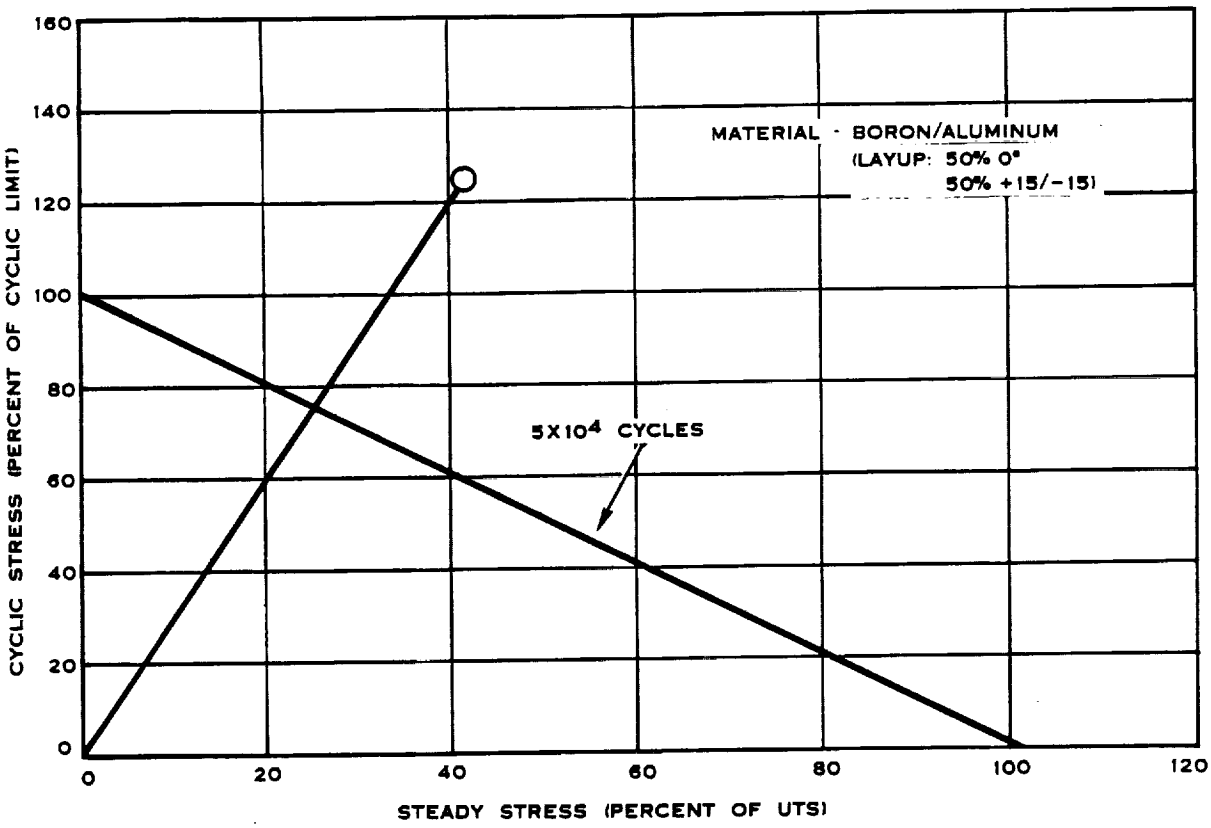

FIGURE 5-39. SR-3C (10) SPAR SPANWISE STRESS
LOW CYCLE FATIGUE

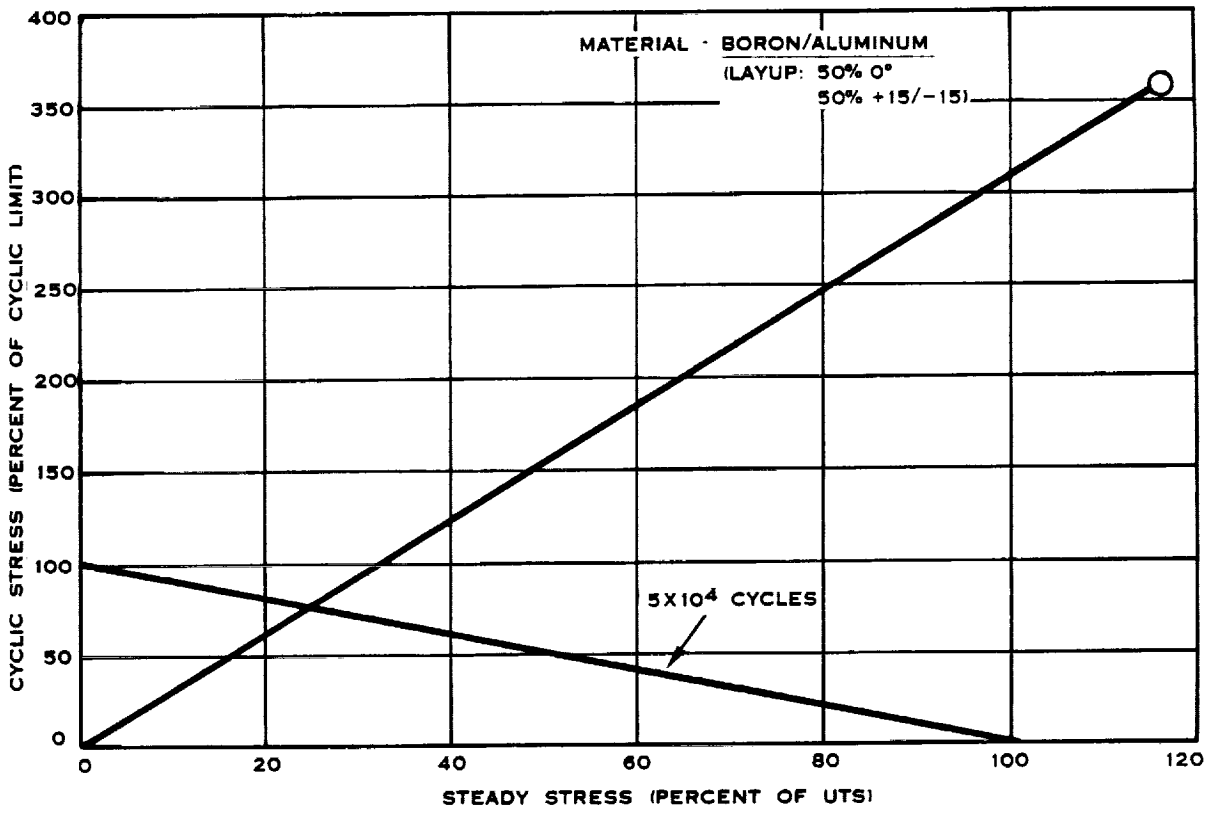

FIGURE 5.40. SR-3C (10) SPAR IN-PLANE SHEAR STRESS LOW CYCLE FATIGUE

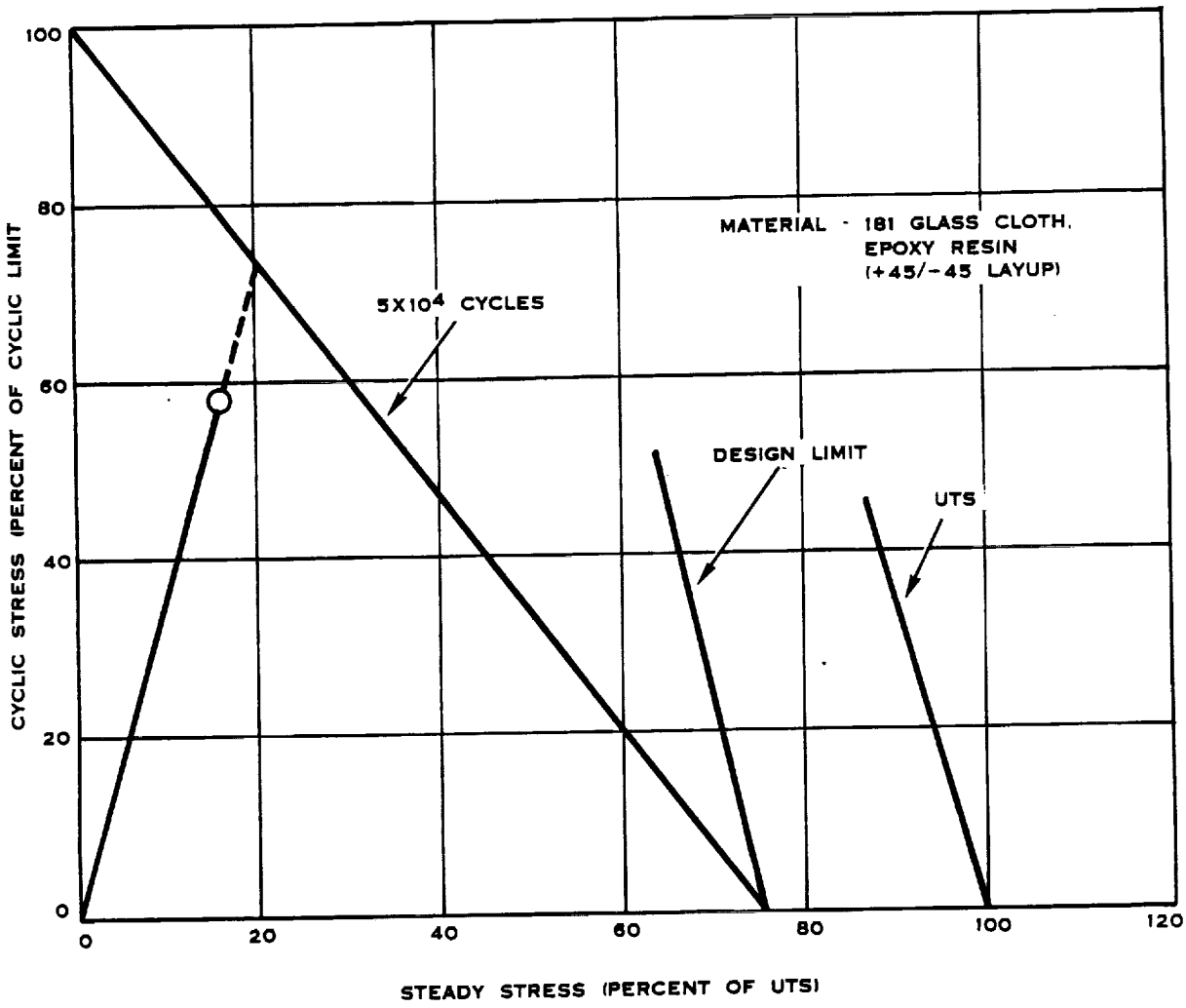

FIGURE 5.41. SR-3C (10) SHELL SPANWISE STRESS LOW CYCLE FATIGUE

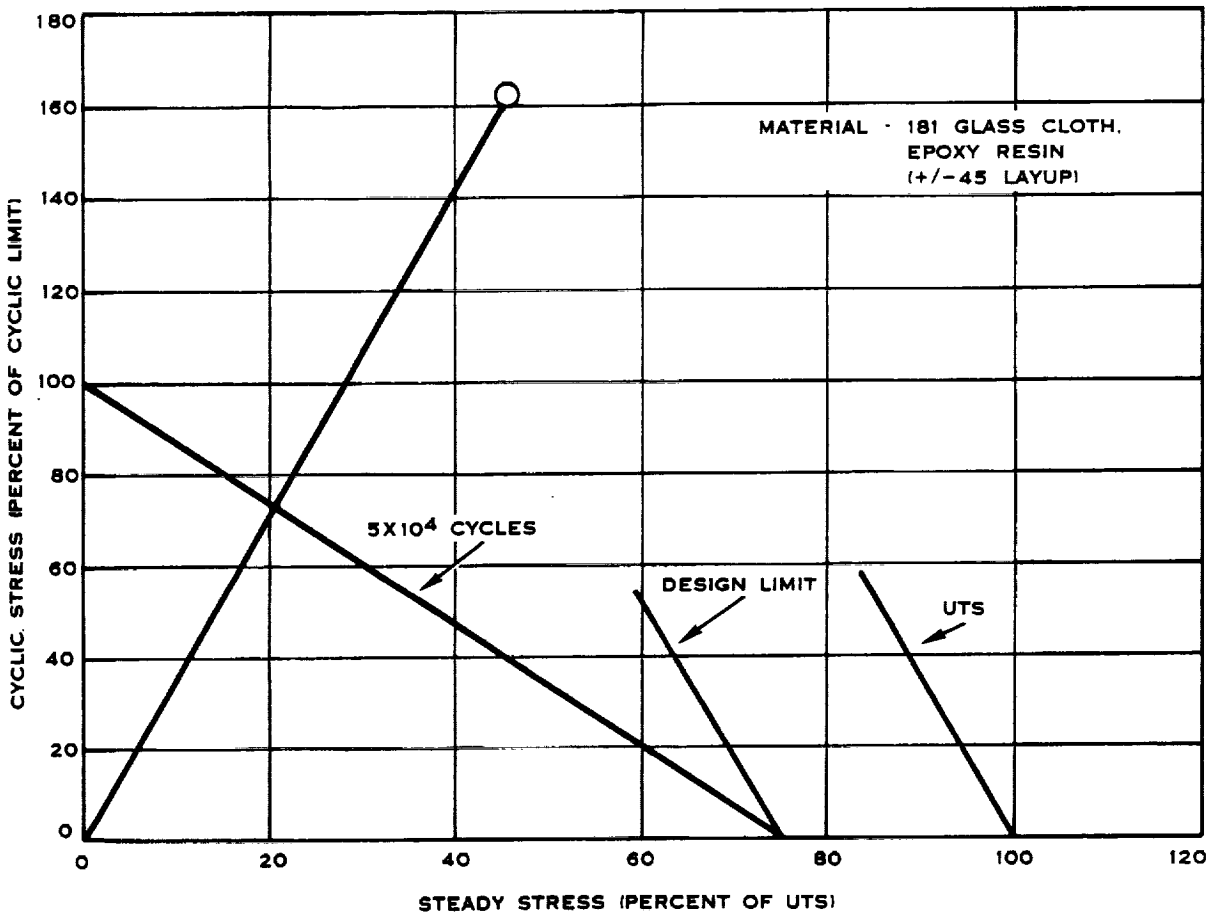

FIGURE 5.42. SR-5A SHELL SPANWISE STRESS LOW CYCLE FATIGUE

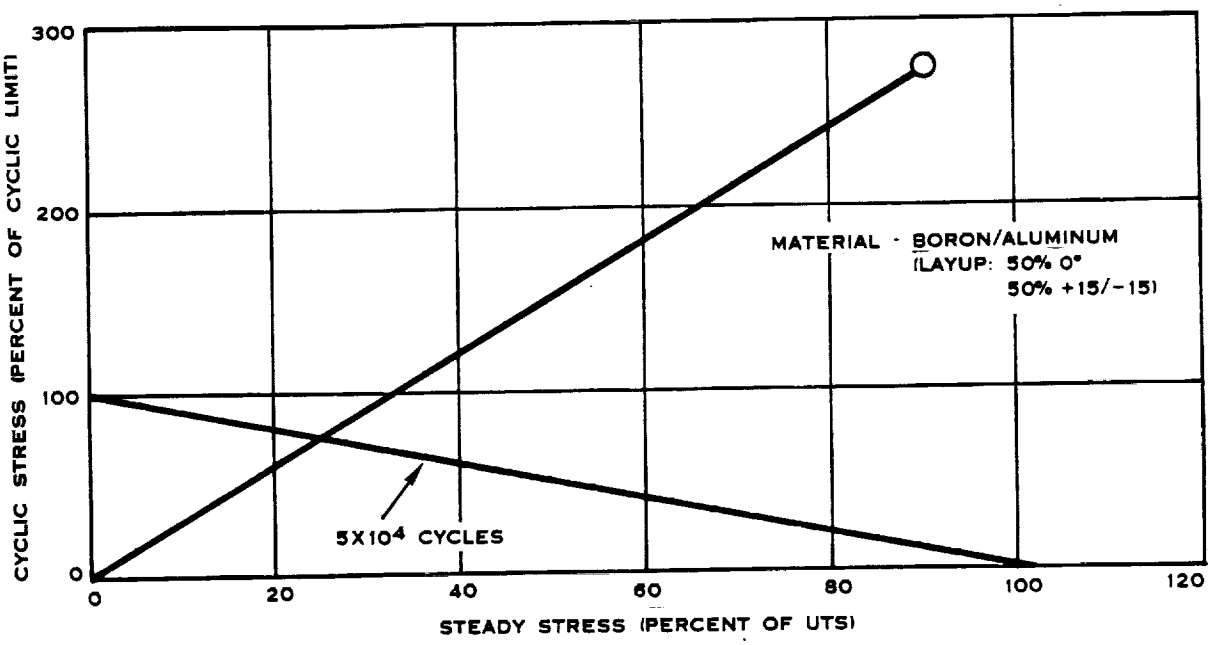

FIGURE 5.43. SR-5B SPAR REINFORCING PAD SPANWISE STRESS LOW CYCLE FATIGUE

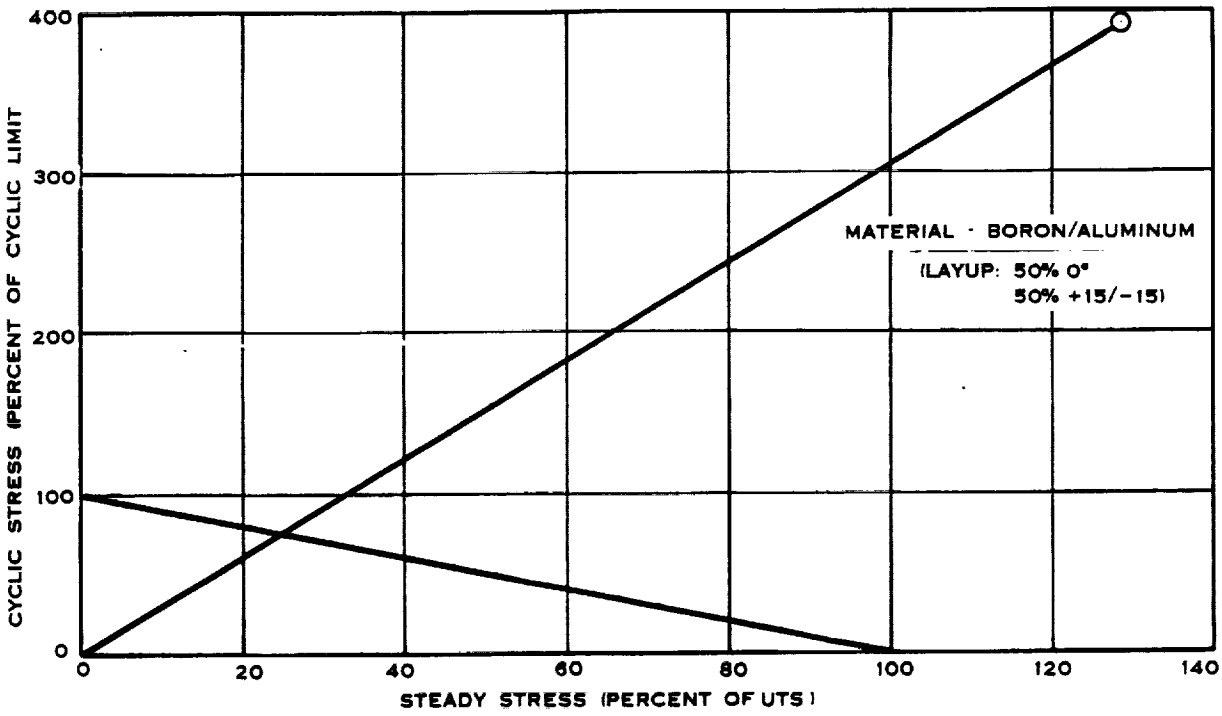

FIGURE 5.44. SR-5B SPAR REINFORCING PAD IN-PLANE SHEAR STRESS LOW CYCLE FATIGUE

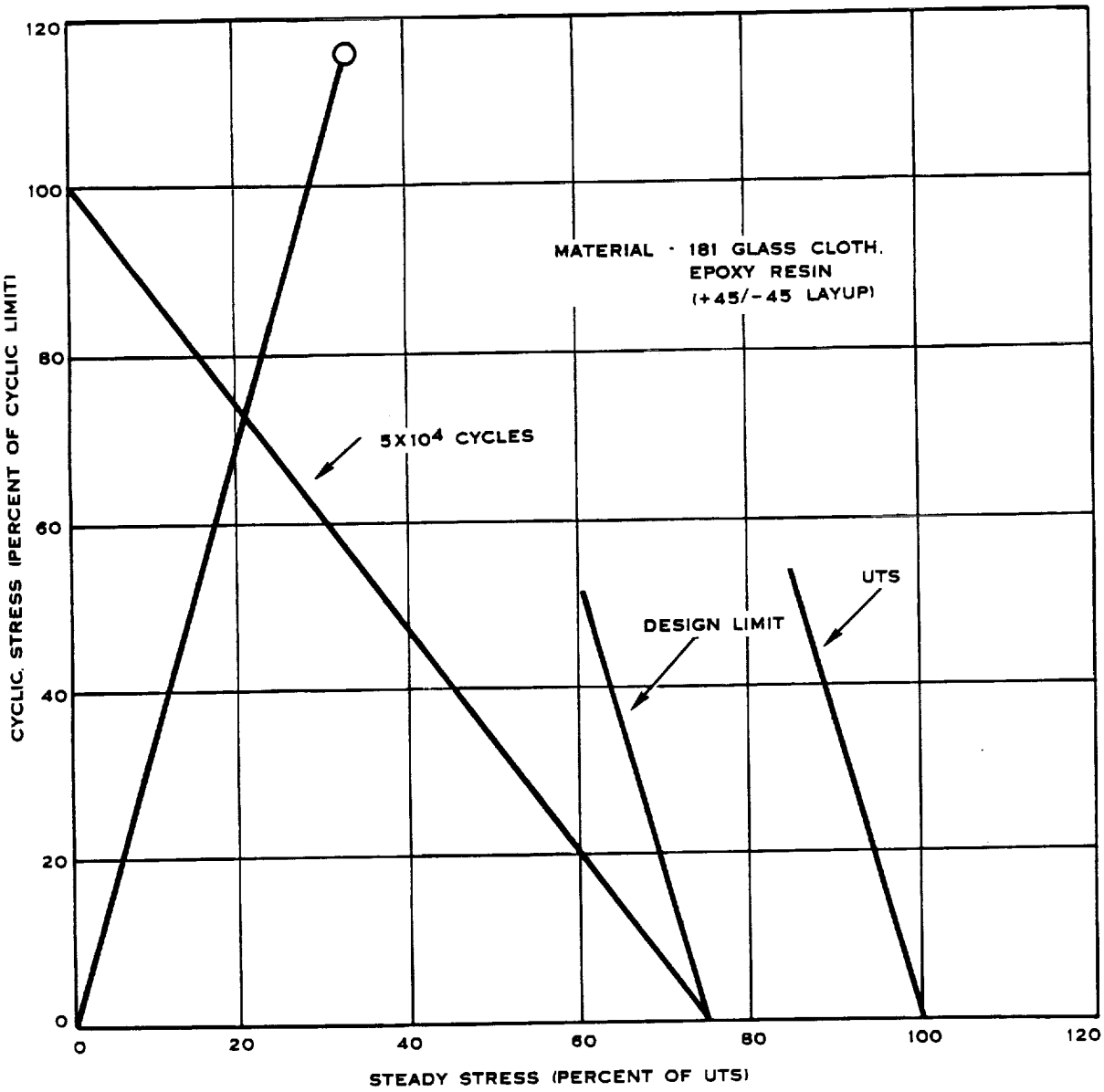

FIGURE 5-45. SR-5B SHELL SPANWISE STRESS LOW CYCLE FATIGUE

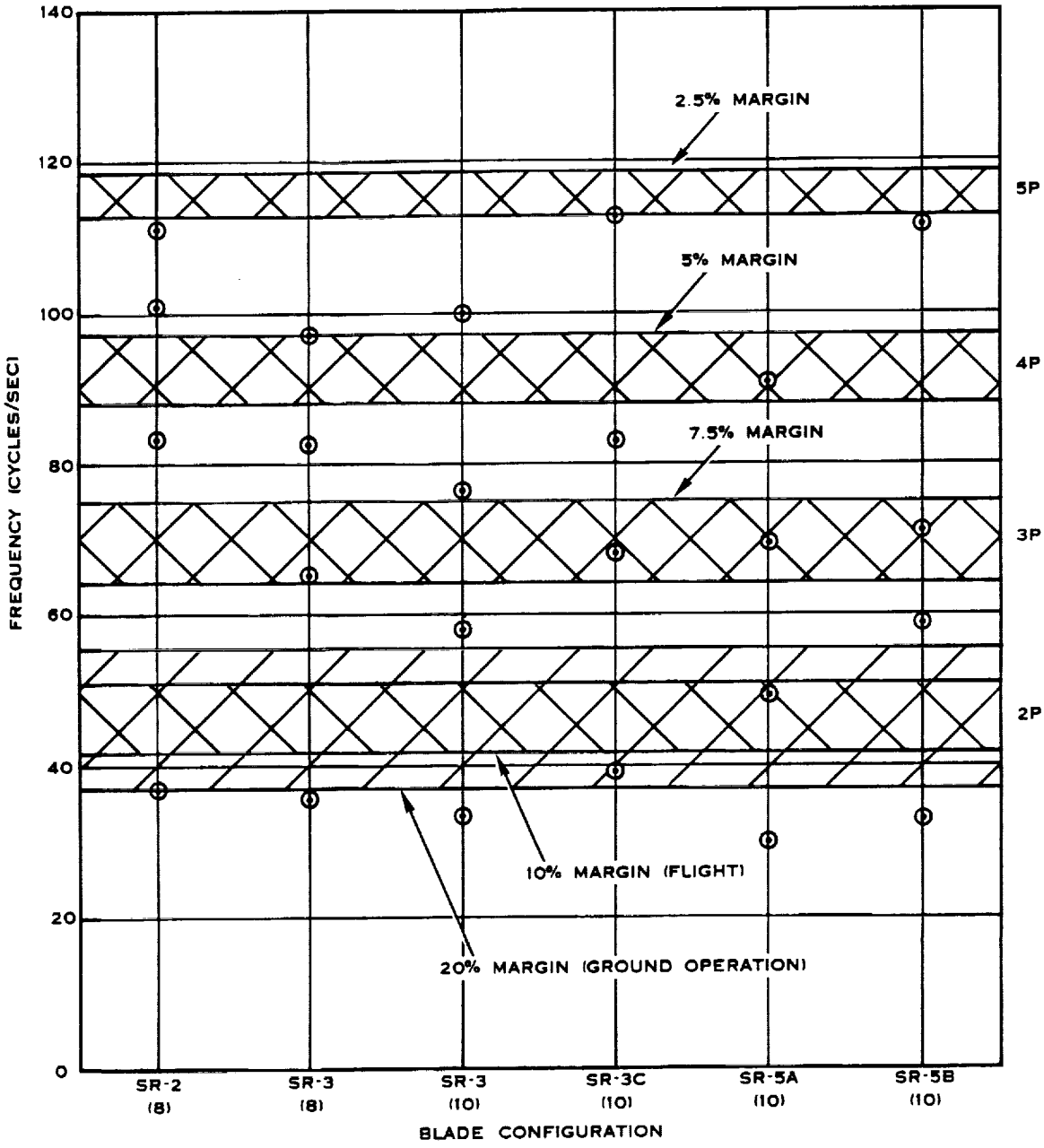

FIGURE 5.46 FREQUENCY SUMMARY, RESONANT FREQUENCIES VS RESONANCE AVOIDANCE ZONES

TABLE 5.9. FOREIGN OBJECT IMPACT SUMMARY

Blade Design	Spar Impact Capacity kg (lb) At Yield	At Failure
SR-2	1.2 (2.6)	2.5 (5.6)
SR-3 (8)	2.6 (5.8)	8.6 (19+)
SR-3 (10)	4.5 (10+)	9.1 (20+)
SR-3C (10)	N/A	.7 (1.5)(1)
SR-5A	N/A	N/A
SR-5B	N/A	1.2 (2.6)(2)

1. To fracture of spar

2. To fracture of reinforcing pads

N/A Not Analyzed

5.14 STABILITY RESULTS

Four of the blade concepts were analyzed for stall and classical flutter. The analysis used was the recently developed F203 rather than the analysis defined in the Design Requirements and Fabrication Concepts documents (Appendices A and B).

The analysis has a linear normal mode complex eigenvalue solution, which provides total damping at high subsonic Mach numbers on a single blade. The initial structural representation can be depicted by BESTRAN or NASTRAN finite element methods, where the response is described by modal deflections, modal frequencies and modal mass for each element. The modes are fully coupled and can be adjusted to account for steady displacements caused by the steady airloads defined by the blade aerodynamic load program, H444.

The flutter analysis, F203, requires that the structural description be transformed to a beam type coordinate system defined at the blade section where the modes are described in three dimensions. Since this is a linear analysis with the definition of the coordinate system as defined above, the inertial and centrifugal effects at large thrust and blade angles can be better approximated.

The transformation is accomplished in a preprocessor (F214) which uses the outupt from BESTRAN or NASTRAN and creates an input file for the flutter analysis.

The equations of motion are generalized in a normal modes approach and are fully coupled. The forcing functions which include quasi-steady and unsteady functions, the effective mass, damping and stiffness terms are generated using linear aerodynamics.

The quasi-steady terms are developed from the vibratory displacements and are provided in tables developed by Jordan, (see Reference 1), along with the unsteady terms. These tables have been modified by methods similar to those used by Cunningham, (see Reference 2), to account for sweep effects. The unsteady aerodynamics, including phase lag terms, are developed as a function of reduced frequency. Prandtl-Glauret corrections are applied to the lift and moment slopes to account for compressibility effects.

The solution is a linear complex eigenvalue one solved by the P-K method (see Reference 3). The aerodynamics are a function of frequency, and simultaneously have a strong effect on modifying the response frequency of the blade. Consequently, it is necessary to iterate the solution as it is modified by the aerodynamics. The results of the above methods produce the complex eigenvectors (or frequencies), and damping for all modes.

By applying Steinman's theory, (see Reference 4), a method of approximating the aerodynamic forces and phase lag in the stalled region was obtained. The resulting new terms are then substituted for some of the aoerdynamic terms in the present analysis, and the solution is carried out using the above mentioned methods. The Steinman aerodynamics uses the local lift and moment curve slopes. In the analysis, the local lift and moment curve slopes are computed using the Hamilton Standard strip analysis program H444, so that the real aerodynamic effects will be considered.

Additionally, an energy approach to the structural response was also developed as a solution to the Steinman aerodynamics. Options are available to allow use of one or all of the above mentioned methods.

For all the options, the output is in the form of damping and eigen frequencies which are plotted as functions of airspeed, RPM, blade angle and altitude. The flutter boundaries can be determined from the points where the damping goes through zero. It is at these points where the response becomes unstable.

If the flutter boundary occurs outside the flight envelope, classical flutter will not be present. If the value of horsepower, obtained at the point where the damping ratio goes to zero, is larger than the power available, then stall flutter will not occur.

Plots of stall flutter claculations and unstalled flutter boundary calculations can be found in Appendix C.

5.15 CONCEPT EVALUATION AND CONCLUSIONS

Each blade concept was evaluated against the design criteria specified in the Design Requirements Document and described in Section 5.5. Table 5.11 summarizes the evaluation of the individual blade concept's stress, frequency, stability, and foreign object impact results. None of the six blade concepts satisfies all of the criteria.

TABLE 5.10. STABILITY SUMMARY

	Stall Flutter	Classical Flutter
SR-2	I	S
SR-3 (8)	I	U
SR-3 (10)	I	U
SR-3C (10)	N/A	N/A
SR-5A	N/A	N/A
SR-5B	S	U

S = Satisfactory
U = Unsatisfactory
N/A = Not Analyzed
I = Inconclusive

It should be noted that only one internal geometry and material selection was analyzed for each blade concept. Various modifications can be made to the concept's structural designs in order to achieve the balance between stress levels, frequency placement and stability margin that is required for a satisfactory design. If the outer blade shapes remain constant as required in this study, the design modifications that are permitted are changing the blade materials and changing the spar width and chordwise location. If composite materials are used in the blade design, then the ply orientation also becomes a design variable.

The shell thickness cannot be varied significantly since the shell stiffness is necessary for basic airfoil integrity and for foreign object impact capability. Also, in a spar and shell blade design, the spar should remain the primary load-carrying component; hence the shell stiffness (i.e., thickness should remain low enough so that the shell only carries a minor portion of the gross blade load.

If the constraint that the outer blade geometry remain constant is removed, then many design modifications become available. Changing the thickness-to-chord ratio and chord-to-diameter ratio will have a significant impact on the

stress levels, frequency placement, and blade mode shapes. Modifying the blade stacking will change the mode shapes and blade stressing, but will have a negligible effect on frequency placement. The blade stability will be primarily influenced by the blade mode shapes.

During any iteration sequence to obtain a satisfactory balance between blade stressing, frequency placement, and stability margin, it must also be noted that the above modifications will affect the aerodynamic and acoustic performance of the blade design. These parameters would also need to be included in the iteration sequence to find a design that satisfies both the design requirements and the aerodynamic and acoustic performance levels.

Considering the possible variations in design variables discussed above and the results of the configurations analyzed, it was concluded that a feasible design could be achieved with a blade configuration similar to SR-3 (either 8 or 10 way) using conventional materials. Configurations with higher aspect ratios (higher activity factors) and higher sweep angles would be much more difficult to design and would probably require use of advanced composite materials.

TABLE 5-11. BLADE CONCEPT EVALUATION SUMMARY

	SR-2		SR-3 (8)		SR-3 (10)		SR-3C (10)		SR-5A			SR-5B		
Frequency Result	S		U		S		U		U			U		
Foreign Object Impact	S		S		S		U		N/A			U		
Stability	I		U		U		N/A		N/A			U		
Stress Results:	Spar	Shell	Spar	Shell	Spar	Shell	Spar		Shell	Spar	Shell	Spar	Reinf Pad	Shell
Blade Component Stress Type	Span	Span	Span	Span	Span	Span	Span	Shear	Span	Span	Span	Span	Span Shear	Span
HCF	S	S	S	S	S	S	U	U	S	U	U	S	U U	U
LCF	S	-	-	U	-	-	U	U	S	-	U	-	U U	U
25% Overspeed	S	S	S	S	S	S	U	U	S	S	U	S	U U	U
40% Overspeed	S	S	S	S	S	S	U	U	S	U	U	S	U U	U

N/A = Not Analyzed
S = Satisfactory
U = Unsatisfactory
I = Inconclusive

6.0 TASK IV - DYNAMIC MODEL FEASIBILITY ANALYSIS

6.1 INTRODUCTION

Previous Prop-Fan model blades (SR-1 thru SR-6) were designed to obtain aerodynamic and acoustic performance data. To do this, they were of solid metal construction to minimize blade deflection. For the next model it is also desired to simulate the aeroelastic properties of the full-size blade.

6.2 OBJECT

The object of this task is to evaluate the feasibility of designing and constructing a dynamic model of the full-size blade configurations studied during the structural design analysis task (reference Section 5.0).

6.3 APPROACH

The evaluation includes the determination of what scaling factors are important, as well as the minimum practical fabrication size for the model. For this task, three configurations were considered. They were:

SR-2 8 way

SR-3 10 way

SR-5 10 way

6.4 SCALING PARAMETERS

There are seven basic parameters generally considered in evaluating scale model tests of rotating lifting surfaces (see Reference 5-7). These are:

Mach Number
Advance Ratio
Reynolds Number
Locke Number
Cauchy Number
Reduced Frequency
Froude Number
Aerodynamic Damping

The following discussions of these parameters are based on the assumption that geometry is scaled proportionally, i.e., the ratio of chord to blade radius and blade built-in-twist remain the same.

In order to achieve proper aerodynamic similarity, the local blade section velocities should be identical to those of the full-scale design. This can be achieved by simultaneously maintaining the full-scale tip-speed (ΩR) and the full-scale advance ratio ($V/\Omega R$) constant. Keeping the tip-speed

constant requires that the rotational speed for the model be inversely proportional to the radius between configurations. Since the tip speed is assumed constant with size, maintaining constant advance ratio requires that the forward speed also remain constant.

Because the flow at forward speed involves local blade section velocities in the transonic range, it is important that the Reynolds Number be the same between the model and full-scale. The Reynolds Number is important to high speed flows because of compressible and boundary layer effects. Flows with different Reynolds Numbers can have shocks located on the blade sections at different positions, different types of flows in the boundary layer, and different attachment points.

Constant Reynolds Numbers cannot easily be maintained at the same time Mach Number and density ratios are kept constant. Reynolds Number is defined as $\rho Vc/\mu$ indicating proportionality to length for constant velocity. Table 6.1 shows the scaling relations for keeping Mach Number constant or for keeping Reynolds Number constant.

Freon 12 has been used as a wind tunnel fluid in fixed wing technology because of its density and Mach Number characteristics. Freon 12 is four times heavier than air. This type of testing is not practical for Prop-Fans because available freon tunnels have no propeller test rig and the state-of-the-art is not that good. This is because the effects of the differences in viscosity are unknown (see Reference 8).

It is generally thought that accepting the differences due to Reynolds Number is the best path to follow.

The Reynolds Number for the 11-ft. diameter Prop-Fan has been calculated to be $Re = 8.55 \times 10^6$ and for the 2-ft. model $Re = 1.57 \times 10^6$, generally not considered too far apart. The test results can be modified, however, by using the results of analytical computations that include the effects of Reynolds Number. This requires the use of aerodynamic section data at different Reynolds Numbers in the calculations.

The ratio of air forces to inertial forces is called Locke Number and is defined as $(\rho C_e a R^4 \Omega^2)/(I_1 \Omega^2)$.

This must remain constant for scaling similarity. It is seen that for a given advance ratio $V/\Omega R$, the air forces are proportional to $\rho\Omega^2R^4$ and the inertial forces are proportional to $\sigma\Omega^2R^4$. The Locke Number simply breaks down to density ratio equals a constant (ρ/σ = constant).

This indicates that the wind tunnel air density should be the same as that in full-scale flight, for a structurally scaled model.

TABLE 6.1. SCALING PARAMETER RATIOS FOR CONSTANT FULL SCALE MACH NO'S AND REYNOLDS NO.

		EXACT	GENERAL	FULL SCALE MACH NO.	FULL SCALE REYNOLDS NO.
REYNOLDS NO.	RE	$\lambda\nu\lambda\ell\lambda\rho/\lambda\mu$	$\lambda\nu\ell\lambda$	$\lambda\ell$	1
MACH NO.	M	$\lambda\nu/\lambda a$	$\lambda\nu$	1	$1/\lambda\ell$
FROUDE NO.	F	$\lambda^2\nu/\lambda g\lambda\ell$	$\lambda\nu^2/\lambda\ell$	$1/\lambda\ell$	$1/\lambda\ell^3$
REDUCED FREQUENCY		$\frac{\lambda\ell\ \lambda w}{\lambda\nu}$	1	1	$1/\lambda\ell$
LINEAR VELOCITY	ν	$\lambda\nu$	$\lambda\nu$	1	$1/\lambda\ell$
ANGULAR VELOCITY	Ω	$\lambda\nu/\lambda\ell$	$\lambda\nu/\lambda\ell$	$1/\lambda\ell$	$1/\lambda\ell^2$
AERO DENSITY	ρ				
STRUCTURE DENSITY	σ	$\lambda\sigma$	1	1	1
STRUCTURE MODULUS	E	$\lambda\rho\lambda\nu^2$	$\lambda\nu^2$	1	$1/\lambda\ell^2$
AERO FORCE	A	$\lambda\rho\lambda\nu^2\lambda\ell^2$	$\lambda\nu^2\lambda\ell^2$	$\lambda\ell^2$	1
ELASTIC FORCE	B	$\lambda_E\lambda\ell^2$			
INERTIAL (RADIAL) AND OSCILLATORY)	C	$\lambda\sigma\lambda\Omega^2\lambda\ell^4$			
GRAVITATIONAL	W	$\lambda\sigma\ell^3$	$\lambda\ell^3$	$\lambda\ell^3$	$\lambda\ell^3$
RESP AMPLITUDE	a	$\lambda_A/\lambda_E\lambda\ell$	$\lambda\ell$	$\lambda\ell$	$\lambda\ell$
FREQUENCY	w	$(\lambda_E/\lambda\sigma)^{1/2}/\lambda\ell$	$\lambda\Omega$	$1/\lambda\ell$	$1/\lambda\ell^2$
ACCELERATION	$\ddot{a}$	$\lambda w^2\lambda\ell$	$\lambda\Omega^2\lambda\ell$	$1/\lambda\ell$	$1/\lambda\ell^3$
DYNAMIC STRESS	ρ	λ_E	$\lambda\nu^2$	1	$1/\lambda\ell^2$
DYNAMIC STRAIN	δ	1	1	1	1
	ϵ	$\lambda w/\lambda_\epsilon$	$\lambda\ell/\lambda\nu^2$	$\lambda\ell$	$\lambda^{3\ell}$

*NOTE: λ IS DEFINED AS THE RATIO OF THE MODEL VARIABLE TO THE RATIO OF THE FULL SCALE VARIABLE.

Similarity in structural stiffness is often evaluated through the use of the Cauchy Number defined as $EIxx/(\rho V^2 R^4)$. This number represents the ratio of flatwise elastic force to the aerodynamic inertial force. Since inertia (I) is proportional to R^4 the Cauchy Number is proportional to $E/\rho V^2$.

For constant density and velocity, the effective Young's modulus must be constant between configurations. For proper coupling between the modes, it is necessary to properly scale the edgewise stiffness and torsional stiffness distributions. Therefore, the ratio of edgewise and torsional stiffness distribution to flatwise stiffness distributions remains the same, i.e., EOyy/EIxx and GJ/EIxxx = constant.

The stiffness parameters can also be simulated by matching the P-order frequencies to the full scale. This assumes that the mode shapes and inertial distributions are the same. If the P-order frequency is constant, then the frequency is kept inversely proportional to size.

Flutter boundaries are generally a function of reduced frequency $b\omega/V$.

If the velocity (V) is constant, the semi-chord (b) is proportional to radius and since ω is inversely proportional to radius, then the reduced frequency must be constant between configurations.

Gravitational forces are usually represented by the Froude Number which is defined as the ratio of centripital force to gravitational acceleration $R\Omega^2/g$. It is felt that the ratio of inertial forces and airloads are much greater than the gravitational force such that the effect of gravity is negligible.

Lastly, the effect of damping. Aerodynamic damping is a very important factor in dynamic response considerations, since it is a primary item in classical type flutter. Except for the effects of Reynolds Number discrepancies, this damping is a function of the airloads which vary as the radius squared (see Table 6.1). The unit loading per square inch is constant for constant Mach Number scaling, or constant reduced frequency.

Structural damping ratio should remain the same if identical scale and identical materials are used. If a different structure is used for the model, then the effect of structural damping should be investigated in a flutter analysis and a calculated increment due to damping should be added to the test results.

6.5 FABRICATION CONSIDERATIONS

All of the above discussion on similarity is predicated on the assumption that the scaled model has similar mode shapes, P-order frequencies, and inertial distributions. This can only occur if the model structure is identical to the full-scale structure in composition as well as geometry. Practically, however, there are manufacturing limitations for the model that are not present for the full-scale configuration. The model blade composition or internal geometry is probably going to be different.

The stiffness and mass distributions must be adjusted to provide similar P-order frequencies using the new construction. This may be accomplished by keeping the inertial mass, and stiffness radial integrations the same as those for the identical scale model.

The mode shapes will probably be quite different, but the gross effects of modal coupling will be similar enough to provide a moderate degree of confidence in the test results. This confidence can be aided by good judgment in determining the stiffness and mass distributions for the test model. One way to do this is to try to match the inboard stiffnesses to those of the identical scale model, while also trying to match the outboard mass to that of the model. Inboard is defined as less than 50% of the blade span while outboard is more than 50% of the blade span. This is important to the primary modes in torsion, edgewise bending, and flatwise bending because of the way that the inertial energy is transferred to the structure displacements during each oscillation for these modes.

Investigating any modes higher than the first four modes is probably not a good idea because the frequencies are very high, there is probably a lot of chordwise bending and very little is known about these modes. For purposes of scaling, the effects of chordwise bending will be ignored. Recent Prop-Fan flutter investigations at Hamilton Standard have shown good results using only the first four modes in an analysis with no chordwise bending (see Reference 9).

If there are differences in any of the parameters or distributions, then the model description can be run on the computer flutter analyses and increments and factors can then be applied to the wind tunnel test results.

6.6 EVALUATION

As previously indicated, the approach to scaling the aeroelastic properties of the configurations is to evaluate the full-scale configuration and then investigate a scaled version of the full-scale blade which is called the exact scale model. Then a configuration with a different type of construction, the properties of which match the exact scale model as closely as possible is evaluated. This configuration is called the aeroelastic model. This was done for the SR-2 8-way, SR-3 10-way, and the SR-5 10-way blades.

Since this work is only a feasibility study, it was decided to investigate the required configurations using the Hamilton Standard section properties program and the uncoupled blade bending and twisting frequency response programs for a first cut at scaling the designs. These programs are respectively called H349, H025, and H027.

The section properties analysis, H349, is a convenient means for changing the construction of a blade and then computing new blade properties. Changing the blade construction involves certain restrictions at the model scale. These restrictions involve such things as the minimum thickness that the spar can be machined to (~.040 inches), the minimum thickness of a fiberglass layer (~.009 inches), and the minimum glue thickness (~.008 inches). These restrictions control the size and shape of the spar and the size and shape of the fiberglass layers on the shell.

The properties from H349 are input to the H025 and H027 blade frequency and response analyses. The blade properties are integrated and the frequencies and mode shapes are computed. It is thought that if the mode shapes, blade frequencies, mass distributions, stiffness distributions, and inertial distributions for the aeroelastic model are close to those of the exact scale model, then the aeroelastic model is representative of the full-scale model. Also, since the structure is confined to the same scaled geometric envelope as the full-scale blade, the sweep effects due to scaling will be minimal. This is based on the assumption that there is little chordwise bending.

By matching the properties and blade frequencies to that of the exact scale model, it is no longer necessary to calculate the scaling parameters because the scaling is implied in the exact scale calculation.

One of the primary purposes of this investigation was to determine the smallest size Prop-Fan model that is practical and feasible, while maintaining those aeroelastic qualities necessary to quantitatively determine blade response over the operating conditions. This will minimize the power required to drive the model as well as minimize the size of the required tunnel.

The three configurations were investigated at full-scale (11-ft. diameter), the 2-foot diameter exact scale model blade, and the 2-foot diameter aeroelastic model blade. These runs are indicated in Table 6.2 for the H349 computations.

Figure 6.1 is a schematic of the SR-3 10-way blade for the exact scale model showing the spar going the whole length of the blade. For this model, the spar takes up the major portion of the load, since the shell is very thin and the spar runs the whole length of the blade.

The aeroelastic version of this model is shown in Figure 6.2. The shell for this configuration is much thicker near mid-span than the exact scale model but the spar is thinner and shorter. This design uses the minimum restrictions on spar and shell thickness as previously outlined. Unlike the exact scale model, the load is transferred to the shell through a gradual thickening of the shell from the spar root to the spar tip. For both models, the cavities are filled with foam.

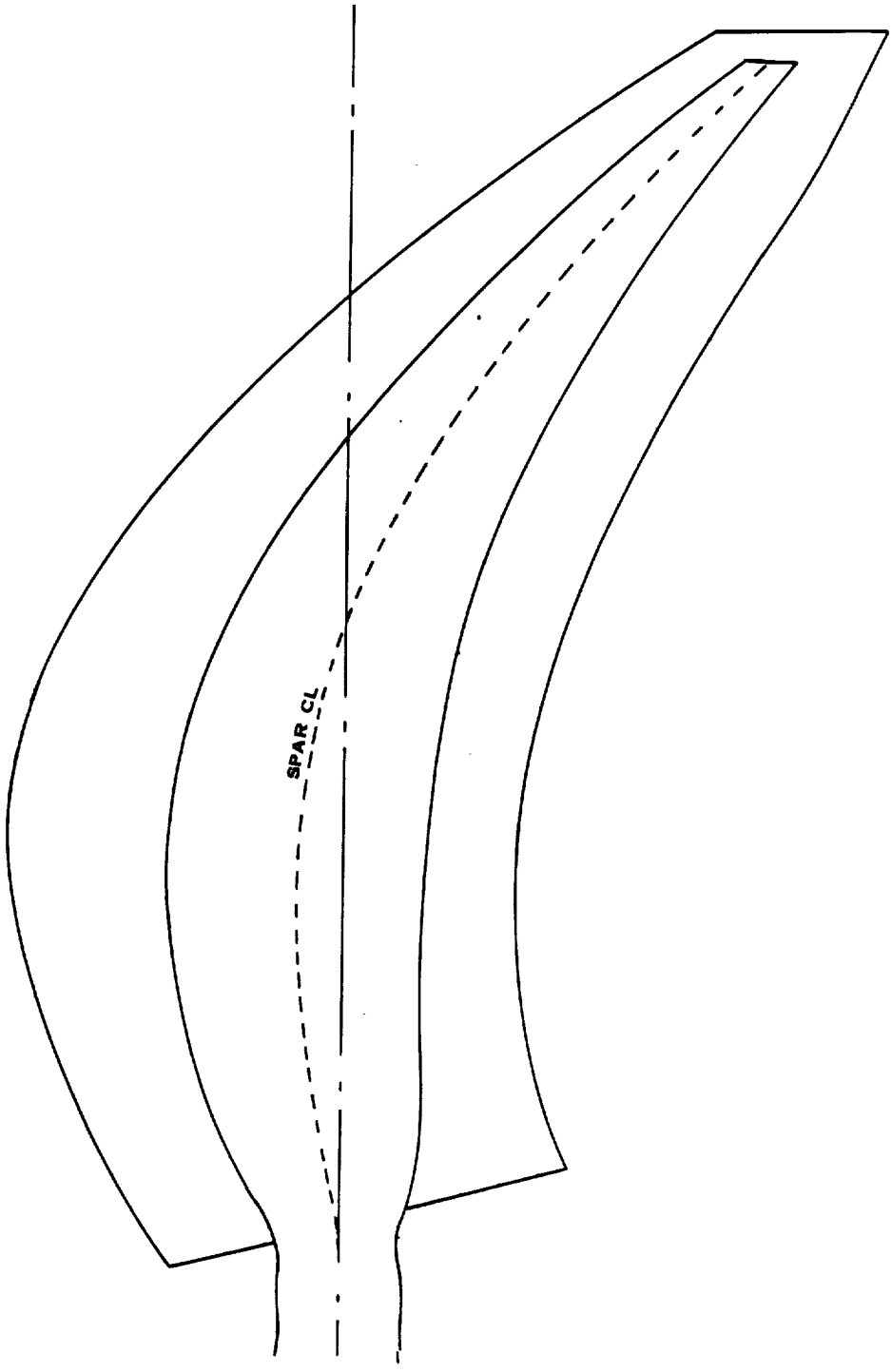

FIGURE 6.1. SR-3 10-WAY 2 FT. EXACTLY SCALED MODEL, FIBERGALSS SHELL, ALUMINUM SPAR

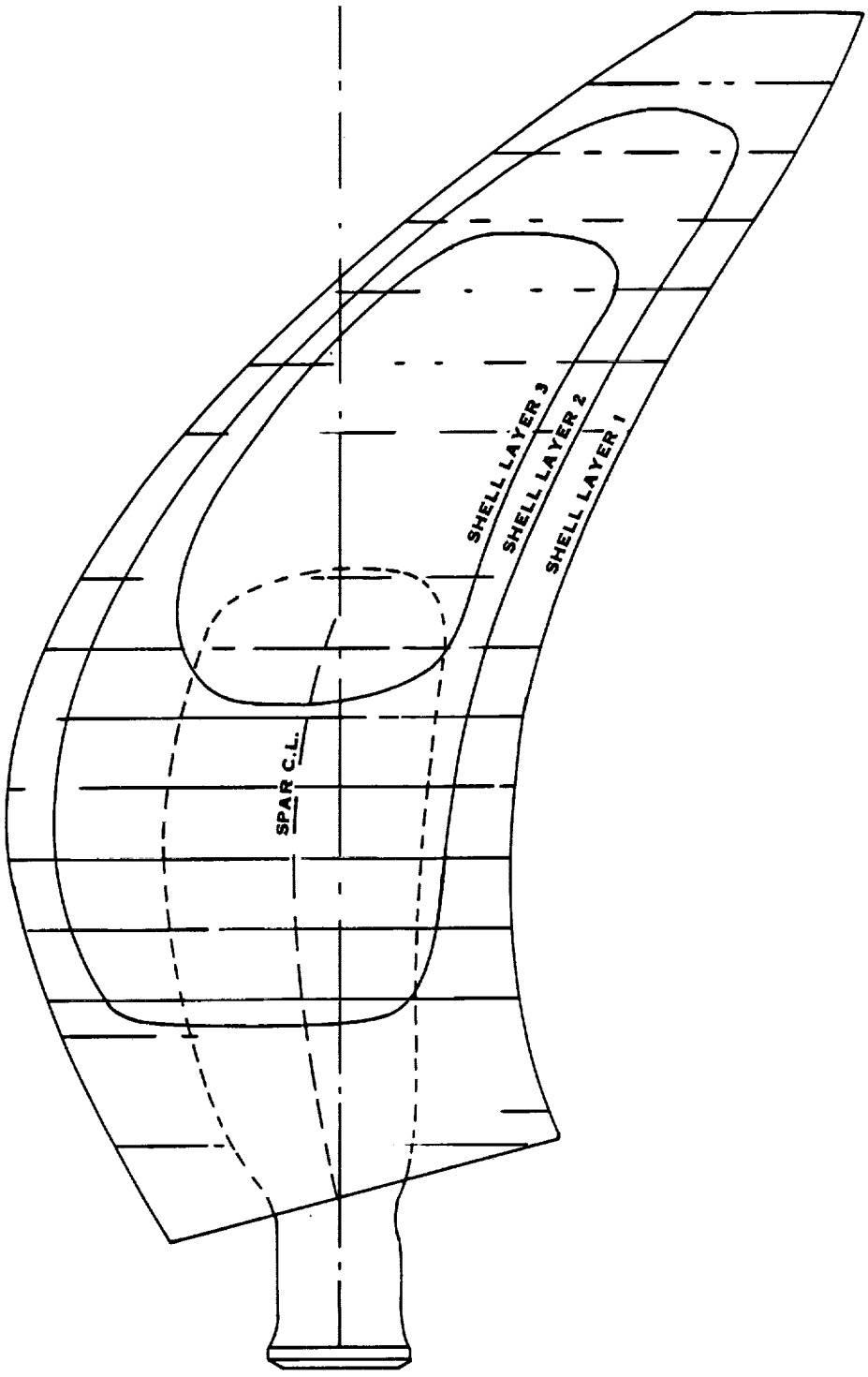

FIGURE 6.2. SR-3 10-WAY 2 FT. AEROELASTIC MODEL, FIBERGLASS SHELL, ALUMINUM SPAR

Schematic diagrams of the SR-2 8-way and the SR-5 10-way will not be shown here because of their similarity to the SR-3 10-way. The primary differences are the shape of the platforms. The SR-2 8-way exact scale model has a hollow spar whereas the SR-2 aeroelastic model has a solid spar.

6.7 RESULTS

The results of running the H349 section properties program are shown in Table 6.2 where blade RPM, centrifugal force, blade weight, polar moment of inertia and radial C.G. location are listed for the model configuration.

The physical section property distributions for the SR-2 8-way models are plotted in Figures 6.3 through 6.7 for both the exact scale configurations and the aeroelastically scaled models. In these figures running mass, equivalent polar area inertia, torsional stiffness, flatwise stiffness, and edgewise stiffness are plotted as a function of propeller radius. The equivalent polar area inertia is representative of the twisting mass inertia when multiplied by the equivalent density.

Theoretically, if all these distributions were identical to the exactly scaled model, then the model can be considered aeroelastically similar to the full-scale configuration. As seen in Figures 6.3 through 6.7, some of the parameters for the SR-2 8-way aeroelastic model do not match those of the exact scale model. More specifically, the mass distribution and the polar area inertia have large discrepancies. However, these discrepancies are mostly inboard where as previously discussed, the effect of stiffness is most important and mass plays a lesser role in the dynamics. One reason for these discrepancies is that the spar on the full-scale SR-2 configuration and hence, the exactly scaled SR-2 model is hollow. The spar on the aeroelastic model is solid.

The stiffness distributions for this model, shown in Figures 6.5 through 6.7, are reasonably close to those of the exact configuration. This is true on the inboard portions because the stiffness is controlled mostly by the outer portions of the spar cross-section. Thus there is little difference between the hollow spar and the solid spar as far as stiffness goes. The outer portions of the exact scale spar are almost solid, so there is less difference between a solid spar and hollow spar.

The conclusion that can be reached is that making the spar solid on the aeroelastic model causes a larger discrepancy in the mass distributions than those of the stiffness distributions.

The P-order Campbell diagrams resulting from computer runs using the H025 and H027 beam analysis for this blade is shown in Figures 6.8 and 6.9. These are the exact scale model and aeroelastic model. It is seen that except for the first flatwise mode, there are substantial discrepancies between the exact scale model and the aeroelastic model. It is seen that except for the first flatwise mode, there are substantial discrepancies between the exact scale model and the aeroelastic model. The second flatwise, first torsion, and

TABLE 6.2. RESULTS OF H349, H025, AND H027 COMPUTER RUNS FOR THE PROP-FAN BLADES

	SR2			SR3			SR5		
CASE NUMBER	1A	1B	1C	2A	2B	2C	3A	3B	3C
RPM	1389	7640	7640	1389	7590	7590	1389	7640	7640
WEIGHT (POUNDS)	25	0.26884	0.479	46.3	0.281	0.264	47.26	0.287	0.268
CF (POUNDS)	61521	2006	3260	68984	2309	2100	78418	2616	2359
POLAR (LB FT^2)	269.8	0.05175	0.0693	299	0.060	0.0529	365	0.0737	0.064
CF TW NOM (IN LB)	7411	39	67	10993	66	75	15558	95	101
RAD C.G. (IN)	25.2	4.5	4.1	27.5	5.0	4.9	30.27	5.5	5.3
STATIC FREQUENCY (CPS)									
1F	20.3	117	90	22.3	125	118	19.7	106	96
2F	65.8	375	275	57.1	315	312	60.4	321	299
1E	121.8	694	591	119.4	657	631	100	571	617
1T	102.53	673	585	100.6	652	618	92.3	504	494
REDUCED FREQUENCY (TORSION)*	0.52	0.621	0.540	0.540	0.586	0.554	0.512	0.511	0.500

*BASED ON V= 982 FT/SEC AND 0.75R CHORD

A = FULL SCALE
B = 2 FT EXACT SCALE
C = 2 FT AEROELASTIC

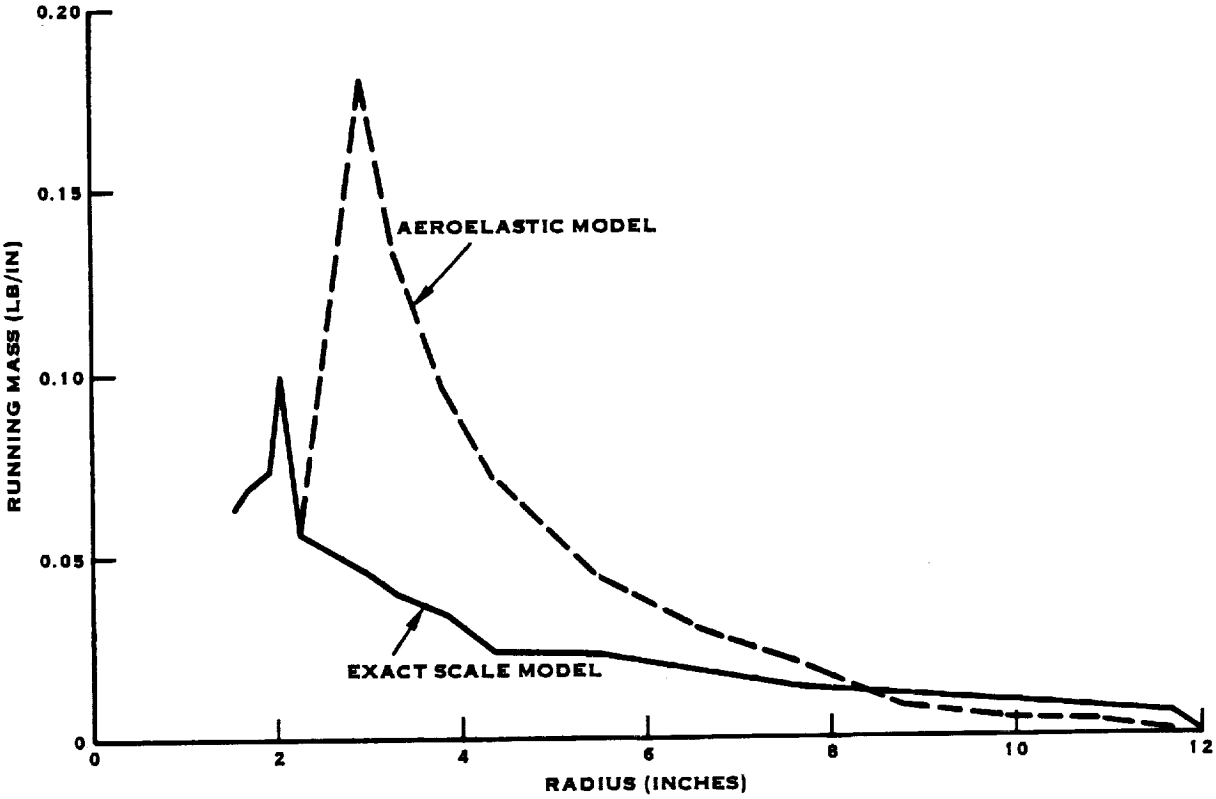

FIGURE 6.3. SR-2 8 WAY 2 FOOT DIAMETER MASS DISTRIBUTION CONPARISON

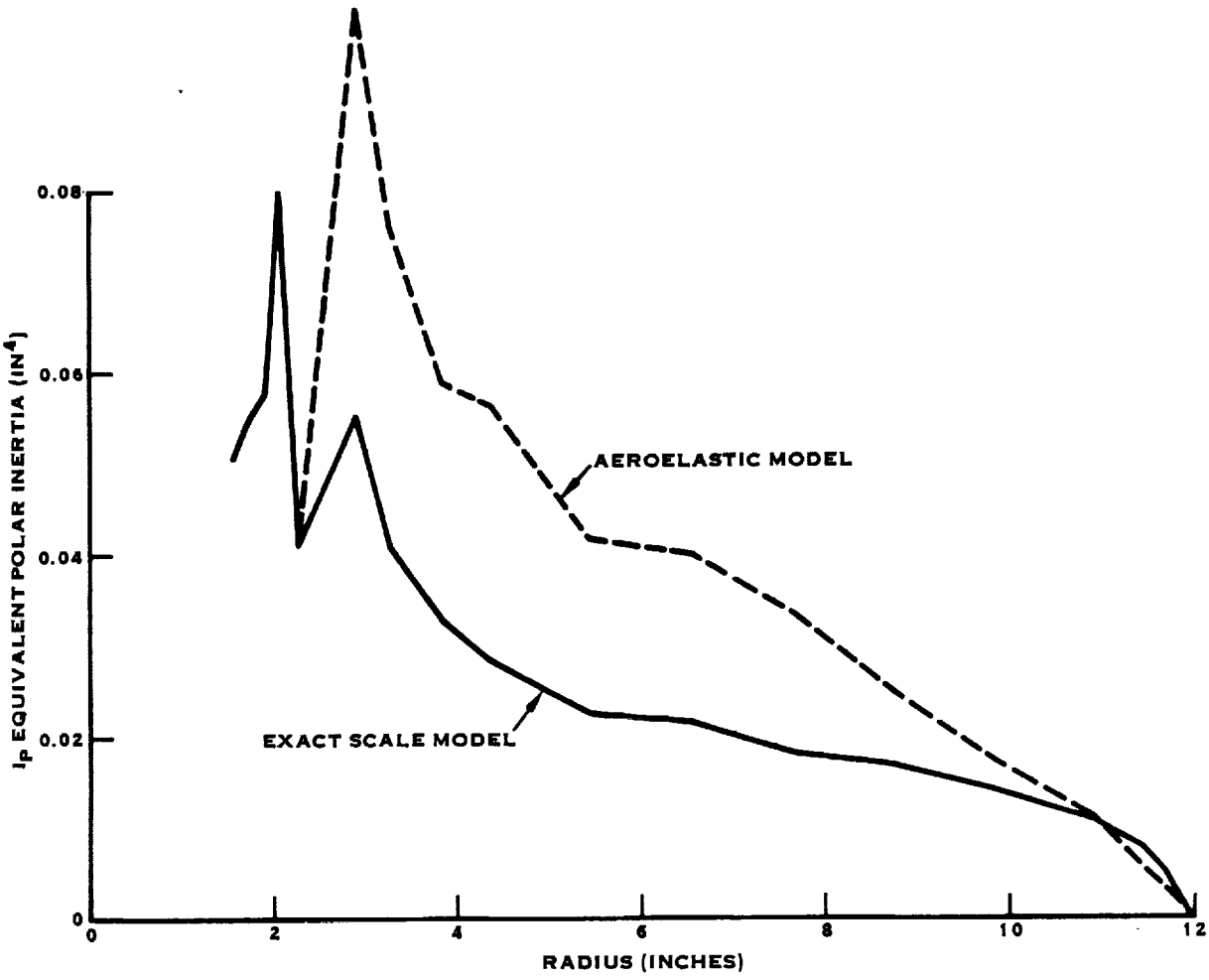

FIGURE 6.4. SR-2 8 WAY 2 FOOT DIAMETER EQUIVALENT POLAR INERTIA DISTRIBUTION COMPARISON

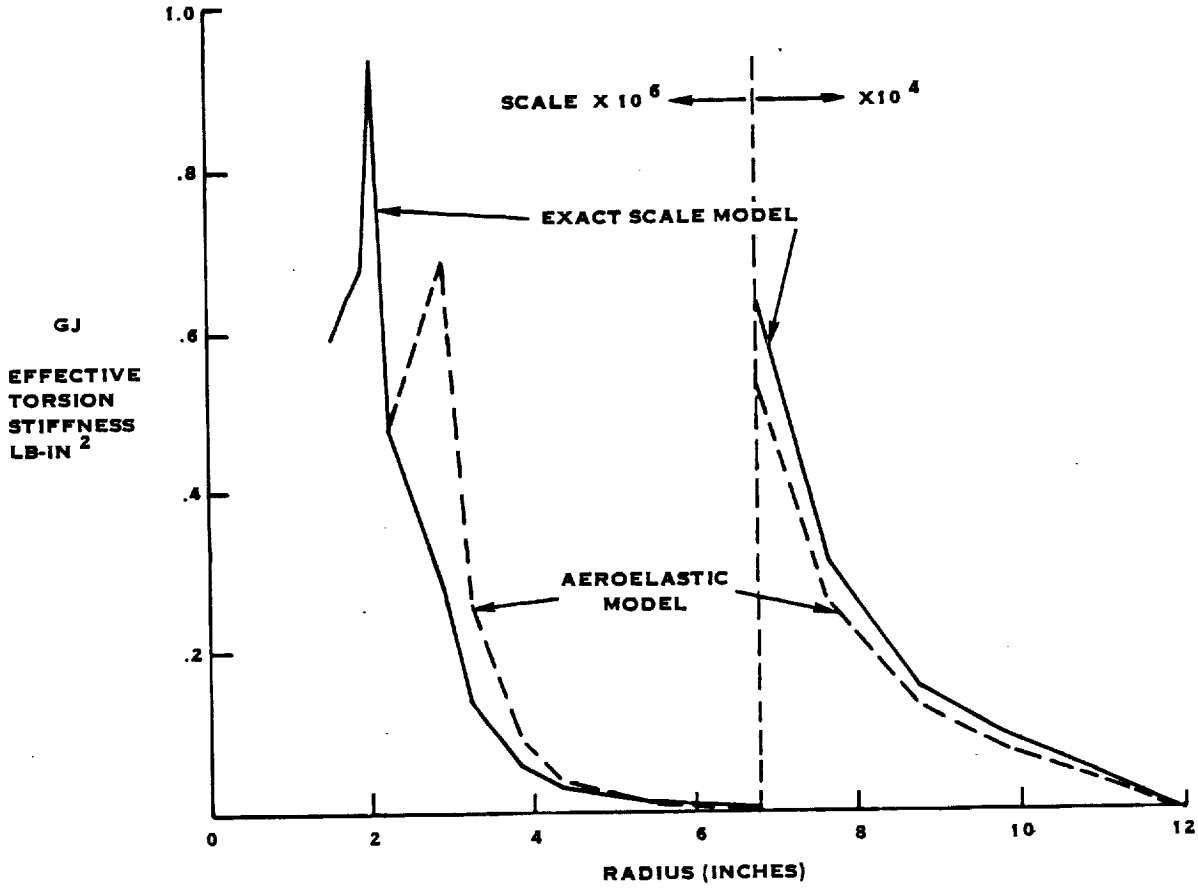

FIGURE 6.5. SR-2 8 WAY 2 FOOT DIAMETER TORSIONAL STIFFNESS COMPARISON

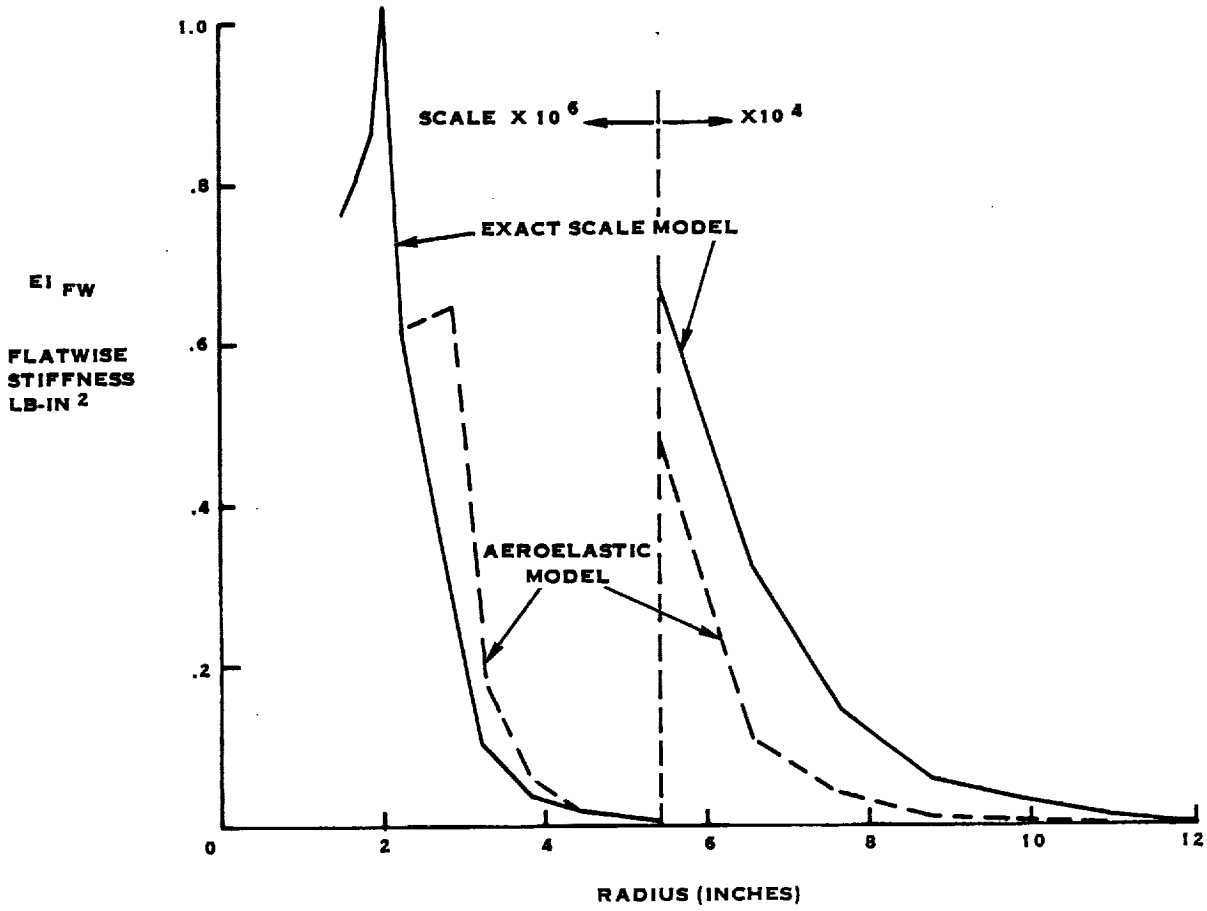

FIGURE 6.6. SR-2 8 WAY 2 FOOT DIAMETER FLATWISE STIFFNESS DISTRIBUTION COMPARISON

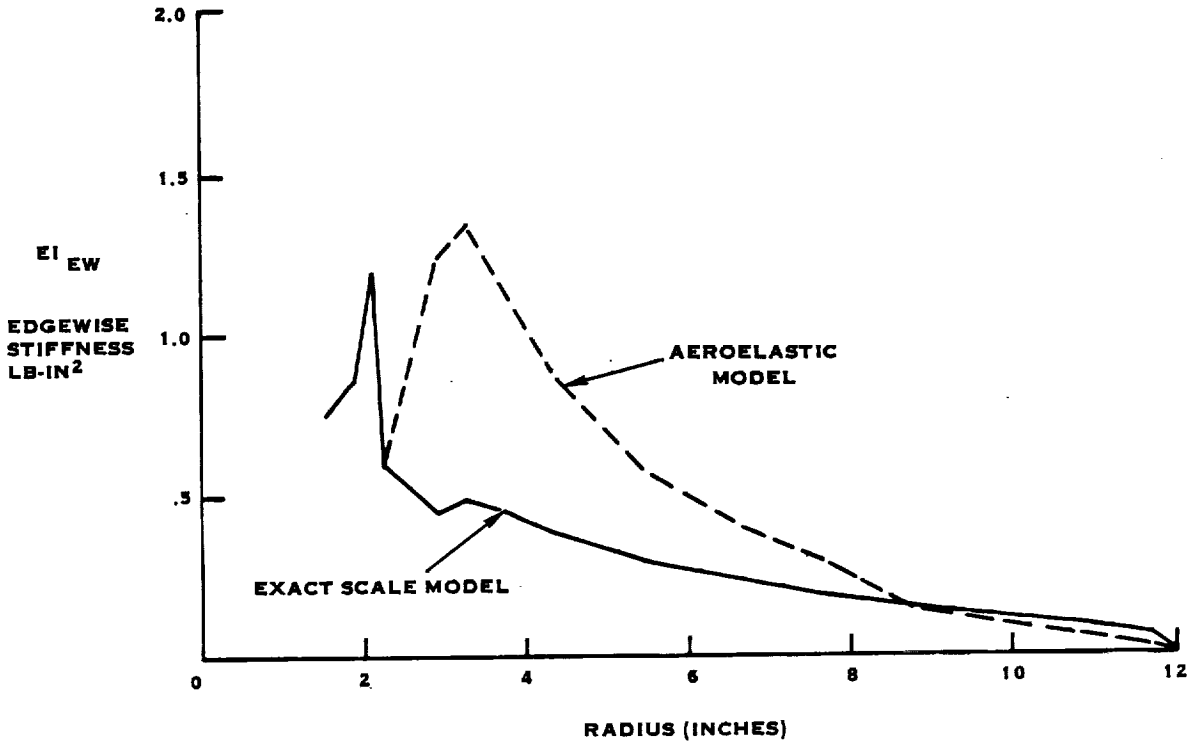

FIGURE 6.7. SR-2 8 WAY 2 FOOT DIAMETER EDGEWISE STIFFNESS DISTRIBUTION COMPARISON

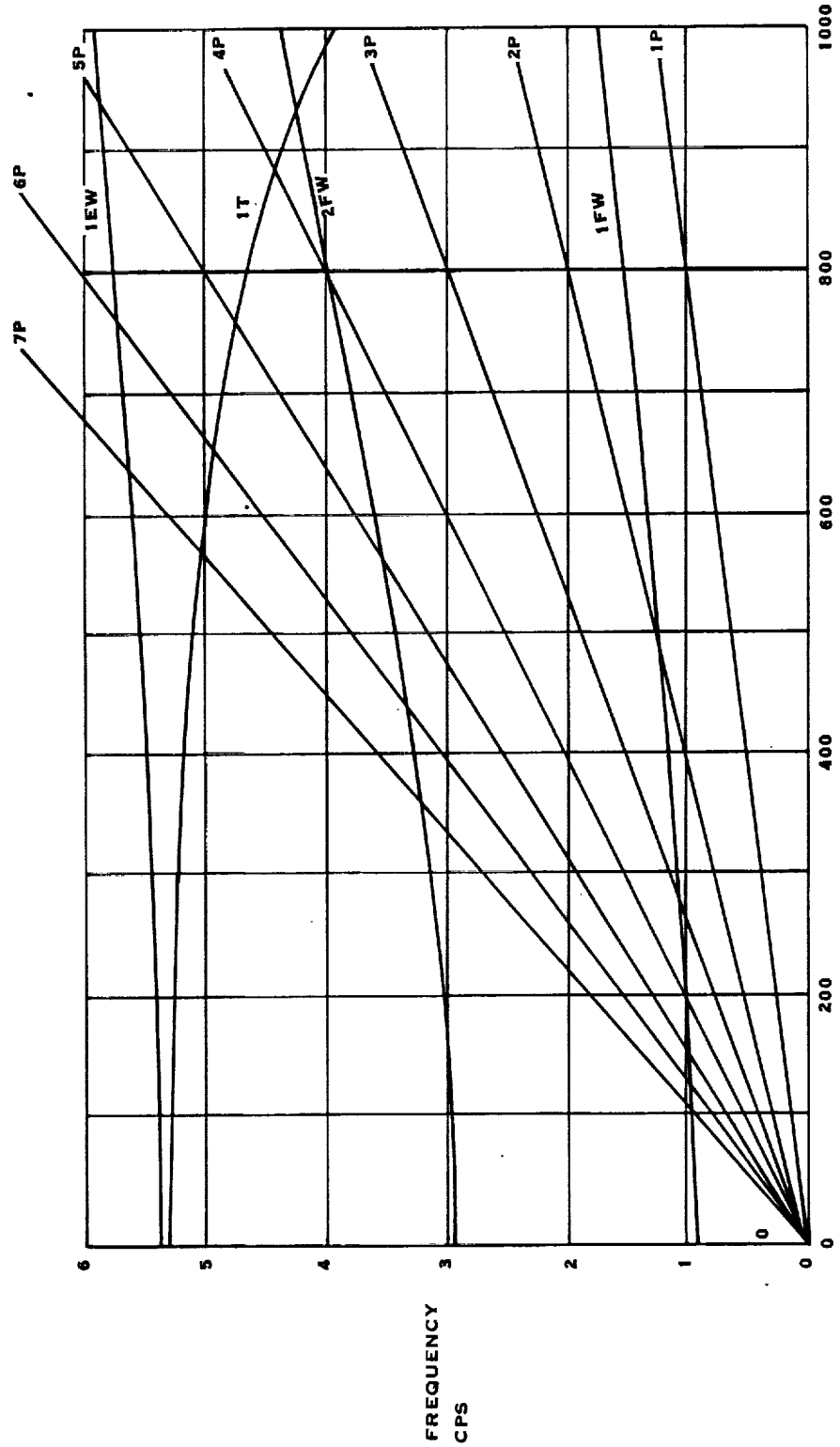

FIGURE 6.8. SR-2 8 WAY 2 FOOT DIAMETER EXACT SCALE CAMPBELL DIAGRAM

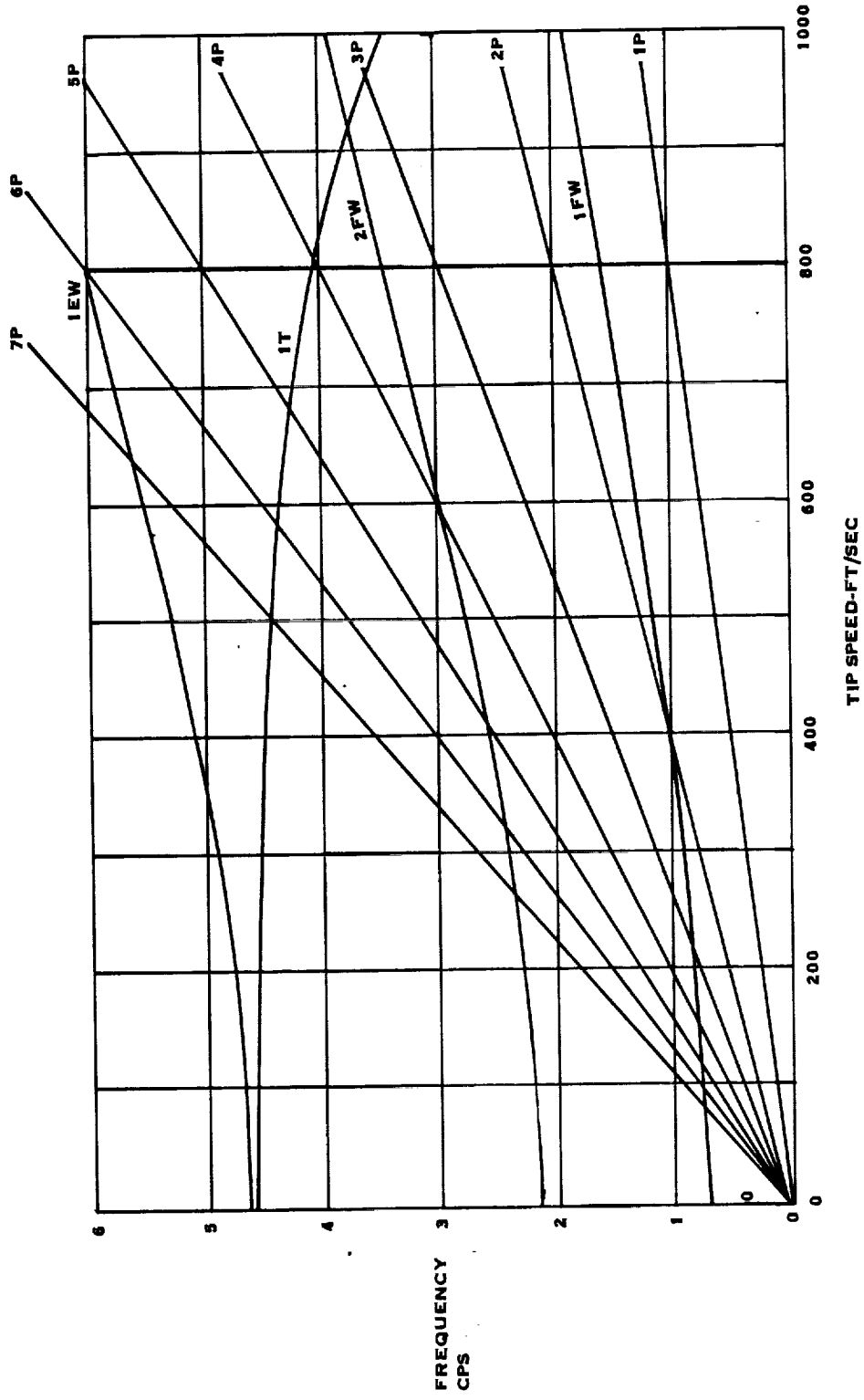

FIGURE 6.9. SR-2 9 WAY 2 FOOT DIAMETER AEROELASTIC SCALE CAMPBELL DIAGRAM

first edgewise discrepancies are primarily due to mass discrepancies. It should be noted that the first edgewise shows a greater effect due to rotational speed. This is probably due to the fact that most of the edgewise bending takes place primarily in the shank region such that the mid-span mass discrepancies have a large effect on the frequencies.

The results of the H349 section property computer runs for the SR-3 10-way configuration are shown in Figures 6.10 through 6.14. Here, mass, polar area inertia, torsional stiffness, flatwise stiffness, and edgewise stiffness are plotted as a function of radius for both the exactly scaled model and the aeroelastic model. Very good comparisons are shown for mass, torsional stiffness, and flatwise stiffness. The polar inertia and edgewise stiffness comparisons are good but could be improved with further structural adjustments on the aeroelastic model. The polar inertia is greater on the aeroelastic model because of the heavier shell bringing more mass to the outer portions of the blade in the chordwise direction. The discrepancy in the edgewise stiffness is in the region where the loads make a transition from the shorter spar to the shell.

The resulting Campbell diagrams are shown in Figures 6.15 and 6.16. The first flatwise and second flatwise modes have very good correlation. First torsion is 3% lower and the first edgewise is about 7% lower than the exactly scaled model at the design speed. The edgewise frequency could probably be improved by beefing up the retention.

Figure 6.17 shows the normalized mode shapes plotted as a function of radius. Comparisons are made between the exactly scaled model and the aeroelastic model for torsion and the first two flatwise modes. The correlation is surprisingly good. Some discrepancy in torsion is due to the increased mass of the aeroelastic model shell.

Figures 6.18 through 6.22 show the SR-5 10-way configuration property distributions plotted as a function of radius. The mass, polar area inertia, torsional stiffness, flatwise stiffness, and edgewise stiffness are plotted for the exactly scaled model and the aeroelastic model. These distributions show good comparisons between the two models and modifications to the aeroelastic model structure could improve the comparison.

This is also true of the frequency response as shown by the Campbell diagrams, Figures 6.23, 6.24 and 6.25. Here blade response or P-order frequency is based on the design rotational speed and is plotted as a function of tip speed. Figure 6.23 is for the full-scale design, Figure 6.24 is for the exactly scaled model, and Figure 6.25 is for the aeroelastic model.

The full-scale configuration was run to check the methods since theory indicates that the exactly scaled model should have an identical curve. This is true for all modes except the edgewise mode which is slightly higher for the model. This frequency may be improved by a modification to the retention.

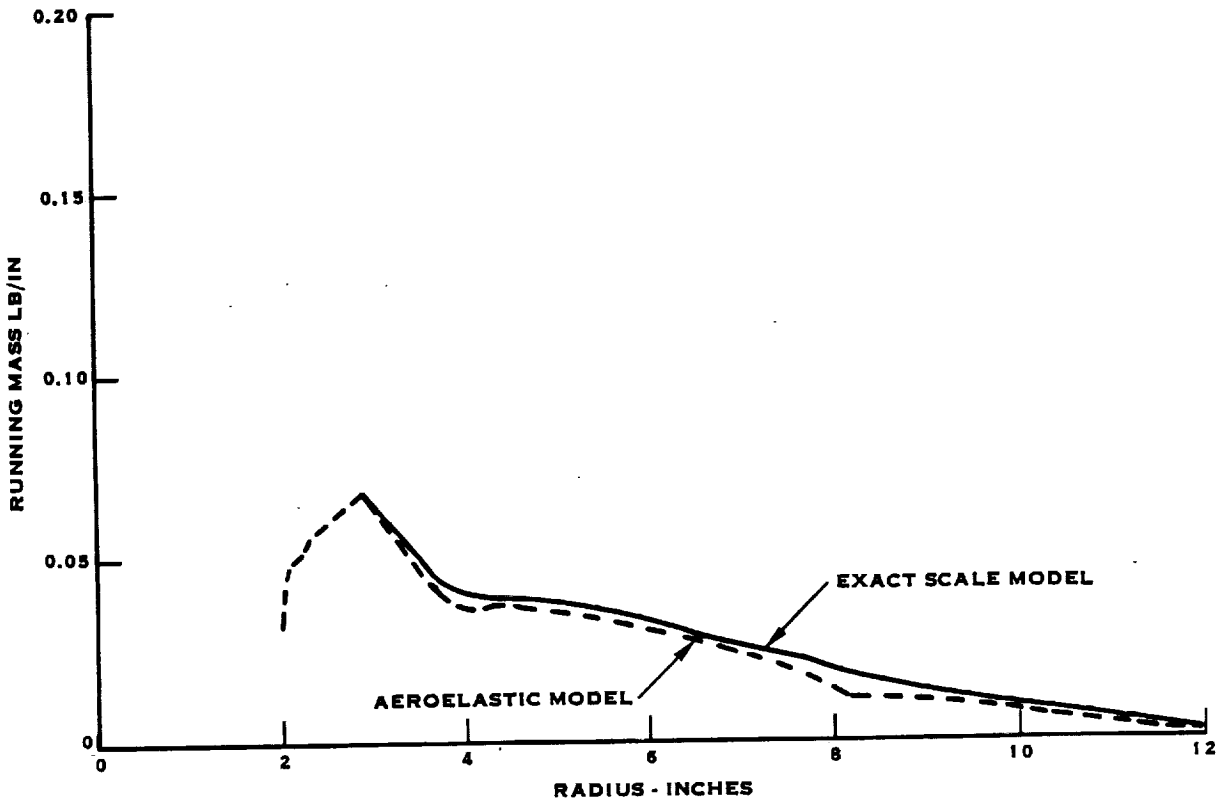

FIGURE 6.10. SR-3 10 WAY 2 FOOT DIAMETER MASS DISTRIBUTION COMPARISON

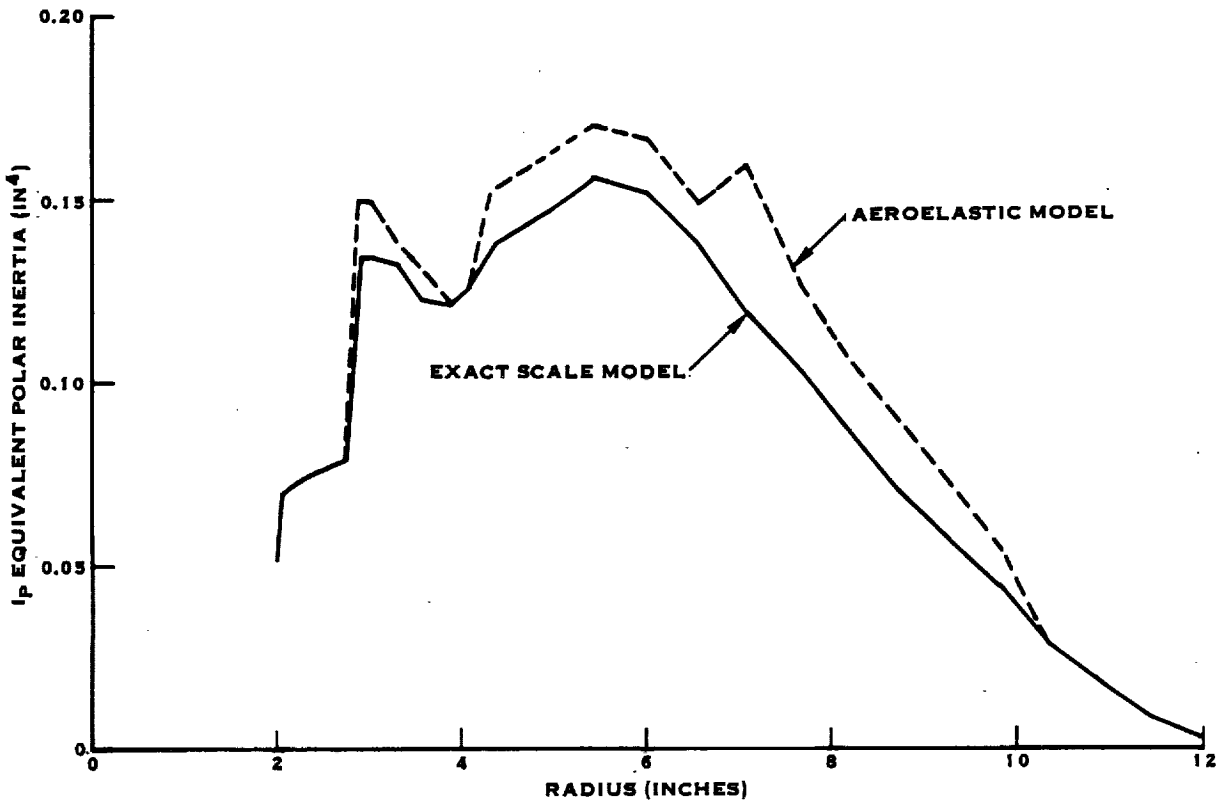

FIGURE 6.11. SR-3 10 WAY 2 FOOT DIAMETER EQUIVALENT POLAR INERTIA COMPARISON

C-2

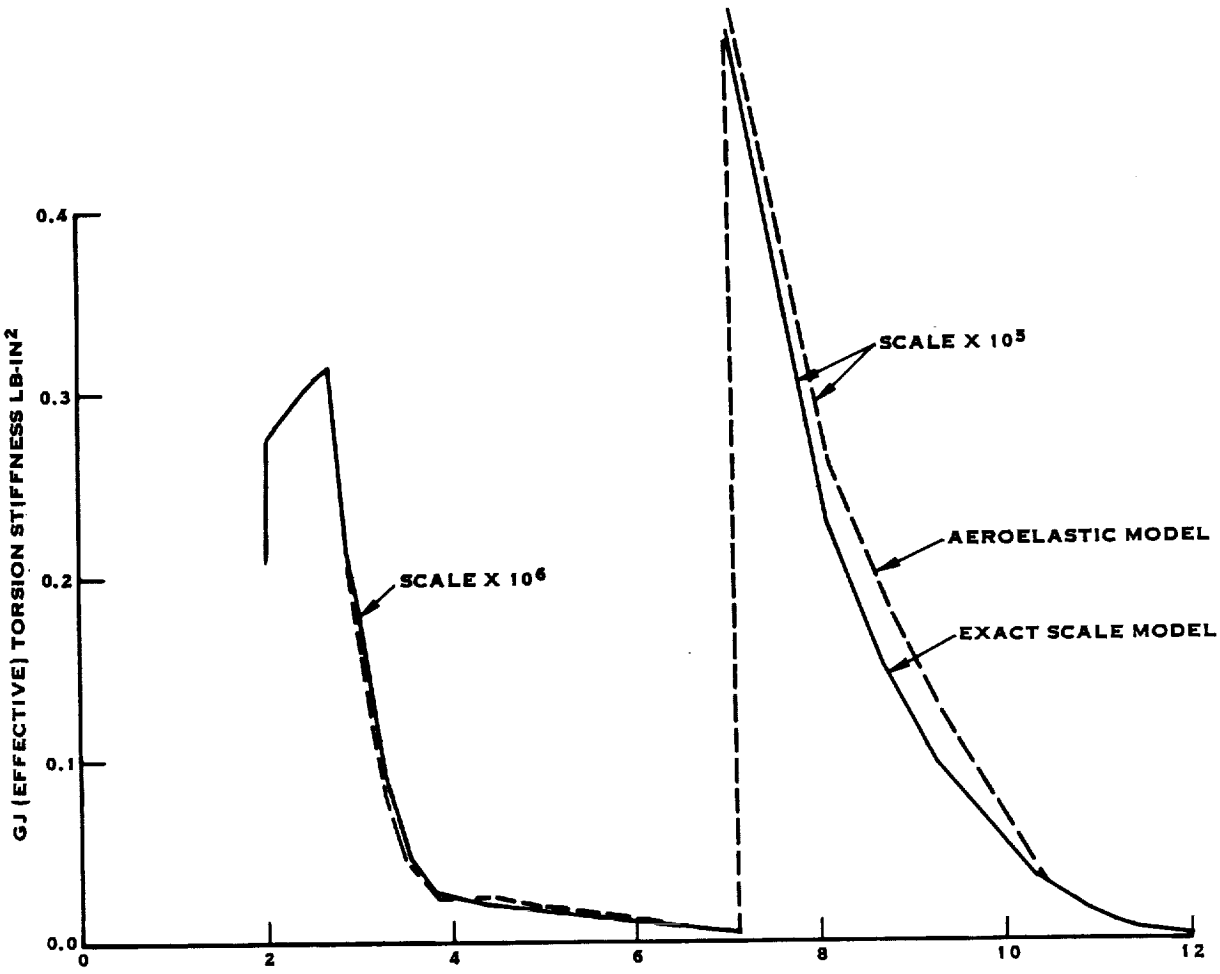

FIGURE 6.12. SR-3 10 WAY 2 FOOT DIAMETER TORSIONAL STIFFNESS COMPARISON

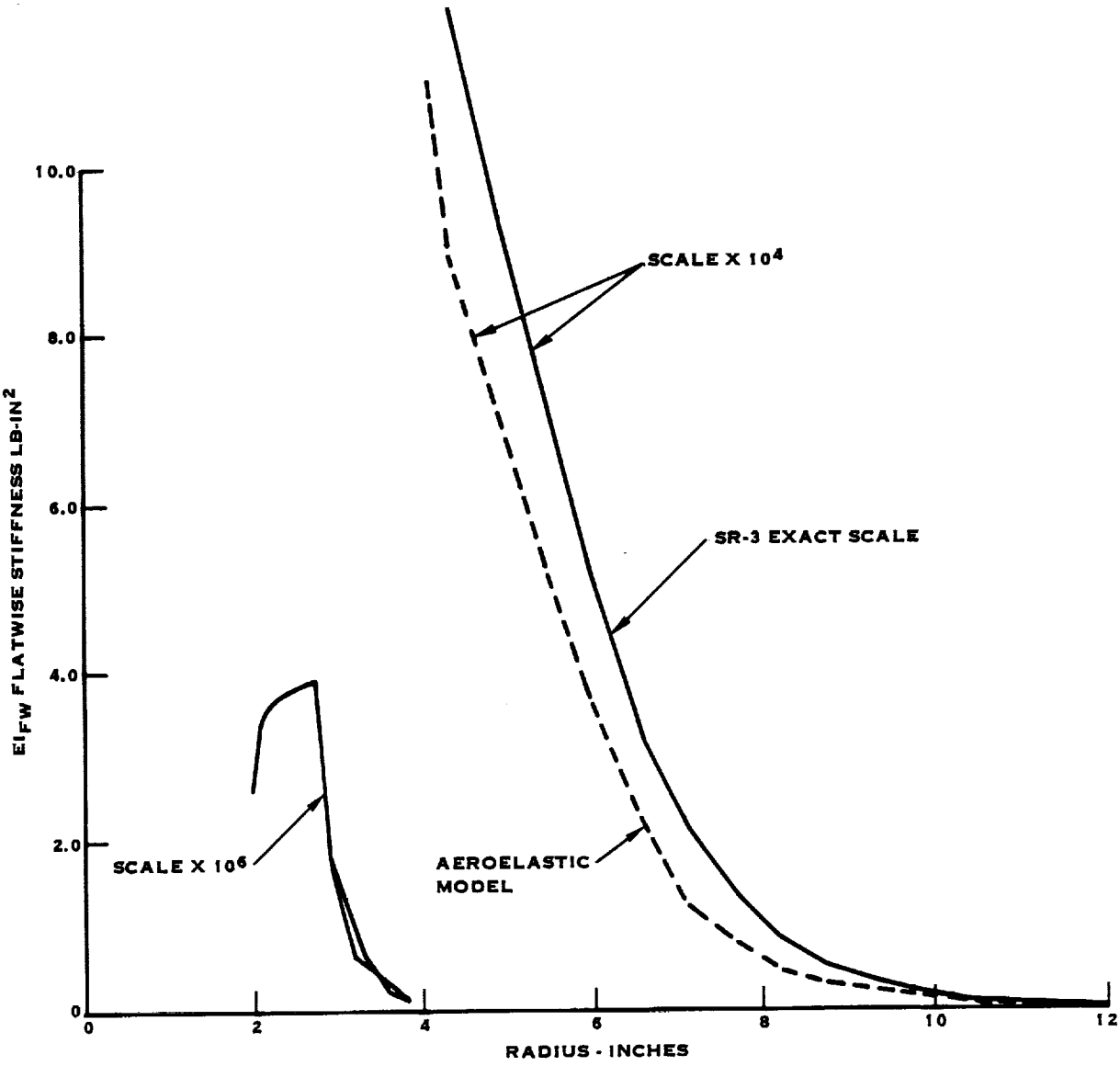

FIGURE 6.13. SR-3 10 WAY 2 FOOT DIAMETER FLATWISE STIFFNESS DISTRIBUTION COMPARISON

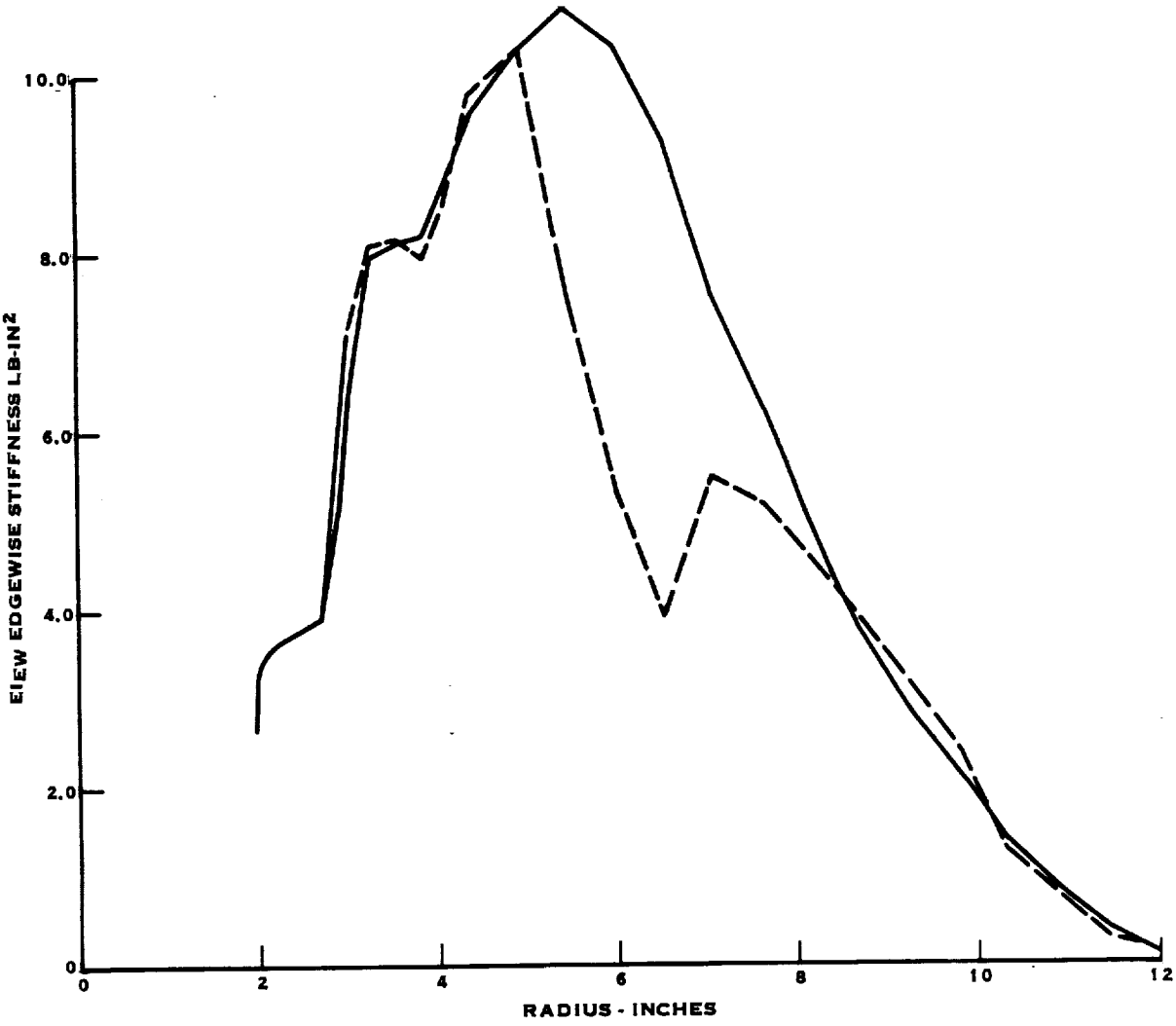

FIGURE 6.14. SR-3 10 WAY 2 FOOT DIAMETER EDGEWISE STIFFNESS DISTRIBUTION COMPARISON

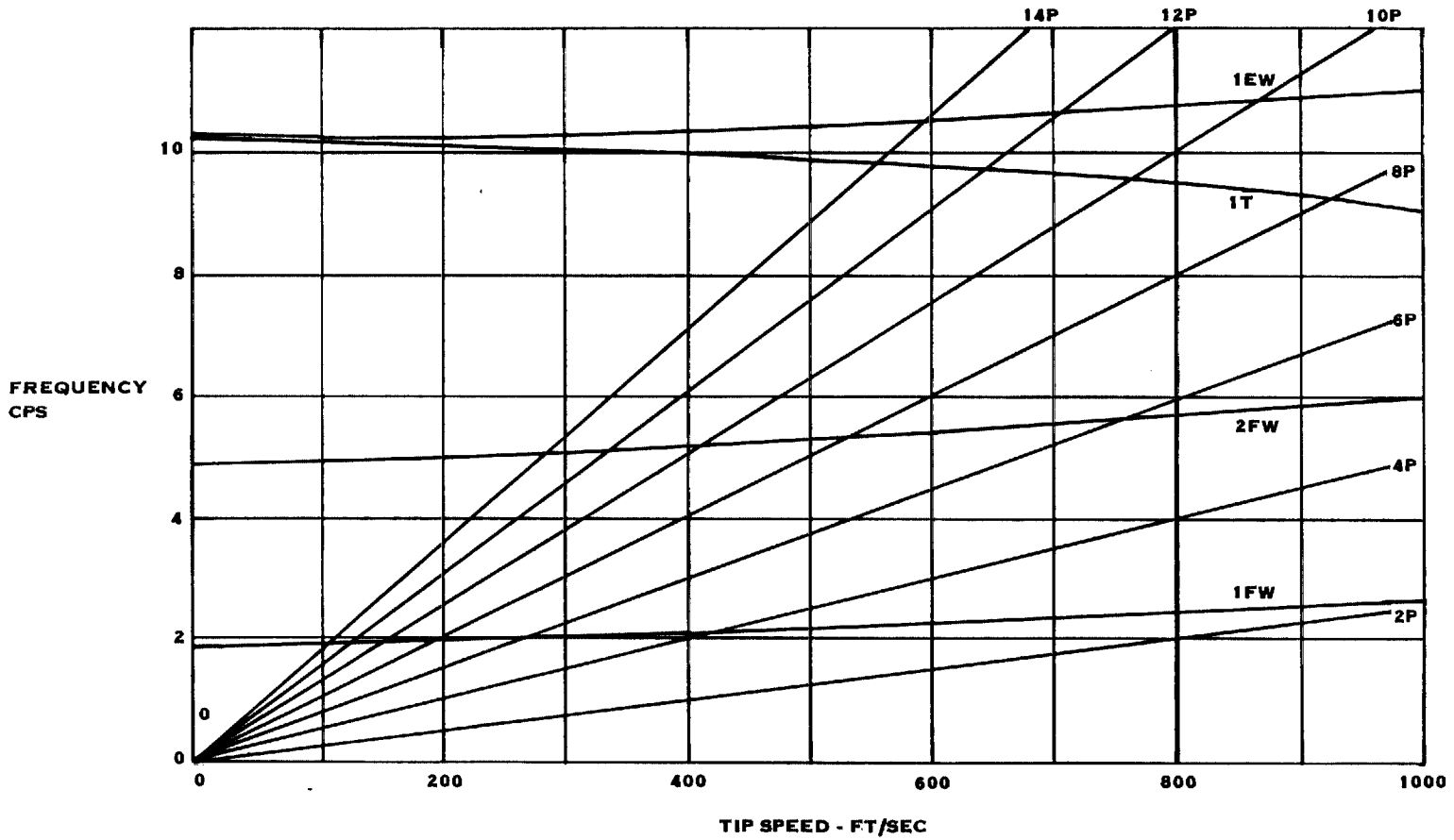

FIGURE 6.15. SR-3 10 WAY 2 FOOT DIAMETER EXACT SCALE CAMPBELL DIAGRAM

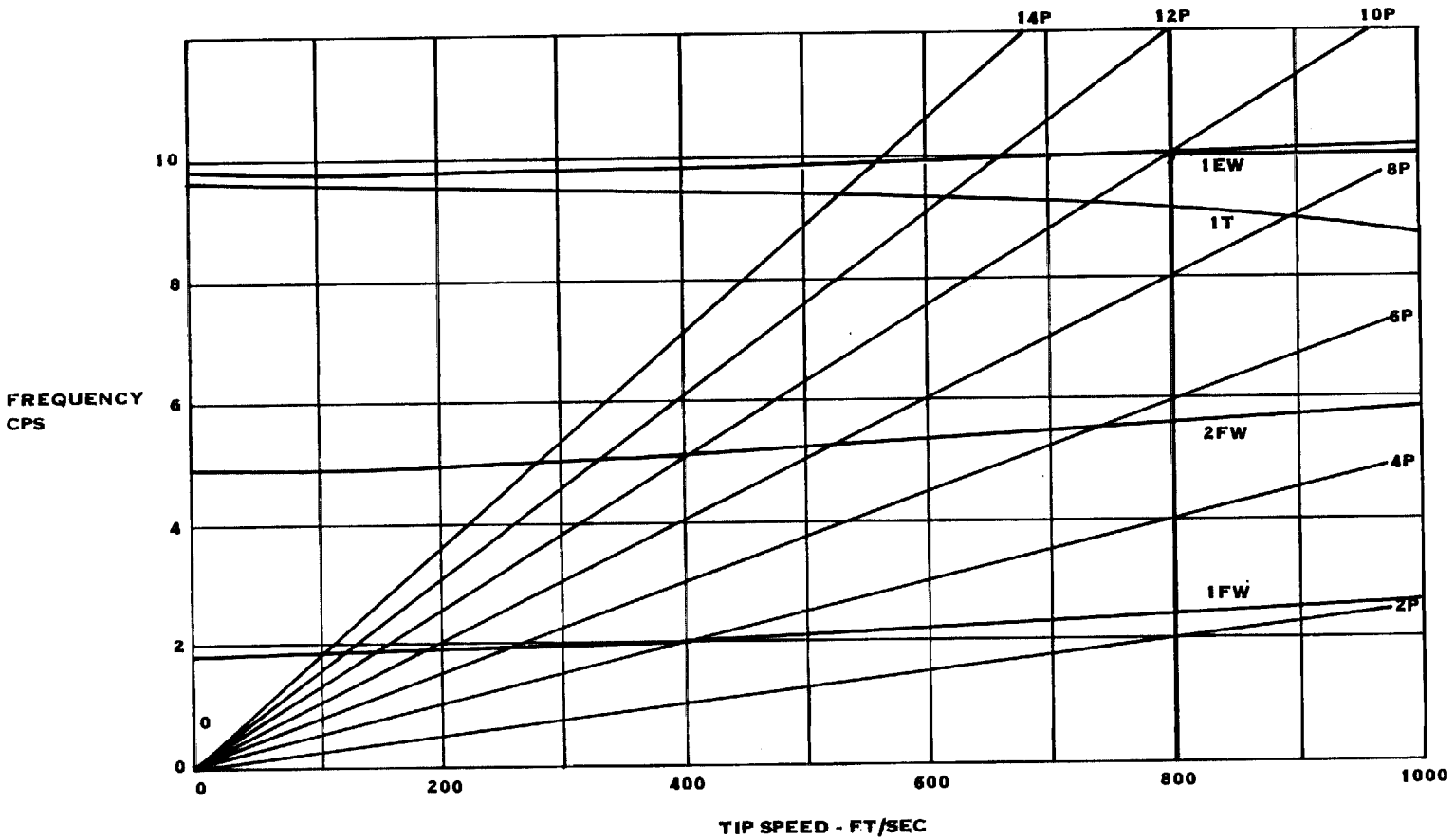

FIGURE 6.16. SR-3 10 WAY 2 FOOT DIAMETER AEROELASTIC SCALE CAMPBELL DIAGRAM

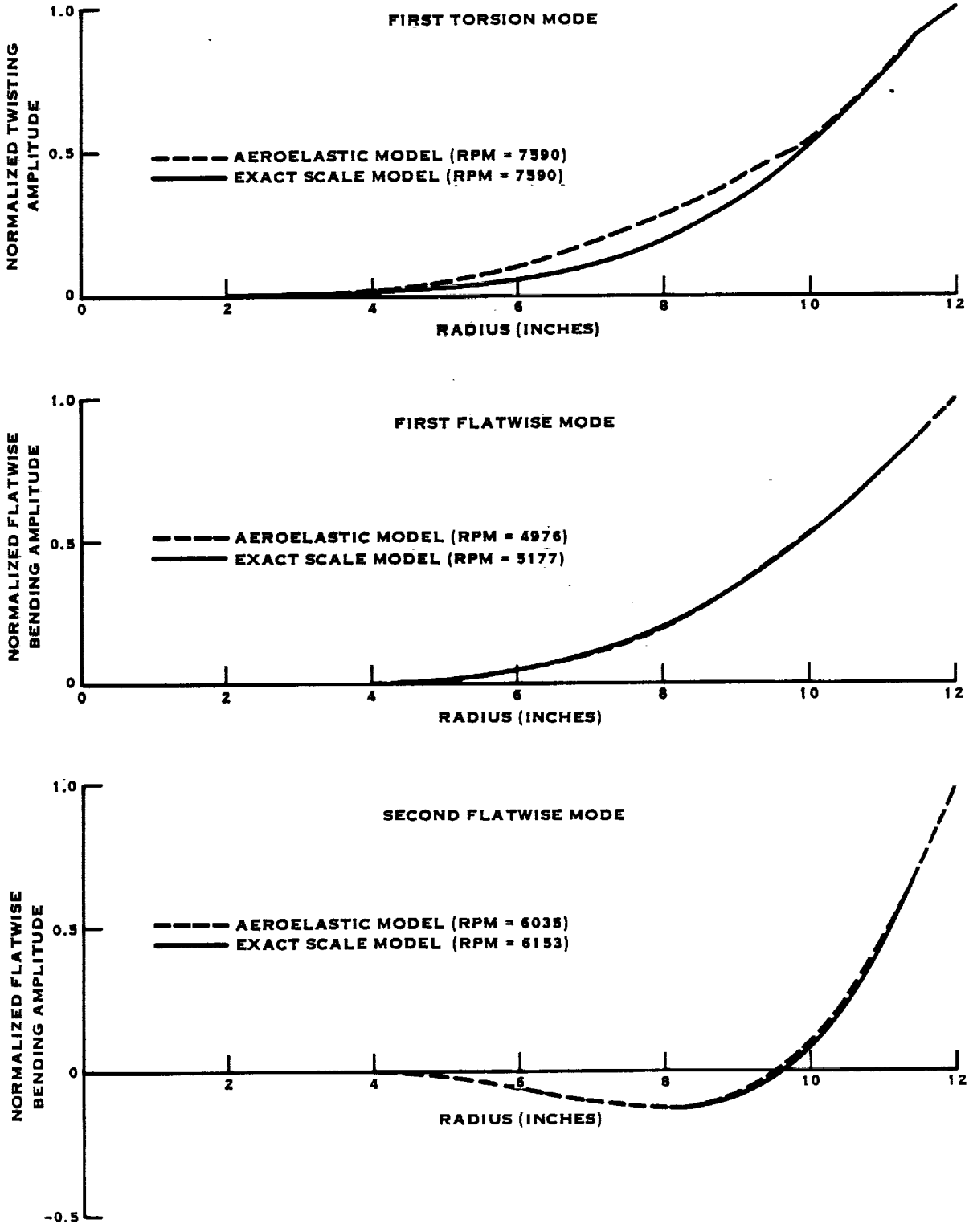

FIGURE 6-17. SR-3 10 WAY 2 FOOT DIAMETER NORMALIZED MODE SHAPE COMPARISON

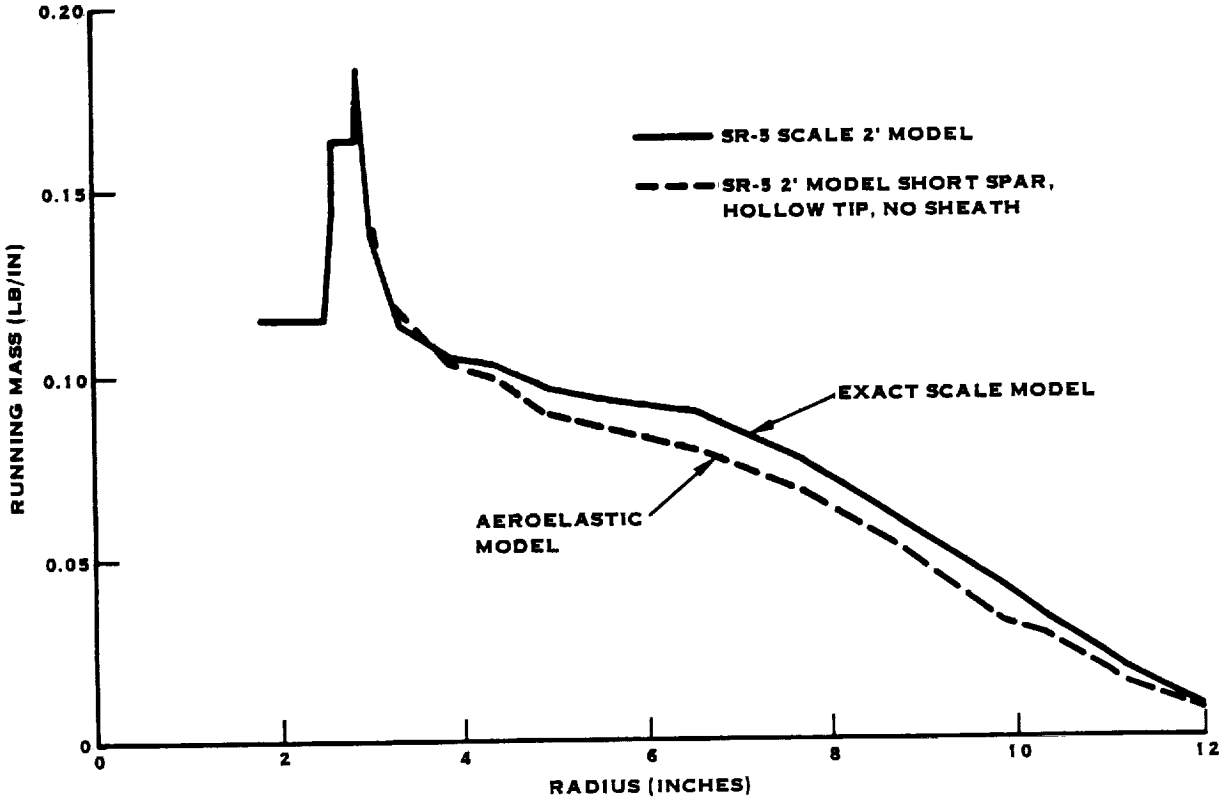

FIGURE 6.18. SR-5 10 WAY 2 FOOT DIAMETER MASS DISTRIBUTION COMPARISON

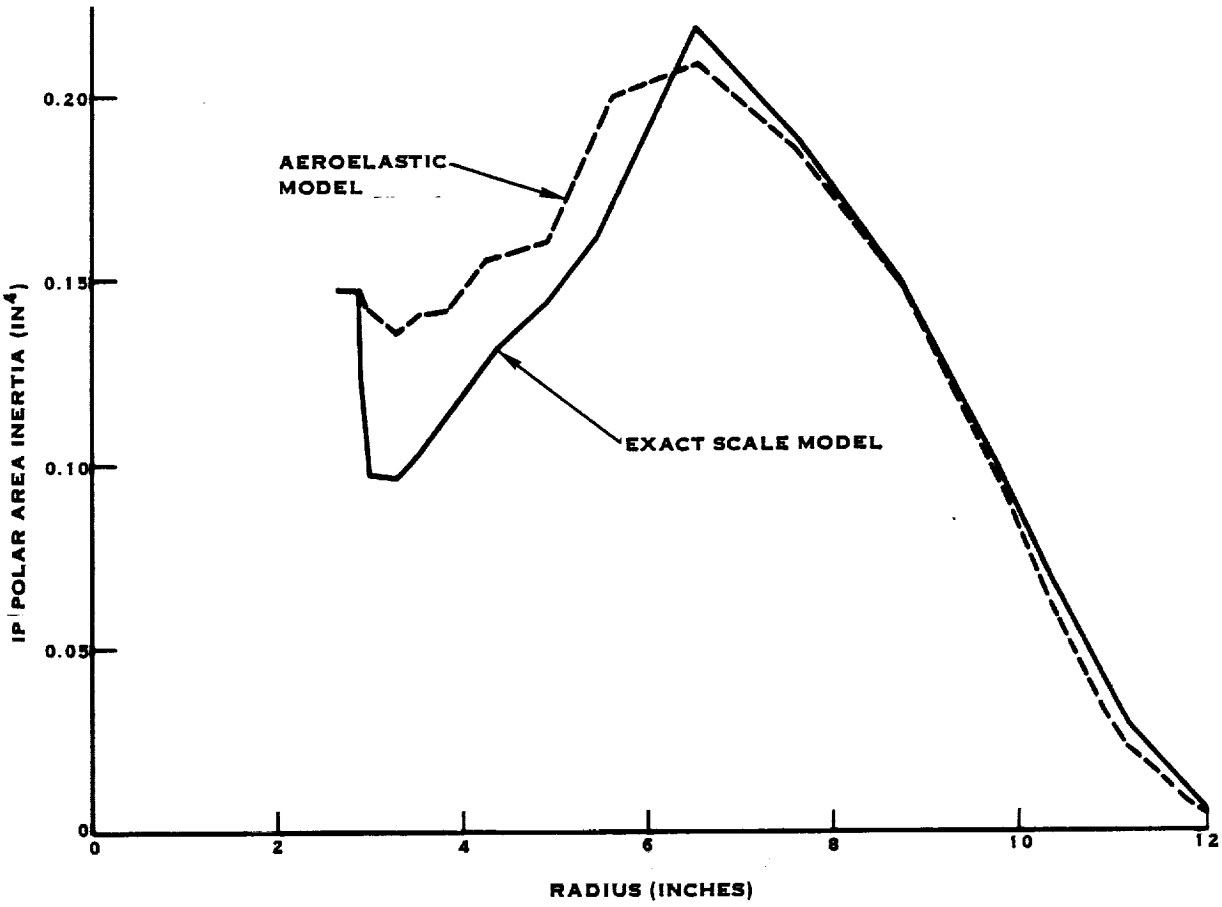

FIGURE 6.19. SR-5 10 WAY 2 FOOT DIAMETER EQUIVALENT POLAR INERTIA COMPARISON

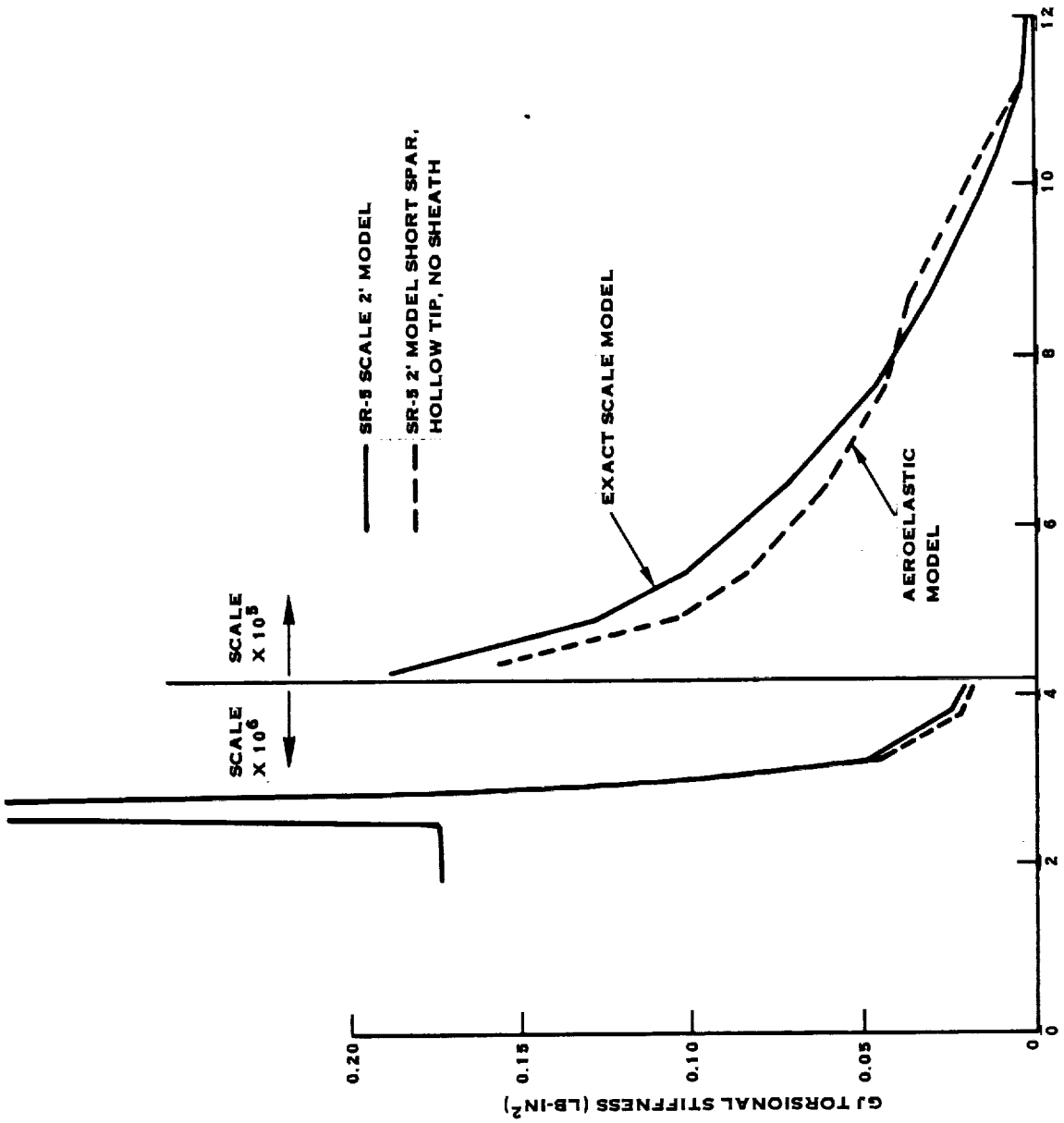

FIGURE 6.20. SR-5 10 WAY 2FOOT DIAMETER TORSIONAL STIFFNESS DISTRIBUTION COMPARISON

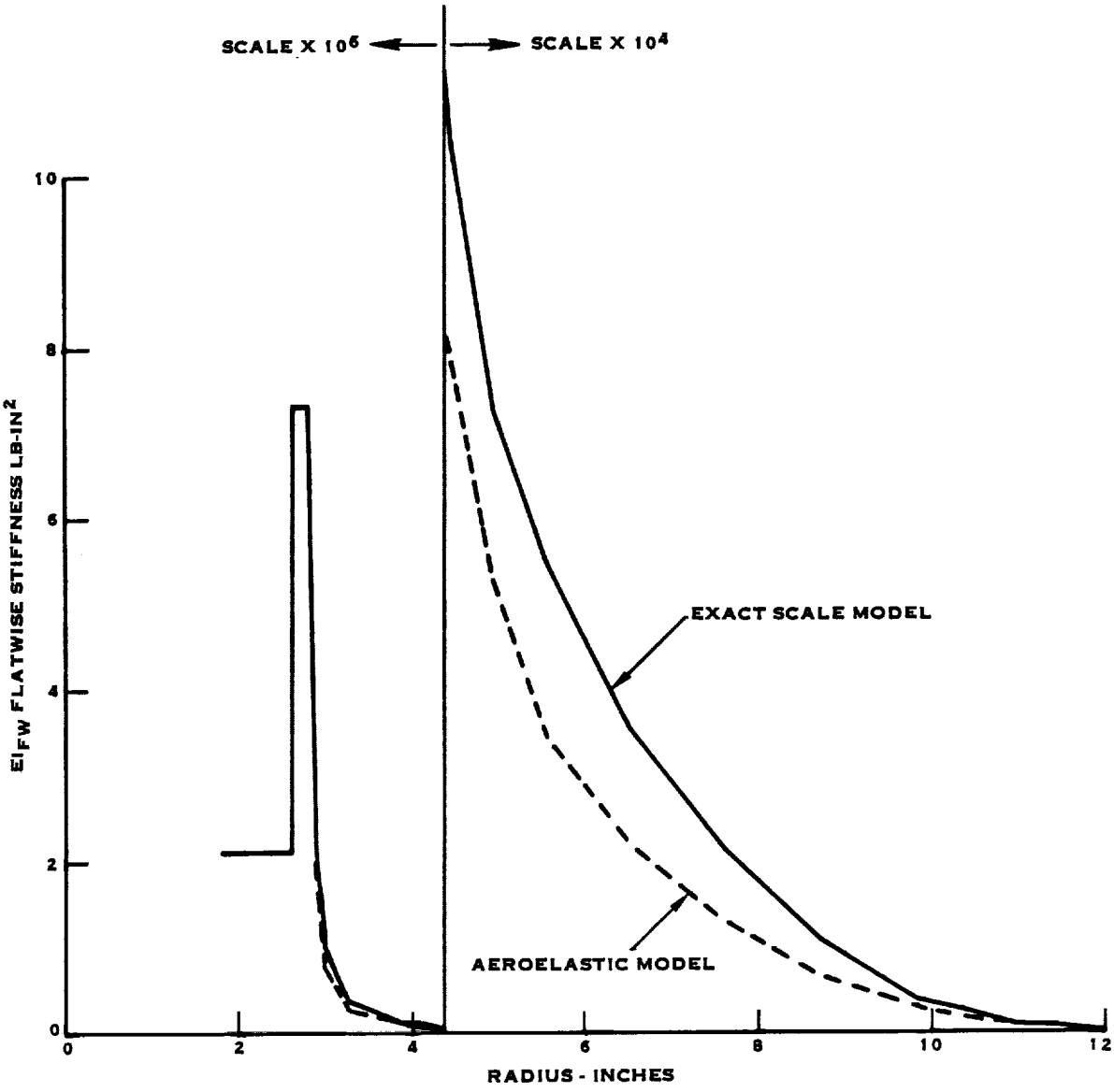

FIGURE 6.21. SR-5 10 WAY 2 FOOT DIAMETER FLATWISE STIFFNESS DISTRIBUTION COMPARISON

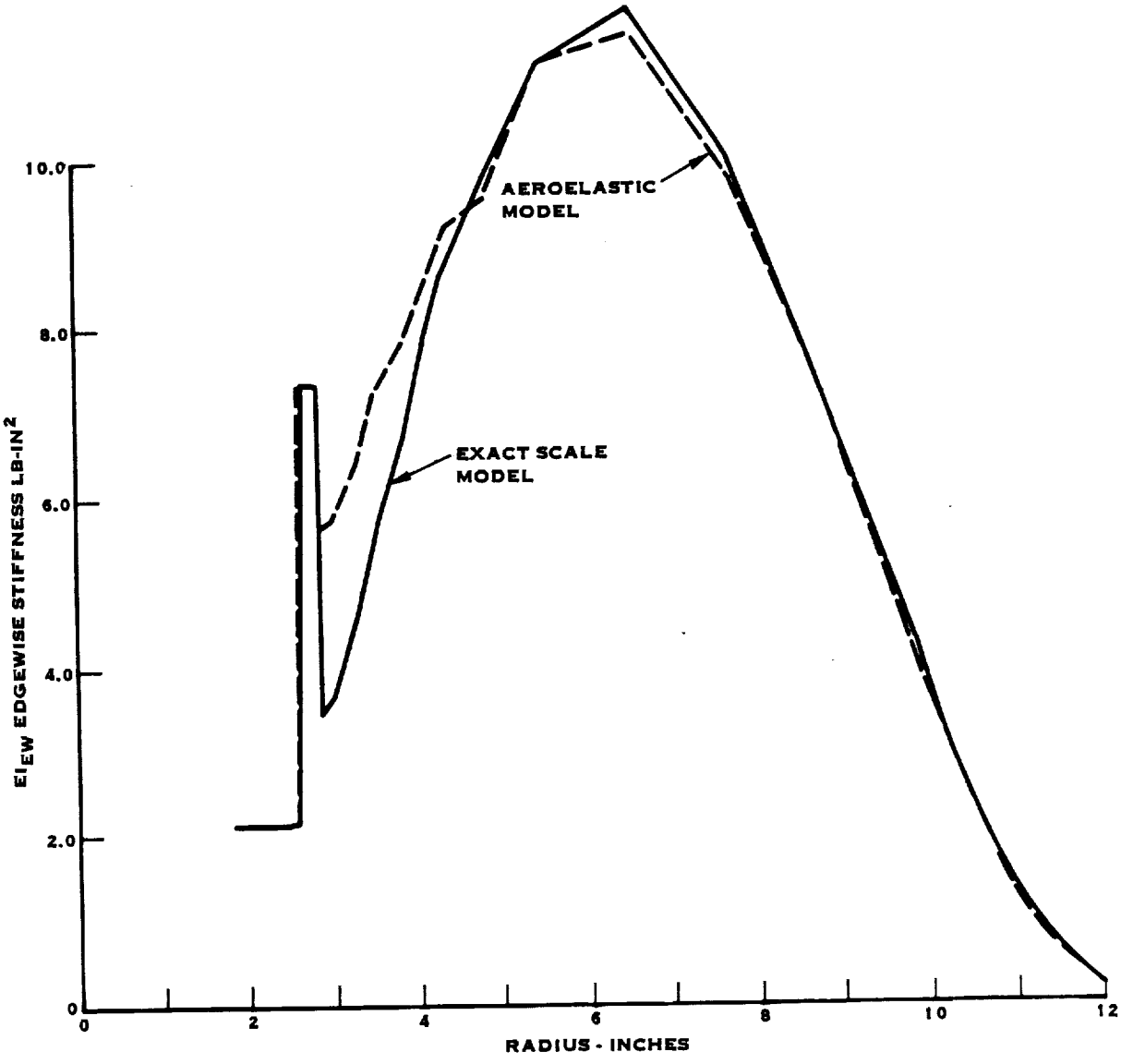

FIGURE 6.22. SR5 10-WAY 2-FT DIAMETER EDGEWISE STIFFNESS DISTRIBUTION COMPARISON

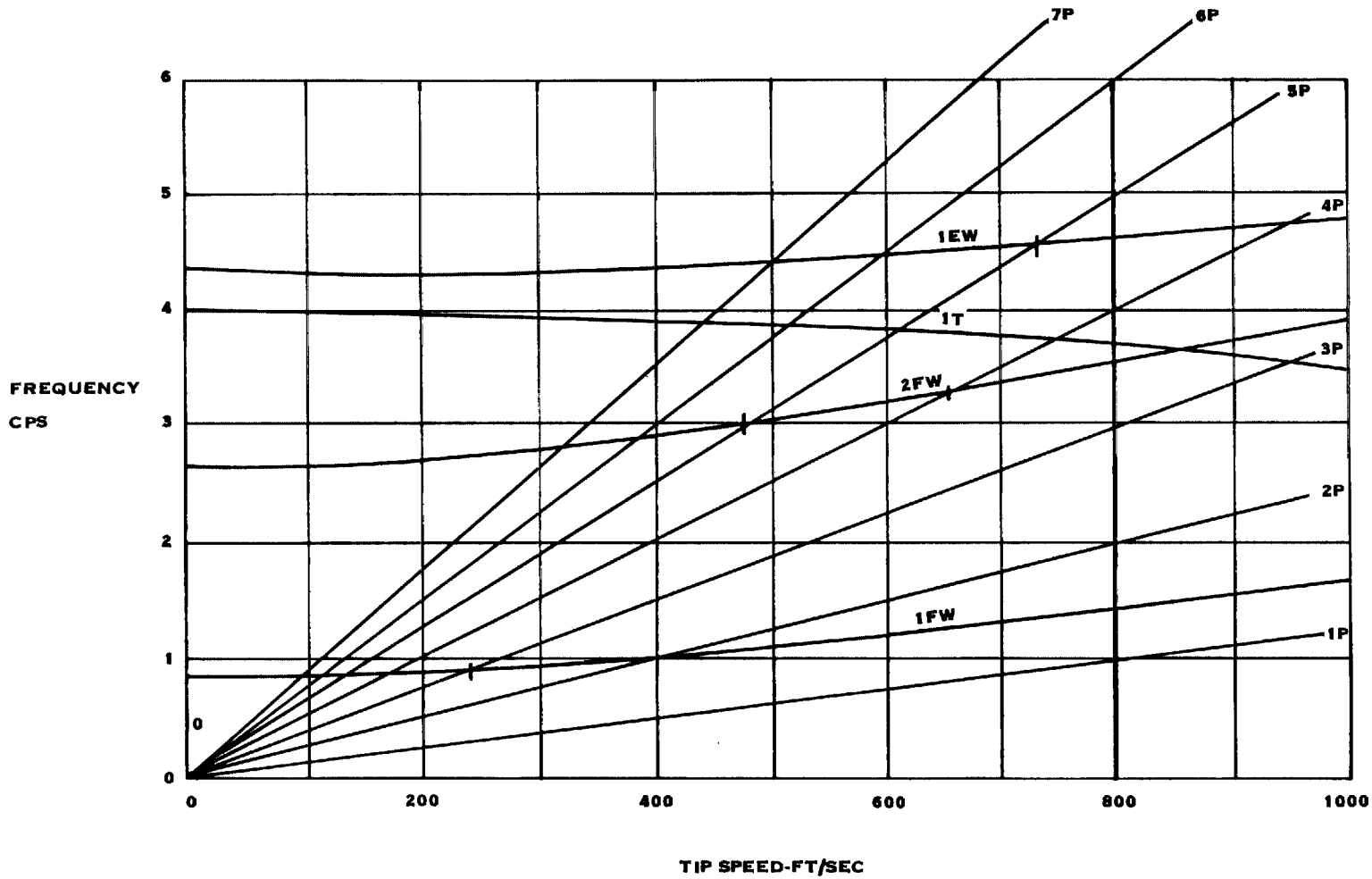

FIGURE 6.23. SR-5 10 WAY 11 FOOT DIAMETER CAMPBELL DIAGRAM

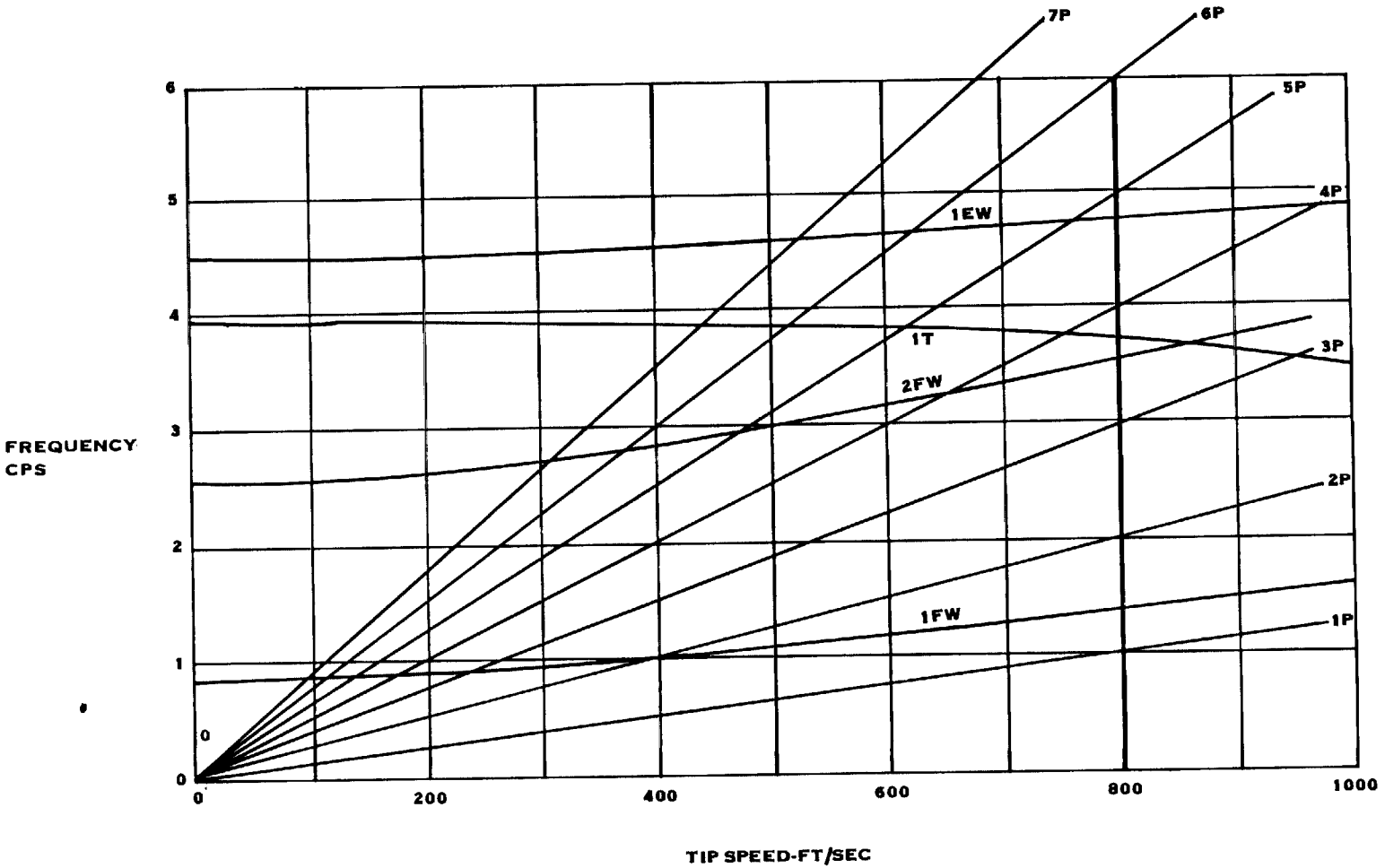

FIGURE 6.24. SR-5 10 WAY 2 FOOT DIAMETER EXACT SCALE CAMPBELL DIAGRAM

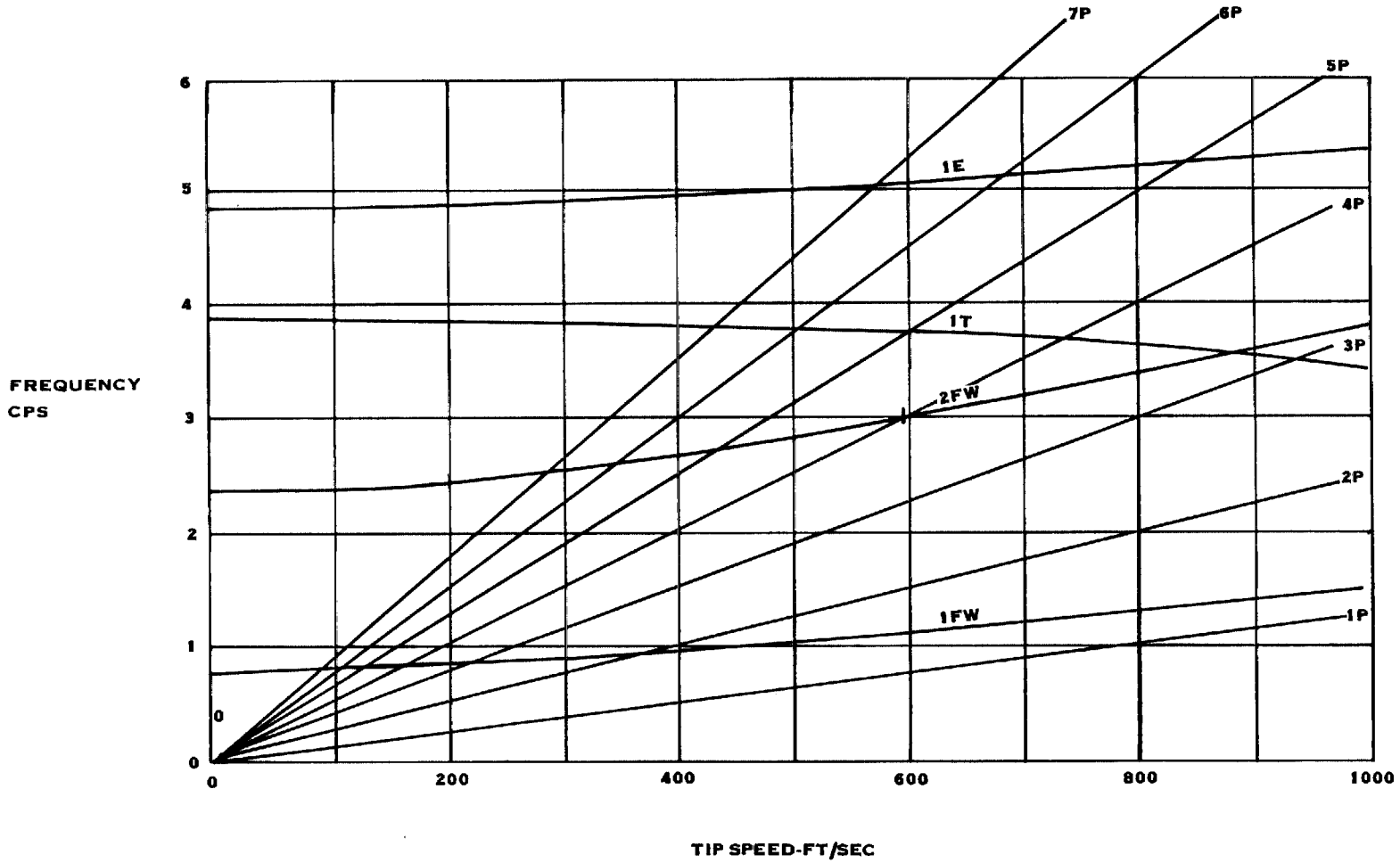

FIGURE 6.25. SR-5 10 WAY 2 FOOT DIAMETER AEROELASTIC SCALE CAMPBELL DIAGRAM

Figure 6.26 shows the normalized mode shapes. The first torsional and first and second flatwise modes are compared between the exactly scaled model and the aeroelastic model. The flatwise comparisons are good but torsion shows some differences, probably due to the mass of the shell.

6.8 CONCLUSIONS

a. Design and fabrication of a 2-foot diameter or larger SR-2 8-way model may be feasible, however the simulation of the properties of the hollow spar with a solid spar in small diameter models may prove to be difficult.

b. Design and fabrication of a 2-foot or larger diameter SR-3 10-way model is feasible.

c. Design and fabrication of a 2-foot or larger diameter SR-5 10-way model is feasible.

d. By inference, the design and fabrication of a 2-foot diameter or larger SR-3 8-way model is feasible.

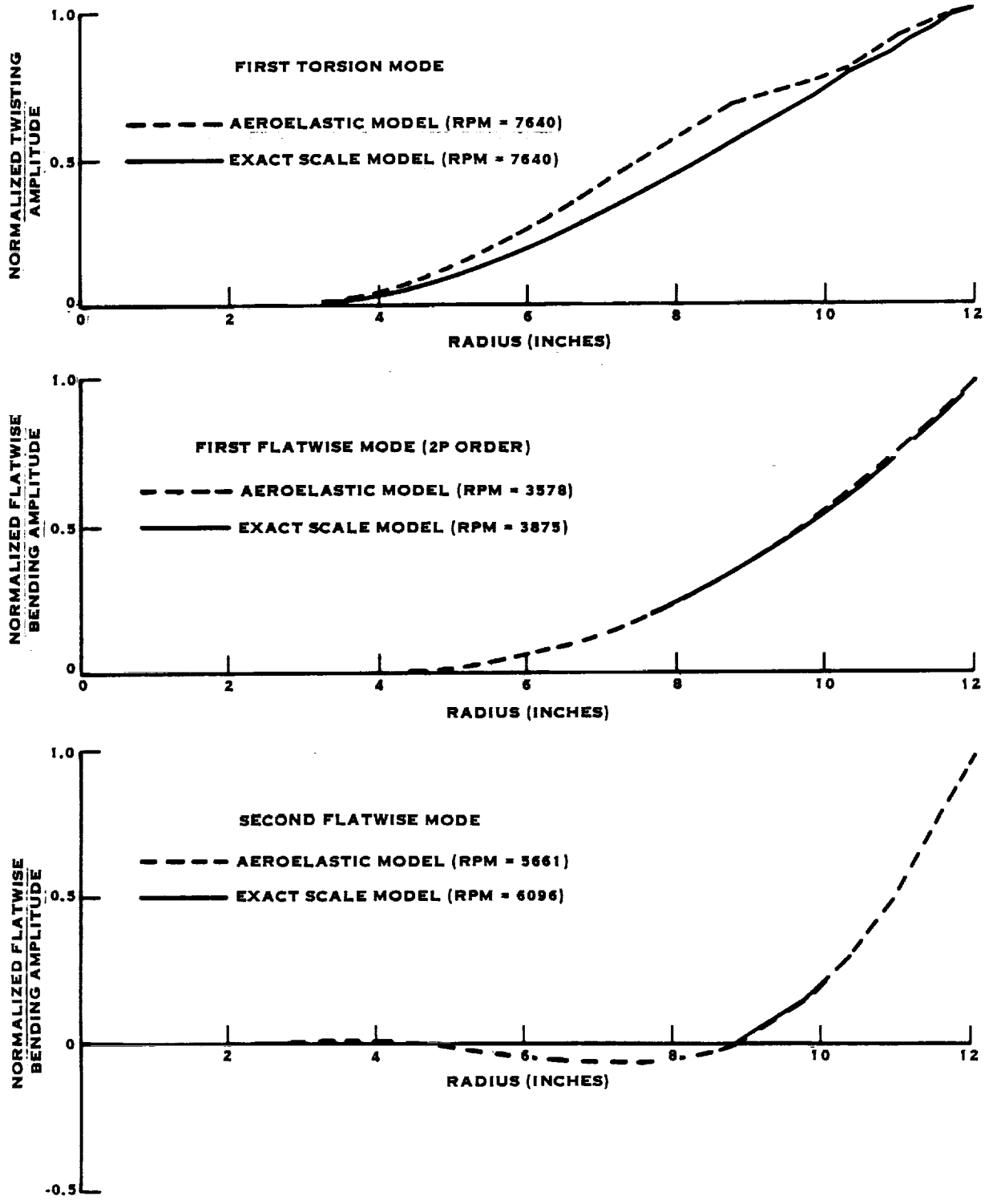

FIGURE 6.26. SR-5 10 WAY 2 FOOT DIAMETER NORMALIZED MODE SHAPE COMPARISON

7.0 TASK V - FULL SIZE BLADE ASSESSMENT AND DEVELOPMENT PLAN

7.1 STRUCTURAL DESIGN

7.1.1 Assessment

The large scale Prop-Fan blades were designed using state-of-the-art technologies. In the area of structural dynamics, the technology is heavily involved with finite element and modal analysis methods. The term structural dynamics is used to encompass frequency and mode shape calculation, vibratory response, and classical and stall flutter stability analysis. Present technology relies on finite element and modal analysis methods because of the complex geometry of the blade. This complexity does not lend itself to the application of beam theory which is routinely used for the design of helicopter and propeller blades. It should also be noted that in some areas of structural dynamics, state-of-the-art technology is in the initial development phase since the Prop-Fan blade has surfaced new and unique design considerations. Because of a lack of thorough analysis procedures in all aspects of the design, a risk or confidence factor exists in each area of the structural analysis. This can only be reduced by correlating predictions to test data.

With the development of the Prop-Fan, Hamilton Standard has been improving design procedures. These improvements in technology take the form of better analytical techniques, empirical modifications to the analysis, or a combination of new analytical and empirical methods. The present structural dynamics methodology, and the shortcomings of the procedures used during this program, were reviewed to assess the strengths and weaknesses.

As noted before, the Prop-Fan blade is modeled with finite elements because of the inherent complexity of the design. Modeling the blade in this manner allows for a detailed description of the blade internal and external structure. The present large scale designs are constructed from a conglomeration of materials, metal or composite spar, fiberglass or Kevlar epoxy shell, bond material, filler foam, and a metallic erosion sheath. Finite element methods allow the combination of all the materials either as a single composite plate element or as individual material layers so that the interaction between material layers can be assessed, such as the stress in the bond holding the shell to the foam and spar. In addition to material flexibility, this modeling procedure completely retains the complex geometric shape along with blade deflections in six degrees of freedom. Under load the blade will untwist, elongate, change camber, etc. These deflections are all retained with finite element methodology. It is important that all blade deflections be retained because the shape of the blade under load may be sufficiently different from the non-rotating, no-load configuration that results obtained using the no-load blade position cannot be applied to the loaded blade position. It has been further established that the loaded blade position must be determined using a nonlinear finite element solution procedure because the deflections are beyond the reasonable limit of linear deflection approximations.

The penalty for the accuracy of finite element methods is time, both manpower and computer. Complex finite element models are time consuming to construct even with the large number of preprocessors specifically developed for Prop-Fan blade design. Also, the long computer running time for a large model is further increased when the solution requires nonlinear methods. But, other than the time factor, finite element methods have proven to be fully satisfactory for establishing the steady state operating position of the blade along with its material stresses.

Frequency and mode shape calculation also relies on finite element methods because the blade vibratory analysis is an extension to the steady-state analysis. Having established the loaded position of the blade and the stiffening effects of the centrifugal field acting on the blade the mode shapes and natural frequencies can be determined using a variety of standard solution procedures. This calculation is relatively straight-forward after the steps used to determine the loaded position of the blade have been completed. The importance of correctly determining the loaded position of the blade is stressed at this point because the frequencies and mode shapes are directly related to the three-dimensional position of the blade in space. This dependence of frequency and mode shape on position is analogous to the dependence of fixed wing frequency and mode shape to center of mass and elastic axis location. The present frequency calculation procedure has been verified with test data and uses established technology so that inaccuracies in the predictions are dependent on establishing the loaded position of the blade and the techniques used to construct the finite element model of the blade.

The NP response analysis of Prop-Fan blades involves the coupling of the blade structure with aerodynamic loads. This coupling is performed with a finite element harmonic response solution. The blade harmonic loads are evaluated using an aerodynamic program that accounts for angular inflow and the aircraft flow field variations. The harmonic air loads due to the non-uniform flow field are then distributed on the blade finite element model for the response calculation. The model used in this calculation has previously been deformed with steady aerodynamic and centrifugal loads. The NP response solution assumes the vibratory motion will be a small displacement about the steady state blade position.

The results obtained using this analytical procedure have not correlated well with existing test data. The predicted blade stresses are lower than the measured blade stresses for the swept configurations. This under-prediction of the stresses is therefore taken into account by increasing the predicted aerodynamic loads with an empirical weighting factor that has been determined from model testing. Many of the approximations that have been applied to the structural and aerodynamic aspects of the NP response calculations have been re-examined and refined to alleviate the need for the empirical correction to the theory but nothing has been uncovered in the current methodology that will improve correlations between theory and experiment. Until the discrepancy in the NP response theory is identified and a new analysis is developed the current empirical correction is sufficient to allow for a satisfactory design.

The classical flutter analysis for Prop-Fan blades has been developed over the past few years and is specifically designed to account for the structural and aerodynamic complexities of the Prop-Fan. The classical flutter theory uses modal analysis methods so the flutter results are directly linked to the accuracy of the frequency and mode shape calculations. The present analysis relies on two-dimensional unsteady aerodynamic theory to predict three-dimensional flow. Therefore, as with the NP predictions, the flutter analysis has been tailored using empirical flutter results to give good correlation with test data. Without tailoring, the analysis predicts blades to be less stable than test results indicate. Because of the lack of a large flutter data base, and the high risk involved if flutter should occur, a conservative approach has been taken to design the blade to ensure classical flutter stability. The present approach is to use the analysis in an untailored form so that flutter predictions will be conservative thereby assuring the integrity of the blade. This analytical approach will continue to be used until a large flutter data base is established or an improved theory can be developed.

The final aspect of the structural dynamics design review is blade stall flutter evaluation. Presently there is no method available to predict stall flutter with any certainty. Stall flutter has been predicted on Prop-Fans using a semi-empirical procedure, and an empirical procedure routinely used for propellers. Both methods have proven unsatisfactory when the results were compared to experimental model stall flutter tests. The risk involved with not having a procedure for predicting stall flutter is low from the viewpoint of a successful experimental test program, because stall flutter only occurs at low to zero airspeeds with high engine power. These conditions would only prevent full power engine operation while the aircraft is on the ground if stall flutter should occur, Also, stall flutter is a non-destructive phenomenon because the amplitude of the self-excited vibration is self limiting and therefore amenable to testing. Accurate assessment of Prop-Fan stall flutter will require a substantial amount of new experimental and theoretical effort.

Upon reviewing the major structural dynamic considerations that go into Prop-Fan design, it is apparent that calculation procedures exist in all aspects of the design except for stall flutter prediction. Even though it was mentioned that stall flutter would not significantly affect an experimental test program, is could affect a commercial development program because Prop-Fan operation could be limited during takeoff and landing. The next section presents a plan for improving state-of-the-art design procedures in all aspects of structural dynamics.

7.1.2 Technology Development Plan

The design assessment evaluation in Section 7.1.1 reviewed current design technology and established the order of priorities for a technology development plan. The priorities fall into the order stall flutter, classical flutter, response to non-uniform inflow, and critical speed calculation. An overview of the advances required to improve design procedures will be presented in the remainder of this section, beginning with stall flutter.

Stall flutter research is of high priority because it is the only aspect of Prop-Fan design that cannot be satisfactorily examined either empirically or theoretically. Unit recently, stall flutter research has centered around dynamic stall of helicopter rotors, stall flutter of turbine and compressor blades, and the avoidance of stall flutter and buffeting of fixed wings. Prop-Fan stall flutter does not fall into the regime of this research. The approach for dealing with stall flutter must proceed first on an experimental path and secondly on an analytical path because elementary knowledge about the problem is not known. For example Prop-Fan stall flutter is initiated by small amplitude blade motion at a high frequency in a stalled flow environment. It is presently not known if this incipient condition behaves as a linear or nonlinear system. A basic piece of information about the linearity of the incipient stall flutter problem can completely define the analytical approach used to model the phenomenon.

Therefore, it is recommended that an experiment be performed to provide data on the unexplored phenomenon of incipient stall flutter of Prop-Fan profiles for the purpose of obtaining direct measurement of steady and unsteady forces and moments. These results will serve as a data base for stall flutter predictions and comparisons to theoretical approaches. In addition to generating new experimental data the existing model Prop-Fan stall flutter test results should be re-examined with the intent of developing empirical prediction methodology. The creation of an empirical Prop-Fan stall flutter data base will have a two fold effect. First the data base will provide necessary information for preliminary stall flutter estimates of new Prop-Fan designs and secondly the data will provide insight into the analytical model needed to develop a general stall flutter theory. Approaching stall flutter technology development in this manner produces empirical data to answer short term questions about Prop-Fan stall flutter while it establishes the groundwork for a general stall flutter theory.

A combined improvement in classical flutter and blade response technology can be obtained by the development of an unsteady lifting surface analysis that rigorously models the three-dimensional flow about the complex Prop-Fan shape. Improvements in the unsteady loading will eliminate many questions concerning the application of two-dimensional aerodynamics to the Prop-Fan model. Rigorous aerodynamic modeling will subsequently shift technology improvements to formulating an aeroelastic analysis that combines three-dimensional aerodynamic and structural effects into a linear harmonic response solution to get angular inflow effects and an eigenvalue solution to get stability results. The aeroelastic analysis will use a modal approach so that finite element methods can be used to establish the steady state operating conditions, natural frequencies, and mode shapes.

Advancements in technology along the path of stall flutter research, lifting surface theory, and an advanced modal solution will eventually lead to a full nonlinear modal response and stability analysis which has the capability of examining the Prop-Fan design over the entire operating spectrum. It is recommended that a modular approach to technology advancement be applied to Prop-Fan development because the Prop-Fan program is a current project that will be immediately influenced by near term advancements. A long term comprehensive plan will not serve the immediate needs of the Prop-Fan and may lag far enough behind commercial development to be obsolete before completion.

7.2 BLADE FABRICATION

7.2.1 Assessment

Development of a full scale Prop-Fan propulsion system will require development of blade manufacturing technology beyond the current techniques used in production at Hamilton Standard. The primary factors prompting this need are the geometry features required to meet aerodynamic and acoustic goals. These unique features are:

- high sweep
- wide chord widths
- low percentage thickness
- high width tapers

The basic Hamilton Standard spar and shell blade approach will continue to be used for new blades with the following new design requirements.

- Spars will have to be swept.
- Spars will have to be hollow to provide tolerable blade weights.
- Spars will have to accommodate larger width to thickness ratios.
- Shells will have to accommodate large variations in plan form shape from root to tip without distorting weave patterns and reinforcement directionality.

In order to accommodate these requirements, several methods of spar manufacture and shell ply generation must be studied and assessed to determine their feasibility. An optimal approach will then be selected for extensive development and testing. The following descriptions of technical development outline the methods of spar manufacture that have been identified as potentially meeting full scale blade needs. The following description of shell technology development applies to any type of resin or fiber that would be used in the full scale blade shell. The primary thrust of this development will be in the technique of laying up the reinforcement to meet shell design requirements for stiffness and strength. In the development of the full scale blade, all of the following approaches will be considered. Only that approach which is eventually determined as optimal will be fully implemented.

7.2.2 Spar Development

7.2.2.1 Mechanical Bending - The primary problem to be addressed in bending a spar tube to achieve the desired sweep will be to apply a machine large enough to bend a spar tube approximately 9 inches in diameter. In the process of bending, wall stabilizing techniques will have to be utilized to

prevent forming creases and wrinkles in the tube walls. An additional factor in this development effort will be the large taper in the tube wall thickness normally utilized in hollow metal spars.

7.2.2.1.1 Assessment - During this phase, a search will be made for installations with the necessary bending capabilities. They will be evaluated for the effectiveness, probability of success, and costs. A selection of an application for further development will then be made. This activity will center largely on reviewing previous applications of candidate equipment. Supplemental evaluation of capabilities will be sought by demonstration of simple tubing specimens with representative wall thickness, diameter, and materials.

7.2.2.1.2 Feasibility Demonstration - This phase will first require adaptation of the selected equipment to handle tapered spar tube blanks. Activity will start with design and procurement of adaptive tooling. A number of test spars of typical design will be produced by the tube reduction process, annealed, and used to perform bending tests on the selected equipment. Evaluation of the test pieces will include defining local wall thickness reductions, shape control, and the degree of cold working in local areas of the spars.

7.2.2.1.3 Hot Form Trials - The manufacture of a quantity of bent spar tubes are required in order to provide specimens for hot forming. Since the hot forming process mechanically forms the spar airfoil and also quenches the steel to produce design strength properties, the die design, press operation, and quenching techniques must be simultaneously developed to produce a spar with the requisite shape and metallurgical properties. Several series of forming trials will be required to optimize the process parameters. Verification of this optimization will be a result of metallurgical examination of test pieces taken from the test spars and their dimensional inspection.

7.2.2.2 Explosive Forming - Explosive forming has been used to both fully form and partially form parts. Its ability to cold form at high deformation rates in a strictly tensile loading is well suited to handling thin, closed parts where buckling is a normal result of mechanical bending. The primary problem to be addressed in the explosive forming development will be control of the charge effects and accommodation of the significant variation in spar wall thickness. Forming dies are usually used as a part back up during explosive forming operations. Their design will have to consider whether full or partial forming will be utilized. A basic limitation to this process will be localized wall thickness reduction in the areas of greatest deformation.

7.2.2.2.1 Assessment - Search for a vendor and site suitable for forming a part of the blade spar's size will be made. Safety considerations will essentially dictate considering only currently approved facilities. Once a site is selected, a development program to analyze the part and predict the charge configuration will be required in order to establish tooling requirements.

7.2.2.2.2 Feasibility Demonstration - During this phase suitable forming tooling will be designed and built. After manufacture of this tooling and installation at the site, a quantity of test spars will be manufactured for explosive forming trials as well as hot forming if the partial forming option is the selected process. This would be more likely as inclusion of blade twist would complicate development of the charge configuration.

7.2.2.2.3 Hot Form Trials - This phase will be required if partial forming of the spar tube is utilized. Starting with a round tube, derived from the traditional tube reduced part, an undersized spar with respect to circumferential lengths in the mid-spar area would be produced. With proper die design and disposition of the charge, the objective of partial explosive forming would be to bump out the leading edge at the mid blade and pivot the tip area back towards the trail edge. Hot forming would then provide for twist, final airfoil, and quenching. Since the reduction characteristics of this process would be significantly different from that derived by bending, a complete metallurgical evaluation would be required to assure materials properties.

7.2.2.3 Welded Steel Spars - The welded steel spar approach will be configured to side step the manufacture of the traditional machined blank/tube reduced spar and go directly to a shaped spar with sweep. The welded spar would be made from two or three pieces. Two of these pieces would comprise the airfoil area of the spar with two welded longitudinal seams probably made with a welding robot. The third piece would comprise the blade spar shank. Attachment of the shank would utilize inertial or electron beam welding in order to produce minimal effects in the weld zone area. Hot forming would still be utilized to establish heat treatment and possibly form the twist distribution in the spar. Extensive structural testing of the welds and an NDT technique for their inspection would be required to qualify welds in the primary spar structure.

7.2.2.3.1 Assessment - During this phase, welding processes would be selected and sample welds surveyed in the spar material with the varied configurations present throughout the tapered spar structure and the retention area. Having established the integrity of the weld structure, the problem of economically producing tapered flat stock suitable for forming the spar airfoil halves would be addressed. It may be noted that grain flow in this stock will be a response to the technique used to form the tapered stock and may be quite different from that produced by the tube reducing of pierced round tubes. If this is the case, then part of the assessment of the tapered flat stock will be to perform extensive specimen fatigue testing.

7.2.2.3.2 Tooling Development - This activity will be required to bring into full scale capability the required tools for the spar manufacture. There are three areas which will require development. The flat tapered sheets will have to be formed into airfoil shaped halves. Possible techniques for this forming would be die hot forming, hydro static pressing, and explosive forming. Once the halves are formed, they will have to be accurately trimmed at the joining edges to a welding configuration. Finally, an automated welding set up would be used to produce the high quality weld of varying cross-sections.

7.2.2.3.3 Manufacturing - Spars would be processed in sufficient quantity to support a blade test program. Spars would be made with the above mentioned tooling and then assembled into blades.

7.2.2.3.4 Blade Test - This phase will be required to verify acceptability of the welded structure. A blade comprehensive test (Destructive Examination) would be used to verify spar stress response to static bending loads prior to performing blade fatigue testing. Blade fatigue testing in zero mean and resonant mean stress modes would establish fatigue life of the spar airfoil. Retention area fatigue testing would establish fatigue life of the blade raceway attachment area under combined centrifugal and cyclic bending loads.

7.2.2.4 Super Plastic Formed Diffusion Bonded - The design characteristics of the Prop-Fan blade may require a hollow titanium spar. Hollow titanium spars have been made at Hamilton Standard by tube reducing blanks, seam welding the tip, and creep forming the twist and airfoil shape. The wide chord and large taper of the Prop-Fan blade spar makes this approach much more difficult. The SPFDB approach which has been used to produce airframe parts such as access doors and formers offers the possibility of manufacturing a spar from flat stock incorporating integral internal wall supports. The basic SPFDB process will be used to produce the airfoil part of the spar. Three pieces of titanium stock, two with tapering thickness representing the face and camber sides and an inner web will be laminated with a stop off pattern separating each layer. After diffusion bonding to produce the patterned seam bonds, internal pressurization would be utilized with the titanium in a super plastic state, to form the airfoil shape and twist. A major extension of this technology will be the accommodation of tapered wall thickness and wall thickness heavy enough to provide useful spar structures. Incorporation of an adequate retention will require additional major extension of this technology. Small test sections with airfoil shape and twist have been produced in past evaluation programs on SPFDB facilities.

7.2.2.4.1 Design Blade Spar - This phase will be required to produce a test spar configuration for process evaluation. The laminated structure with seam bonds and integral internal bracing will require generation of a design configuration that provides for a transition from the expanded laminated airfoil into a retention with a continuous heavy wall raceway. Establishing this design configuration will dictate the facilities and tooling to be assessed in the next phase.

7.2.2.4.2 Assessment - During this phase an evaluation of facilities useable for this process will be made. A furnace capable of holding a spar die and reaching 1800°F will be required. Low and moderate pressure argon service will also be required. The die design will provide the necessary inert gas envelope required to protect the titanium from oxygen. Some facilities to be considered will be the hot form furnace at Hamilton Standard, braze furnace facilities within UTC and specialty vendors working with SPFDB process development. Airfoil and transition specimens will be prepared, processed, and evaluated as part of this assessment phase.

7.2.2.4.3 Tooling Development - This phase will be used to design, procure, and process develop a full scale spar facility. Included in this effort will be large scale specimens to prove out the dies and process.

7.2.2.4.4 Manufacture Spars - Full scale complete spars will be provided for use in test blade manufacture.

7.2.2.4.5 Manufacture Blades - This phase will provide the required number of blades for structural testing and will provide a comprehensive examination blade for destructive testing.

7.2.2.4.6 Experimental Stress Analysis and Fatigue Test - This phase will provide a full ESA and blade fatigue test sequence to determine the fatigue strength of the titanium SPFDB blade structure.

7.2.3 Shell Development

7.2.3.1 Seam Development - The Prop-Fan blade configuration will produce three separate problem areas novel to composite shell propeller blade development. The planform geometry with exceptional sweep and taper will not permit one piece of cloth to be wrapped around both sides of the blade with a butt seam over the spar as has been done in the past. Large multiple darts, open gores, and cloth directionality changes up to 90° will occur if this layup technique is maintained. In addition, the thinner airfoils prevent full wrap around of the shell at both lead and trail edges. Butt seams will be displaced to the edges and arranged in the available taper thickness. In order to assess adequate shell resistance to air loads, bending fatigue, and foreign object damage, test specimens will have to be designed, manufactured and tested. The specific layup configuration to be used on Prop-Fan shells will be derived from evaluation of these tests.

7.2.3.2 Ply Generation - Over and above techniques of utilizing the existing specified cloth material, it will be necessary to consider alternate forms of ply generation that will inherently accommodate the plan form and thickness characteristics of the Prop-Fan blades. If the seam locations near the edges prove unsatisfactory, economically prohibitive, or difficult to control in manufacture, then ply generation development will be required. The former location of seams over the spar has protected them from the fatigue and impact loads. A more continuous structure at the edges which would be provided by alternative ply generation techniques would then be required to eliminate edge orientated seams.

Two techniques that will be assessed are braiding and weaving. A sequence of events that would provide for development of an alternate ply generation technique will include the following tasks:

- Qualified vendors will be evaluated and one selected to set up a ply generation application on their equipment.
- Tooling will be provided for that equipment and samples procured.

- A preliminary materials characterization program will be run to provide shell design limits.
- A shell design will be made to satisfy overall blade design requirements.
- Full scale shell plies will be procured from the vendor equipment.
- Blades will be manufactured using the alternative shell plies.
- The blades will be subjected to fatigue, frequency, and FOD testing to verify required shell properties.
- The materials characterization program will be completed utilizing materials generated by the alternate process in the mode of manufacturing full scale shell plies.

7.2.4 Development Tests

7.2.4.1 Metallurgical and Process Examinations - The following table lists the various metallurgical examination and process evaluation testing to be done by section of this plan for a full evaluation of each section as if it were the optimal approach selected.

Section	Description of Test	Type of Specimen	Number of Specimens Req.
7.2.2.1	Bend Tubing	Constant Section Tubes	10
	Bend Tubing	Tapered Spars	20
	Section and Etch	Cut Up Spars	15
	Hot Form	Bent Spars	30
	Metal Structure	Micros	45
7.2.2.2	Explosive Forming	Tapered Spars	30
	Hot Form	Formed Spars	30
	Section and Etch	Cut Up Spars	30
	Metal Structure	Micros	100

7.2.2.3	Weld Sections	Micros	100
	In Process Base Matl	Micros	50
	NDT	X-Ray	100
		Acoustics Emission	100
		Ultrasonic	100
	Spar Comprehensive	Section Spar	15
	Blade Comprehensive	Full Blade	1
7.2.2.4	Form and Bond	Partial Spar Sections	20
	Form and Bond	Full Spars	30
	Sections of Specimens	Micros	100
	Spar Comprehensive	Section Spar	5
	Blade Comprehensive	Full Blade	1

7.2.4.2 Mechanical Properties - The following table lists the various mechanical tests to be done by section of this plan for a full evaluation of each section as if it were the optimal approach selected.

Section	Description of Test	Type of Specimen	Specimens Req.
7.2.2.3	Weld Specimen	Static Tensile	20
		Bend Test	100
		Fatigue Tensile	32
		Cup Rupture	100
		Fatigue Flexure	64
	Base Material	Static Tensile	30
		Fatigue Tensile	24
		Fracture Tuffness	4
	In Process	Static Tensile	32
2.2.2.4	S.P.F.D.B. Base Matl.	Static Tensile	32
		Fatigue Tensile	10
7.2.3.1	Seam Effects Verification	Static Tensile	30
		Fatigue Tensile	32
		Fatigue Flexure	32
		Peel	12
		Impact	30

7.2.3.1	F.O.D. Whirl	Part Blade	20
	Edge Impact	Full Blade	3
	Blass Missile Gouge	Full Blade	1
7.2.3.2	Zero Mean Fatigue	Full Blade	4
	Resonant Mean Fatigue	Cropped Blade	4
	E.S.A.	Full Blade	1

7.2.5 Facilities

The following table summarizes areas of facilities development that will be required to pursue each potential course of spar process development that has been covered in this plan. The use of each area has been described in the previous sections.

Section	Type of Facility	Development Purpose of Facility
7.2.2.1	Tubing Bender	Handle up to a 9" diameter tapered wall tube.
7.2.2.2	Explosive Forming	Handle open end tapered tube.
7.2.2.3	Plate Reducing	Produce tapered flat stock in HS44 steel.
	Robotic Welding	Weld edges of spar.
	Inertia/Electron Beam Welding	Attach retention to spar.
7.2.2.4	S.P.F.D.B.	Form and bond spar configuration with attached retention.
7.2.3.2	Braiding/Weaving	Produce shaped shell plies with controlled thickness and mechanical properties.

References

1. Jordan, P.F., "Aerodynamic Flutter Coefficients for Subsonic, Sonic, and Supersonic Flow (Linear-Two-Dimensional Theory). Rep. No. Structures 141, British R.A.E., April 1953, ARC. R&M 2932-1953.

2. Barmby, J.G., Cunningham, H.J., and Garrick, I.E., "Study of Effects of Sweep on the Flutter of Cantilever Wings," NACA TN 2121, June 1950.

3. Hassig, Herman, "An Approximate True Damping Solution of the Flutter Equation by Determinant Iteration", J. Aircraft, Vol. 8, No. 11, November 1971.

4. Steinman, D.B., "Aerodynamic Theory of Bridge Oscillations," American Society of Civil Engineers Transactions, Paper No. 2420, October 1949.

5. Wolowics, C.J., Bowman, J.S., Gilbert, W.P., "Similitude Requirements and Scaling Relationships as Applied to Model Testing", NASA Technical Paper 1435, August, 1979.

6. Hunt, G.K., "Similarity Requirements for Aeroelastic Models of Helicopter Rotors", C.P. No. 1245 Aeronautical Research Council Current Papers, Structures Dept., R.A.E., Farnborough, 1973.

7. Scroton, C., Lamborne, N.C., "Similarity Requirements for Flutter Model Testing", Agard Manual on Aeroelasticity, Volume IV, Chapter 6, 1960.

8. Jones, J. Lloyd, "Transonic Testing in Existing Wind Tunnels", Agard - Facilities and Techniques for Aerodynamic Testing at Transonic Speeds - Agard-CP-83-71, August 1971.

9. Turnberg, J., "Classical Flutter Analysis F187 for Swept, Twisted Propellers in Subsonic Flow", Vibration memorandum No. 1004, July, 1981.

APPENDIX A

UNITED TECHNOLOGIES
HAMILTON STANDARD

DESIGN REQUIREMENTS

FOR

ADVANCED TURBOPROP BLADES

Prepared as part of

Propeller Blade Structural Design Study

NASA Contract NAS3-22394

April 1, 1980

Revised June, 1980

UNITED TECHNOLOGIES HAMILTON STANDARD

TABLE OF CONTENTS

UNITED TECHNOLOGIES HAMILTON STANDARD

I. INTRODUCTION

In recent years, considerable attention has been directed toward reducing aircraft fuel consumption. Studies have shown that the inherent efficiency advantage that turboprop propulsion systems have demonstrated at 0.65 Mn may now be extended to the higher cruise speeds of todays turbofan powered aircraft. In order to achieve this goal, new propeller designs will require advancements such as thin, high speed airfoils and aerodynamic sweep.

A program to conduct structural design studies of large scale blades of this type has been funded by NASA LeRC. This program includes the establishment of structural concepts for the fabrication of several of the Prop-Fan model blade configurations in large scale, and the definition of their structural properties.

This document contains a description of the design process, a description of the analysis procedures which will be used during the study, and sets forth the requirements to which the blades will be designed.

UNITED TECHNOLOGIES HAMILTON STANDARD

II. APPROACH TO ANALYSIS

During the program, a total of five blade configurations will be analyzed. One of these configurations (SR-2) will be analyzed using a beam analysis method, while the others will be analyzed using a finite element analysis method. These methods are described below.

Beam Analysis Method (Ref. Figure 1)

The blade aerodynamic inplane and out-of-plane loads are calculated using a computer program (H444). The input to this program is the blade operating condition.

If composite laminates are used in the blade design, the elastic properties will be calculated using a composite material laminate analysis program, H250. This program has the capability to calculate the laminate stress allowable based on the orthotropic stress allowables of each layer.

The blade aerodynamic data, aerodynamic loads, and fabrication method are entered into a computer program (H882) which creates streamline airfoil sections. The airfoil sections are based on a "library" of airfoil coordinate data for many standard airfoils over a wide range of thickness ratios and camber levels. Internal cross-section geometry coordinates, where required, and lead edge sheath definitions are also created in H882. The streamline airfoil sections are then stacked relative to one another by computer program H883 to produce the aero-acoustically dictated three-dimensional blade shape. The blade shape is generated by fairing the streamline airfoil sections and internal blade geometry using spline curves in computer program H884. Orthagonal planes are cut through the faired blade geometry at desired radial locations for beam property calculations and manufacturing dimensional definition.

Blade section properties are calculated by computer program H886, based on the radial station cross-sections. Equivalent cross-sectional properties for non-homogenous blade components are also calculated using their elastic modulii and density ratios. Pertinent cross-sectional properties are then integrated along the blade span to determine weight, blade stiffness distribution, and mass distribution.

UNITED TECHNOLOGIES
HAMILTON STANDARD

FLOW DIAGRAM

BEAM ANALYSIS

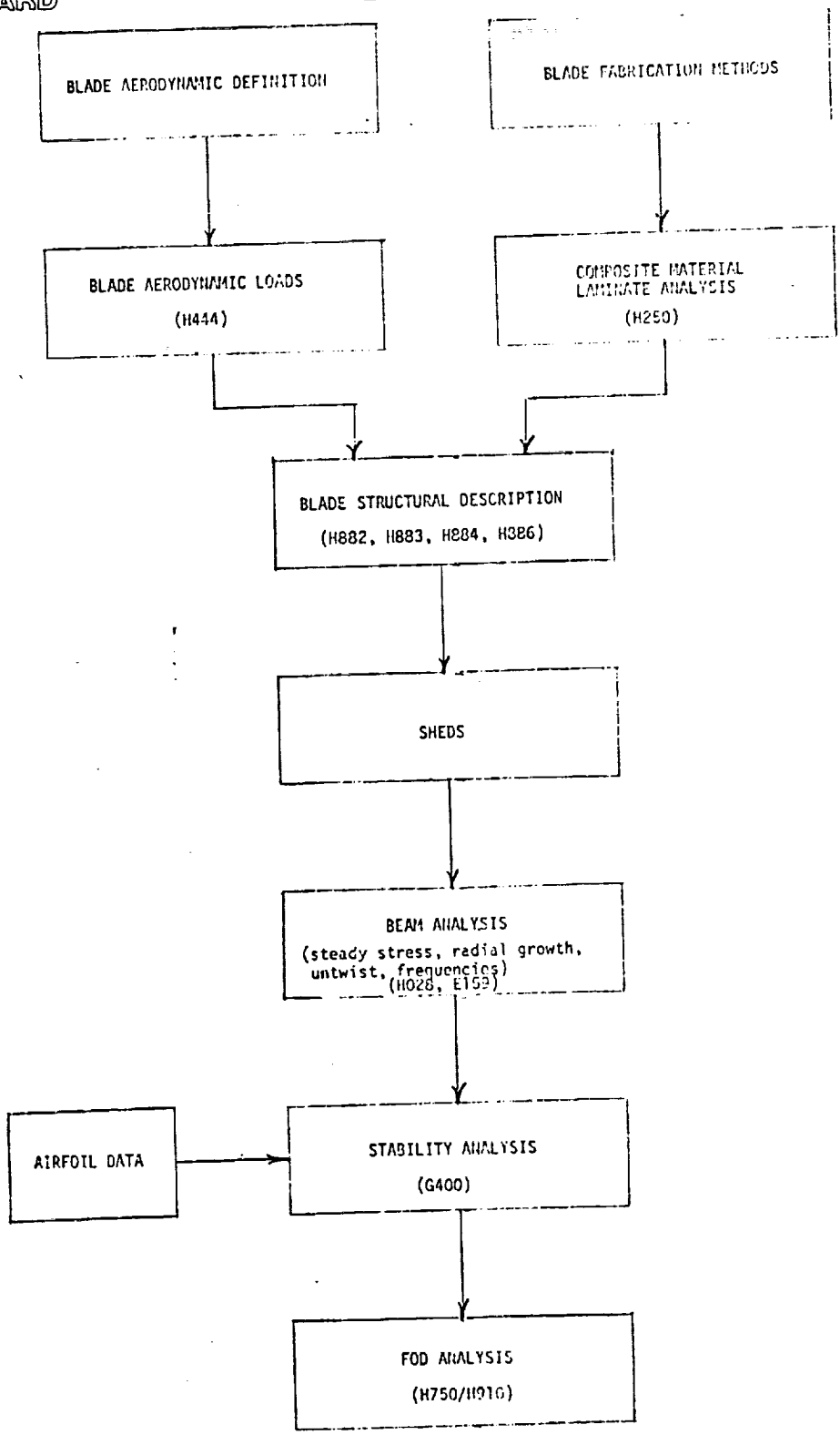

FIGURE 1

The data generated during the preceeding programs is stored in a common computer data base storage system called SHEDS (Structured Hamilton Standard Engineering Data Storage). This common data base is accessed by the beam theory programs for the structural definition of the blade.

The steady state stress analysis program (H028) uses the aerodynamic loading distribution along the blade span and normal to the cross-section's chord. The loading distribution is resolved into in-plane and out-of-plane components and an iterative algorithm is used to determine the final deflected position. The resultant steady bending moment is resolved into flatwise and edgewise components which are used to calculate the steady state stress distribution along the blade span. Computer program E159 uses a Myklestad procedure to generate the uncoupled blade flatwise, edgewise and torsion modes required in the response program.

An aeroelastic dynamic time history response analysis computer program (G400) will be used to calculate blade steady and cyclic stresses, blade and hub moments, blade displacements, and blade damping. This analysis is a single blade multi-purpose computer program characterized by a rigorous modeling of the blade and accounting for the non-linear and time varying structural twist. The differential equations of blade bending (flatwise and edgewise) and torsion are solved using a Galerkin procedure wherein the normal uncoupled mode shapes, their spanwise derivatives and the spanwise derivative of the blade (non-linear) twist are combined to describe the coupled blade deflections. Appropriate airfoil data are input to the program. For the Prop-Fan, the airfoil data is comprised of coefficients of lift, drag, and moment vs. angle of attack for Series 16 airfoils. Two types of solutions are available: eigensolutions of various linearized equation sets for coupled frequency and/or stability analysis purposes, and time-history solutions of the complete non-linear equations for harmonic analysis and/or transient aeroelastic response calculation purposes. Transient time histories can be generated in numerical and/or plotted form. A moving block spectral analysis technique is employed to display the predominant response modes giving the frequencies and damping under loaded conditions. If the damping is negative, system instability is indicated and the time histories show increasing amplitude. This method will be used to determine classical stability as well as stability in areas of dynamic stall.

The blade design will be subjected to a Foreign Object Damage analysis using computer programs H750/H910. These programs are a three mode interactive blade impact program which utilizes a fluid missile model which is interactive with the dynamic modal response of the blade.

Finite Element Analysis Method (Ref. Figure 2)

The blade aerodynamic data, aerodynamic loads and fabrication methods are entered into SHEDS using computer programs H250, H444, H882, H883, H884, and H886 in the same manner as the Beam Analysis Method.

The finite element model is generated using program F018. This program utilizes the blade data from SHEDS and allows the designer to generate the model interactively on a computer terminal.

The finite element analysis will be performed using a computerized general purpose three-dimensional finite element program known as BESTRAN-H552. This is a program comprising several specialized subprograms which work together, based on the methods of finite element analysis. The analysis will calculate steady stresses and deflections at speed. Frequency, mode shape, and stress distributions will be calculated at rest and at speed and used to generate the Campbell Plot.

The frequency and mode shape data are then used in computer program G400, described in the Beam Analysis Method, to determine stability.

The blade design will then be subjected to a Foreign Object Damage analysis using computer programs H750/H910.

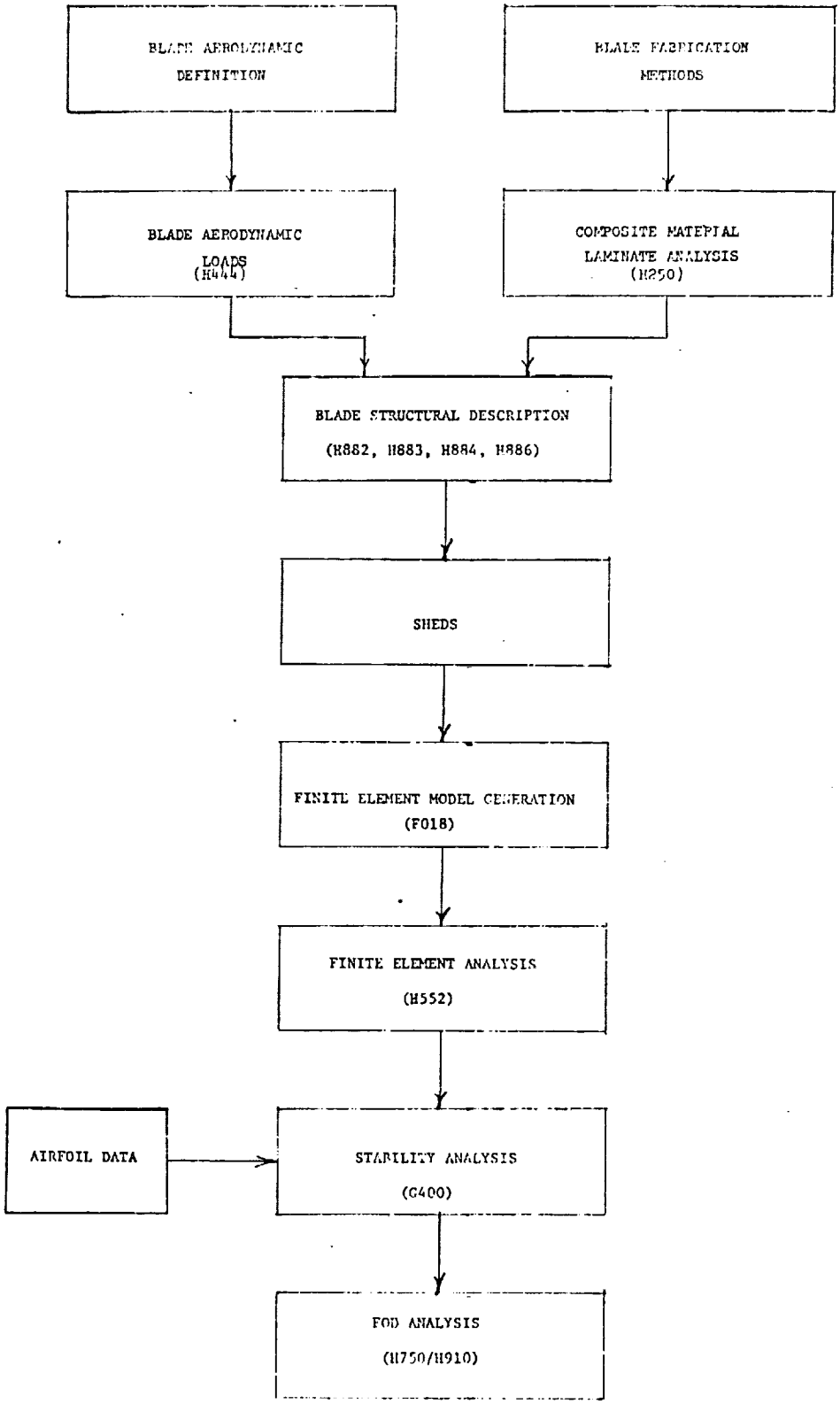

FIGURE 2

III. DESCRIPTION OF ANALYSES

A. Aerodynamic Loads (H-444)

The once-per-revolution (1P) airloads are computed by means of the Hamilton Standard strip analysis program (Deck No. H444) utilizing two-dimensional compressible airfoil data. An operating condition is defined in terms of shaft horsepower, propeller rotational speed, pressure altitude, velocity, ambient temperature and inflow angle. These parameters in turn define the non-dimensional coefficients required to do a strip analysis, namely, advance ratio, J and power coefficient, Cp, defined as:

$$J = v/nD$$

$$C_p = P/\rho\, n^3 D^5$$

where v = true airspeed, feet per second

n = propeller speed, rps

D = diameter, feet

P = power, ft. lbs./ second

ρ = density, lb. sec.^{2}/ft.^{4}

The advance ratio and inflow angle define the blade advance angle radially and azimuthally.

An iterative procedure is then utilized to calculate the blade angle at the given operating condition to absorb the proper power coefficient, Cp. For example, for the eight bladed Prop-Fan eight azimuthal positions are examined and the elemental power coefficient is intergrated both azimuthally and radially until the required Cp is attained.

Once the blade angle is determined, the elemental in-plane force (Fr) and the elemental out-of-plane force (Fp) are calculated at the advancing and retreating positions. From these results, the change in in-plane and out-of-plane force (Fr & Fp respectively) are determined. These loads are then used in the multiazimuth analysis (H045) which is used in the determination of the excitation factor defined in IIID. The loads are also used as an input to the BESTRAN analysis (H552).

B. Mechanical Loads

1. Steady Tension (H-028 or H-552)

The most obvious load on a propeller blade is due to centrifugal force. Centrifugal force acts on blade mass elements to produce radial tensile forces which are additive from the blade tip, R, down to any radius, r_1, being studied. The total centrifugal load developed at radius r_1, is found by integrating as follows:

$$C.L. = \omega^2 \rho \int_{r_1}^{R} Ardr$$

where ω is the angular rotation speed, ρ is the mass density of the blade material, A is the blade cross sectional area and r_1 is the radius of the blade section. This force is a pure tensile load when the cross section mass centers are aligned on a single axis perpendicular to and passing through the axis of rotation. This is commonly called the "stacking axis".

2. Steady Bending (H-028 or H-552)

As a propeller blade rotates through the air, each portion of the blade produces a lift and drag force. The magnitude of these forces are determined by the specific characteristics of airfoil shape and its operating parameters as shown in Figure 3.

At any blade radial position, these aerodynamic forces, calculated with a strip analysis program, can be resolved into two vectors, thrust (T), and torque (Q), as shown in Figure 4. Also illustrated is the origin of a secondary aerodynamic steady load, aerodynamic twisting moment. This comes from the distance between the quarter chord point and the stacking axis which is commonly the centerline of the blade retention bearing and the axis about which the blade angle control mechanism torque is applied.

Summing these thrust and torque forces along the span of the blade yields the total thrust and torque per blade. These distributed forces produce bending moments in the cantilevered blade. From the preceding discussion of steady centrifugal loads, it is obvious that by offsetting the centers of gravity of the

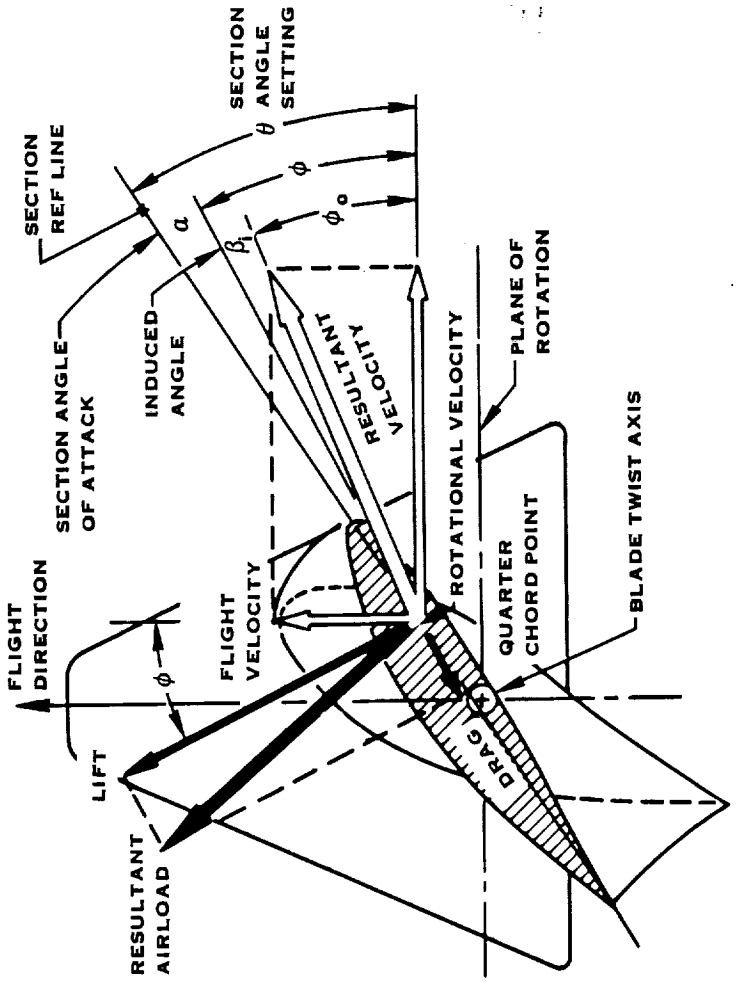

BLADE AERODYNAMIC LOAD RELATIONSHIPS

FIGURE 3.

DEVELOPMENT AND RESOLUTION OF PROPELLER BLADE AIRLOADS

FIGURE 4

blade cross sections from the radial stacking axis in a systematic fashion, centrifugal bending moments can be developed in addition to the tensile loads. These moments are in a direction which tends to return the displaced mass center to the radial axis and are called centrifugal restoring moments. In some blades initial displacements along the local section chordline (sweep) and/or perpendicular to the local section chordline (offset) are built into the blade in order to generate restoring moments which reduce the aerodynamic bending moments.

3. Steady Untwist (H-886 or H-552)

Since a propeller blade operates in a radial centrifugal force field there are forces developed that tend to align the blade parallel to the plane of rotation. Resolution of these forces about the stacking axis into centrifugal twisting moments can be seen in Figure 5. In this figure the total cross sectional mass of a typical blade radial element is separated into two centers of mass, one for the leading edge portion of blade at distance "a" from the plane of rotation; and one for the trailing edge portion of the blade at distance "b" from the plane of rotation. Radial centrifugal force vectors, originating from the propeller rotational axis can be drawn through each of these mass centers. Each of these vectors may be separated into radial components parallel to the blade centerline and in-plane components, P_L and P_T, parallel to the plane of rotation.

The two components, at moment arms "a" and "b" generate a centrifugal twisting moment about the stacking axis which tries to align the section with the plane of rotation. This twisting moment for any specific section varies sinusoidally with the angular position of that section with respect to the plane of rotation. Consequently, the twisting moment about the stacking axis varies sinusoidally with section blade angle referenced to the plane of rotation over a period of 90°.

The twisting moments of each incremental cross section of a blade can be summed from tip to root resulting in a net twisting moment about the stacking axis at the blade root. In most operating conditions this centrifugal twisting moment is opposite in sense to the previously discussed aerodynamic twisting moment. The net twisting moment is a torque that must be carried by the blade angle control mechanism in order to maintain blade angle setting.

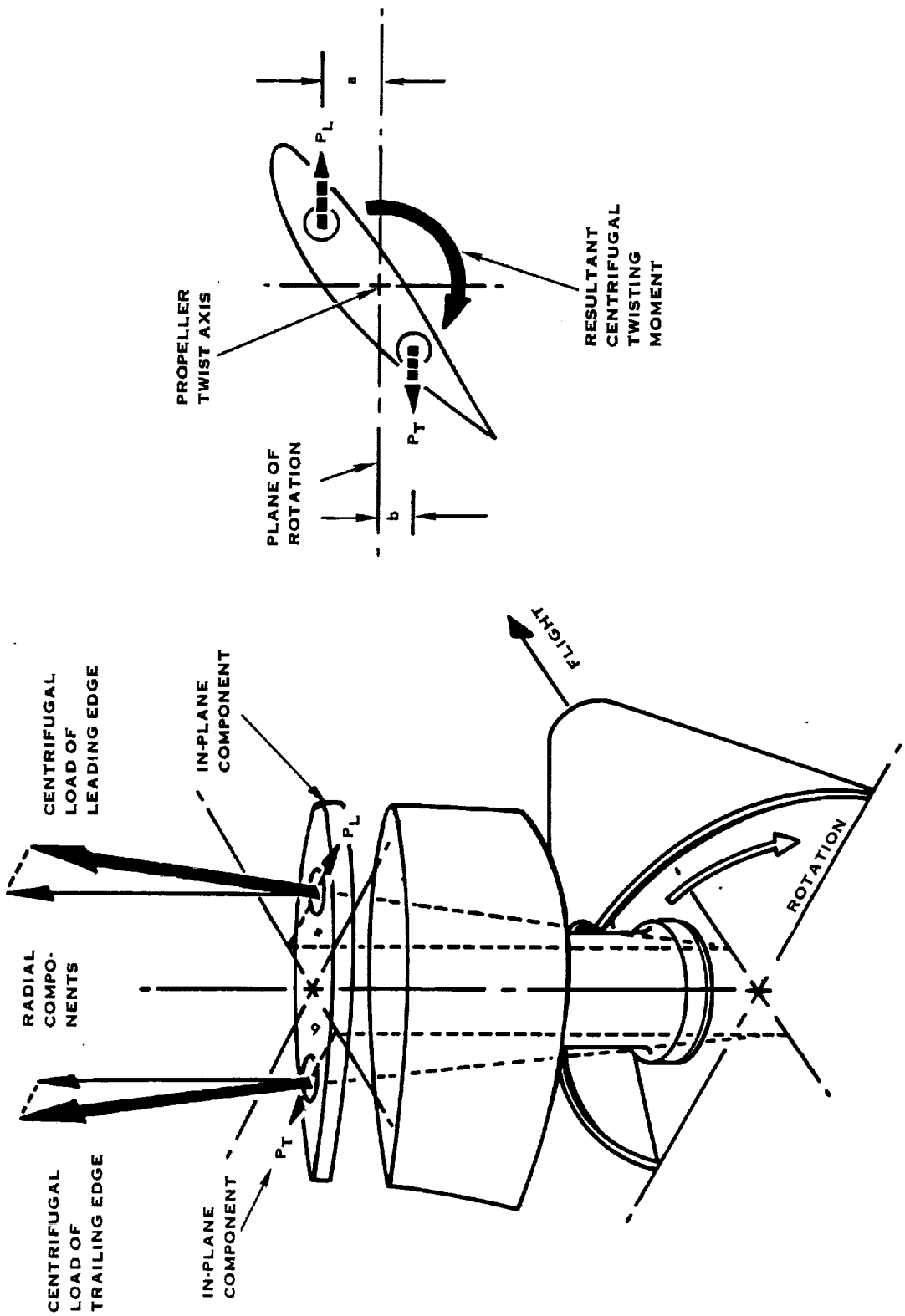

FIGURE 5. CTM DEVELOPMENT OF PROPELLER BLADE CENTRIFUGAL TWISTING MOMENT

These same offset mass forces lead to twisting moments within the blade even when the net root twisting moment is zero. This is because a blade has a built in twist distribution and there can be no single blade angle setting which results in a zero twisting moment for all incremental sections along its radial length. These internal centrifugal twisting moments, balanced by aerodynamic twisting moments, act to reduce the built in twist distribution of the blade, thus the common term "untwist". It is normal to correct for the untwist by building in a compensating amount of pretwist. As with sweep and offset, pretwist can only be exactly correct for one operating condition.

The basic explanation of the mechanical loading of a blade given above has been in beam theory terms. The blade is assumed clamped at some fixed location near the center of rotation. The classical beam section properties are calculated for an appropriate number of blade segments along the blade radial length. The radial increment between segments is chosen depending on the rapidity of geometric variation. These sections are then stacked in space relative to a radial line, the stacking axis, which passes through the axis of rotation. The mechanical body forces are then determined for the appropriate rotational speed by summing from tip to root. The mathematical description of a twisted, tapered, rotating beam subjected to distributed aerodynamic loading is a complicated process. The methods, however, are well established and proven by over forty years of application. The use of modern computers has made this task very straightforward.

All of the same mechanical loads can be calculated using finite element analysis methods. The method in common use at Hamilton Standard is called BESTRAN. BESTRAN is a broad based system written in FORTRAN language that is similar to but much less comprehensive than NASTRAN. Identical results have been obtained on comparative running of the two programs. BESTRAN is more commonly used at HS than NASTRAN because of a wide variety of pre- and post-processing methods that are keyed to BESTRAN.

An auxiliary program, ST570, is used for analyzing steady stresses and deflections in rotating structures. It applies to structures that can be modeled as plates or shells of arbitrary shape and thickness. The analysis recognizes centrifugal stiffening effects. There are eleven element types available which include types for isotropic or anisotropic materials. Several blade types have been analyzed using BESTRAN. Detailed comparisons with measured stresses and deflections confirm the applicability of this analysis method.

C. Critical Speeds (E-159)

Every piece of rotating machinery has one or more "critical speeds". This critical speed results from the coincidence of some periodic, speed dependent forcing function and the natural frequency of the machine or some part of the machine. Certainly any bladed rotating device must be examined for critical speeds because of the many modes of resonant vibration the individual cantilevered blades can have and the various ways these blades modes can combine to produce rotor modes. The periodic forcing functions can be mechanical in origin such as gyroscopic precession, unbalance, engine firing torques, etc. or aerodynamic in origin such as an inclined flow field or a distorted flow field which becomes periodic to the propeller as it rotates through it. It is important to note that this discussion does not include "self excited" vibratory response--flutter phenomena. Flutter involves the interaction of the elastic motions of the blade and the aerodynamic loading and is discussed in Section F.

In propellers, the foundation of a critical speed study is the determination of the blade frequencies. Vibratory deflections that meet fatigue strength criteria are small enough so that aerodynamic coupling can be neglected. The hub to tip diameter ratios and the hub geometry is such that blade dynamic response is not influenced by hub dynamics. The blade retention stiffness and blade angle control mechanism stiffness must be considered as well as centrifugal stiffening effects.

The range of blade frequencies that are of interest is determined by the number of periodic forcing functions possible and the strength of those excitations. For Prop-Fans of eight blades or more, excitations up to 5 per revolution are judged to be significant. This judgement is preliminary and will be biased by the configuration and operating regime of each individual installation. Accepting the 5 per revolution judgement as appropriate for this study, all blade frequencies that fall above 5 per revolution at maximum operating speed need not be considered. This can be seen from Figure 6 which is an example of a standard Campbell Plot. Here the first, second, and third modes would be studied for intersections with integer order exciting frequencies, but the fourth mode would not be considered because there is no critical speed near the operating regime.

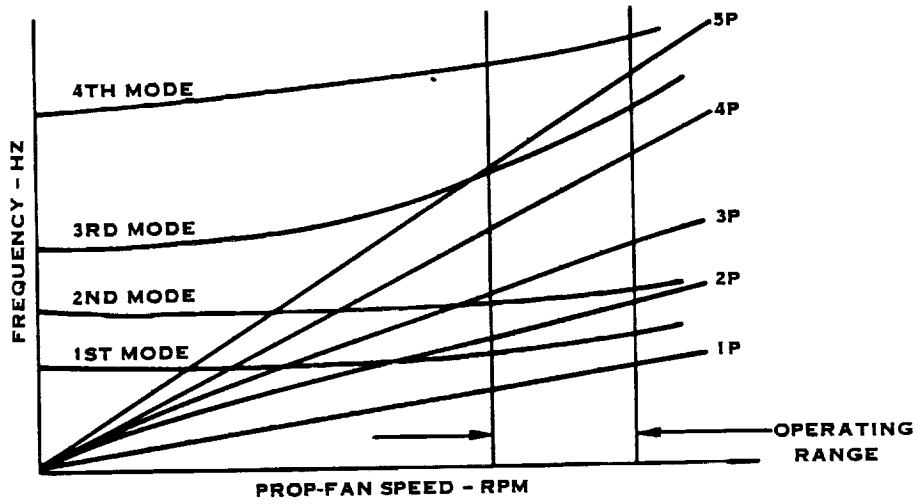

FIGURE 6. CAMPBELL PLOT

The intersection of a blade frequency and an interger order excitation line is studied because it represents the possibility of excitation at resonance where the amplitude of response is limited only by the available damping. The location of the critical speeds can be altered by the possible modes of rotor vibration and the dynamic characteristics of the rotor mounting. Rotor modes can be divided into four basic categories.

1) Those in which the sum of the vibratory moments on the propeller shaft is zero, but the sum of the forces is finite. This mode is called "symmetrical" and is characterized by in-phase bending of the blades which results in a fore and aft reaction on the rotor mounting.

2) Those in which the sum of the vibratory moments on the propeller shaft is finite, but the sum of the forces are zero. This mode is called "unsymmetrical" and is characterized by a lateral or whirling reaction on the rotor mounting.

3) Those in which neither a vibratory moment nor a vibratory force is transmitted to the rotor mounting. This mode is called "reactionless" since the forces and motions are confined to the propeller; no loads or motions are transmitted to the rotor mounting.

4) Those in which both moments and forces are transmitted to the rotor mounting. This mode can occur only at 1P frequency due to an inclined flow field or gyroscopic action. The 1P mode is unique in that it does not involve resonance although having blade frequencies near 1P will increase the stress response due to inertial magnification.

The first three categories are illustrated in Figure 7. The third category is of particular interest with eight and ten bladed Prop-Fans. The number of reactionless modes possible for an eight bladed rotor span the range from 2P to 6P, 7P and 9P are whirl modes and 8P is a symmetrical mode. Critical speeds for the first six exciting orders can be accurately predicted from a knowledge of the rotor alone. Critical speeds from 7P to 9P would require a knowledge of the rotor mounting impedance. As mentioned earlier, however, excitations beyond 5P are weak enough to be ignored. With a ten bladed rotor, the reactionless modes extend from 2P through 8P, 9P and 11P are whirl modes and 10P is a symmetrical mode.

ROTOR VIBRATION MODES

FIGURE 7.

The static and rotating blade frequencies can be calculated by beam theory or finite element analytical methods. The beam method will be discussed first.

For the theoretical analysis of the flexural vibration of a propeller blade, it must be constrained so that at some defined location near the center of rotation only uniform rotational motion is possible. This condition of end fixity was chosen to cover both symmetrical and unsymmetrical rotor modes. The system is furthermore assumed to be linear, with small vibratory displacements, and simple beam bending theory is used. The differential equations of equilibrium are first derived and transformed into integral equations, and they are then examined in the form of a matrix equation for a segmented blade, which permits the evaluation of vibratory response, critical speeds, and normal modes by simple classical methods.

The finite element program used for frequency determination is the same as described in Section III B. An auxiliary program, VIBR, is used that can perform vibration analysis of a wide variety of simple and complex structures. It determines vibratory response in the form of modal displacements for all possible degrees of freedom on systems excited by specified vibratory forces at the nodes or for specified vibratory frequencies. Problems involving bending, longitudinal and torsional vibrations, gyroscopic coupling effects, and combinations of effects can be solved. Resonant frequencies are found by a determinant search. Stress and deflection mode shapes can be generated and plotted out for any of the determinate cross-overs. Twenty-five element types are available to describe the blade which attests to broad based applicability of this analysis.

D. Aerodynamic Excitation (H039 & H045)

The primary source of vibratory stresses in a turbine-driven aircraft propeller is the periodic variation in aerodynamic forces caused by asymmetry in the direction and velocity of inflow to the propeller. Such periodic variations in force cause excitations at frequencies which are integer multiples of the propeller speed. These excitations are referred to as "P" orders - 1P, 2P, 3P, etc. The most important of these P-order excitations is the fundamental or 1P because it is, by far, the greatest in magnitude.

The unsymmetrical inflow to the propeller is caused by two major factors; 1) overall misalignment between the thrust axis and the incoming air velocity, and, 2) distortions to the free-stream flow due to the lift on the aircraft wing and disturbances due to flow past the other parts of the aircraft (fuselage, nacelle, etc.). The misalignment or angular inflow causes mostly 1P excitation while the distortions tend to cause both 1P and higher order excitations.

The aerodynamic excitations due to unsymmetric inflow are evaluated by first determining the pattern of flow coming into the propeller for various flight operating conditions. This is done by computerized analysis (H039) which calculates the disturbances caused by the individual structural components of the aircraft (wing, fuselage, nacelle, etc.) and superimposing them to give the total flow-field seen by the propeller.

This program has the capability to handle three lifting surfaces (the wing, the pylon, and the tail surface) either separately or simultaneously. The lift for each of these surfaces is predetermined, with the total lift being equal to the aircraft gross weight. The propeller and nacelle can be located anywhere in the flow-field except on the centerline of any of the three lifting surfaces. The flow-field effects analyzed for the lifting surfaces are; circulation due to lift, cross flow and rectilinear flow. The effects of thickness and sweep of the surface are accounted for. The lifting surface velocity components are computed by standard vortex methods that assume the velocity is proportional to the circulation functions and is inversely proportional to radius as given by:

$$v_w = \frac{1}{4\pi} S_w \int \frac{1}{r} \, d\Gamma$$

and

$$d\Gamma = \frac{dL}{\rho U}$$

where

v_w = Velocity component radius r

r = Radius from the center of the vortex.

$d\Gamma$ = Circulation function or vortex strength element

S_w = Surface semi-span

dL = Incremental lift along the span

ρ = Air density

U = Local blade section velocity

The velocity component is determined in the plane of the propeller and assumes an elliptical spanwise lift distribution. The resulting velocity is an integrated effect that includes the bound vorticies as well as the trailing vortex sheet.

The cross flow effect is a flow disturbance caused by the component of the free stream normal to the lifting surface chord passing around the lifting surface planform. The surface is assumed to have an elliptical cross section and the complex velocity potential is calculated for flow perpendicular to the major axis of the ellipse.

The lifting surface rectilinear flow is a flow distrubance caused by the finite thickness of the surface. The surface is again assumed to have an elliptical cross section and assumes that the chord and thickness are constant. The complex velocity potential is calculated for flow parallel to the major axis.

The flow field effects analyzed for the fuselage and nacelle are cross flow and rectilinear flow.

The cross flow is treated as a complex velocity potential where the equations are solved by treating the body as a number of equivalent cylinders. The potential function is determined by distributing doublets of unknown strength, oriented vertically, along the body axis. The doublet strength is then determined by setting the velocity potential equal to zero on the body surface.

For rectilinear flow, the body is assumed to be an asymetric rankine solid containing a single point source.

For each of the components (wing, fuselage, nacelle, etc.) the velocity perturbation is computed and superimposed on the free stream flow field in the plane of the Prop-Fan. Axial and tangential flow components are then calculated.

These flow components are then input to a multiazimuth airload program (H045). This program accomplishes aerodynamic strip-analysis calculations at many azimuthal positions to obtain time-history variations of the aerodynamic loads. Harmonic analysis is then performed on these loads and the blade dynamic response is computed for each P-order harmonic.

Since the 1P aerodynamic excitation is the most important by virtue of its magnitude, it is a principal factor controlling the design of a propeller blade. It has been found that the magnitude of the 1P excitation is roughly proportional to the product of the inflow angle and the equivalent airspeed squared. Therefore a parameter called Excitation Factor (EF) was defined as $EF = \psi \left(\frac{Ve}{348}\right)^2$, where ψ is the inflow angle in degrees and Ve is the equivalent airspeed in knots. Excitation Factor is a convenient measure of the severity of 1P aerodynamic excitations, and the manner in which EF varies with flight conditions is an important consideration.

This method was used to estimate the excitations due to the flow fields for Prop-Fan installations on the DC-9 and B767 aircraft. The results of these two studies were used to establish the excitation factor to be used in this program. The excitation factor is input to the response program (H026).

E. Response (H-026)

The response of a propeller to periodic unsteady aerodynamic loads as measured by stress or deflection amplitude is determined by four items:

1. The magnitude of the unsteady applied air loads.

2. The total stiffness of the blade which must include the centrifugal enhancement of the static stiffness.

3. The instantaneous elastic angular deflection of the blade since it is a first order influence on the angle of attack of the distributed airfoil sections. Bending motions and cross sectional distortion also affect the thrust and torque generated by a propeller blade. These latter two distortions are negligibly small because of the inherent stiffness and mass of a propeller blade relative to the magnitude of the cyclic air loads.

4. The proximity of a critical speed to a predominant harmonic of the unsteady airload.

For this study, it is desirable to define an excitation factor which is a measure of the total vibratory excitation, including the nP harmonics. The way a blade responds to nP excitations is dependent upon critical speed locations or nearness to resonance. In order to define an equivalent excitation factor, a magnification factor will be assumed and applied to the nP excitations.

With beam modeling, all four of these effects are handled. The method requires a complete multi-degree of freedom model of the rotating blade and a harmonic description of the unsteady air loading. The air loads are applied with proper periodicity as distributions of thrust and torque forces along the blade radial span. The twist deflections are iterated until equilibrium is achieved. The resulting modified radial airload distribution is then used to calculate the bending moments in the rotor coordinate and local blade coordinate systems. The moments are modified by applying a dynamic magnification factor based on the proximity of the harmonic content of the unsteady loading and the critical speeds. This modified moment distribution is used to calculate blade deflection and stressing. The blade root moments and shear forces are also summed at the rotor attachment to predict rotor hub and attachment loadings.

The use of a finite element model of the blade results in a more exact description of the blade structure but the interaction of this model with the applied airload is not as well modeled as with the beam approach. This is not an inherent limitation of the finite element approach, the methodology has not yet been developed. For this study the maximum and minimum airload distributions will be calculated. These airloads will be applied to the blade model as line loads at the appropriate nodes representing the center of pressure for each radial airfoil section. Stresses and deflections will be calculated for each load case and the maximum difference anywhere in the airfoil will be determined. This stress range will be combined with the appropriate steady stress and used for the fatigue life determination.

F. Flutter (G-400)

In the past, flutter in the classical sense, has not been a problem for conventional propeller designs and conventional operating conditions. The Prop-Fan, however, with its high activity factor operates at dynamic pressures much greater than those found in the conventional propeller environment. The Prop-Fan also has more blade sweep than conventional propellers. These factors cause more concern about blade stability. For this design study, classical flutter will be investigated using a single-blade, multi-degree-of-freedom aeroelastic analysis.

This program has been under development at UTRC for approximately six years and is used extensively in the research activities at UTRC as well as at Sikorsky and Hamilton Standard. This analysis is a single blade, multi-purpose computer program characterized by a rigorous modeling of the blade and accounting for the non-linear and time varying structural twist. Although developed in response to the specialized requirements of composite, bearingless rotors, the dynamic equations developed for this analysis are sufficiently general for valid application to all conventional rotor systems: articulated, semi-articulated, teetering and hingeless, as well as to propellers, Prop-Fans, and wind turbines. The differential equations of blade bending (flatwise and edgewise) and torsion are solved using a Galerkin procedure wherein the normal uncoupled bending mode shapes, their spanwise derivatives, and the spanwise derivative of the blade (nonlinear) twist are combined to describe the coupled blade deflections. Two types of solutions are available: eigensolutions of various linearized equation sets for coupled frequency and/or stability analysis purposes, and time-history solutions of the complete nonlinear equations for harmonic analysis and/or transient aeroelastic response calculation purposes.

Because of its interest in Prop-Fans, Hamilton Standard has incorporated sweep in the nonlinear portion of this analysis, such that it can be considered a curved beam dynamic response analysis. The aerodynamic description includes the use of predetermined static airfoil data, constant or variable (multiple harmonic and spanwise variable) inflow, and unsteady dynamic stall data. The blade dynamic description allows the use of three flatwise, two edgewise and two torsion modes to determine higher order as well as once-per-rev responses.

This analysis produces the following output: blade steady and cyclic stresses, blade and hub moments, blade displacements, blade damping. Transient time histories of these quantities can be generated in numerical and/or plotted forms. A moving block spectral analysis technique is employed to display the predominant response modes giving the frequencies and damping under loaded conditions. If the damping is negative, system instability is indicated and the time histories show increasing amplitude. This aeroelastic method will be used to determine classical stability as well as stability in areas of dynamic stall.

Unlike classical flutter, stall flutter has normally been investigated on propellers. This problem has been handled successfully in the past using a stall flutter parameter which relates blade stiffness to forward speed, and by using the above mentioned multi-degree-of-freedom aeroelastic analysis.

The damping ratio will be plotted as a function of horsepower. The point of instability is determined where the damping ratio goes to zero. If this horsepower value is larger than the power available, then stall flutter is not possible.

G. Foreign Object Damage Analysis (H-750/H-910)

The evaluation of foreign object impact resistance involves three steps:

1) The definition of the impact conditions;

2) The determination of the gross impact loads, blade response, and blade stressing from the gross structural blade characteristics; and

3) The determination of local stressing based on detailed local stress analysis.

The first step is fundamental to all of the blade designs since it depends only on the engine characteristics, size and density of the foreign object, the airspeed, and the radial impact position on the blade. For this program, the operating condition which previous analyses have shown to be the most severe will be used. A preprocessor determines the penetration of a cylindrical mass (representing the object) into the plane of the rotor and thus defines the fundamental impact parameters of size, weight, velocity and angle of impact of the slice of theingested foreign object, which are needed for the second step of the analysis.

Having defined the impact conditions, the gross blade impact load, response, and stressing with time will then be calculated using the 3 dimensional (3 mode) computer program, H750/H910. The data stored in the SHEDS system for the blade designs are the structural characteristics that are used by H750/H910 in the FOD analysis.

The Three-Mode-Interactive Blade Impact Program utilizes a fluid missile model which is interactive with the dynamic modal response of the blade. This feature is essential to the analysis of FOD impacts, since the changing impact angle due to blade twist, the physical size of the missile, the changing rate at which it spreads on the blade surface during the impact event and the spreading mass thickness distribution have a large influence on blade response. The three-mode analysis uses the three beam-type modes of vibration to characterize the gross blade dynamics; i.e., the first flatwise bending, the first edgewise bending and the first torsional modes. Although coupling between blade modes is accounted for in the dynamic characteristics input to the three-mode analysis, only the dynamic response of the blade flatwise and torsional modes are coupled in the impact. This makes the calculated blade response stresses slightly conservative.

The accuracy of the analytical methods has been confirmed by several tests. In addition, the pressure distribution as calculated for the fluid missile model used by the three-mode analysis correlates quite well with test data.

After defining the gross blade characteristics, and the resulting impact loads, gross stresses, and response with time for the various impacts, the blade will then be analyzed for local stressing in the impact region. This stress will be calculated using the impact load distribution and magnitude from the gross impact analysis. The gross blade stresses and the local blade stresses are then compared to appropriate material stress allowables and to the foreign object damage limits as defined in the Design Requirements Document to determine if the blade design satisfies all of the specified design requirements.

IV. DESIGN REQUIREMENTS

A. Configurations

The configurations which will be structurally analyzed are listed in the following table.

BLADE DEFINITION

	SR-2	SR-3 8-way	SR-3 10-way	SR-5
Tip Speed (ft/sec)	800	800	800	800
Tip Diameter (feet)	11	11	11	11
Number of Blades	8	8	10	10
Tip Sweep (degrees)	0	35	35	48
Activity Factor	203	234	187	210

B. Operating Conditions

This section defines the operating conditions to be used during the design study.

1. Load Spectrum

Condition	Altitude	Airspeed	SHP	Fan rpm
T.O./Climb	Sea Level	0.2Mn	9075	1389
Max Climb	35,000 feet	0.8MN	4537	1389

2. Foreign Object Damage

The foreign object damage analysis will be conducted at the take/off climb condition.

3. Excitation Factor

The maximum excitation factor was determined to occur at the following condition:

Condition	Altitude	Airspeed	Weight
Climb	Sea Level	190 Knots	250,000 lbs.

4. Centrifugal Twisting Moment

The centrifugally induced twisting moment at the blade root about the blade retention bearing centerline will be calculated at maximum rated speed as a function of blade angle setting. This will permit scaling for other operating speeds and blade angles by the relationships discussed in Section III B.3. This twisting moment must be combined with aerodynamic and friction twisting moments in order to size the blade angle control mechanism.

5. Overspeed

All elements of the rotating propeller will be designed to withstand 125% overspeed or 150% centrifugal load with no inelastic deformation.

All elements of the rotating propeller will be designed to withstand 140% overspeed or 200% centrifugal load. This includes the blade, retention, disc, and blade angle control mechanism. Local inelastic deformation will be permitted in all of these elements at this overspeed but the propeller will be capable of changing pitch after exposure to 140% overspeed.

6. Flutter

Classical flutter boundaries will be determined by degrading the torsional frequency at various propeller rpms and forward speeds.

Stall flutter will be calculated for various horsepowers and propeller rpms.

7. Aerodynamic Loads

The aerodynamic loads will be determined for the conditions listed in IV B.1.

8. Mechanical Loads

a. Steady Tension

The steady tension loads will be determined at 100%, 125%, and 140% of maximum rated speed.

b. Steady Bending

The centrifugally induced steady bending loads will be determined at 100%, 125%, and 140% of maximum rated speed. The aerodynamically induced steady bending moment will be determined at maximum rated thrust and 100% speed only. Propeller overspeeds are generally associated with a loss in thrust due to a blade angle fault or application of negative torque, so that centrifugally induced bending moments are dominant at 125% and 140% overspeed conditions.

c. Steady Untwist

The centrifugally induced steady untwist loads will be determined at 100%, 125%, and 140% of maximum rated speed. The aerodynamically indueed twisting loads will be determined at maximum rated thrust and 100% speed only. The centrifugal loads would be dominant at the overspeed conditions.

d. Other

Other loads are present but, particularly for large commercial transport aircraft, the load limits set by the airframe and passenger comfort keep the resulting propeller stressing well within the capacity of the propeller. These loads include: gyroscopic, hard landings, gusts, etc.

C. Critical Speed Margins

The aerodynamically induced cyclic loads during cross-wind operation on the ground are commonly more severe than experienced when the aircraft has forward airspeed. For the 2P excitation, the ground operation critical speed margin shall be a minimum of 20% of propeller speed and resonant frequency. The flight margin shall be a minimum of 10% of

propeller speed and resonant frequency. This margin shall be reduced inversely as the exciting order is increased from 3P up to 5P. No 1P critical speeds shall be permitted in the propeller operating speed range and the minimum margin shall be 40% of maximum propeller operating speed. In determining these margins, the effect of blade angle on frequencies will be included.

D. Aerodynamic Excitations

The equivalent design 1P Excitation Factor (EF) will be 4.5. The basic EF due to 1P only is 3.30.

Normally, EF is only used as a measure of the 1P excitation. However, for design purposes it is desirable to define a quantity which is a measure of the total vibratory excitation, including the nP harmonics. The way a blade responds to nP excitations is dependent upon critical speed locations or nearness to resonance. For the purpose of defining an Equivalent Design Excitation Factor it was assumed that the nP excitations for the Prop-Fan would have a magnification factor of 3, and 1P magnification factor was assumed to be unity.

The relative magnitude of the 1P and nP excitations are as follows:

Order	Un-magnified	Magnified
1P	1.00	1.00
2P	0.125	0.375
3P	0.037	0.111
4P	0.016	0.048
5P	0.008	0.024

The Equivalent Design Excitation Factor is a combination of all the P-orders, including the magnification estimate and consideration of the manner in which harmonics combine to give total amplitude.

E. Distortion Criteria

During normal operation a propeller blade distorts elastically due to steady and cyclic loads. The cyclic deformations are small as compared with a helicopter blade, small enough so that accurate structural response can be determined without inclusion of aeroelastic coupling for all cyclic excitations except that at 1P frequency. At 1P frequency the aeroelastic effects commonly are less than 10% of the basic loading. Consequently, the elastic distortions due to cyclic loading will not be evaluated. Due to steady loads a propeller blade can change diameter,

sweep, offset, twist and camber. Width and thickness changes are insignificant. Of these five geometric changes, only offset variations have no aero-acoustic effect. The magnitude of the other four distortions will be determined to permit comparisons between construction concepts.

No absolute limits will be set on distortion, other than those implied by stress and buckling limits. The acceptability of distortions within the stress and buckling limits should be determined by their affect on aero/acoustic performance over the operating range. In this program, the distortions will be used as an evaluation of the fabrication concept.

F. Flutter Margins

Classical flutter should not be encountered up to the maximum design rotational and forward speeds with the torsional frequency degraded by 15%.

The propeller shall be free of stall flutter up to 120% of maximum (baseline) power at 100% rpm.

G. FOD Criteria

The foreign objects are classified into three categories as follows: minor, moderate, and major impacts. Major and moderate impacts correlate with Group I and II definitions in FAR Advisory Circular 33-1B dated April 22, 1970. Minor impacts include sand, small stones, and birds up to about four ounces. Moderate impacts include two inch hailstones and birds up to two pounds. Major impacts include a single bird up to four pounds. The damage criteria are as follows:

Minor Impacts - no damage allowed to basic blade structure. Operation will continue without impediment.

Moderate Impacts - Damage can include loss of material or airfoil distortion. Operation shall continue at 75% power minimum for five minutes. No metal fragments shall be lost which can penetrate the aircraft fuselage pressure shell. Roughness shall be tolerable and as a guide, rotor unbalance force shall be kept below 5,000 pounds.

Major Impacts - Damage can include loss of material or airfoil distortion. Ability to feather the propeller must be maintained. A shutdown must be accomplished without catostrophic effects on airframe structure. As a guide, the rotor unbalance force shall be kept below 25,000 pounds. No metal fragments shall be lost which can penetrate the aircraft fuselage pressure shell.

H. Stress Margins

The combined steady and cyclic stresses will be plotted on modified Goodman Diagrams for the materials of construction. The strength boundaries will represent a high probability of survival derived from experimental data on specimens and full scale structures. As a minimum, the boundaries will represent $x - 3.5\sigma$ lines. The start-stop stress range will be reflected against a boundary for a life of 50×10^3 cycles. The high cycle combined stresses will be reflected against a boundary for 100×10^6 cycles or infinite life.

The maximum elastic (nominal x k_T) stressing due to a 125% overspeed and the nominal stressing due to a 140% overspeed will be kept below the 0.2% offset yield strength for homogenous metal materials. The change in elastic modulii will be kept below 5% for fiber reinforced resin material regarding these same overspeed requirements.

I. Features

1. Repairability

Consideration will be given to the use of materials in the blade which can be repaired in the field in the event of minor damage in service.

2. Replacement

The blade retention design will allow for the replacement of a single blade in a Prop-Fan assembly while installed on an engine.

3. Leading Edge Protection

The outer portion of the blade leading edge will be protected with a partial chord width metal sheath.

4. Lightning Protection

Lightning protection will be incorporated in the blade.

5. Ice Protection

The inner portion of the blade leading edge will be protected with electric heaters.

6. Life and Reliability Goals

The blade will be designed for the following goals:

Maximum Continuous Stress Level	Infinite Life
Replacement Life	35,000 hours
Mean Time Between Blade Removals (8 blade set)	50,000 hours

APPENDIX B

UNITED TECHNOLOGIES
HAMILTON STANDARD

FABRICATION CONCEPTS

FOR

PROP-FAN BLADES

Prepared as part of

Propeller Blade Structural Design Study

NASA Contract NAS3-22394

May 15, 1980

UNITED TECHNOLOGIES HAMILTON STANDARD

CONTENTS

UNITED TECHNOLOGIES HAMILTON STANDARD

I. INTRODUCTION

In recent years, considerable attention has been directed toward reducing aircraft fuel consumption. Studies have shown that the inherent efficiency advantage that turboprop propulsion systems have demonstrated at 0.65 Mn may now be extended to the higher cruise speeds of today's turbofan-powered aircraft. In order to achieve this goal, new turboprop designs will require advancements such as thin, high speed airfoils and aerodynamic sweep.

A program to conduct structural design studies of large scale blades of this type has been funded by NASA LeRC. This program includes the establishment of structural concepts for the fabrication of several of the Prop-Fan (advanced turboprop) model blade configurations in large scale, and the definition of their structural properties.

This document discusses Hamilton Standard's blade design philosophy, describe several large-scale blade fabrication concepts, and discusses their advantages and disadvantages. Hamilton Standard's recommendations of the fabrication concepts for the Prop-Fan blade designs to be structurally analyzed in the design phase of the program are presented. A discussion of the analyses that will be used in the design phase is also included.

II. DESIGN PHILOSOPHY

The blade structural design philosophy at Hamilton Standard has evolved over several decades of blade design, analysis, testing, and manufacturing, and millions of flight hours of propeller experience. Dedication to reliability and safety of flight has helped make Hamilton Standard the free world leader in the design and manufacture of propellers. At Hamilton Standard, a new propeller is designed using well-established criteria based on: 1) state-of-the-art analytical tools verified by extensive testing; 2) design material properties and strengths established from Hamilton Standard's own material specimen tests and full-scale component tests; and 3) a wide variety of fabrication methods using materials that range from metals to the latest in advanced composites.

During the iterative design procedure, the following major goals are achieved:

- Conservative stresses, designed to give unlimited service life.
- Dynamic stability, through critical speed placement and adequate flutter margins
- Resistance to foreign object damage, by minimizing damage to the primary structure of the blade
- Optimum material distribution and effectiveness, to minimize weight, shank retention loads and pitch change loads
- Minimum blade distortion, by providing adequate torsional and bending stiffness

In addition, the blade design must incorporate other features where required, such as lightning, ice and erosion protection. Consideration must also be given to minimizing the maintenance requirements of the blade. These features are not determining factors in blade structural design and will not be discussed in this report; however, the various fabrication concepts will be evaluated with regard to incorporating these features. For this Prop-Fan blade structural design study, the design criteria to achieve these goals are specified in the Design Requirements Document. How these goals and the design criteria influence the choice of a blade fabrication concept is discussed below.

A. STRESS

A propeller blade is designed so that the stress levels due to the blade loads at all operating conditions will permit an unlimited service life (10^8 cycles). The loads acting on a typical blade design are shown in Figure 1. The loads in the blade (tension,

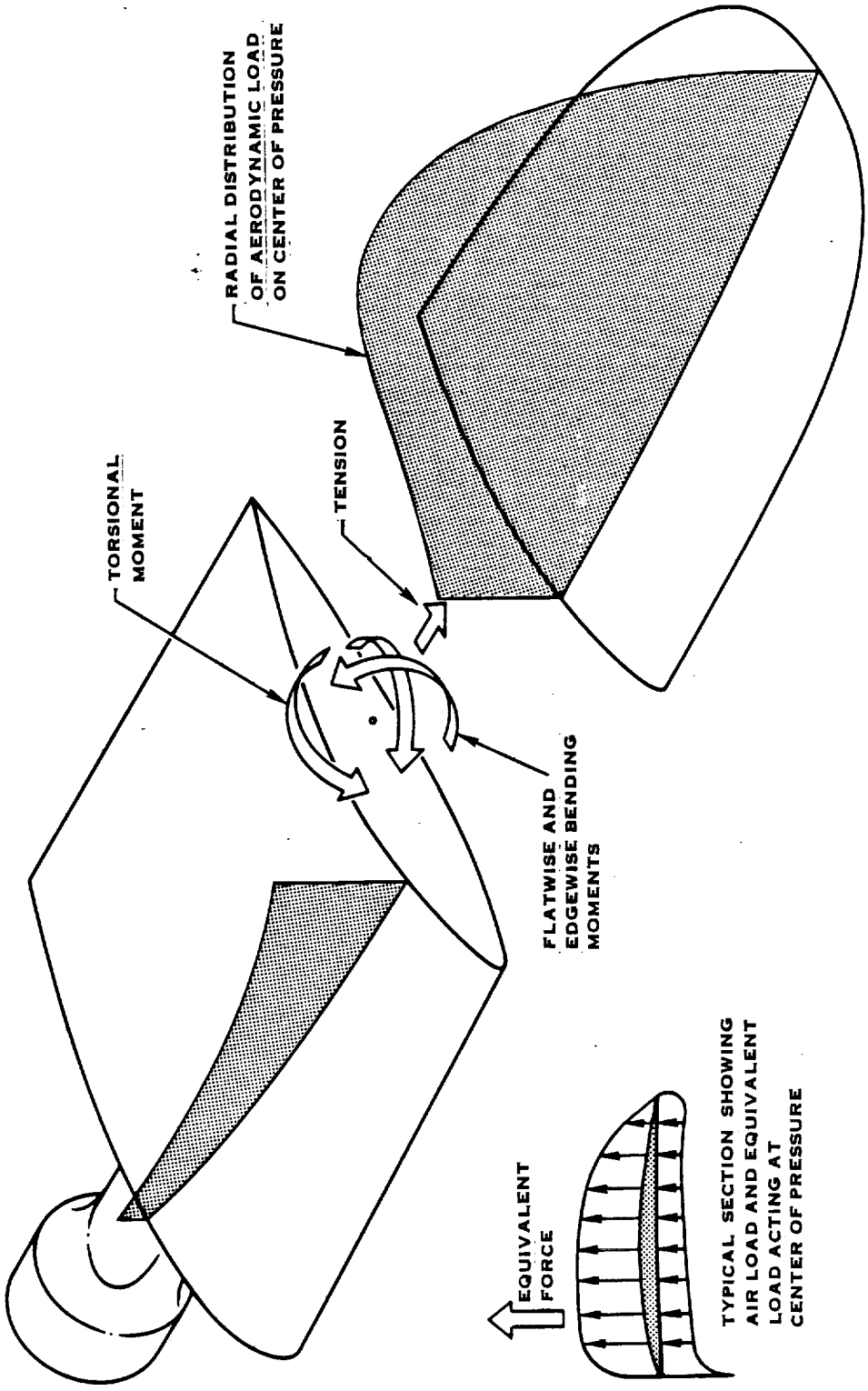

FIGURE 1. TYPICAL BLADE LOADS

bending and torsion) increase from the tip to root. When combined with a typical blade structure, these loads produce critical stress areas, illustrated in Figure 2. In order to minimize the stress magnitude in these critical areas, the capacity is increased smoothly from tip to root, thereby accommodating the load distribution efficiently. An efficient blade design will also possess smooth mass and stiffness distributions to avoid high stress gradients, especially in the blade-to-shank transition area.

The structural analysis methods used to predict blade design stresses have produced results that have been correlated with experimental data for many blade designs of various size, shape, and fabrication. Extensive material testing and full-size component testing have provided conservative fatigue stress design limits for many materals currently used in production blades and also for materials being used in experimental blade programs. Choosing and distributing materials so that the calculated blade stresses are within these conservative stress limits will ensure that the blade design has an unlimited service life (10^8 cycles) under all operating loads.

B. DYNAMIC STABILITY

Dynamic stability of a propeller blade design can be insured by providing adequate critical speed margins and flutter margins. The structural analysis methods used to predict blade stresses can also predict resonant frequencies of the blade design. Carefully controlled comparisons have demonstrated excellent correlation between analytical predictions of frequencies and experimental results.

The frequency response of the blade can be modified by altering the mass and stiffness distributions of the blade. This may be done to increase the critical speed margins and/or flutter margins. A greater ability to modify these distributions for a selected fabrication concept or material combination will provide increased freedom to tune the blade frequency response while not significantly affecting the blade stressing.

C. FOREIGN OBJECT DAMAGE RESISTANCE

The blade design must withstand varying foreign object impacts while sustaining no damage or limited damage, as specified in the Design Requirements Document. The accuracy of the FOD analysis programs in use at Hamilton Standard has been confirmed by comparison with experimental data from several specially conducted tests. The bending deflection and twist, in addition to the analytical impact pressure distribution, has shown excellent correlation with test data. In designing for small object FOD resistance, the primary blade structure should be protected from the impact, and should be isolated from any sustained damage.

As the size of the foreign object and the impact load increases, more structural capacity is needed beyond that required by body loads and air loads. Minor impacts can

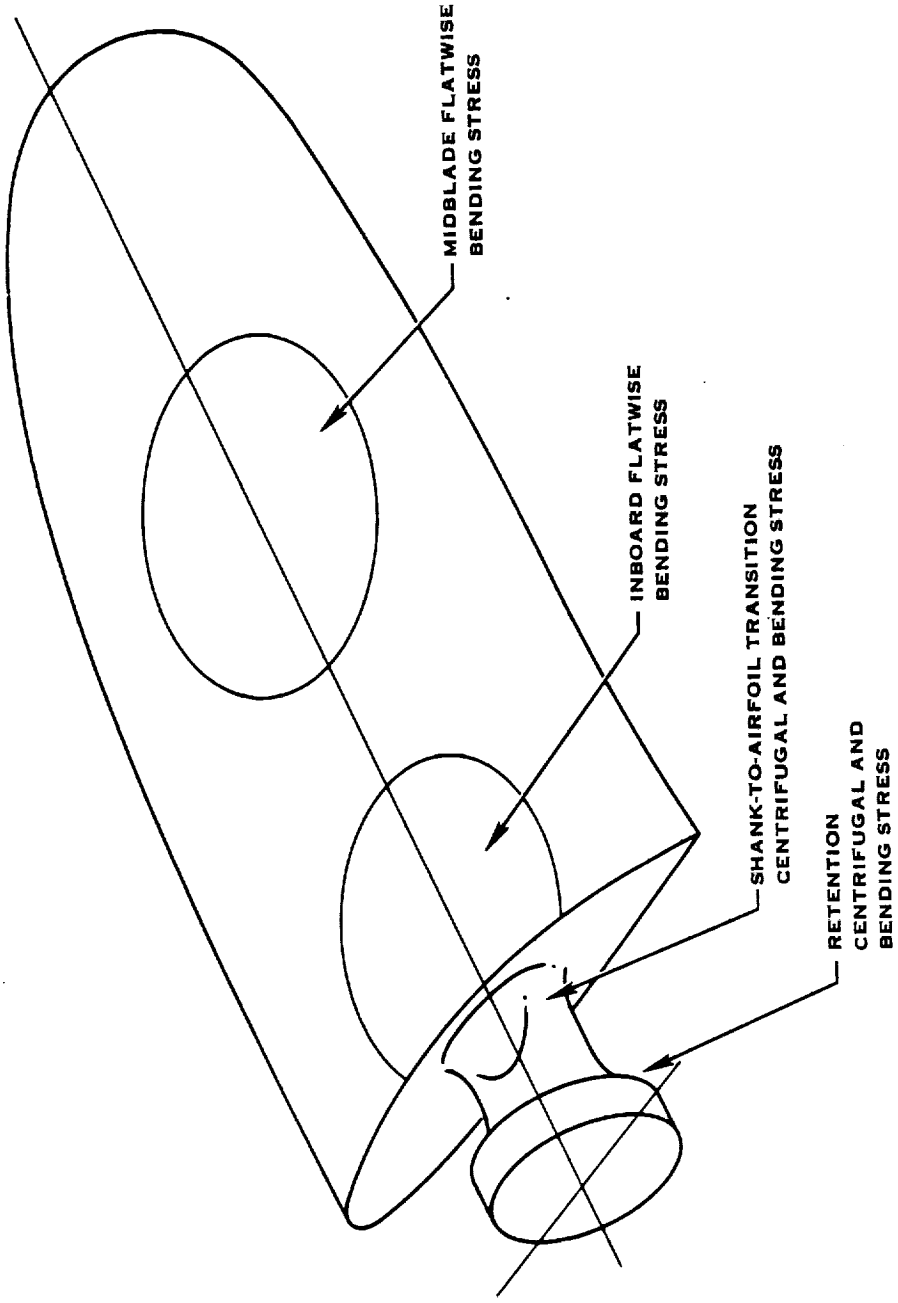

FIGURE 2. TYPICAL CRITICAL STRESS AREAS OF A PROPELLER BLADE

usually be tolerated without an increase in stiffness. Moderate impacts may require increasing the chordwise leading edge strength and stiffness. Major impacts will involve the stiffness and strength of the entire blade, especially the primary structure of the blade. Blades at Hamilton Standard are designed for maximum FOD resistance not only for flight safety but also for repairability. A high damage threshold permits a maximum impact without damage, for a given blade geometry. Beyond that damage threshold, materials and fabrication methods are chosen to limit the sustained damage and for ease of repair.

The chordwise and spanwise stiffness and strength properties are important in absorbing both the local and gross impact loads. Chordwise and spanwise loads are produced by the impact at the local impact site. These loads will then spread through the blade as a whole, resulting in gross cantilever bending and torsion loads at the shank and retention area. By tailoring the blade's frequency response, and elastic and structural properties, the blade impact response and stressing can be minimized, within the other blade design requirements and constraints.

D. MATERIAL DISTRIBUTION AND EFFECTIVENESS

Optimum material distribution and effectiveness is a major goal of every blade design at Hamilton Standard. The cross-sectional geometry provides the strength and stiffness to accommodate the local air loads and local FOD impact loads. Summed along the blade span, the cross-sectional properties also dictate the spanwise bending stiffness distribution and the spanwise mass distribution, which influence the blade frequency response, the blade FOD response and stressing, and the blade deflections under load. As the blade loads increase toward the root, the cross-sectional stiffness and strength should also increase to accommodate the load, and should match the load distribution to prevent high stress gradients.

Since the bending and torsional stiffnesses depend on both the area and the distance from the cross-sectional principal centers or axes, and the centrifugal load requires only a sufficient cross-sectional area, the material in a blade design will be most effective if it is near the outer airfoil contour. For this reason, hollow blades are more efficient than solid blades. The spanwise distribution of load capacity should increase from tip to root to withstand the increasing body loads, cantilever bending loads, and torsional loads. From a frequency response viewpoint, material should add stiffness in addition to mass in order to be used efficiently.

Both the chordwise and spanwise distribution of material will influence the centrifugal twisting moment (CTM). In general, the cross-sectional mass should be concentrated near the mid-chord to minimize the CTM. For a straight blade design, the CTM is influenced mostly by the thickest or most inboard airfoil sections. For a swept blade design, the CTM is affected also by the amount of sweep and the size of the tip area.

To minimize the CTM of the swept tip, the mass at the tip should be kept as low as possible without compromising stiffness and strength, by careful selection of chord width, thickness ratio, and material.

The overall blade mass should be optimized with respect to blade stiffness, strength, and FOD resistance; and retention, hub, and pitch change mechanism size and weight. A lower blade weight will allow a smaller and lighter retention and hub. A low blade CTM will result in a smaller and lighter pitch change mechanism, which will also favorably influence the hub design.

E. BLADE DISTORTION

Blade design aero-acoustic performance is dependent upon the accurate location of the desired shape in space, under operating conditions. Deviation from the initial blade geometry can significantly influence the performance. If the elastic distortion does become significant, the deformed blade shape must be re-analyzed for its aero-acoustic performance. Iteration may be required to determine the final blade deformed shape and the aerodynamic loads for this shape. In order to minimize the need for such iteration, high bending and torsional stiffness is desirable. The chordwise bending stiffness will govern the amount of airfoil shape and camber distortion, and the spanwise bending and torsional stiffness will control the spanwise blade deflection.

Pre-deforming the blade shape to give the desired shape at a specific operating condition can be done to compensate for the blade distortion. However, other operating conditions must be analyzed at the blade shape corresponding to those operating conditions to determine the aero-acoustic performance. A structural and aero-acoustic blade analysis will be more complex and time consuming than the standard analysis procedure, in which only initial blade shape is analyzed at the various operating conditions.

F. SPECIAL CONSIDERATIONS FOR PROP-FAN BLADES

The shape of a Prop-Fan blade introduces design considerations not found in the same degree in previous propeller designs. These are listed in Figure 3. The Prop-Fan blades have a reduced thickness-to-chord ratio and increased chord-to-diameter ratio than standard turboprop blades. This is illustrated in Figures 4 and 5 for the P-3, an in-service propeller with solid aluminum straight blades, and the SR-3 Prop-Fan design. The wider, thinner sections of the Prop-Fan blades may have reduced section stiffness. The introduction of sweep results in a revision and magnification of centrifugal and aerodynamic loads. These revised loads and reduced section stiffness can increase the blade distortion. The sweep of the blade, by changing the mass moment distribution about the pitch change axis, can increase the torsional inertia loads, moddifying the preferred initial twist distribution and increasing the gross torsional loads that must be accommodated by the pitch change mechanism.

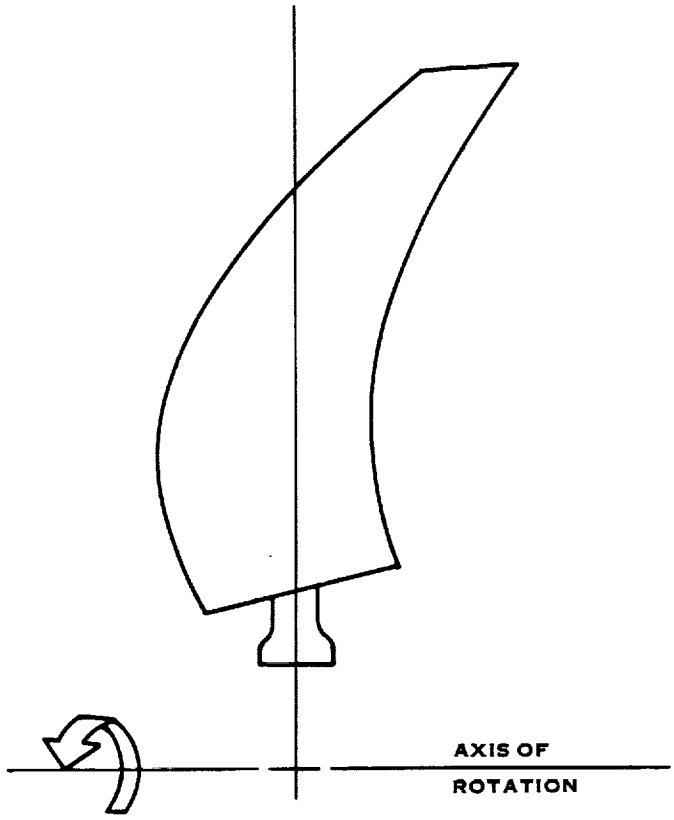

- SWEEP IMPROVES AERO-ACOUSTIC PERFORMANCE
- t/b REDUCED FOR HIGH-SPEED AERODYNAMICS
- b/D INCREASED AT MID-BLADE FOR STRUCTURAL THICKNESS AND STIFFNESS
- THINNER TIP SECTIONS REDUCE CHORDWISE BENDING STIFFNESS
- SWEEP AND REDUCED STIFFNESS INCREASE BLADE DISTORTION
- SWEEP INCREASES MIDBLADE TRAILING EDGE STRESS
- SWEEP INCREASES ROOT TORSIONAL LOADS

FIGURE 3. SPECIAL CONSIDERATIONS FOR PROP-FAN BLADES

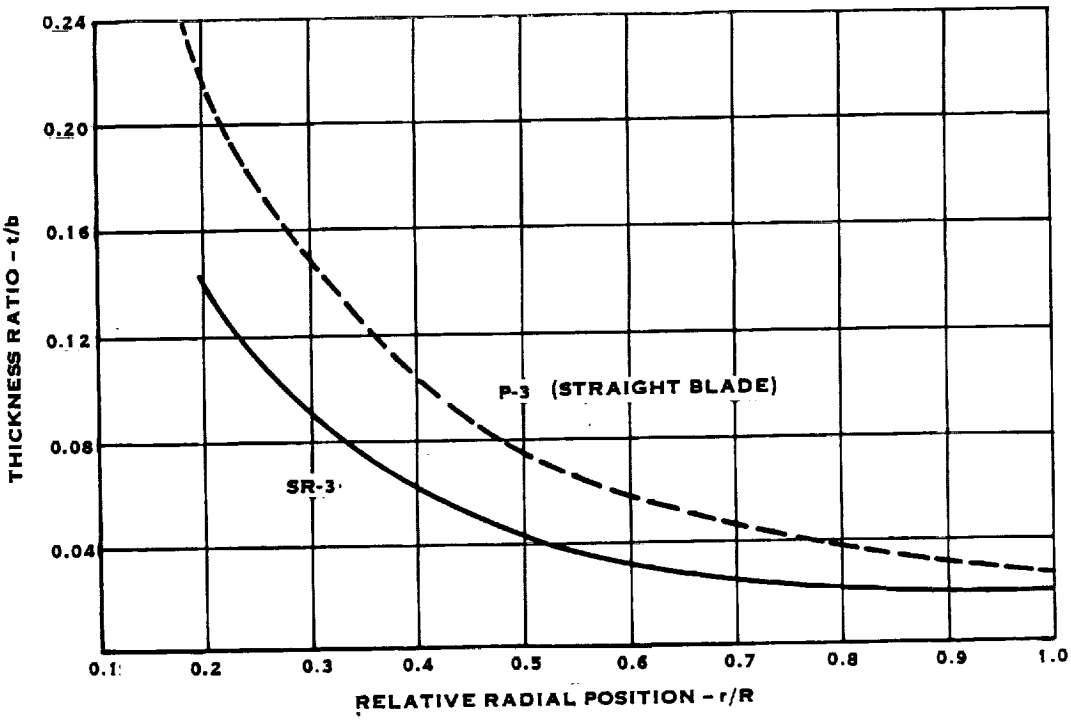

FIGURE 4. THICKNESS RATIO COMPARISON

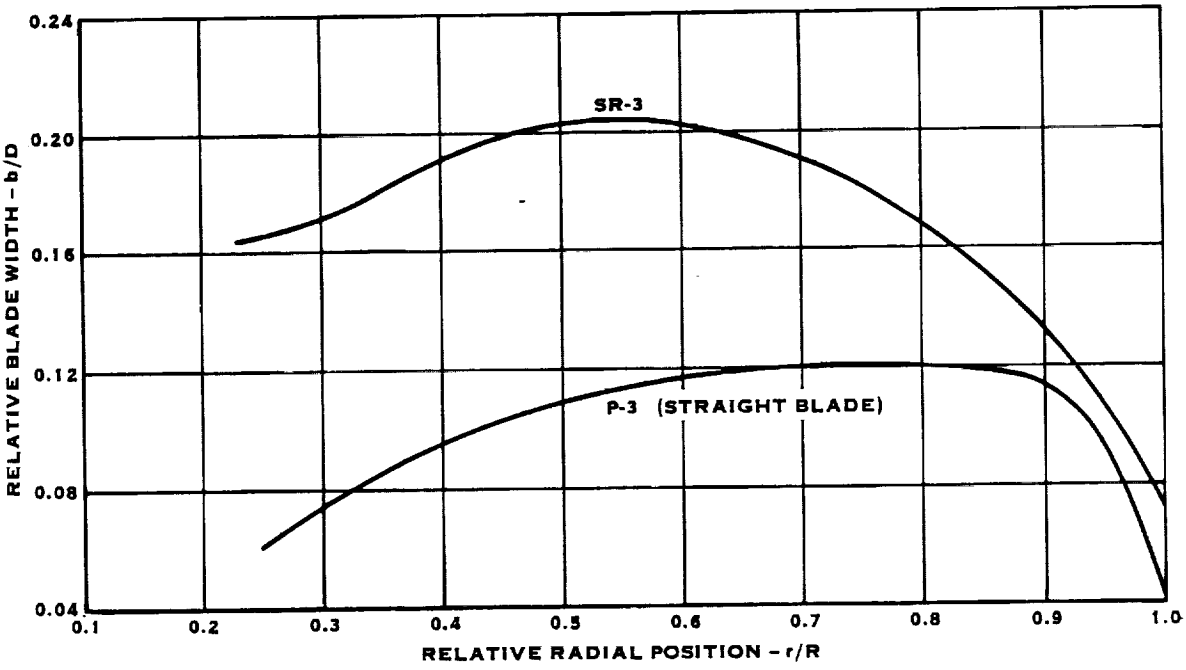

FIGURE 5. PLANFORM COMPARISON

III. MATERIALS

Two major types of materials are used in propeller blade fabrication: metals and composites. Comparisons of the commonly used metals and composites are given in Tables 1 and 2, respectively.

The typical metals that are used are aluminum, steel and titanium (see Table 1). Of these, titanium offers the highest specific ultimate strength (ultimate strength divided by density) and specific fatigue strength (fatigue strength divided by density), but also the highest cost. The ability to form small inside radii is desireable for hollow component designs; steel can be hot-formed to the smallest radius-to-wall thickness ratio. Steel is also better suited for a tube reduction/die forming process, which is also used to form hollow components. Super-plastic forming/diffusion-bonding (SPF/DB), an advanced technology hollow-forming process, has been used experimentally to form hollow components. Titanium is currently used for SPF/DB components; however, steel may also be a candidate material. In the SPF/DB process, the component pieces are selectively diffusion bonded and then expanded plastically at elevated temperature in a die of the desired shape.

There are two major advantages in using metals as blade materials. The first is the high shear strength of metals. The resin matrices that are available are much lower in shear strength than metals. This could be overcome if it were practical to use metals as matrices. At this time, only aluminum can be considered for use as a matrix with boron fibers, although limited work has been done with titanium as a matrix. This limited shear strength of resin matrix composites is a major design limitation in areas of rapid geometry or loading change, or in areas of high flange load transfer where shear loading dominates. The second major advantage of metals is their ductility. Because unlimited service life is desired, normal operating stresses in Prop-Fan blades are well within the elastic range of any material and ductility is not important, except as it may affect the crack propagation rate. Under the impulsive load conditions of large foreign object impact, such as two- to four-pound birds, the ability to yield locally and still retain virgin strength and elastic moduli can become valuable. Resin matrix materials do not have this ability. The resin and the resin-to-fiber bond are flexible (low in modulus) but brittle. A fiber-reinforced resin matrix composite, where the fiber is characteristically much stronger than the matrix, can accommodate strains beyond the strain capability of the matrix or matrix-to-fiber bond only by fracture. The fracturing is initially confined to the resin and the resin-to-fiber bond, and is commonly called "crazing". As the density of crazing increases, fiber fracture will occur. Even without fiber fracture, crazing is usually accompanied by a reduction in modulus, and a reduction in resistance to cyclic stressing and general environmental effects. In this latter respect, crazing is similar to initial porosity in the resin.

UNITED TECHNOLOGIES HAMILTON STANDARD

TABLE 1. COMPARISON OF METAL MATERIALS

	ALUMINUM	STEEL	TITANIUM
MATERIAL AND PROCESSING COST COMPARISON (BASED ON FORGED ALUMINUM)	1.0	2.5	10.–15.
AVAILABILITY (LEAD TIME, SOURCES, ETC.)	VERY GOOD	GOOD	POOR
MATERIAL PROPERTIES			
DENSITY (LBS/IN^3)	0.10	0.283	0.16
SPECIFIC ULTIMATE STRENGTH ($\frac{PSI}{e} \times 10^{-6}$)			
TENSION	0.64	0.65	0.81
SHEAR	0.38	0.39	0.53
SPECIFIC STIFFNESS ($\frac{PSI}{e} \times 10^{-6}$)			
E	103	102	99
G	40	39	39
MATERIAL CHARACTERISTICS			
MACHINABILITY	VERY GOOD	FAIR	POOR
MINIMUM INTERNAL FORMING RADIUS (R/T_{WALL}) (HOLLOW COMPONENTS)	3:1	2:1	3:1
TUBE REDUCTION/DIE FORMING SUITABILITY (HOLLOW COMPONENTS)	FAIR/GOOD	VERY GOOD (SPHERODIZED)	FAIR
SPF/DB SUITABILITY (HOLLOW COMPONENTS)	NOT DEVELOPED	POSSIBLE	DEVELOPED, NEEDS EVAL.
REPAIRABILITY - SURFACE FLAWS (NICKS, SCRATCHES, ETC.)	GOOD	GOOD	FAIR

TABLE 2. COMPARISON OF COMPOSITES MATERIALS

	RESIN MATRIX							METAL MATRIX
	FIBERGLASS EPOXY		KEVLAR EPOXY		CARBON EPOXY	BORON EPOXY	BORON ALUMINUM
	UNIDIRECTIONAL	WOVEN (181 CLOTH)	UNIDIRECTIONAL	WOVEN (181 CLOTH)	UNIDIRECTIONAL	UNIDIRECTIONAL	UNIDIRECTIONAL
MATERIAL COST COMPARISON (PER LB. RELATIVE TO FIBERGLASS)	1.0	1.0	2.5	2.5	10	28	39
MATERIAL PROPERTIES							
DENSITY (LBS/IN^3)	0.065	0.065	0.050	0.050	0.055	0.071	0.100
SPECIFIC ULTIMATE STRENGTH ($\frac{PSI}{\rho}$ x 10^{-6})							
UNIDIRECTIONAL TENSILE	2.46	0.68	4.00	1.50	3.21	2.65	1.63
TRANSVERSE TENSILE	0.07	0.65	0.09	1.44	0.14	0.14	0.16
UNIDIRECTIONAL COMPRESSIVE	1.38	(1)	0.65	(1)	3.21	4.87	1.80
TRANSVERSE COMPRESSIVE	0.31	(1)	0.38	(1)	0.54	0.55	0.24
± 45° CROSS-PLY TENSILE	(1)	0.41	(1)	0.60	0.41	0.40	0.24
IN-PLANE SHEAR: UNIDIRECTIONAL	0.08	0.22	0.17	0.32	0.21	0.21	0.10
± 45° CROSS-PLY	(1)	0.38	(1)	0.64	1.17	1.06	0.11
INTERLAMINAR SHEAR	0.08	0.10	0.18	0.14	0.23	0.18	0.19
SPECIFIC STIFFNESS ($\frac{PSI}{\rho}$ x 10^{-6})							
UNIDIRECTIONAL	84.6	47.7	220.0	90.0	375.0	413.8	346.9
TRANSVERSE	23.1	45.4	16.0	86.0	30.4	37.2	204.1
± 45° CROSS-PLY	–	36.9	19.0	22.0	41.8	35.7	195.2
IN-PLANE SHEAR: UNIDIRECTIONAL	7.2	12.5	6.0	6.0	11.6	9.7	96.9
± 45° CROSS-PLY	–	21.5	60.8	60.0	98.6	109.0	111.0
MATERIAL CHARACTERISTICS							
INJECTION MOLDING SUITABILITY	POOR	EXC	POOR	VERY GOOD	POOR	POOR	NOT SUITABLE
REPAIRABILITY - SURFACE FLAWS (NICK, SCRATCHES, CRACKS, ETC.)	FAIR	VERY GOOD	FAIR	GOOD	GOOD	POOR	POOR

(1) INSUFFICIENT DATA AVAILABLE

Metal matrix and resin matrix composites are also used in blade fabrication concepts, and are listed in Table 2. Composites can provide specific ultimate strengths and stiffnesses, in a unidirectional direction, that are higher than metals. However, the transverse properties of resin matrix composites are typically lower, as is the shear strength. The fibers are usually cross-plied to increase these properties, but then the maximum stiffness and strength are lower than the unidirectional properties. The interlaminar shear stiffness and strength remains unchanged by fiber orientation; the interlaminar shear stress must be examined in critical areas of the blade. The cost of metal matrix composites may prohibit their use unless the high strength is necessary to satisfy the design requirements. The resin matrix composites vary in stiffness, strength, and cost; their application will depend upon the stiffness and strength required in the design. The resin matrix composites are also well-suited for repair of surface nicks, gouges and cracks.

A resin injection molding process, an advanced technology process under development that can reduce the number of manufacturing steps, can be used with some of the resin matrix composites. Injection molding is limited to those fibers that can be procured in cloth form. Chopped fiber composites can be injection molded but are not desirable from a design viewpoint due to significantly lower stiffness and strength.

In hollow components, a fill material is used in the cavities and contributes greatly to the structural integrity of the component by preventing buckling and secondary panel behavior. Foam is typically used as a fill material; however, its brittle nature requires that it be subjected to low loads only. Metal honeycomb can provide greater FOD impact capacity due to its greater shear capacity. It must be machined to the exact cavity shape as a detail part and be bonded in place, and hence is more costly. Super-plastic forming/diffusion-bonding (SPF/DB) technology can be applied to manufacturing hollow components with internal web structures; this web structure would perform the same function as a fill material. However, extensive development of these SPF/DB components is required to ensure that the design satisfies the required load and FOD impact criteria.

IV. FABRICATION CONCEPTS

Hamilton Standard's blade design experience includes fabrication concepts and methods ranging from solid blade designs to all of the various hollow types, using both metal and composites. New blade fabrication concepts such as super-plastic formed/diffusion-bonded (SPF/DB) blade structures, have been investigated as potential Prop-Fan fabrication methods. Many of these concepts are shown in Figure 6. These concepts are discussed below, along with a discussion of their advantages and disadvantages. A summary of the fabrication concepts is given in Table 3.

The sweep of the Prop-Fan blade will strongly influence whether the features of a fabrication concept are an advantage or a disadvantage. The Prop-Fan blade also has a lower thickness ratio than standard turboprop blades. These two factors will be significant in the evaluation of the fabrication concepts, and may preclude the use of traditional straight blade fabrication concepts as Prop-Fan fabrication methods.

A. SOLID BLADE

The basic blade fabrication concept is a solid blade design. This concept is illustrated in Figure 7. A solid blade design can be either metal or composite material. In order to direct the centrifugal load smoothly into the shank and minimize stress gradients in the blade-to-shank transition area, the leading edge and trailing edge root area of the blade design may be tapered smoothly into the shank. Rubber-covered foam cuffs are usually used in this area to form the airfoil shape if root aerodynamic performance is important. These foam cuffs are sufficiently stiff to maintain the airfoil shape since the airloads are low in this area of the blade.

Since the primary loading on a propeller blade is due to bending, the highest blade stresses will occur in the outer fibers. The material near the neutral axis carries very little bending load and contributes little to the bending capacity of the blade. This inefficient use of material in a solid blade design will result in unnecessary weight in the blade, retention, hub and pitch change mechanisms.

A solid metal blade design is the most straightforward concept and is used on many current turboprop blades. However, on the Prop-Fan, a large retention and hub would be required to accommodate the centrifugal load, as well as a large pitch change mechanism to accommodate the centrifugal twisting moment (CTM). Stresses in the shank area, trailing edge area, and midblade area (see Figure 2) may be above the fatigue stress limit of the selected material when the steady and vibratory bending stresses are added to the centrifugal stress.

The primary disadvantage of a solid metal blade in service usage is that this design has no capability to isolate damage. Any cracks that are initiated due to nicks

UNITED TECHNOLOGIES HAMILTON STANDARD

ORIGINAL PAGE IS OF POOR QUALITY

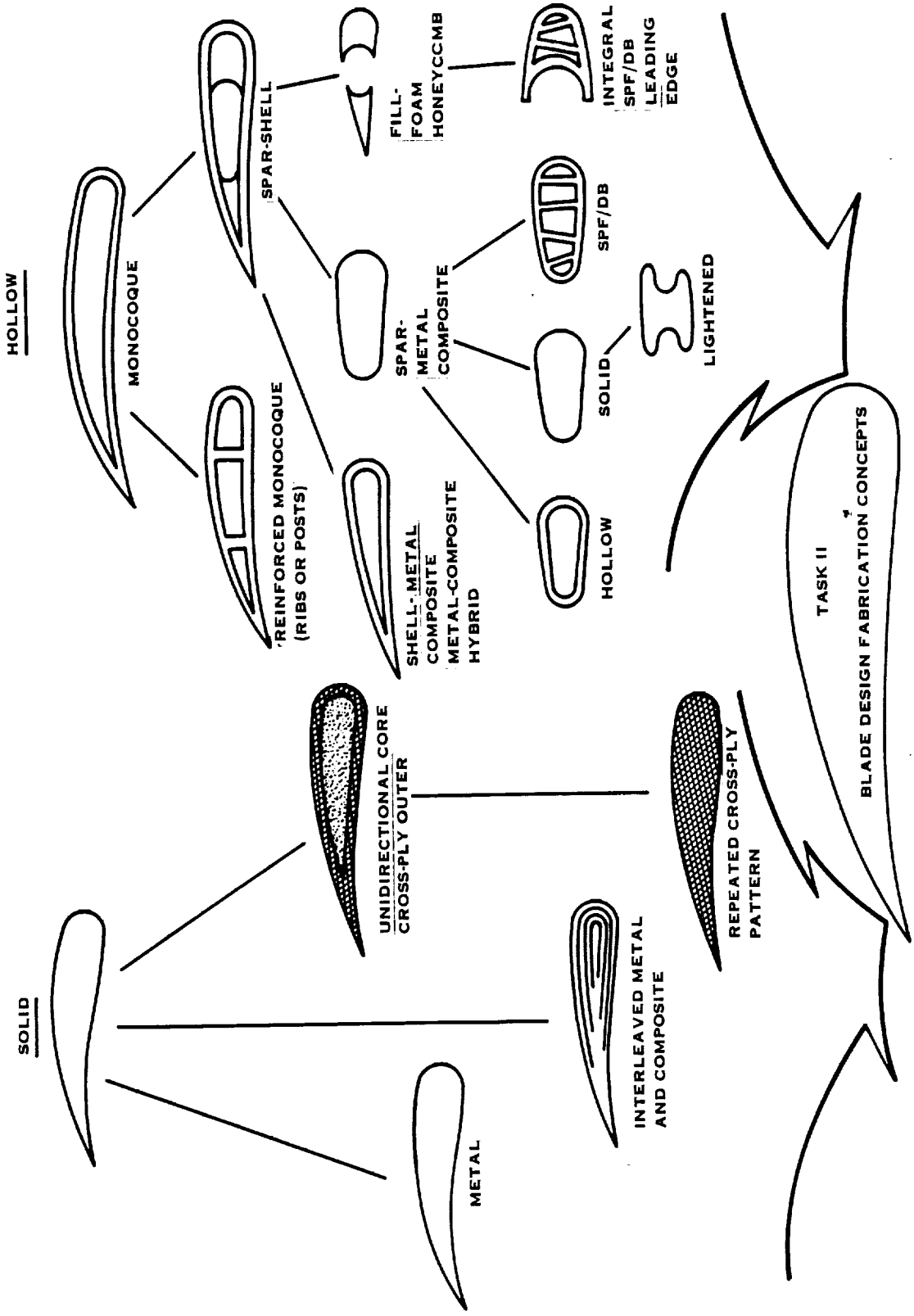

FIGURE 6. BLADE FABRICATION CONCEPTS

UNITED TECHNOLOGIES HAMILTON STANDARD

TABLE 3. BLADE FABRICATION CONCEPT COMPARISON

	BLADE FABRICATION CONCEPTS			
	SOLID	MONOCOQUE	MODIFIED MONOCOQUE	SPAR AND SHELL
HAMILTON STANDARD EXPERIENCE	PRODUCTION	LIMITED PRODUCTION	STUDIED	PRODUCTION
SWEPT SHAPE SUITABILITY:				
• MANUFACTURABILITY	EXC	REQ. DEVEL.	REQ. DEVEL.	VERY GOOD
• STRUCTURAL SUITABILITY	POOR	POOR	FAIR	GOOD/EXC
• DISTORTION RESISTANCE	FAIR	POOR	GOOD	VERY GOOD
LOAD LEVEL:				
• RETENTION	HIGH	MODERATE	MODERATE	MODERATE
• PITCH CHANGE	HIGH	MODERATE	MODERATE	LOW
SHEAR LAG RESISTANCE	EXC	POOR	EXC	EXC
DESIGN FLEXIBILITY - ABILITY TO MODIFY STRUCTURAL CHARACTERISTICS	POOR	FAIR	FAIR	EXC
RESISTANCE TO FOREIGN OBJECT DAMAGE: (1)				
• IMPACT LOAD CAPACITY	GOOD/EXC	POOR	FAIR	GOOD/EXC
• DAMAGE ISOLATION ABILITY	POOR	POOR	POOR	FAIR/EXC
• REPAIRABILITY (SURFACE DAMAGE, CRACKS)	FAIR	FAIR/POOR	FAIR/POOR	FAIR/GOOD

(1) HIGHLY DEPENDENT ON MATERIAL AND MANUFACTURING PROCESS

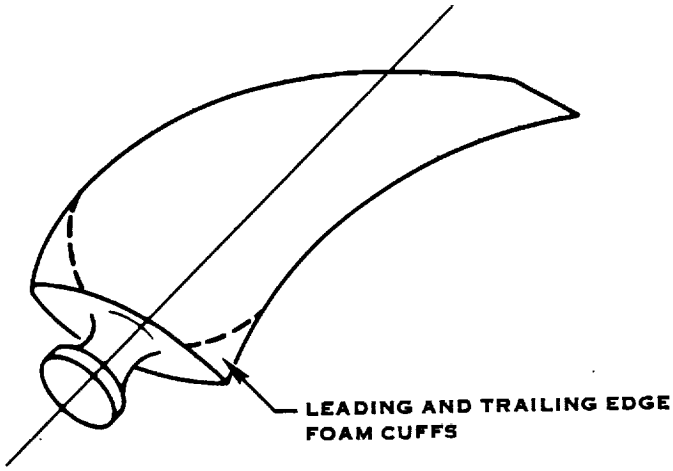

DISADVANTAGES

- NO DAMAGE ISOLATION
- LIMITED MATERIAL CHOICES
- INEFFICIENT USE OF MATERIAL

FIGURE 7. SOLID BLADE DESIGN

or corrosion are in the primary structure of the blade, and may propagate due to fatigue, leading to failure. Frequent inspection of the blades is required, along with frequent maintenance to blend out surface nicks and gouges before they develop into fatigue cracks. This procedure cannot be avoided if this surface damage is to be detected.

Another disadvantage of a solid metal blade from a design viewpoint is the inability to modify the basic stiffness and weight distributions of the blade, without significantly changing the external airfoil shape, to reduce locally high bending stresses or to tune the frequency response of the blade.

A solid composite blade could be fabricated from metal matrix or resin matrix composites. The reduction in material density compared to solid metal will result in lower blade loads, thus allowing a smaller retention, lighter hub, and lighter pitch change mechanism. By varying the orientation of the fibers in the layers, the stiffness and strength distribution can be modified somewhat to tune the frequency response of the blade. This stiffness modification can also be used to reduce locally high bending stresses in critical areas.

As with the solid metal design, the main disadvantage of a solid composite blade is the lack of damage isolation capability. In a composite design, a crack can propagate through the structure of the blade, although at a lower rate than in a metal design. Both metal matrix and resin matrix composites may experience undetected interlaminar shear and separation from an FOD hit. Subsequent normal usage or repeated FOD impacts may cause major damage to the blade and result in large portions of the blade being lost. A severe interlaminar separation can also have a significant effect on the frequency response of the blade depending on the location and extent of delamination, since the structural properties of the blade will change.

The shank area and retention area for a solid composite blade require detailed evaluation to determine a successful design due to the low shear strengths of the materials and limited available space. A solid composite blade will probably be mated to a solid metal shank/retention or to metal components in the shank/retention area in order to carry the retention contact stresses in the bearing. A large shear joint will be required in order to transfer the bending and centrifugal loads into the metal components with low unit shear stressing. The bending and shear stresses in the composite and shear joint must be within the established fatigue stress limits for normal service loading and within critical ultimate stress limits for FOD impact loading.

B. MONOCOQUE DESIGN

A metal or composite monocoque blade design makes more efficient use of the material since is eliminates the material near the neutral axis that does not contribute

significantly to the blade stiffness. Figure 8 illustrates a monocoque blade design. As with a solid blade design, the leading edge and trailing edge root area of the blade may be tapered to direct the load smoothly into the shank. The airfoil shape would be maintained by using rubber-covered foam cuffs. Because the weight is reduced, the centrifugal stress is lower than for a solid blade design. Particular attention must be given to the secondary stresses due to local bending loads in the airfoil-to-shank transition area (Figure 2).

Damage isolation is not achieved in a monocoque design, whether metal or composite materials are used. Fatigue crack propagation can lead to the loss of a major portion of the blade since all cracks occur in the primary structure of the blade. In order to withstand minor FOD impact without damage, the tip area wall thickness would have to be greater than that required by the normal operating stress levels. Past experience at Hamilton Standard has shown that this required wall thickness reduces the potential weight savings of a metal or composite monocoque construction when proper inner radii are included, particularly in the thin airfoil sections of the Prop-Fan blade designs.

Shear lag susceptibility is also a problem in a monocoque design. Shear lag causes the tensile bending stress in a wide beam flange to decrease as the distance from the web increases. This phenomenon is illustrated in Figure 9. Elementary bending theory predicts a uniform tensile bending stress in the top panel of the box beam. Since the panel acquires its tensile stress from the shear stresses in the side panels, the tensile bending stress is not uniform but is higher at the edges than in the center of the panel. This effect will result in stresses near the leading and trailing edges of the blade that are above those predicted by beam theory. This effect must be included when establishing the size of the leading and trailing edge inner radii.

Because of the sweep of the Prop-Fan blades, a method of manufacturing a one-piece metal monocoque blade would require development. Super-plastic forming/diffusion-bonding technology should be considered as a possible manufacturing process during the development of a metal monocoque design. Actual material properties and strengths will exist in the diffusion bond area. This process will also form the small leading and trailing edge inner radii. Development would also be required to form a one-piece composite monocoque blade, since the fibers may not be able to form the required inner radii. A two-piece monocoque design that is joined at the leading and trailing edges may be suitable for the swept Prop-Fan blade designs. The stress concentration problems due to the small leading and trailing edge inner radii could be reduced in a two-piece design by pre-machining large radii. However, the joint between the two pieces would require extensive evaluation since it will be subjected to high shear stressing. In addition, the leading edge joint design must permit the blade to satisfy the FOD design requirements. Repeated FOD hits may cause severe damage to the blade, especially the leading edge area.

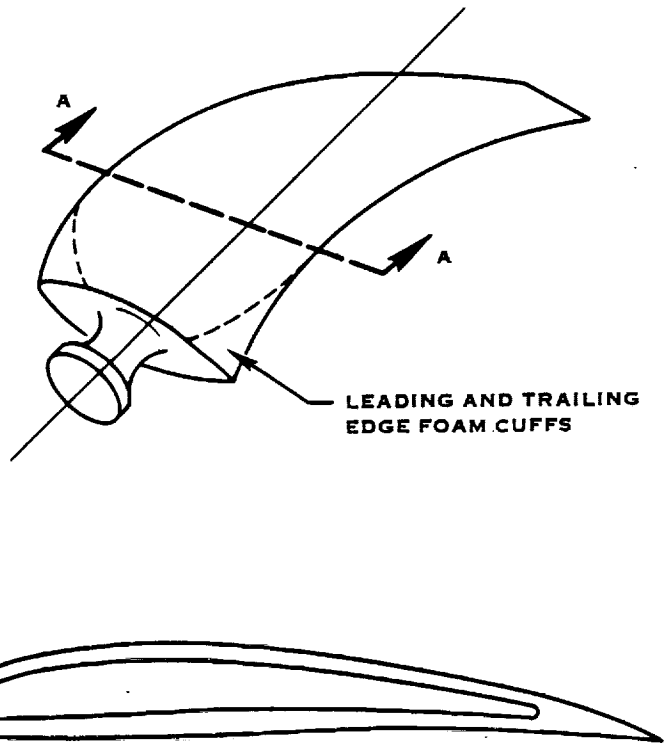

CROSS-SECTION A-A

DISADVANTAGES

- NO DAMAGE ISOLATION
- SUSCEPTIBLE TO SHEAR LAG
- GENEROUS INNER RADII ARE REQUIRED AT LEADING AND TRAILING EDGES
- MINIMUM WALL THICKNESS GOVERNED BY FOD DENTING DAMAGE

FIGURE 8. MONOCOQUE DESIGN

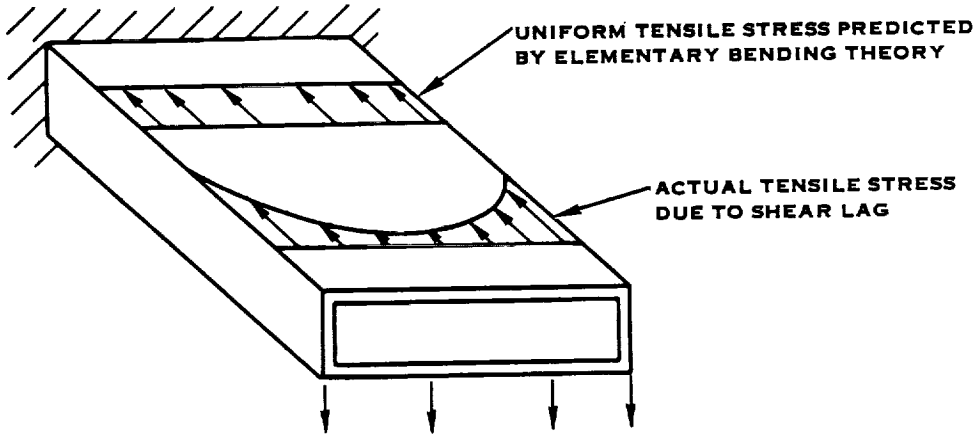

CANTILEVER BOX BEAM LOADED AT END

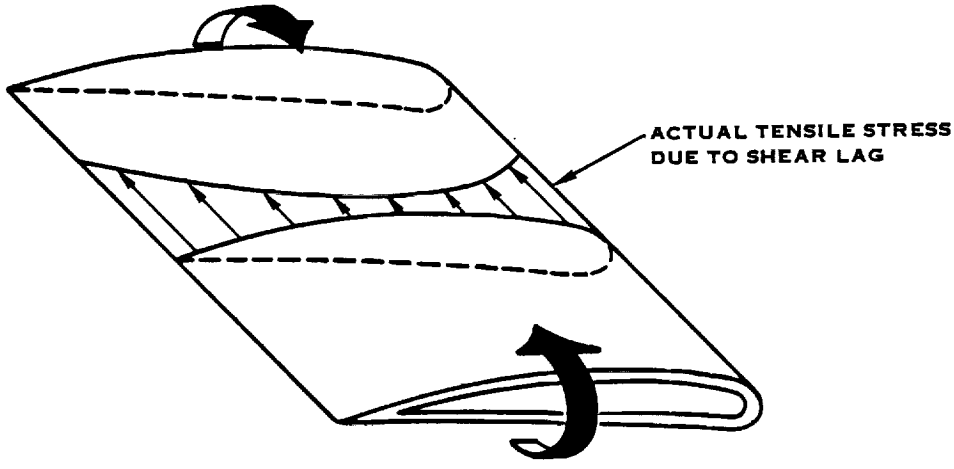

BLADE UNDER BENDING MOMENT

FIGURE 9. SHEAR LAG DEFINITION

With either a one-piece or two-piece monocoque design, the basic mass, stiffness and strength distributions are dictated by the wall thickness, which will be primarily determined by FOD impact criteria. These distributions can be modified somewhat by increasing the wall thickness or changing the external airfoil shape. However, the material added by increasing the wall thickness is less effective in adding stiffness since it is added to the inner wall. In a composite design, varying the fiber orientation can change the strength and stiffness distributions slightly, but their orientation will be primarily dictated by FOD impact criteria.

As with a solid composite blade, the retention area of a composite monocoque design will also require detailed evaluation. The composite blade will probably be mated to a solid metal shank/retention area or to metal components in the shank/retention area. The stresses in this critical area must be below the material fatigue stress limits for normal operating stress levels and below critical ultimate stress limits for FOD impact loads.

C. MODIFIED MONOCOQUE BLADE

A modified monocoque blade design, either metal or composite, improves the basic monocoque design by adding integral internal webs between the face and camber sides to provide additional shear capacity beyond that available at the leading and trailing edges. This design is shown in Figure 10. The internal webs give increased bending and shear stiffness to the blade.

The shear lag problem of a monocoque design can be eliminated by properly spacing the internal webs in regard to the skin wall thickness. The bending stresses in the cirtical blade areas (Figure 2) can probably be designed to be within the material fatigue stress limits since the bending stiffness is greater than a monocoque design. The leading and trailing edge root areas of the blade may also be tapered to direct the load smoothly into the shank, with foam cuffs providing the airfoil shape.

By varying the number and thickness of the internal webs, the stiffness and mass distribution of the blade design can be modified to a small degree to reduce locally high bending stresses and tune the frequency response of the blade. However, since the outer wall thickness remains the primary governor in blade stiffness, this modification of the stiffness distribution may be small.

Although a modified monocoque design with integral internal webs eliminates the shear lag problem, many of the disadvantages of the monocoque design are also present in this design. Damage isolation remains a primary disadvantage, for either a metal or composite design. The wall thickness is still governed by the minor impact FOD criteria, rather than by the normal operating stress levels.

UNITED TECHNOLOGIES HAMILTON STANDARD

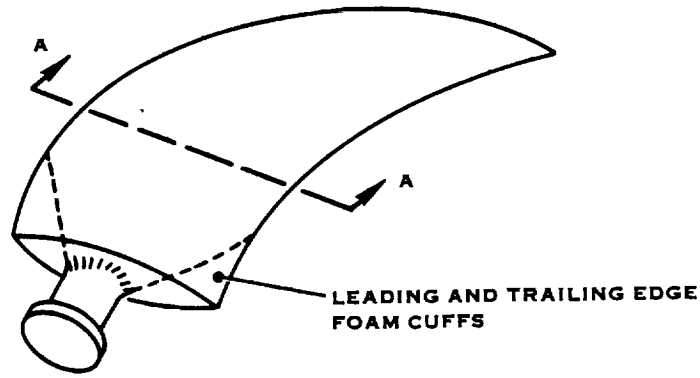

CROSS-SECTION A-A SHOWING INTEGRAL INTERNAL WEBS

DISADVANTAGES

- NO DAMAGE ISOLATION
- GENEROUS RADII AT ALL INNER JUNCTIONS
- MINIMUM WALL THICKNESS GOVERNED BY FOD DENTING DAMAGE

FIGURE 10. MODIFIED MONOCOQUE DESIGN WITH INTEGRAL INTERNAL WEBS

Manufacturing a one-piece design will require advanced methods due to the Prop-Fan geometry. Super-plastic forming/diffusion-bonding technology may be applicable in manufacturing a one-piece metal swept blade. However, development is required to determine internal web design and wall thickness and also to control the stresses in the leading and trailing edge areas. Manufacturing a one-piece composite swept blade design will require extensive development in order to incorporate the internal webs.

A two-piece design approach may be suitable for swept blade designs. The joints between the two pieces will require detailed evaluation; high shear stresses can occur at these joints. The leading edge joint must also withstand FOD impacts; repeated impacts may cause severe structural damage.

D. SPAR AND SHELL BLADE

All of the blade concepts discussed so far have in turn made more efficient use of material, but the inability to isolate surface damage has been a disadvantage of each concept. A particular type of modified monocoque design, a spar and shell design (illustrated in Figure 11), can provide this damage isolation capability with the proper choices of spar and shell materials. In general, it is necessary for the spar and shell to be separated by a low modulus layer, such as adhesive, or for the spar and shell to be made from materials with different crack propagation characteristics, such as metal and composite. The various spar and shell fabrication and material concepts are summarized in Table 4.

In the spar and shell design, the spar is the primary structural component. Through judicious selection of thickness and/or material, the objective is to make the shell the secondary structure, loaded by the spar-governed deflections and carrying only the cross-sectional air loads. If the shell becomes damaged, possibly from an FOD impact, that damage can be isolated from entering the spar, the primary structure of the blade. The shell also acts to protect the spar from erosion, nicks and gouges. In the unlikely event of a loss of a portion of the shell following service-induced damage, the spar remains intact to carry the gross loads. A spar and shell design will minimize the resulting imbalance if a portion of a blade is lost. This low imbalance will permit continued operation at partial power for a short time, or allow a controlled shutdown of the engine, if necessary. Proper choice of spar and shell materials also provides for easy repairability of any shell damage, permitting re-use of the blade and extending its service life.

A spar and shell design is lighter than a solid blade design, and also lighter than a pure monocoque design of the same structural capacity and materials. The lighter weight will permit a lighter retention, hub, and pitch change mechanism. In addition, the stresses in the critical areas of the blade (Figure 2) can be designed to be within the material fatigue stress limits, due to the low centrifugal loads and low bending loads.

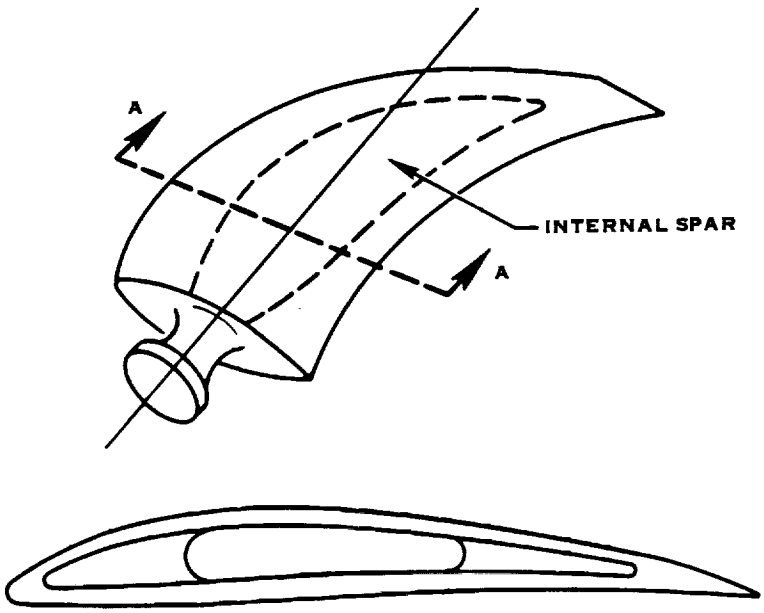

CROSS SECTION A-A SHOWING SOLID SPAR

ADVANTAGES

- SPAR IS MAJOR STRUCTURAL COMPONENT AND IS RELATIVELY INDEPENDENT OF AIRFOIL IN SIZE AND LOCATION
- DAMAGE ISOLATION IS POSSIBLE
- WALL THICKNESS OF SPAR AND SHELL CAN BE VARIED INDEPENDENTLY
- WIDE CHOICE OF SPAR AND SHELL MATERIALS

FIGURE 11. SPAR AND SHELL DESIGN

TABLE 4. SPAR AND SHELL FABRICATION CONCEPT COMPARISON

SPAR DESIGN	SOLID		SOLID	SOLID	HOLLOW	HOLLOW	HOLLOW	HOLLOW
SPAR MATERIAL SHELL MATERIAL	METAL METAL	METAL COMPOSITE	COMPOSITE METAL	COMPOSITE COMPOSITE	METAL METAL	METAL COMPOSITE	COMPOSITE METAL	COMPOSITE COMPOSITE
HAMILTON STANDARD EXPERIENCE	STUDIED	PRODUCTION	STUDIED	STUDIED	PRODUCTION	PRODUCTION	STUDIED	STUDIED
SWEPT SHAPE SUITABILITY • MANUFACTURABILITY - SPAR - SHELL	EXC GOOD	EXC EXC	VERY GOOD[1] GOOD	VERY GOOD[1] EXC	REQ. DEVEL. GOOD	REQ. DEVEL. EXC	VERY GOOD[1][2] GOOD	VERY GOOD[1][2] EXC
• STRUCTURAL SUITABILITY	FAIR	VERY GOOD	FAIR/POOR	GOOD	GOOD	VERY GOOD	FAIR/POOR	GOOD
• DISTORTION RESISTANCE	GOOD	VERY GOOD	GOOD	VERY GOOD	VERY GOOD	EXC	GOOD	VERY GOOD
LOAD LEVEL • RETENTION	HIGH	MODERATE/ HIGH	MODERATE	LOW/ MODERATE	MODERATE	LOW/ MODERATE	LOW/ MODERATE	LOW
• PITCH CHANGE	HIGH	MODERATE	HIGH	MODERATE	MODERATE	LOW	MODERATE	LOW
SHEAR LAG RESISTANCE	EXC	EXC	EXC	EXC	GOOD	GOOD	GOOD	GOOD
DESIGN FLEXIBILITY - ABILITY TO MODIFY STRUCTURAL CHARACTERISTICS	FAIR	GOOD	GOOD	VERY GOOD	GOOD	VERY GOOD	VERY GOOD	EXC
RESISTANCE TO FOREIGN OBJECT DAMAGE[2] • IMPACT LOAD CAPACITY	GOOD	GOOD	FAIR	FAIR	GOOD	GOOD	FAIR	FAIR
• DAMAGE ISOLATION ABILITY	GOOD	EXC	FAIR	GOOD	GOOD	EXC	FAIR	GOOD
• REPAIRABILITY - SHELL ONLY (SURFACE DAMAGE, CRACKS)	POOR	GOOD	POOR	GOOD	POOR	GOOD	POOR	GOOD

(1) SHANK AND RETENTION AREA REQUIRES DEVELOPMENT
(2) HIGHLY DEPENDENT ON MATERIAL AND MANUFACTURING PROCESS

All loads are directed from the shell into the spar over the full length of the spar. A large mutual contact area between the shell and spar will provide for load transfer from the shell to the spar with very low unit stressing. The loads then move directly into the retention.

Since the spar and shell are separate components, different materials can be used for each component. Advanced materials may be used without adding unnecessary costs since the concept allows for use of the material where it provides the best return. Separate spar and shell components permits varying the mass, stiffness and strength distributions along the blade by modifying the materials and component designs. This design flexibility can be used to reduce locally high bending stresses and to tune the blade frequency response. The ability to modify the chordwise stiffness and strength, inherent in the spar and shell concept, can be used to improve the distortion resistance and the FOD impact capacity.

E. RETENTION CONCEPT

The Prop-Fan blade designs will incorporate a variable pitch retention scheme. Although the retention and pitch change design is independent of the fabrication concept, the size of the retention and pitch change mechanism is directly influenced by the loads transmitted from the blade. These loads must be minimized to design a lightweight retention, hub, and pitch change mechanism.

Single-row and double-row angular contact ball bearing retention schemes have been concepted since these schemes are commonly used in turboprop designs. These retention designs also allow for blade replacement as specified in the Design Requirements Document. The axial retention force limit is plotted in Figure 12 for single-row and double-row retentions for a range of pitch change diameters and ball diameters, for 29 balls per race. The axial retention force, for sizing purposes, can be equated not only to the centrifugal load but also to the bending moment load through the relationship: $F = 2M/r$, where F is the axial load, M is the bending moment, and r is the pitch radius. This curve can be used to determine a specific retention size. The retention stiffness and other required parameters for use in the Task III blade analysis will be determined for this specific retention size.

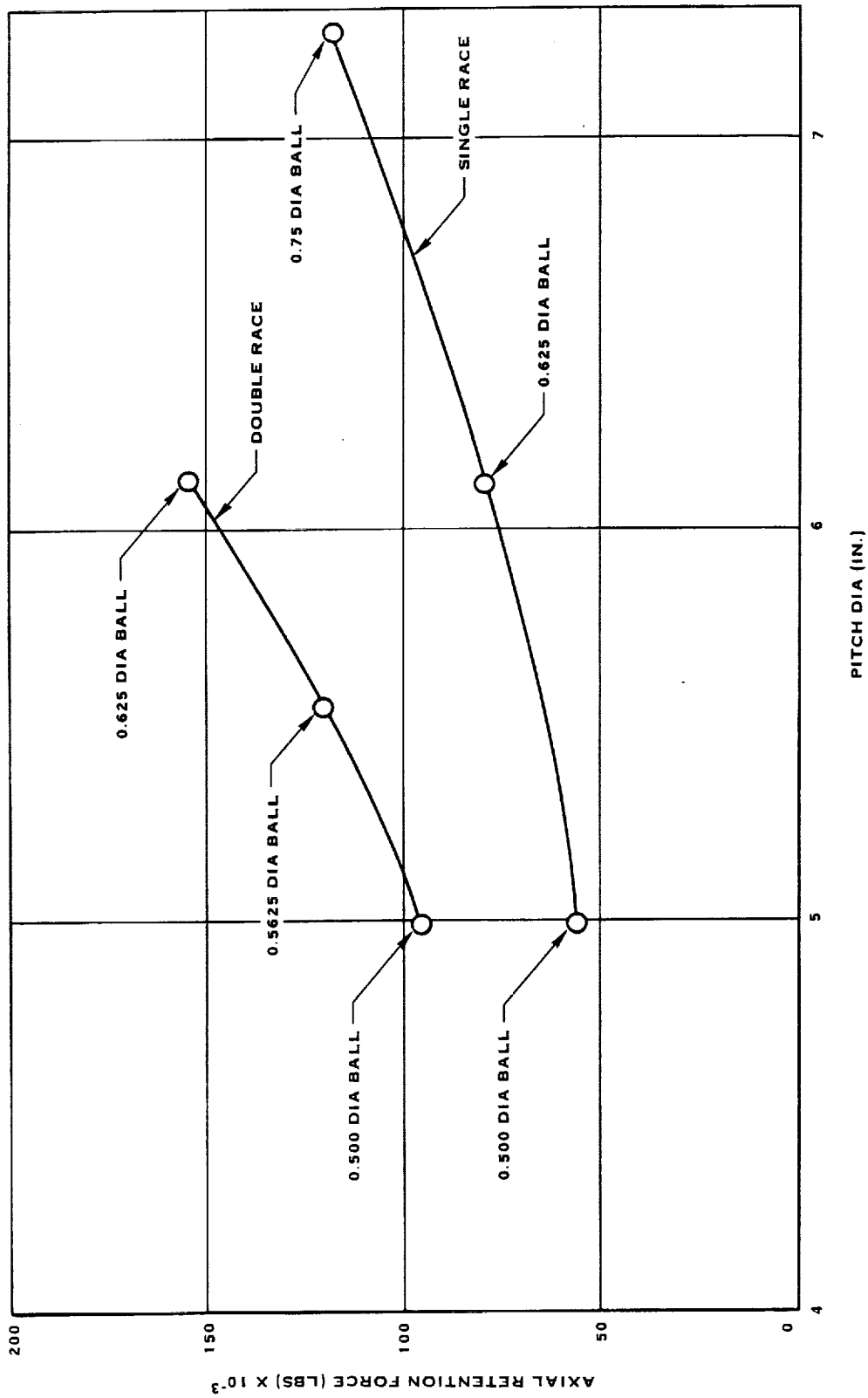

FIGURE 12. BLADE RETENTION STUDY (29 BALLS/RACE)

V. RECOMMENDED CONCEPTS

Hamilton Standard's blade design experience, ranging from service-proven designs to advanced designs, is summarized in Table 5. The experimental designs, produced and tested but not yet in service, represent Hamilton Standard's efforts to incorporate state-of-the-art technology into production blade applications. The advanced design concepts represent new methods being investigated in blade and blade component manufacturing, resulting in increased structural capacity, lighter weight, and simplified manufacturing.

From the various fabrication concepts shown in Figure 6 and previously discussed, and based on Hamilton Standard's experience with various fabrication concepts, the recommended fabrication concepts to be evaluated in Task III have been chosen. The recommended concepts for each Prop-Fan blade design are:

SR-2 (8 way):	Metal spar,	Composite shell
SR-3 (8 way):	Metal spar,	Composite shell
SR-3 (10 way):	Metal spar,	Composite shell
SR-5 (10 way):	Metal spar,	Composite shell
	and	
	Composite spar,	Composite shell

The spar and shell design allows greater design flexibility than the other fabrication concepts. This design flexibility implies high assurance that the blade requirements will be satisfied for all of the blade designs. The spar and shell fabrication method offers:

- Excellent damage isolation and repairability
- Lower weight, higher load capacity
- Lower retention, hub and pitch change mechanism weight
- Greater design flexibility for reducing local stresses, tuning blade frequencies, and absorbing FOD impact loads
- Lower cost by using smaller amounts of expensive materials and proven, existing manufacturing techniques
- Good adaptibility to resin injection fabrication processes currently being evaluated

TABLE 5. BLADE DESIGN EXPERIENCE

- Production Designs - Service Proven

  Solid Aluminum (Many large and small installations)

  Hollow Steel Spar/Fiberglass Shell (P-2, E-2/C-2)

  Solid Aluminum Spar/Fiberglass Shell (DHC-7, OV-10D)

  Hollow Steel Spar/Hollow Steel Shell (B-377, KC/C-97)

- Limited Production Designs - Produced and with Limited Service

  Lightened Steel Spar/Polyimide Shell (C4 Wind Tunnel Blade)

  Monocoque Aluminum (L-1649)

- Experimental Designs - Produced and Tested

  Solid Titanium (SR-3 Model Blade)

  Hollow Steel Spar/Boron Epoxy Shell (JT9D Fan)

  Solid Titanium Spar/Boron Aluminum Shell (F100 Fan)

  Hollow Composite Boron/Al Spar (AVLABS)

  Monocoque Steel (C-132)

  Hollow Titanium Spar/Fiberglass Shell with Boron Tip (CP49T)

- Advanced Designs - Studied

  Super Plastic Formed/Diffusion Bonded (SPF/DB) Structures:

  Integral Sheath

  Spar

  Monocoque Design

  Monocoque Design with Reinforcing Ribs

C-3

For each Prop-Fan blade design, a composite shell was chosen since it provides greater design flexibility, better distortion resistance, lower pitch change loads and better damage isolation when compared to a metal shell. A metal spar is the primary spar concept since the retention and shank are an integral part of the spar and since it has no interlaminar shear problem. A second fabrication concept for the SR-5 is given, in accordance with the work statement. This concept also incorporates a composite shell, but has a composite spar. The composite spar design will require detailed evaluation of the interlaminar shear stress, due to both normal operating loads and FOD impact loads, and of the bending and shear joint stress in the retention and shank area where it will mate to metal components.

VI. STRUCTURAL ANALYSIS METHODS

The primary method in use at Hamilton Standard to perform blade structural analysis is based on beam theory. Close agreement of measured and calculated stresses and natural frequency values of numerous straight, high aspect ratio (length-to-chord) blade designs over the past forty years demonstrate that beam theory analyses are valid and accurate. The SR-1 and SR-2 Prop-Fan model blades were analyzed successfully with beam theory. When analyzing a highly swept blade design, such as the SR-3 and SR-5 Prop-Fan model blades, the standard beam analysis were significantly in error in predicting stresses, retention loads, and resonant frequencies above the first bending mode. For this reason, these beam programs have been recently improved to accommodate the mass and elastic axis offset associated with swept blades. In addition, a more sophisticated aeroelastic dynamic response analysis program, also based on beam theory, has been put into use for analyzing swept blades. These beam theory programs will be used to analyze the SR-2 blade design.

The SR-3 and SR-5 blade analyses will be performed using finite element methods. The finite element methods, incorporated in an in-house program called BESTRAN, were used very successfully in analyzing the APSI (Advanced Propulsion System Integration) advanced composite fan blade, a metal spar and metal matrix composite shell design. The APSI analytical results for frequencies, mode shapes, deflections, and stress distribution matched measured data taken during the structural verification program prior to the aerodynamic test program. The full range of the planned aerodynamic test program was completed on the first build of the fan without any restrictions due to structural limitations. BESTRAN has also been used to design several Prop-Fan model blades. Analytical results were in excellent agreement with measured data.

A. BEAM THEORY ANALYSIS

Beam theory analysis will be used for the structural analysis of the SR-2 Model design. The Design Requirements Document will serve as the standard of acceptability for the results of these analyses. The beam theory analysis sequence is shown in Figure 13. The blade design process is iterative. The blade loads, stressing, and dynamic characteristics are calculated and are continually compared to the material allowables and design requirements as delineated in the Design Requirements Document. Should these comparisons indicate an unacceptable condition, appropriate modifications will be made and this process repeated.

Blade Strip Analysis Program (H444) - The strip analysis program, H444, calculates the airloads using two-dimensional compressible airfoil data. The input to the program is the definition of the operating condition being studied: shaft horsepower, propeller rotational speed, pressure altitude, velocity, ambient temperature and air

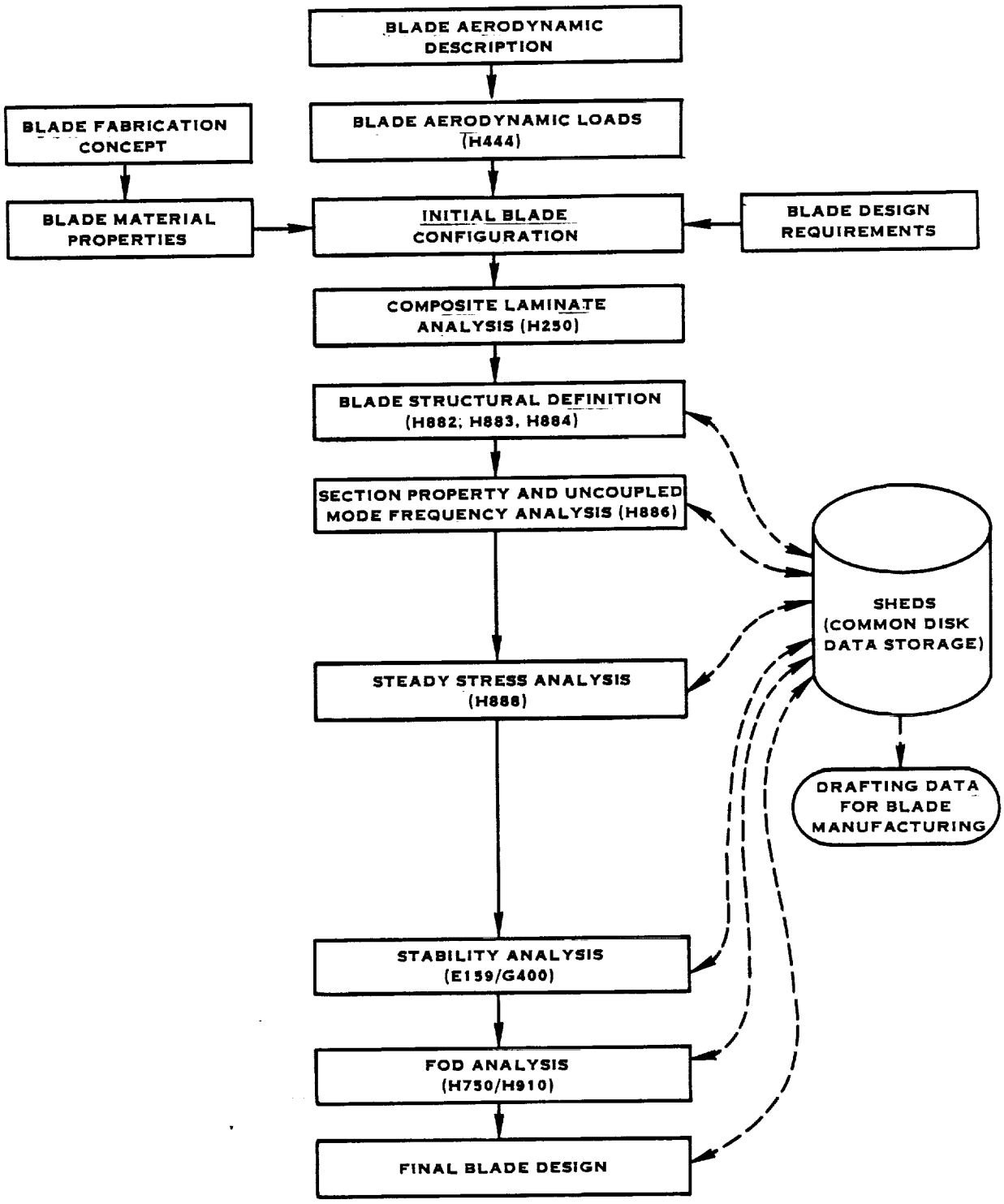

FIGURE 13. BEAM THEORY ANALYSIS BLADE DESIGN SEQUENCE

inflow angle (or excitation factor). This program then calculates the in-plane and out-of-plane airload distribution and also the aerodynamic twisting moment distribution for the given operating condition.

Composite Laminate Analysis (H250) - If composite laminates are used in the design, the composite laminate analysis program, H250, will be used to calculate the elastic properties and strengths of the laminate. The elastic properties and strength of each layer and the layer orientation are required input, and the elastic properties and strengths of the laminate in two orthogonal directions are generated by the program.

Blade Configuration Description - Structural (H882, H883, H884, H886) - These computer programs form the basis for the beam theory structural analysis of propeller blades by converting material properties and geometric definitions into beam characteristics. These programs have evolved from beam theory analytical methods that have been in use at Hamilton Standard for many years. The structural characteristics of the propeller blade beam models are stored in a common computer data base storage system called SHEDS (Structured Hamilton Standard Engineering Data Storage). This common data base is accessed by the beam theory programs for the structural definition of the blade. The SHEDS system and related analysis programs lend themselves very well to this blade design study, as they make maximum utilization of the computer storage capabilities, speed up the design process (i.e., the blade input description does not need to be input for each program), and greatly reduce the chances for human error. The blade design is input to SHEDS using programs H882, H883, and H884.

The blade configuration is input to the SHEDS system from the fabrication concept, the material properties, the aerodynamic description, and the blade structural configuration definition. The fabrication concept has been chosen in Task II for each blade configuration.

The material properties include the elastic properties of the materials used in the fabrication concept, and can include spar material, shell material, sheath material, and hollow cavity fill material. The aerodynamic description of the blade includes: blade angle, airfoil chord, airfoil thickness, airfoil camber, and streamline angle at various radial stations; airfoil types and meanline descriptions; and airfoil stacking, sweep and offset descriptions. The structural configuration description will depend upon the selected fabrication concept, and can include the spar width and shell thickness distributions, leading edge sheath description, and blade shank/retention description.

The blade shape is then generated by fairing the streamline airfoil sections and internal blade geometry, if applicable, using spline curves in H884. Orthogonal planes are cut through the faired blade geometry at desired radial locations for beam property calculations and manufacturing dimensional definition.

Blade section properties are calculated in H886, based on the radial station cross-sections. Equivalent cross-sectional properties for non-homogeneous blade components are also calculated using their elastic moduli and density ratios. Pertinent cross-sectional properties are then integrated along the blade span to determine weight, blade stiffness distributions, and mass distributions. Beam theory analysis programs use the cross-sectional data calculated in H886 to calculate blade natural frequencies (static and rotating), steady-state and vibratory stress, deflection, centrifugal load, and centrifugal twisting moments. The H886 program also calculates the coupled flatwise and edgewise bending frequencies and uncoupled torsional frequency.

Airfoil Steady Stress (H028/H888) - The section properties and weights calculated at the various radial stations and stored in SHEDS are used by the steady-state stress program, H888, to calculate the steady-state bending stresses and the centrifugal stresses, under the combined whirling body and aerodynamic loads. These steady-state stresses are calculated at any specific operating condition by giving the horsepower and torque for that condition. H028 is a card-input program and H888 is an interactive program for use on a CRT terminal; both perform the same analysis.

Stability Analysis (E159/G400) - Stability calculations will be made using E159/G400. The uncoupled blade flatwise, edgewise, and torsional frequency modes are calculated by E159 using the blade information stored in SHEDS. The E159 program also extracts the necessary data from the SHEDS system for input into the aeroelastic dynamic response analysis program, G400. The G400 program is a single blade, multi-purpose computer program characterized by a rigorous modeling of the blade and accounting for the time-varying structural bending and twist deformations. The ability to analyze swept blades has been incorporated into the program, such that it can be considered a curved beam dynamic response analysis.

The required input to G400 includes the aerodynamic and structural definition of the blade (from SHEDS), and the aerodynamic flow field description at the desired operating condition. The G400 program produces the following output: blade steady and cyclic stresses, blade and hub shears and moments, blade in-plane and out-of-plane displacements, blade section angles of attack and blade damping. Transient time histories of these quantities can be generated in numerical and/or plotted forms. A moving block spectral analysis technique is employed to display the predominant response modes giving the frequencies and damping under loaded conditions. If the damping is negative system instability is indicated and the time histories show increasing amplitude. This aeroelastic method will be used to determine classical stability as well as stability in areas of dynamic stall.

Foreign Object Damage Analysis (H750/H910) - The blade designs will be analyzed for foreign object damage resistance using the programs H750 and H910. The evaluation of foreign object impact resistance involves three steps: 1) the definition of the

impact conditions; 2) the determination of the gross impact loads, blade response, and blade stressing from the gross structural blade characteristics; and 3) the determination of local stressing based on detailed local stress analyses. The first step is fundamental to any and all blade designs since it depends only on the engine characteristics, size and density of the specified foreign object, the airspeed, and the radial impact position on the blade. A pre-processor determines the penetration of a cylindrical mass (representing the bird) into the plane of the rotor and thus defines the fundamental impact parameters of size, weight, velocity and angle of impact of the slice of the ingested foreign object, which are needed for the second step of the analysis.

Having defined the impact conditions, the gross blade impact load, response, and stressing with time will then be calculated using the three dimensional Three-Mode-Interactive Blade Impact Program, H750/H910. The data stored in the SHEDS system for the blade designs are the structural characteristics that are used by H750/H910 in the FOD analysis.

The Three-Mode-Interactive Blade Impact Program utilizes a fluid missile model which is interactive with the dynamic modal response of the blade. This feature is essential to the analysis of FOD impacts, since the changing impact angle due to blade twist, the physical size of the missile, the changing rate at which it spreads on the blade surface during the impact event and the spreading mass thickness distribution have a large influence on blade response. The three-mode analysis uses the three beam-type modes of vibration to characterize the gross blade dynamics; i.e., the first flatwise bending, the first edgewise bending and the first torsional modes. Although coupling between blade modes is accounted for in the dynamic characteristics input to the three-mode analysis, the dynamic response of the blade is handled with uncoupled modes. This tends to put the calculated blade response stresses on the conservative side. The calculations performed by the three-mode analysis include local spanwise bending and torsional stressing at the impact station, chordwise bending at the impact station and secondary impact due to missile deflection and blade twist, in addition to gross blade stresses.

Through judicious tailoring of the blade design's fundamental natural frequencies, inertias, elastic axis, and center of gravity, by changing the shell ply layup and thickness, and spar location and size (for a spar and shell design) it is possible to minimize the gross blade impact response and stressing within the other blade design requirements and constraints.

After defining the gross blade characteristics, and the resulting impact loads, gross stresses, and response with time for the various impacts, the blade will then be analyzed for local stressing in the impact region. This stress will be calculated using the impact load distribution and magnitude from the gross impact analysis. The gross blade stresses and the local blade stresses are then compared to appropriate material stress allowables and to the foreign object damage limits as defined in the Design Requirements Document.

B. FINITE ELEMENT ANALYSIS

Finite element analysis will be used for the structural analysis of the SR-3 (8 way), SR-3 (10 way), and SR-5 blade designs. The finite element analysis blade design sequence is shown in Figure 14.

Finite Element Model Generation (IDS-3 System or F018) - The finite element models can be generated by the IDS-3 System, a software system incorporating a minicomputer central processing unit and a random access disk memory device. The output of the system can be viewed interactively on a CRT terminal. The model can also be generated using F018, and allows the designer to generate the model interactively using a CRT terminal. The key benefits of the IDS-3 system or F018 are reduced cost and improved accuracy during model generation. The design process is more creative due to elimination of repetitive drawing tasks. Greater accuracy is achieved by machine processing and storage of the digital data. The input to these systems is the blade aerodynamic and structural definition that is generated in the SHEDS system in the same manner as in the beam analysis method.

Finite Element Analysis (BESTRAN-H552) - The finite element analysis will be performed using an in-house, computerized general purpose three-dimensional finite element program known as BESTRAN (H552). BESTRAN is a computer program written in FORTRAN language comprising several specialized subprograms which work together, based on the methods of finite element analysis. This program is well-suited for a three-dimensional representation of a blade. BESTRAN is comparable in accuracy and sophistication of solution to NASTRAN, level 16.0, but does not have the same breadth. NASTRAN is also in-house and operating at Hamilton Standard, and has found wide application to diverse problems. BESTRAN will be used for the Prop-Fan blade designs because it has been used more frequently than NASTRAN for blade design at Hamilton Standard, and numerous time saving pre- and post-processing subroutines particularly suited to spar/shell blade design are in-place and operating.

BESTRAN will calculate the radial, chordwise, and shear stresses and deflections at any operating condition, and can also be used to calculate the static and rotating frequencies and mode shapes. The frequencies will be used to determine the critical speed margins and to confirm the swept beam method frequencies used in G400 for the final design stability analysis. The stresses and deflections due to the steady and cyclic air loads will be calculated by applying equivalent line loads to the nodes at the equivalent chordal center of pressure.

Foreign Object Damage Analysis (H750/H910) - The foreign object damage resistance analysis will be performed by the same method as described in the beam analysis section, except the frequencies predicted by finite element analysis will be used to confirm the dynamic input.

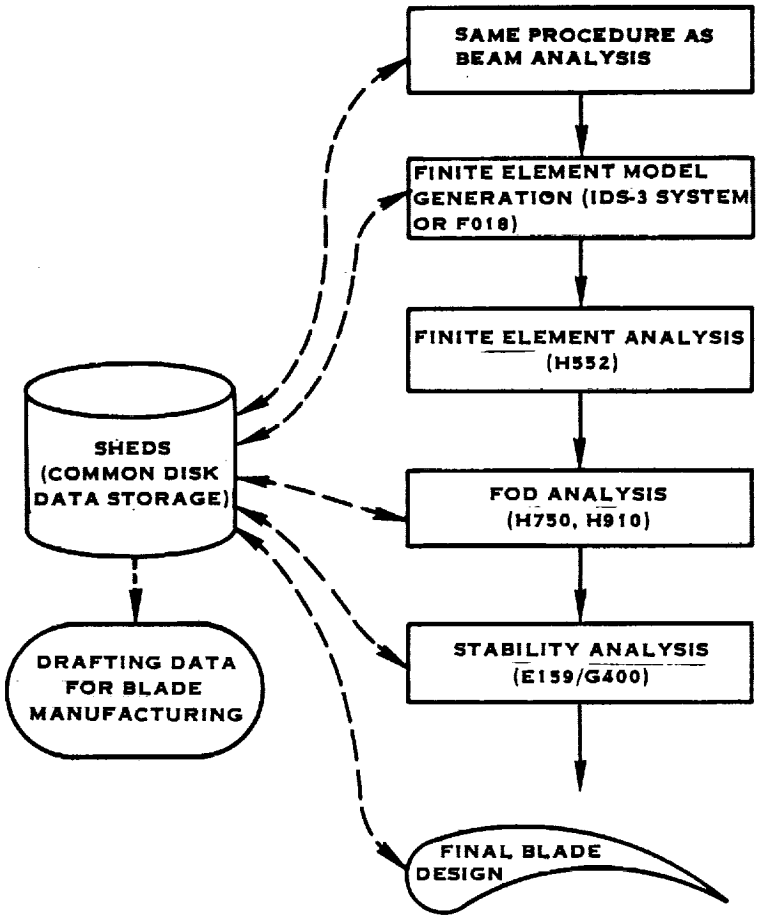

FIGURE 14. FINITE ELEMENT ANALYSIS BLADE DESIGN SEQUENCE

Stability Analysis (E159/G400) - The stability analysis will be performed using E159/G400, as described in the beam theory section, using the finite element frequency and mode shape results to confirm the dynamic input from beam model analysis.

APPENDIX C

DEFLECTION CONTOUR PLOTS

This appendix presents the individual blade concept deflection contour plots. The displacement that is plotted is the node point displacement resolved normal to the chord at the .75 r/R station. The rotation is the local rotation about an axis parallel to the pitch change axis.

The following plots are presented:

Blade Concept	Operating Condition	Contour Plot	Figure
SR-3 (8)	Cruise, steady-state	Deflection	C-1
SR-3 (8)	Takeoff, steady-state	Deflection	C-2
SR-3 (8)	Takeoff, cyclic	Deflection	C-3
SR-3 (10)	Cruise, steady-state	Deflection	C-4
SR-3 (10)	Takeoff, steady-state	Deflection	C-5
SR-3 (10)	Takeoff, cyclic	Deflection	C-6
SR-3C (10)	Cruise, steady-state	Deflection	C-7
SR-3C (10)	Takeoff, steady-state	Deflection	C-8
SR-3C (10)	Takeoff, cyclic	Deflection	C-9
SR-3 (8)	Cruise, steady-state	Rotation	C-10
SR-3 (8)	Takeoff, steady-state	Rotation	C-11
SR-3 (10)	Cruise, steady-state	Rotation	C-12
SR-3 (10)	Takeoff, steady-state	Rotation	C-13
SR-3C (10)	Cruise, steady-state	Rotation	C-14
SR-3C (10)	Takeoff, steady-state	Rotation	C-15

Displacement and rotation plots are not included for the SR-2, SR-5A, and SR-5B. This type of information cannot be obtained from the beam analysis that was used on the SR-2. The plots for the SR-5A and SR-5B are not presented since the data is no longer available. The data for the SR-5A and SR-5B presented in Table 10-1 was obtained from computer printouts.

STRESS CONTOUR PLOTS

This appendix presents contour plots of percent of allowable stress limit for high cycle fatigue for the components of the blade concepts. Section 4.12 described the procedure for calculating the percent of allowable stress limit. This percentage was determined for each element in the finite element models, and iso-contour plots were made. In these plots, a value of 100% means the stress state is at the material allowable stress limit. A value of greater than 200% is plotted as 200%.

The following plots are included:

Blade Concept	Blade Component	Stress Type	Component Surface	Figure
SR-3 (8)	Spar	Spanwise	Face	C-16
SR-3 (8)	Spar	Spanwise	Camber	C-17
SR-3 (8)	Shell	Spanwise	Face	C-18
SR-3 (8)	Shell	Spanwise	Camber	C-19
SR-3 (10)	Spar	Spanwise	Face	C-20
SR-3 (10)	Spar	Spanwise	Camber	C-21
SR-3 (10)	Shell	Spanwise	Face	C-22
SR-3 (10)	Shell	Spanwise	Camber	C-23
SR-3 (10)	Spar	Spanwise	Face	C-24
SR-3 (10)	Spar	Spanwise	Camber	C-25
SR-3 (10)	Spar	In-Plane Shear	Face	C-26
SR-3 (10)	Spar	In-Plane Shear	Camber	C-27
SR-3 (10)	Shell	Spanwise	Face	C-28
SR-3 (10)	Shell	Spanwise	Camber	C-29

Plots are not included for the SR-2 since plots of this type cannot be obtained from the beam analysis that was used. Plots for the SR-5A and SR-5B are not included since the data is no longer available. The data in the plots in Section 4.12 was obtained from computer printouts.

FREQUENCY DIAGRAMS AND MODE SHAPES

Campbell frequency diagrams for the blade concepts are presented as follows:

Blade Concept	Figure
SR-2	C-30
SR-3 (8)	C-31
SR-3 (10)	C-32
SR-3C (10)	C-33
SR-5A	C-34
SR-5B	C-35

Mode shapes for the resonant frequencies at cruise condition are also included:

Blade Concept	Figure
SR-3 (8)	C-36
SR-3 (10)	C-37
SR-3C (10)	C-38
SR-5A	C-39
SR-5B	C-40

STABILITY PLOTS

Plots of the stall flutter damping ratio for the SR-3 (8), SR-3 (10), and SR-5B concepts are shown in Figure C-41 through C-44, respectively. As mentioned in Section 4.15, a negative damping ratio prediction is inconclusive in determining stall flutter. Figure C-45 through C-48 show the stability boundary and the LAP flight profile, plotted against altitude, for the same design concepts.

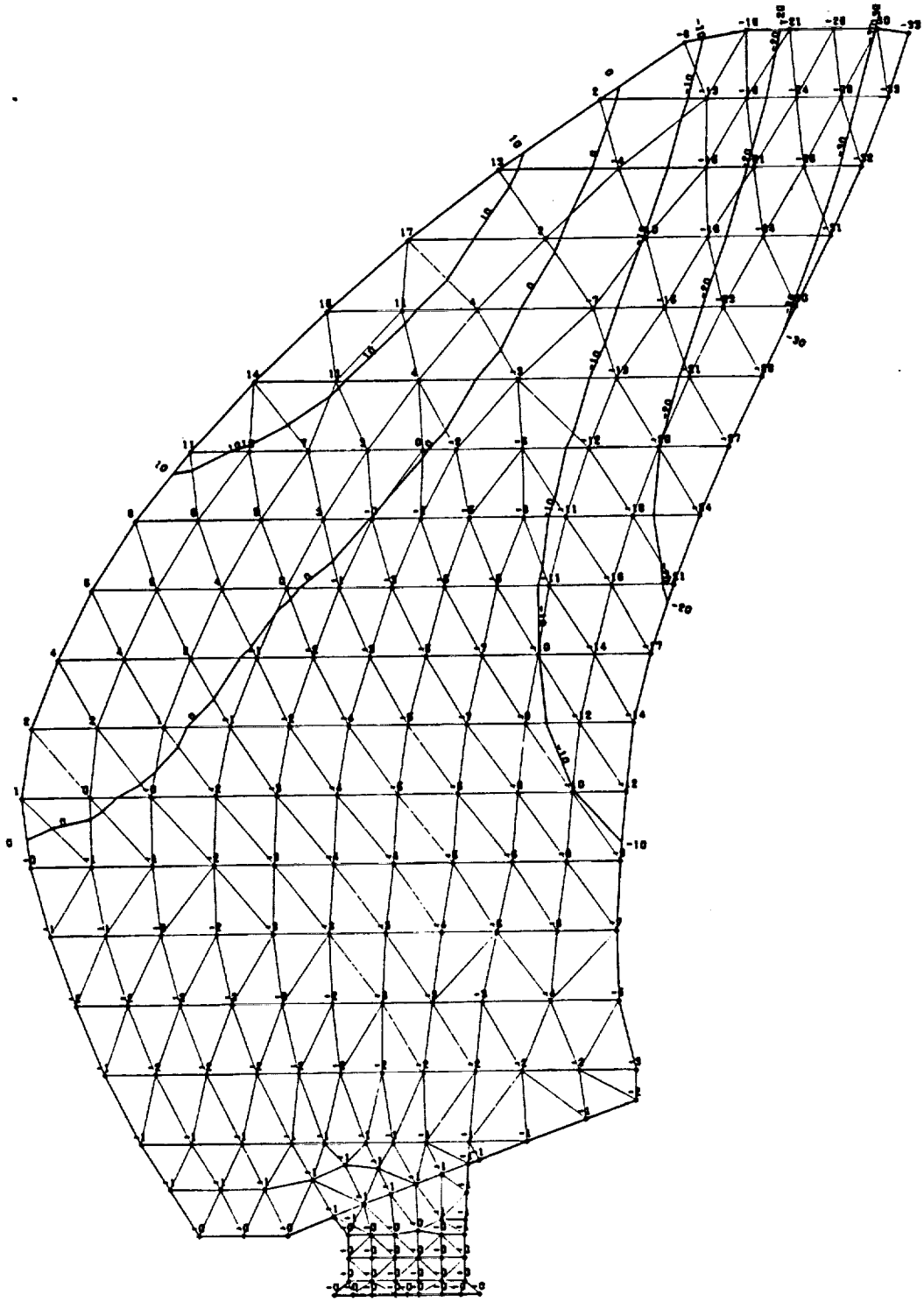

FIGURE C-1

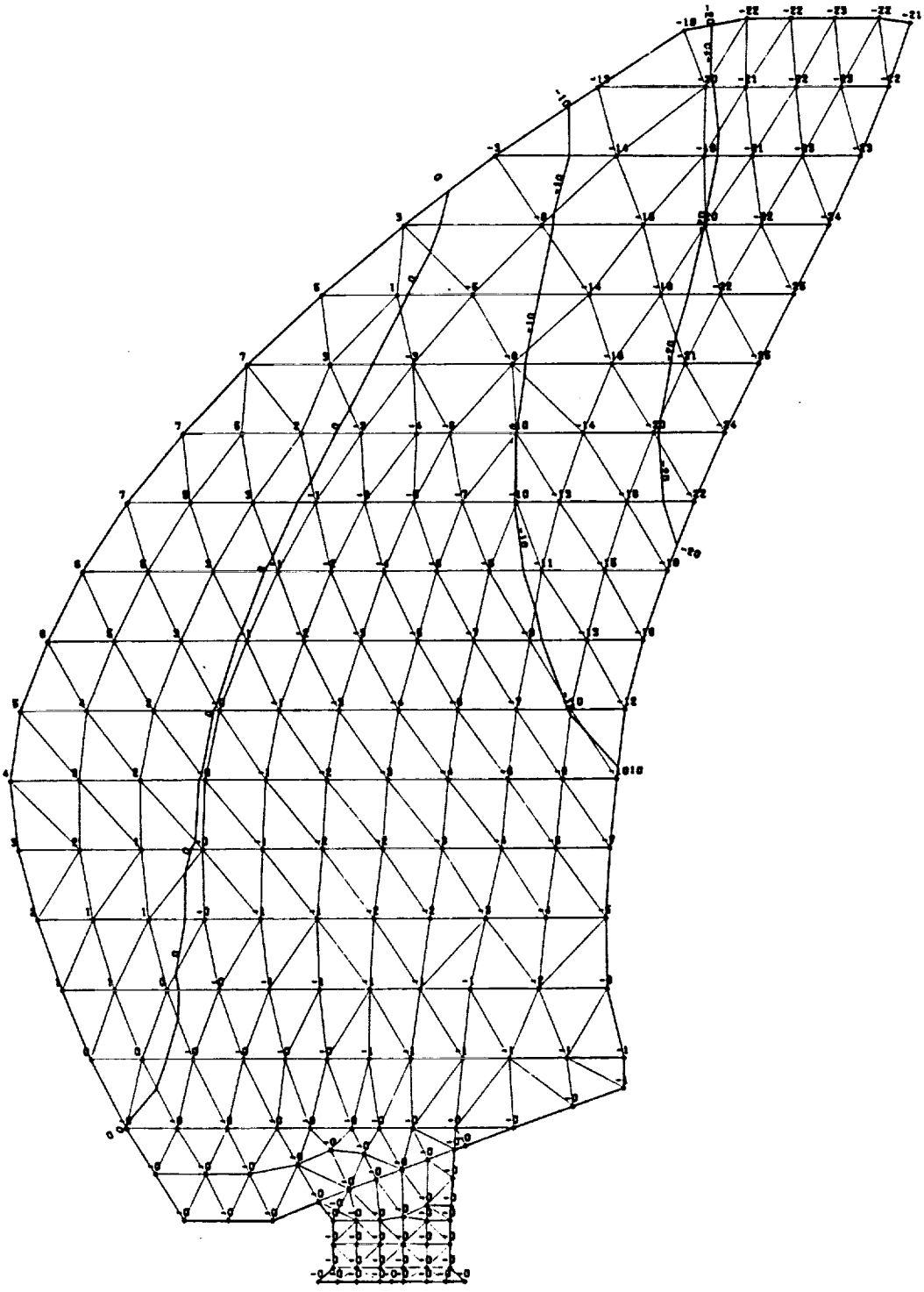

FIGURE C-2

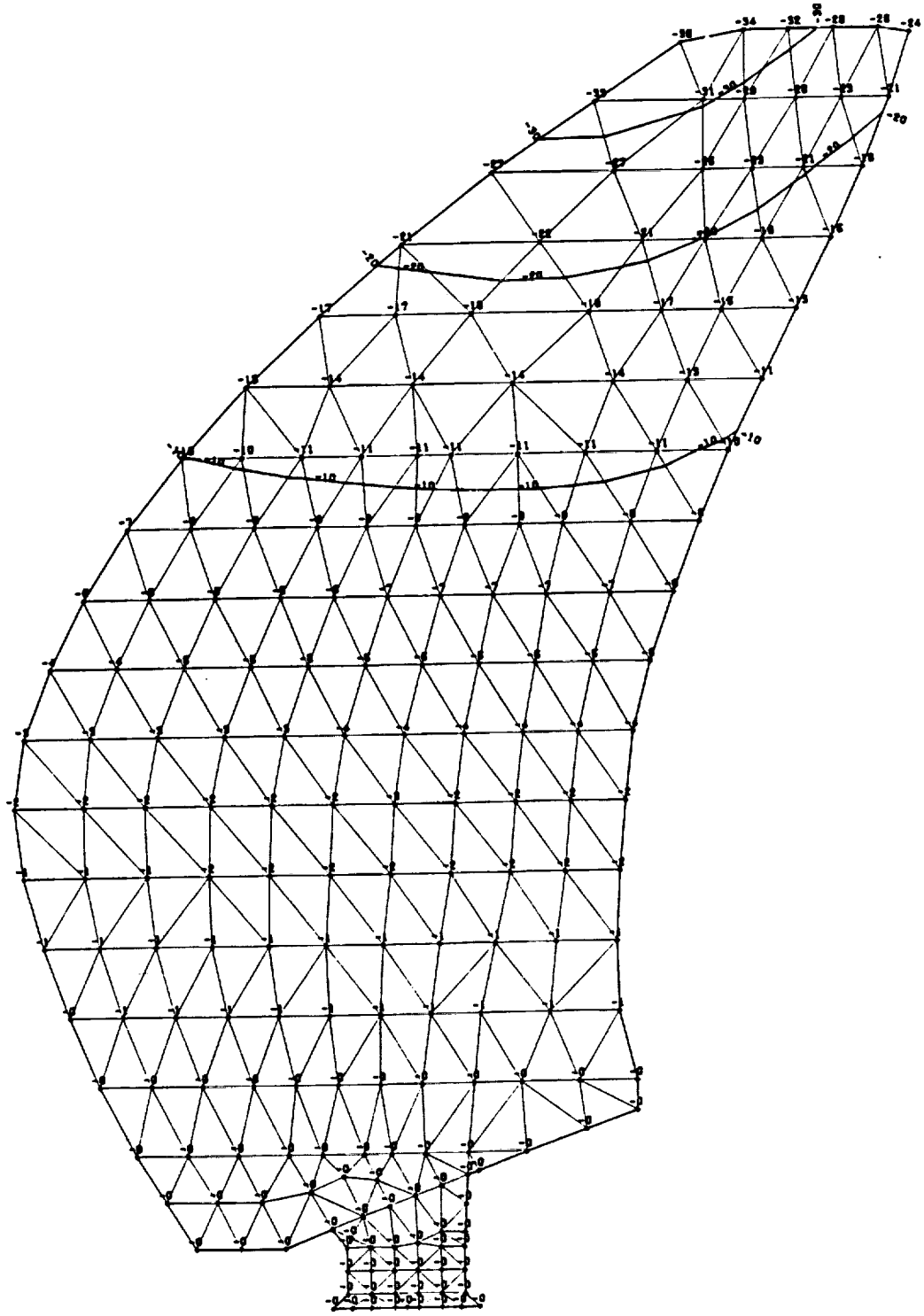

FIGURE C-3

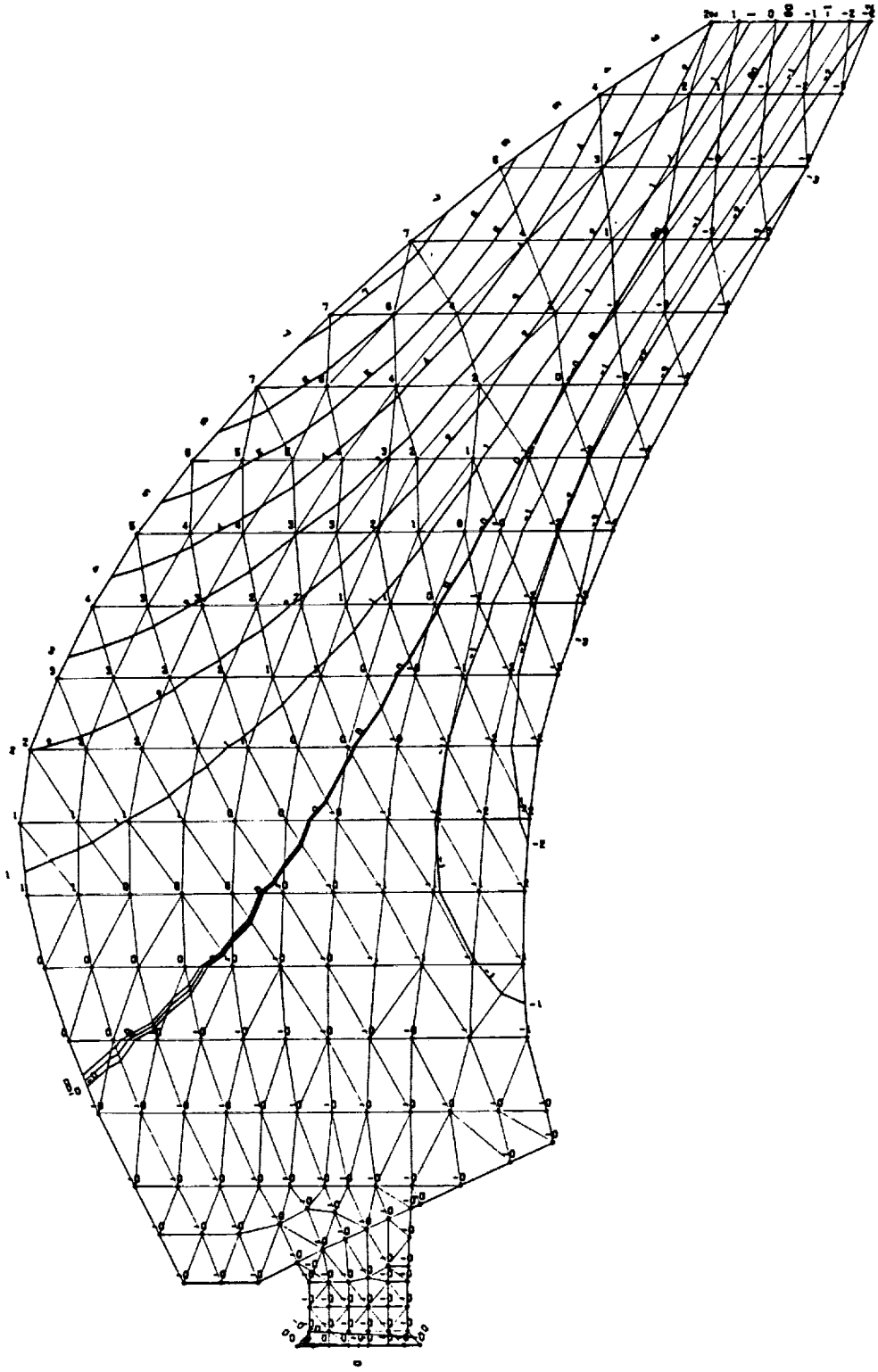

FIGURE C-4

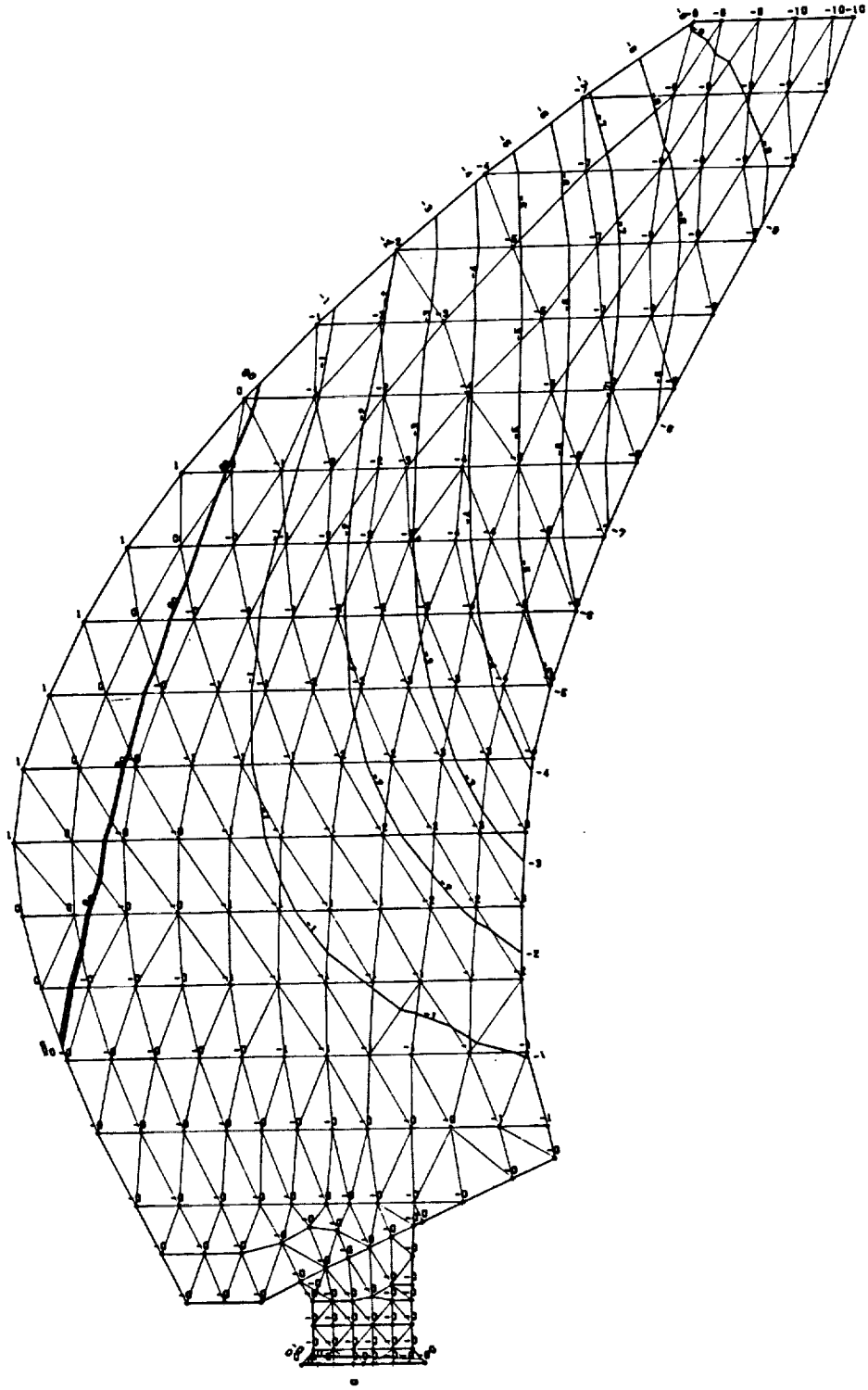

FIGURE C-5

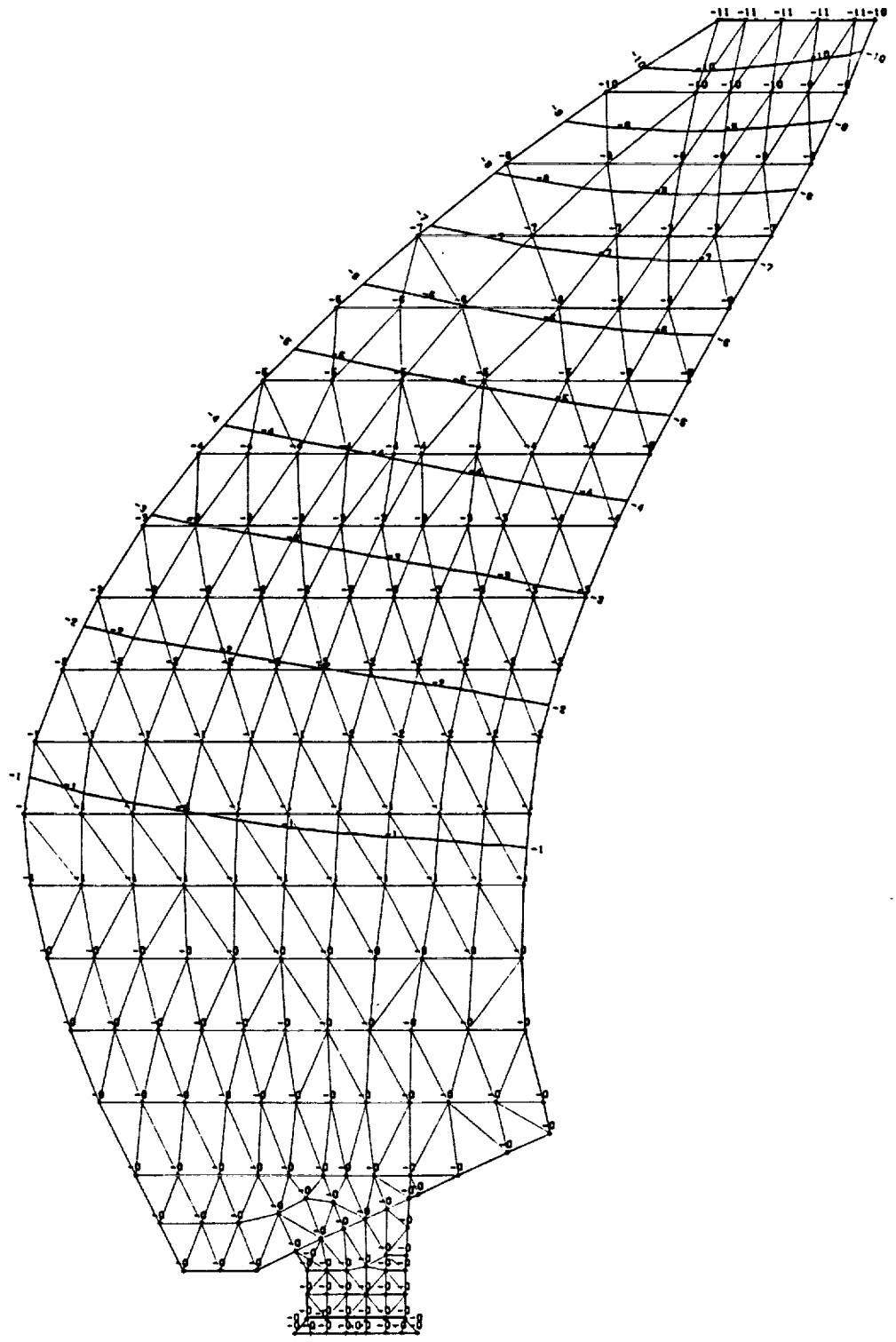

FIGURE C-6

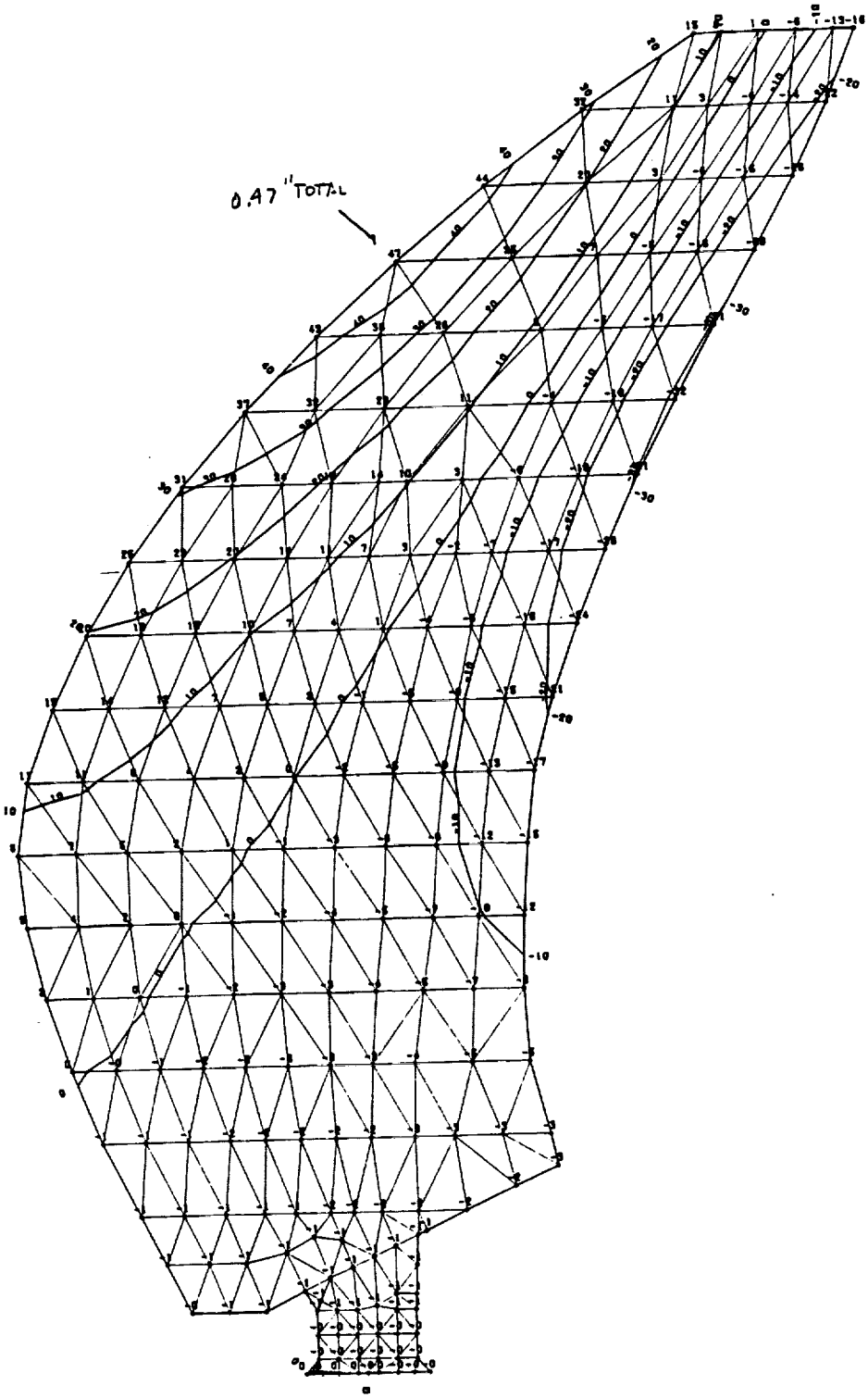

FIGURE C-7

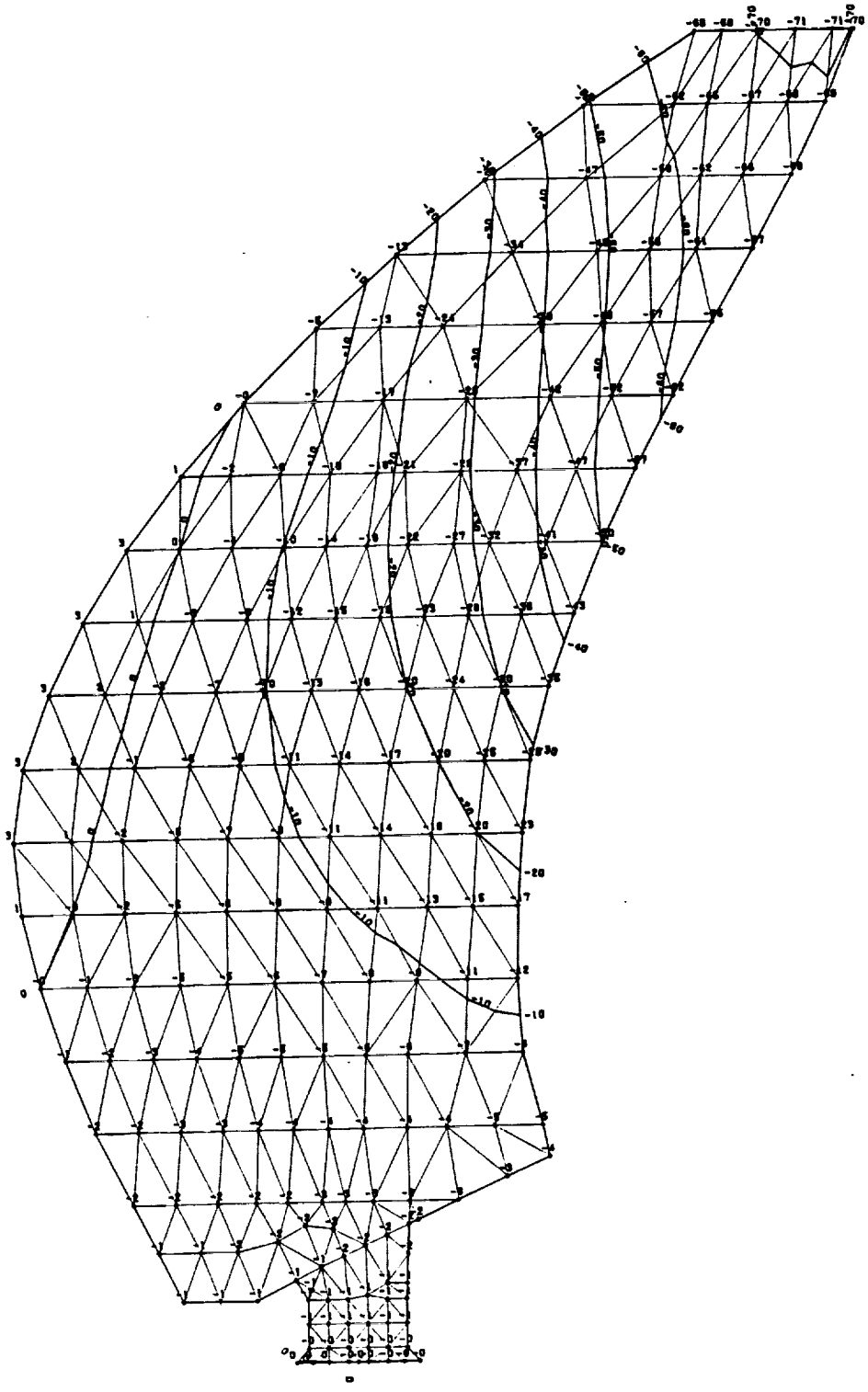

FIGURE C-8

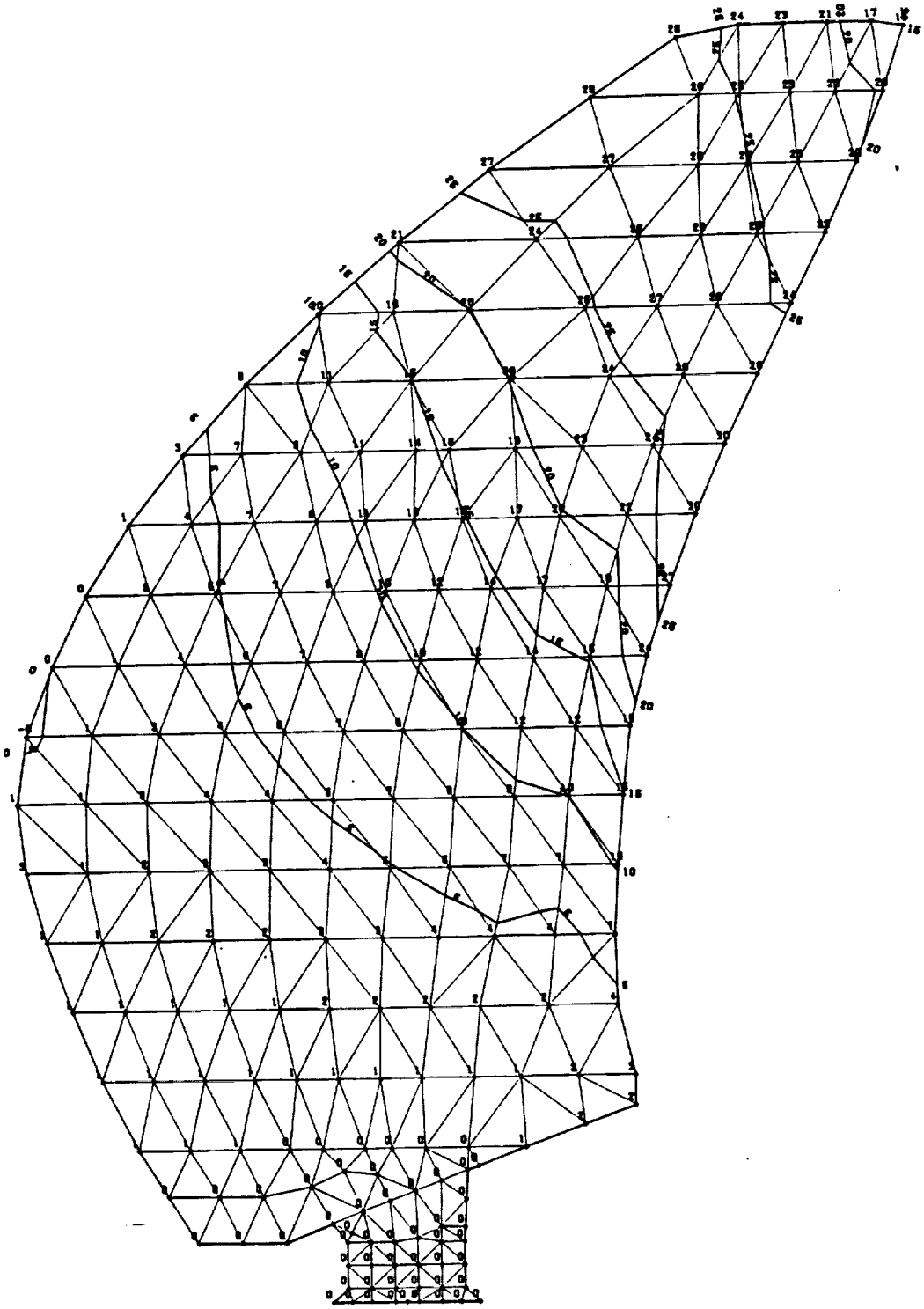

FIGURE C-9

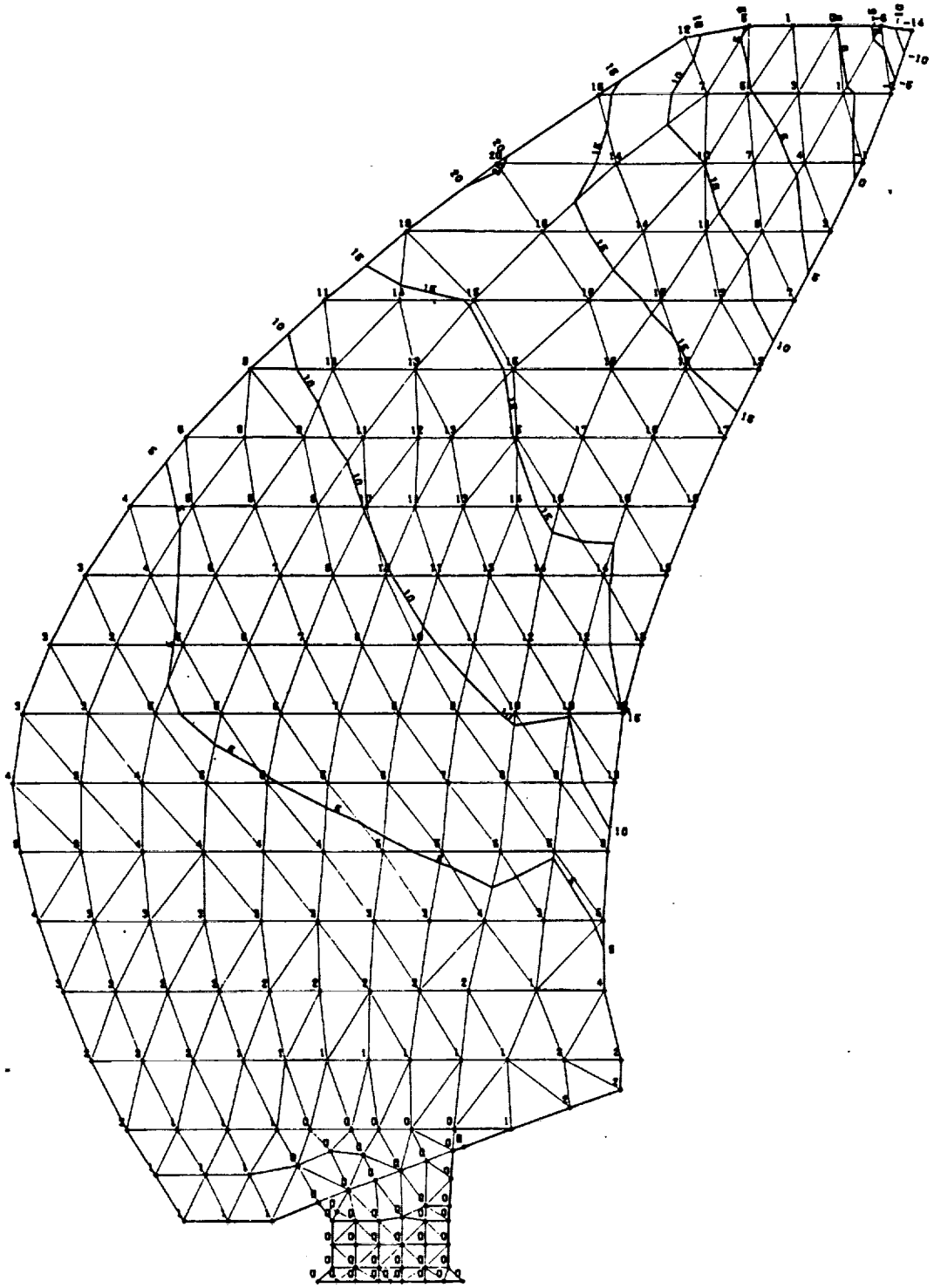

FIGURE C-10

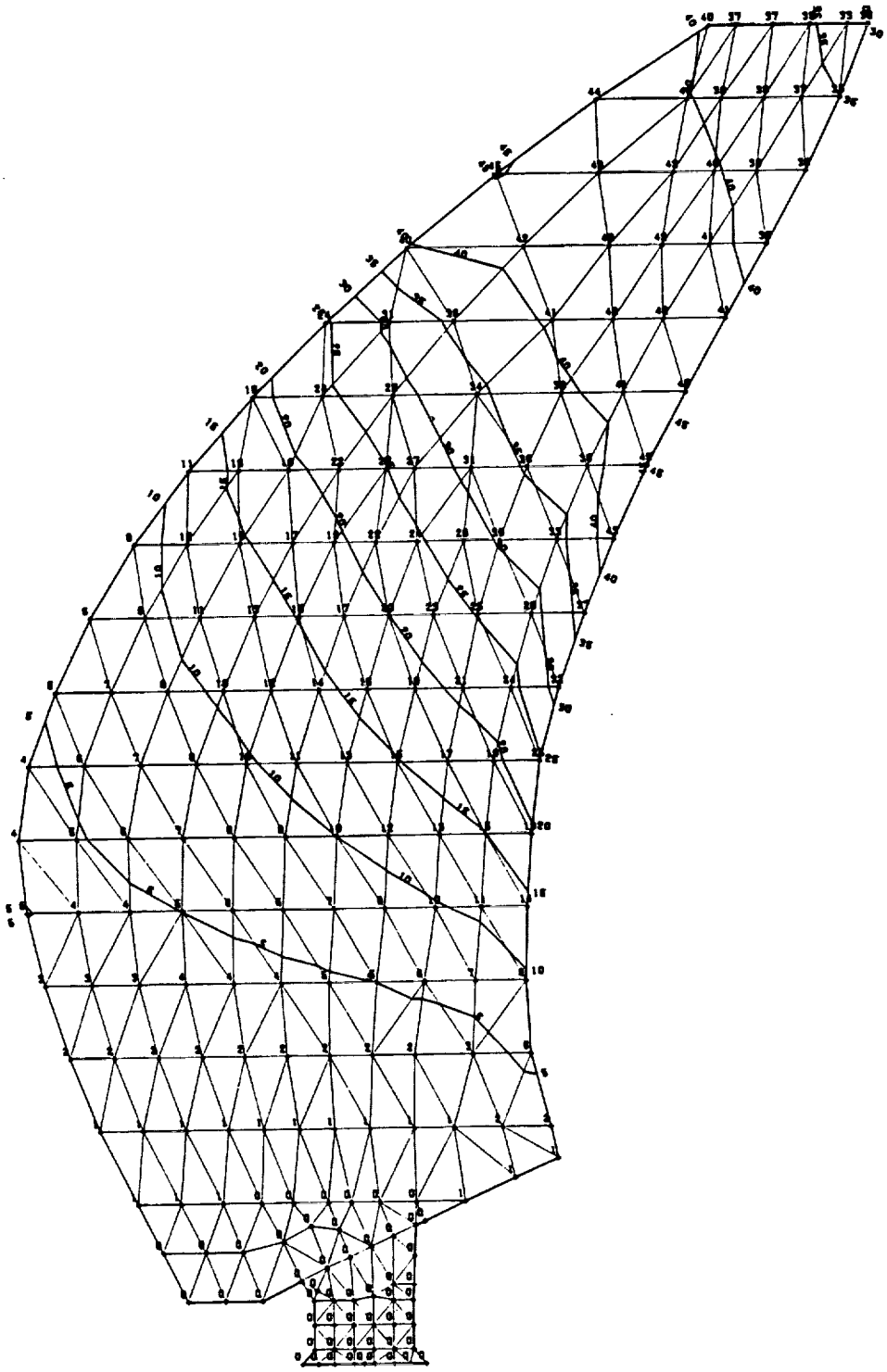

FIGURE C-11

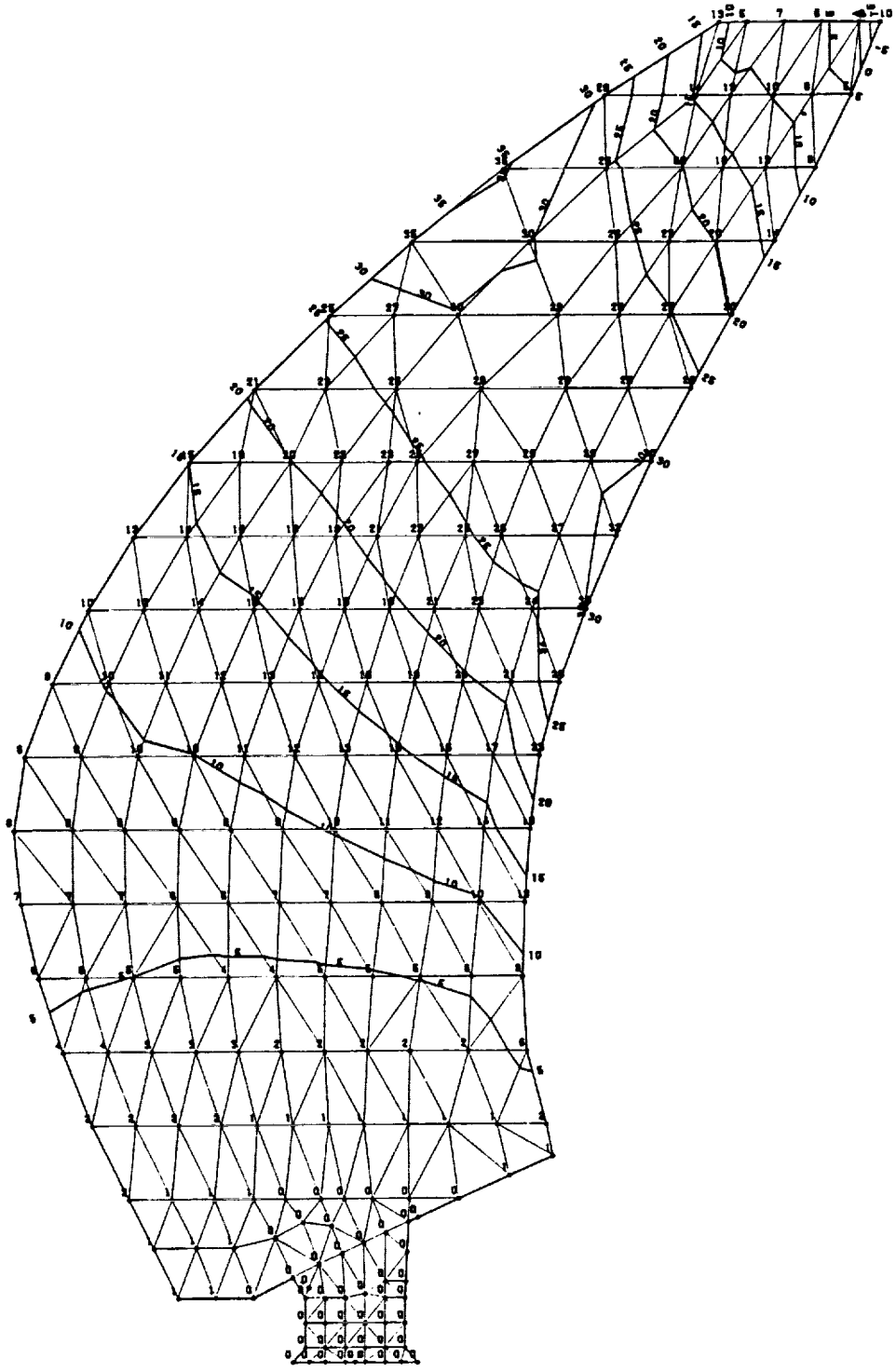

FIGURE C-12

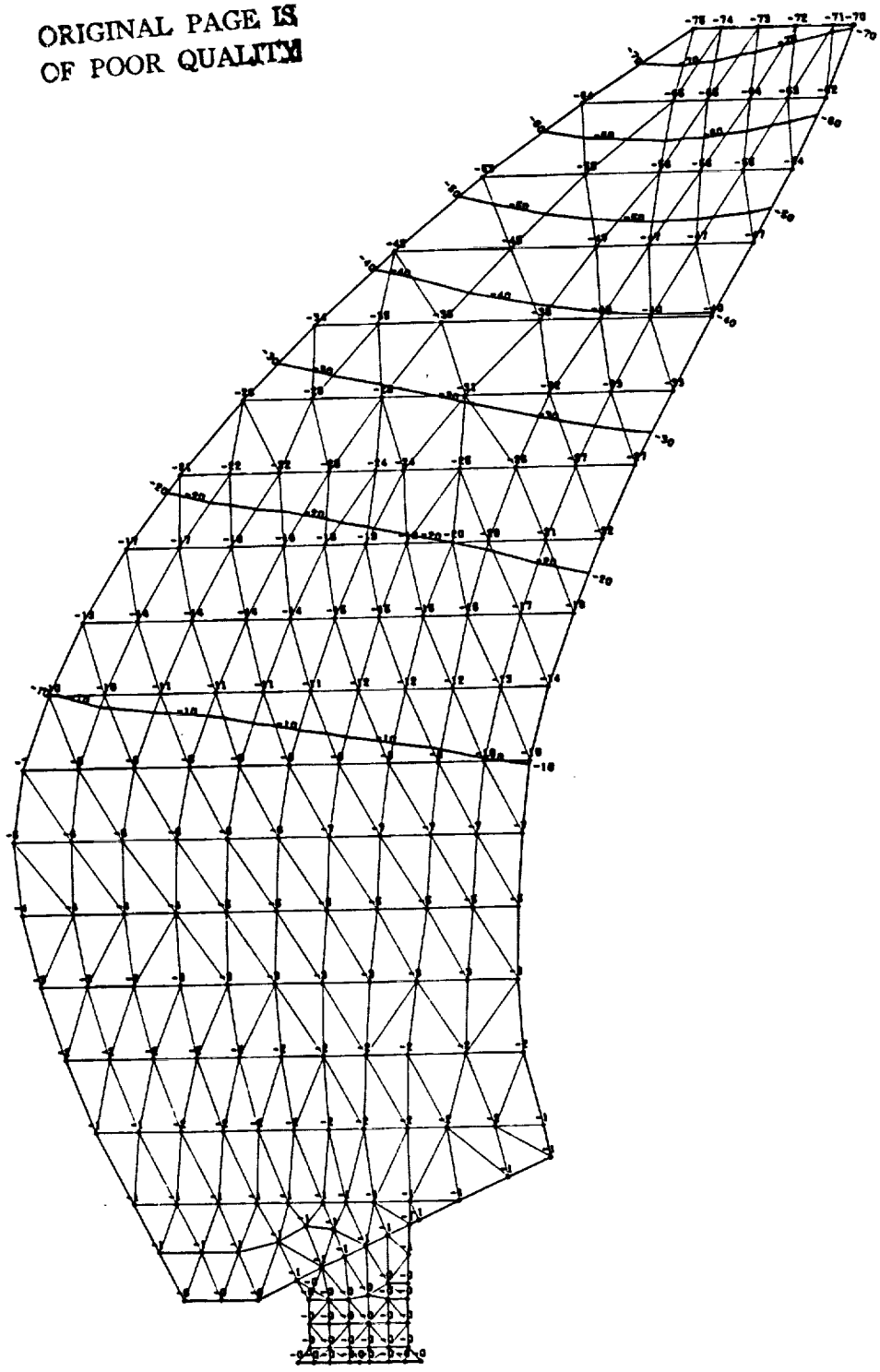

FIGURE C-13

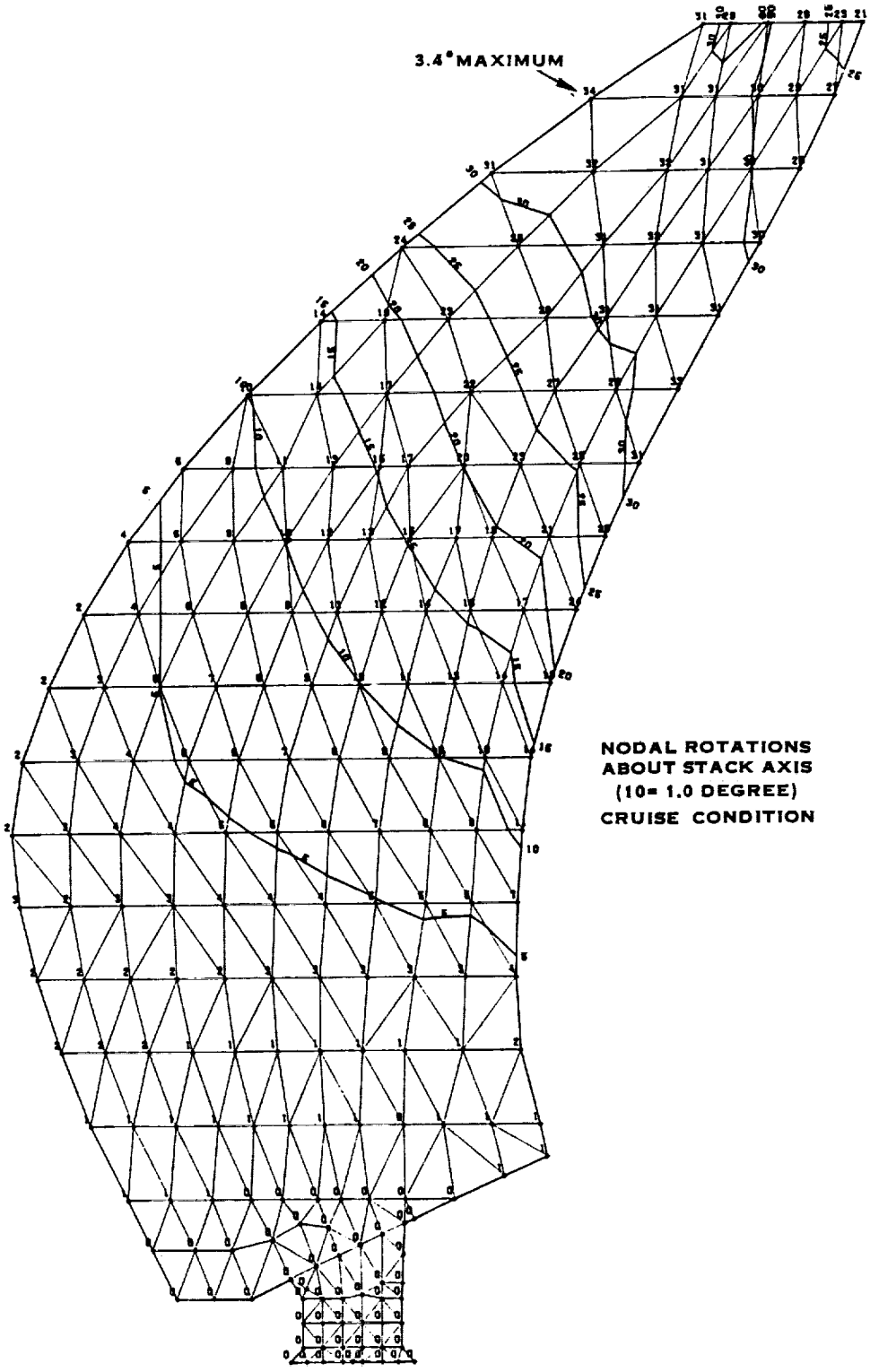
3.4° MAXIMUM
NODAL ROTATIONS
ABOUT STACK AXIS
(10= 1.0 DEGREE)
CRUISE CONDITION

FIGURE C-14

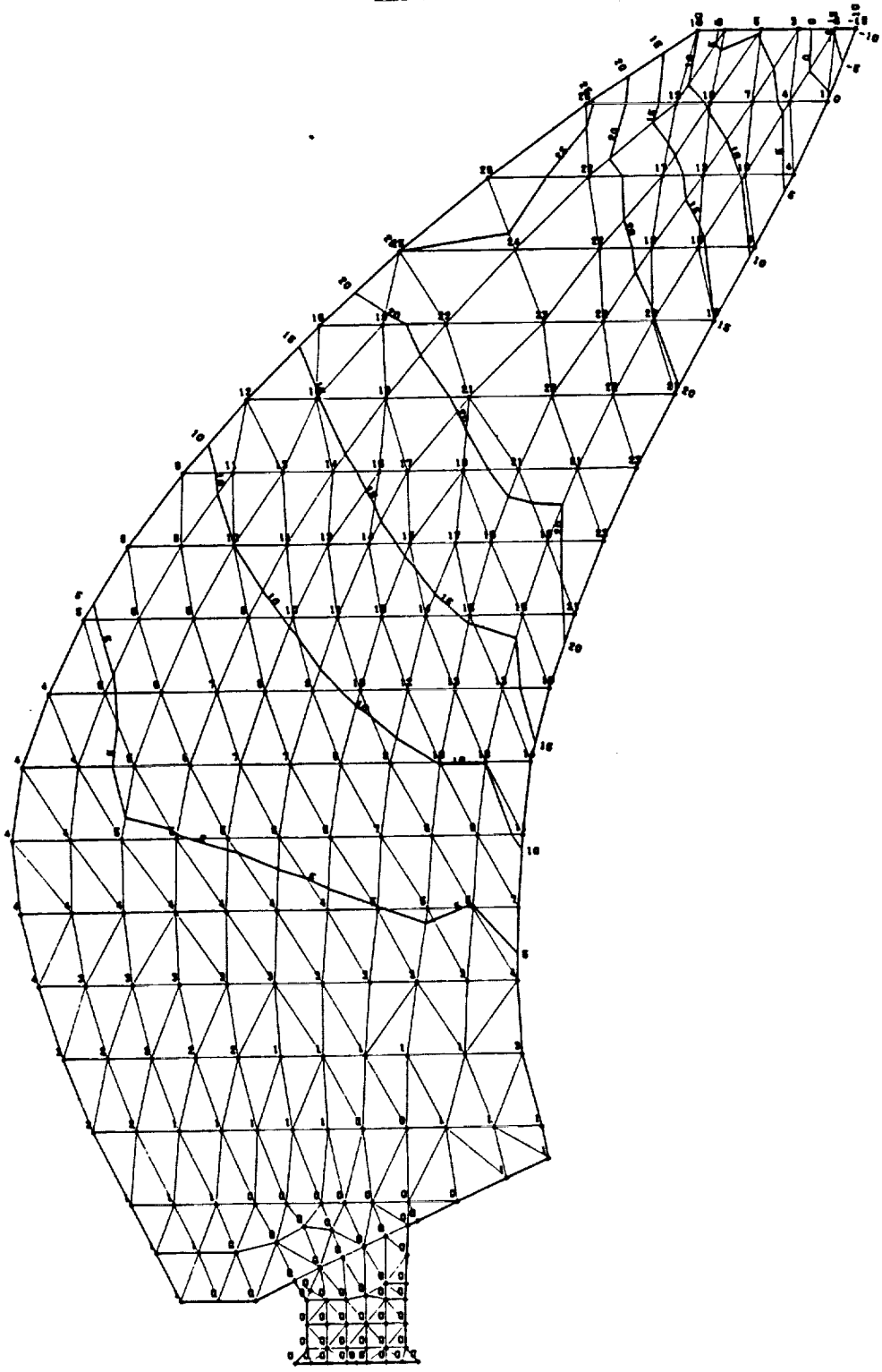

FIGURE C-15

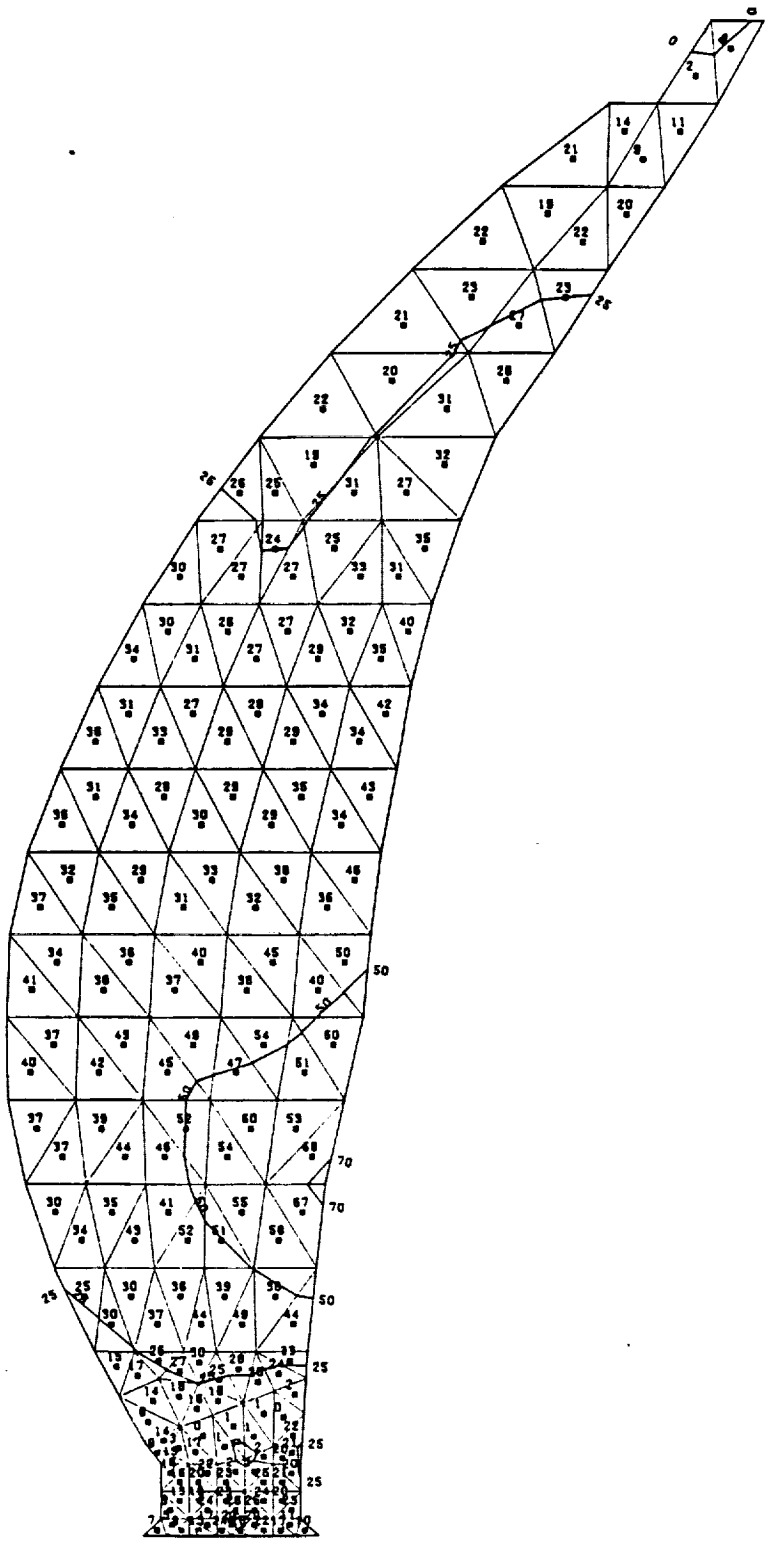

FIGURE C-16

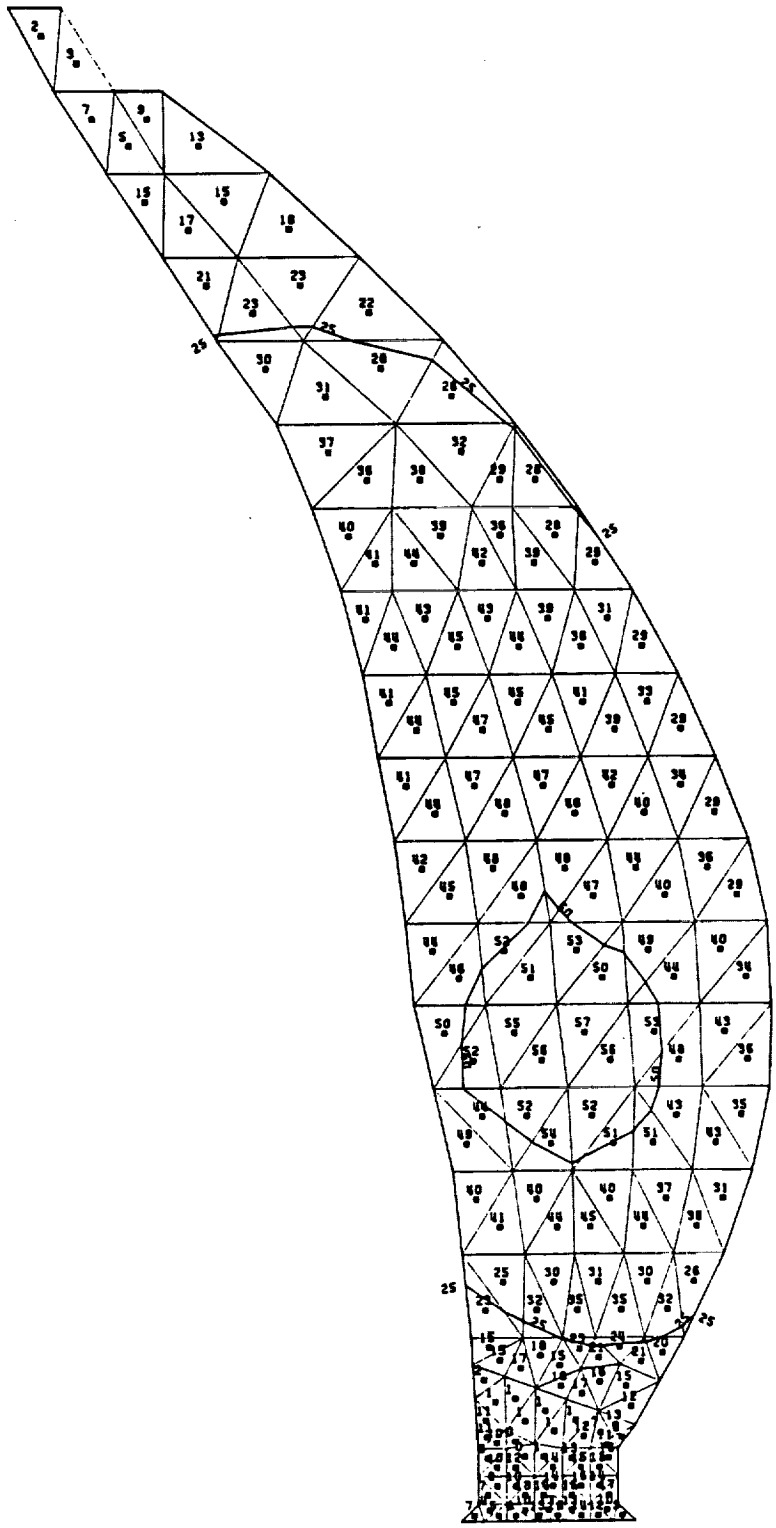

FIGURE C-17

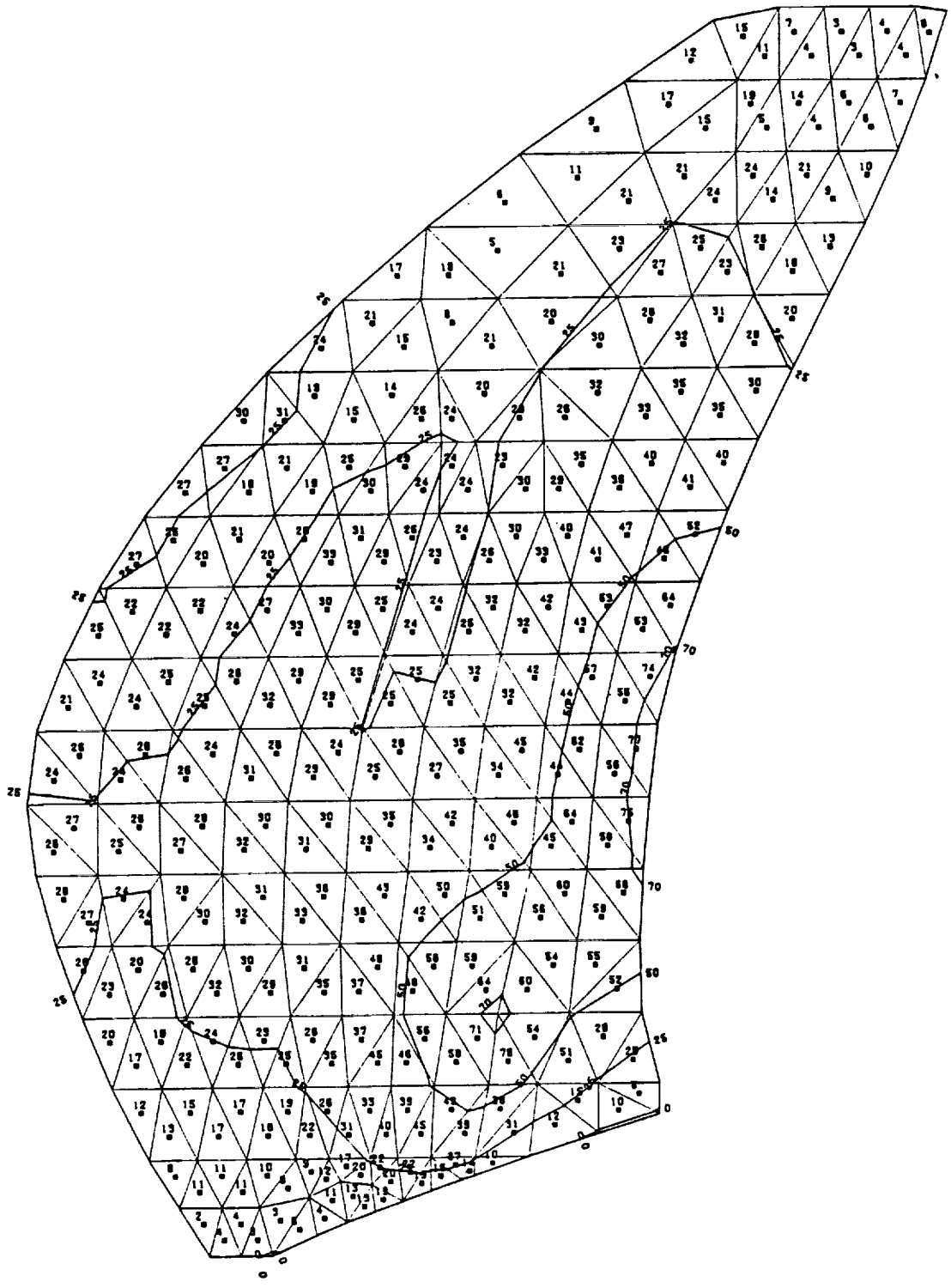

FIGURE C-18

ORIGINAL PAGE IS
OF POOR QUALITY

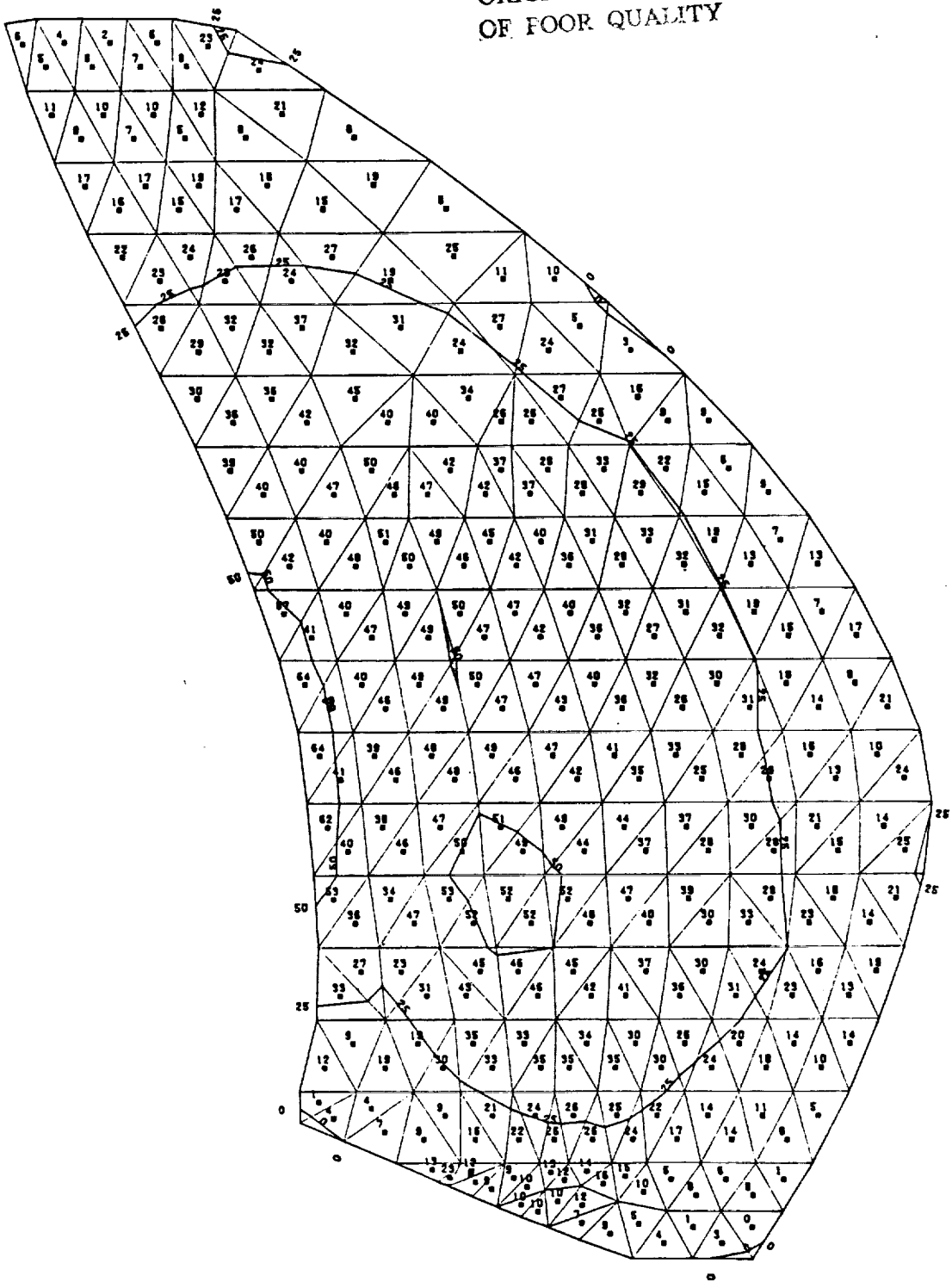

FIGURE C-19

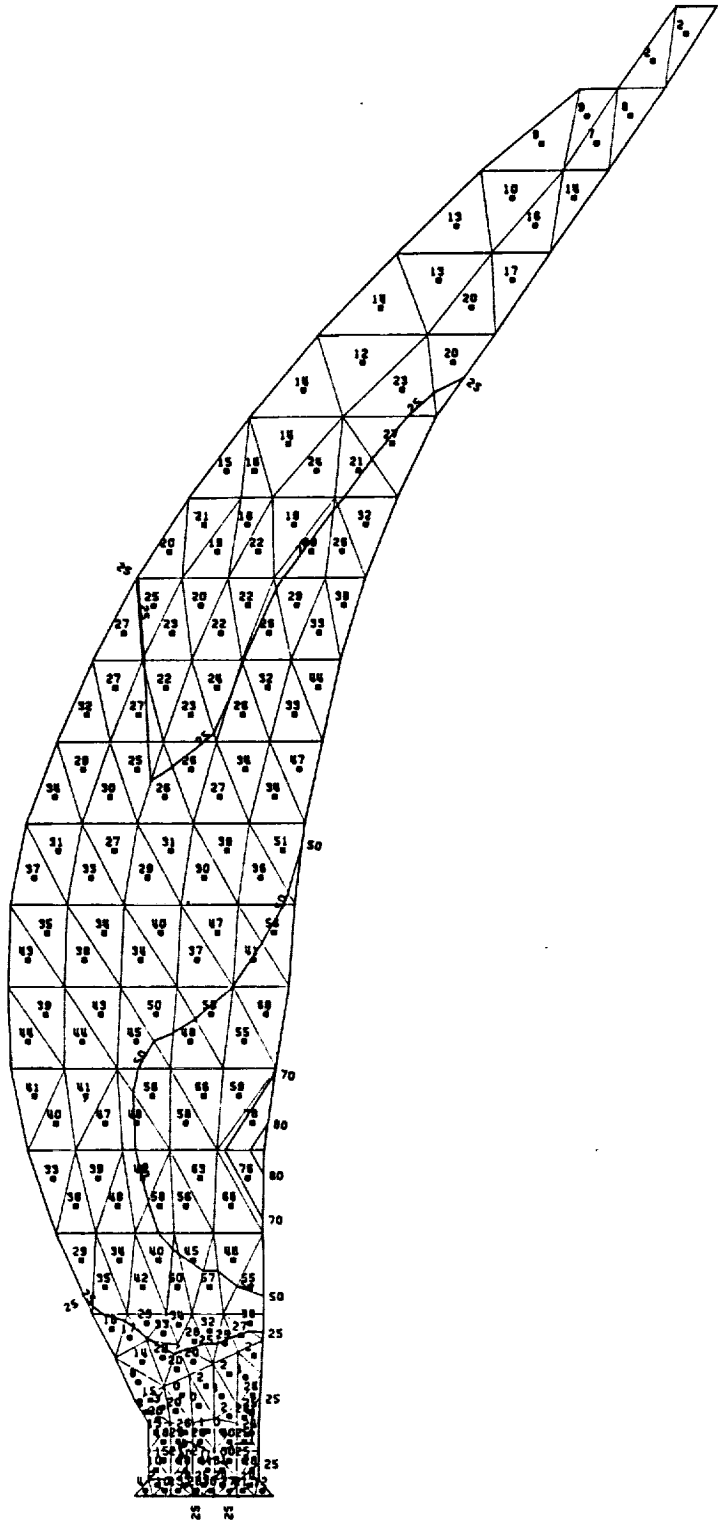

FIGURE C-20

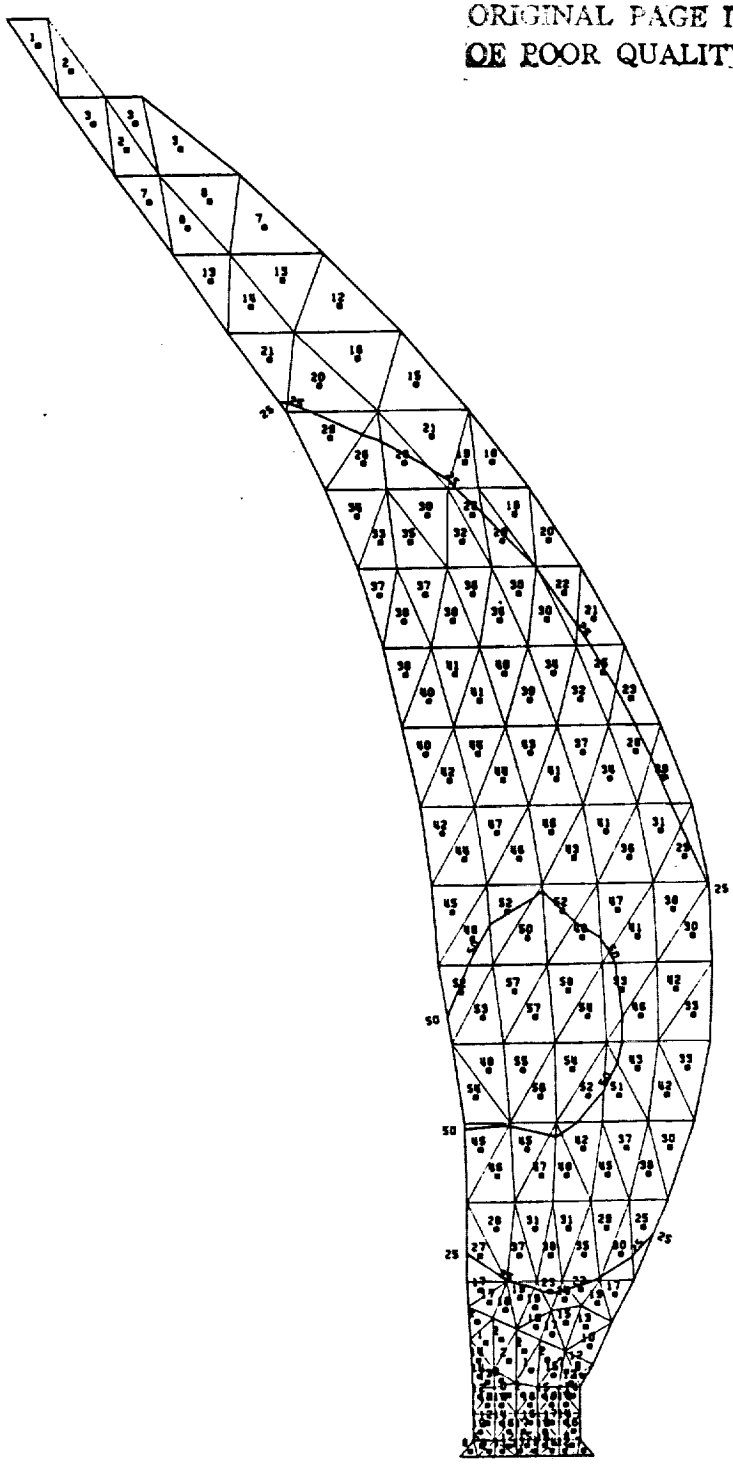

FIGURE C-21.

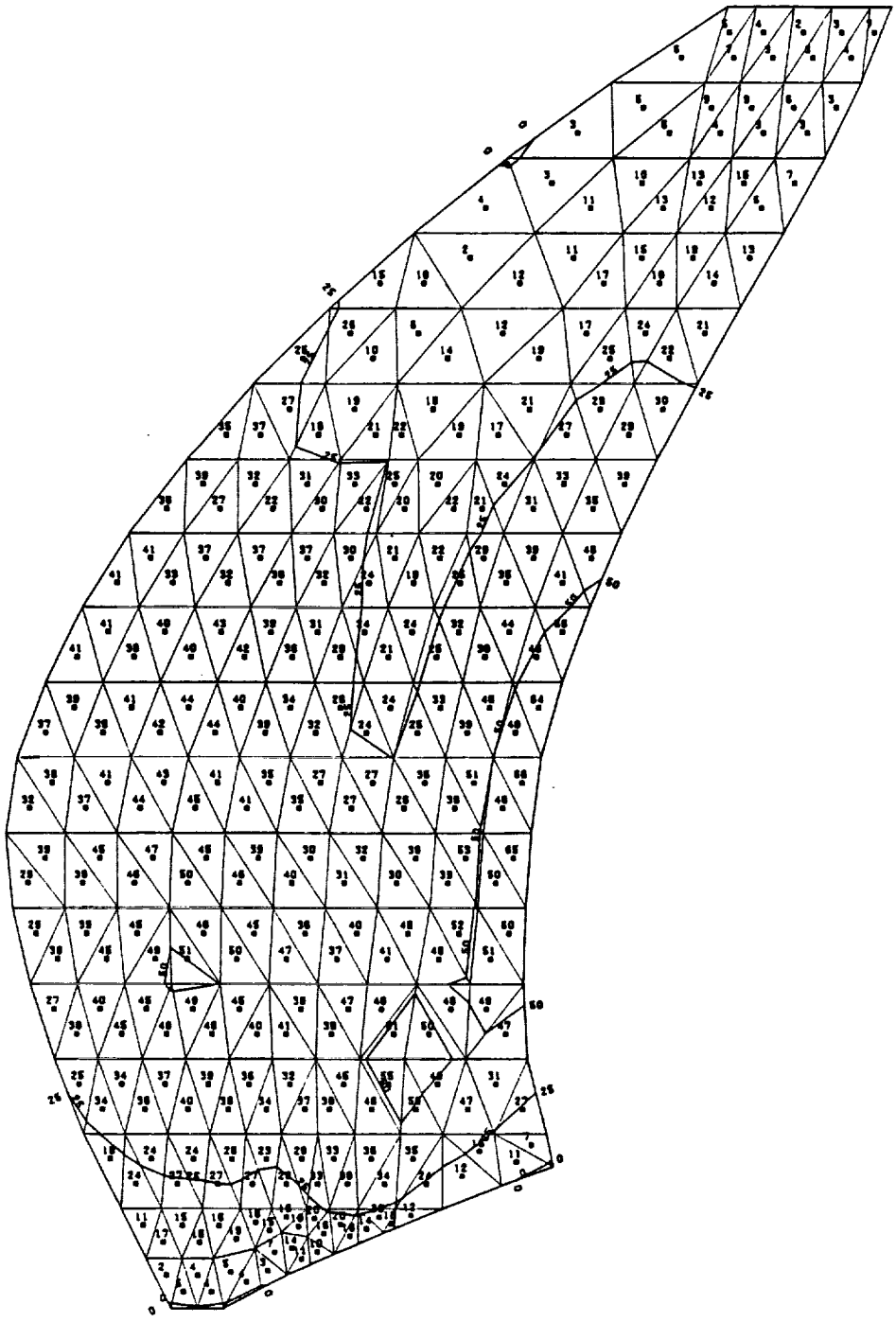

FIGURE C-22.

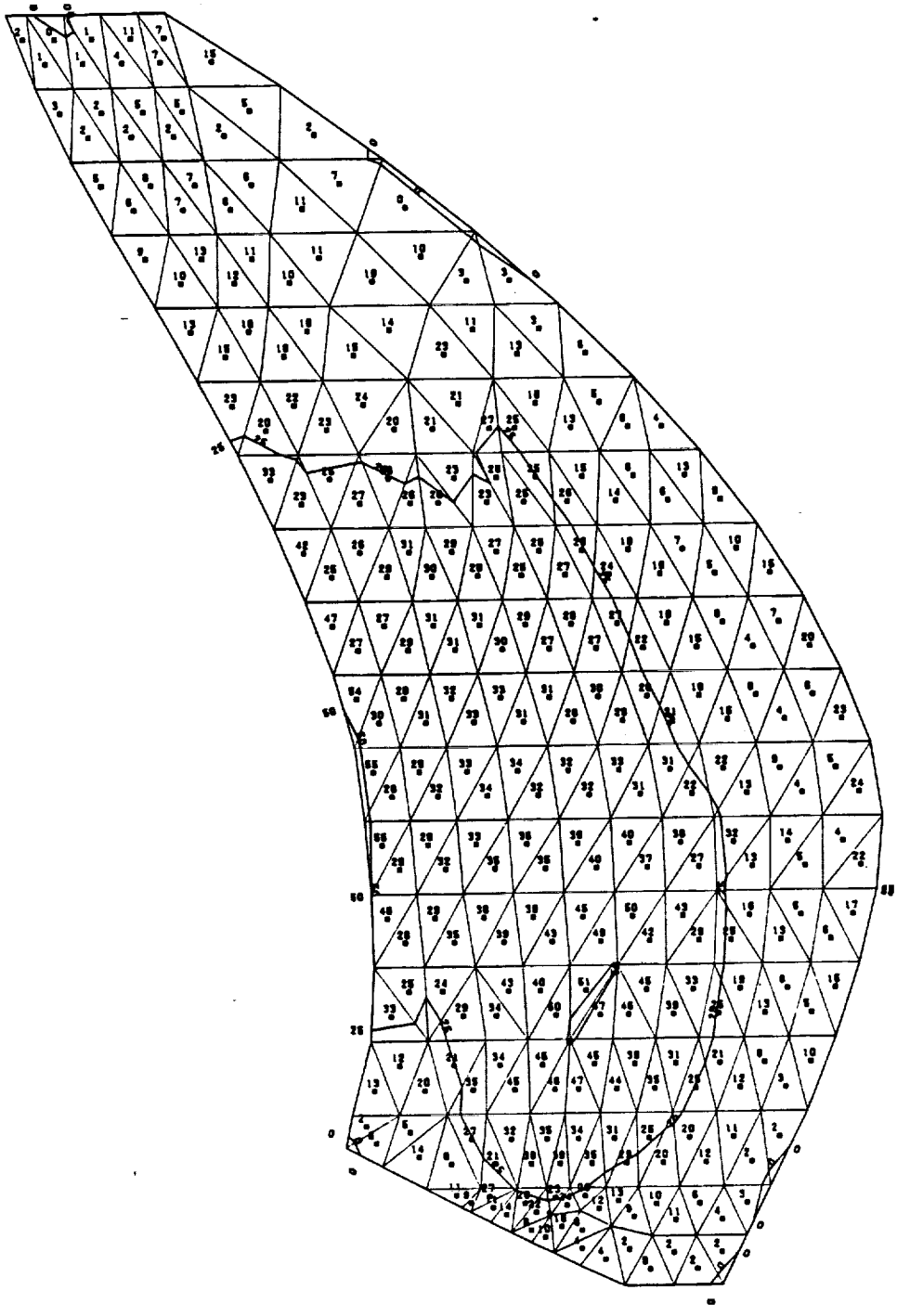

FIGURE C-23.

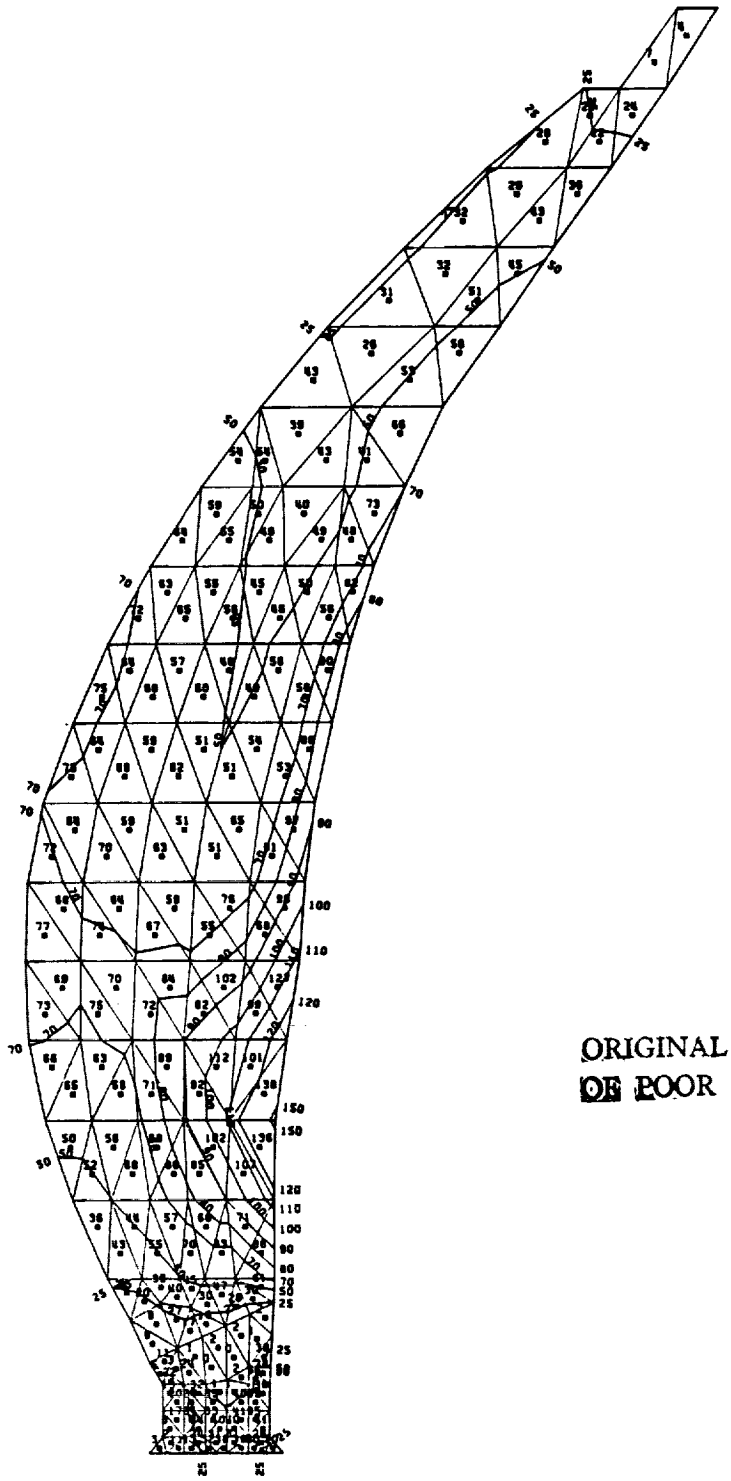

ORIGINAL PAGE IS
OF POOR QUALITY

FIGURE C-24.

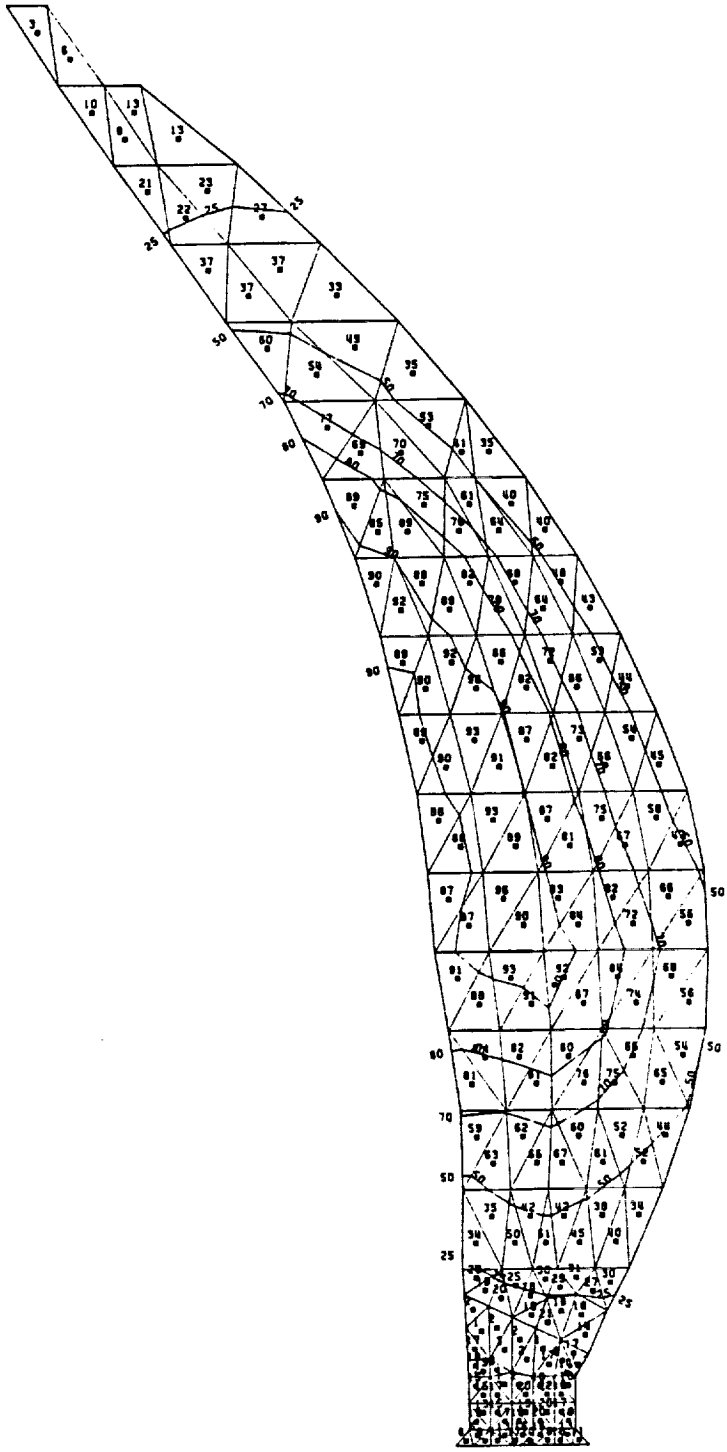

FIGURE C-25.

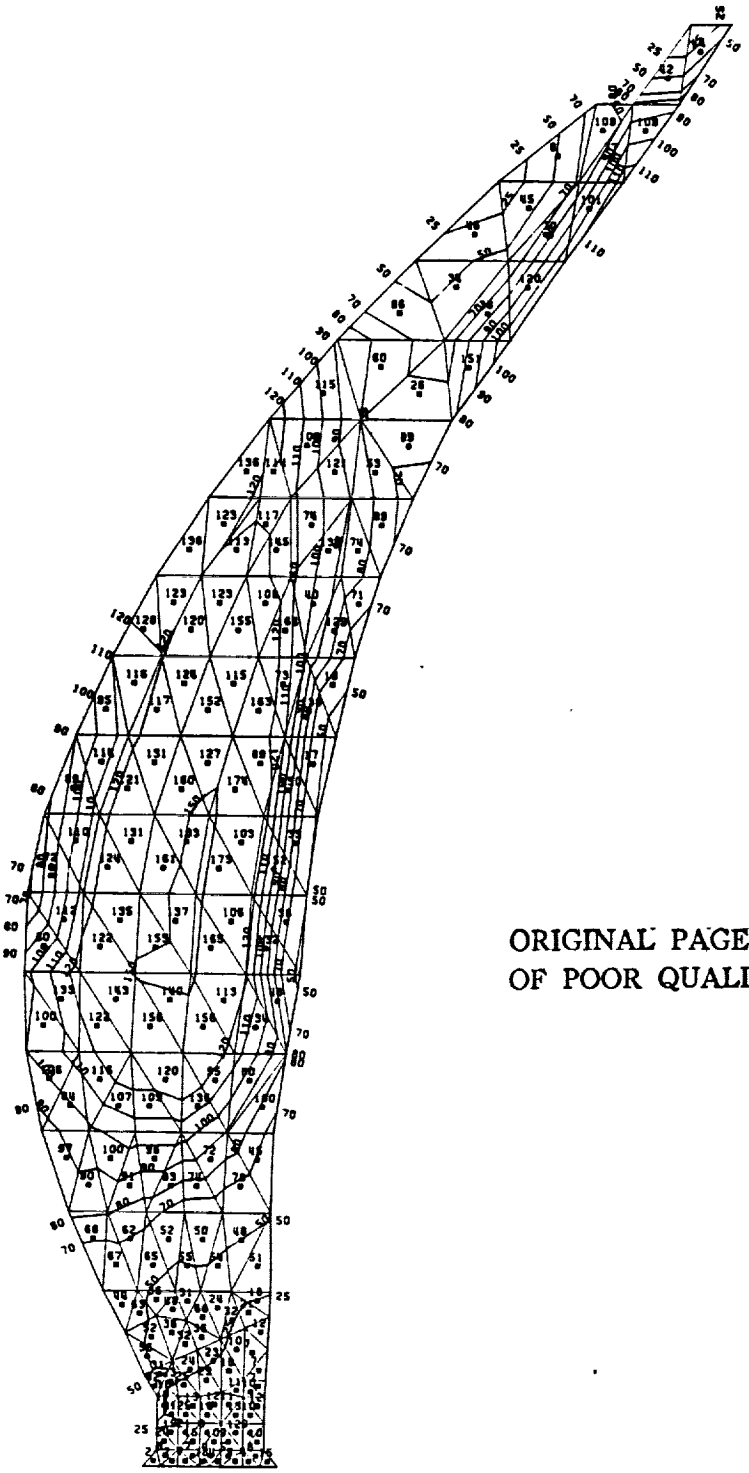

ORIGINAL PAGE IS
OF POOR QUALITY

FIGURE C-26.

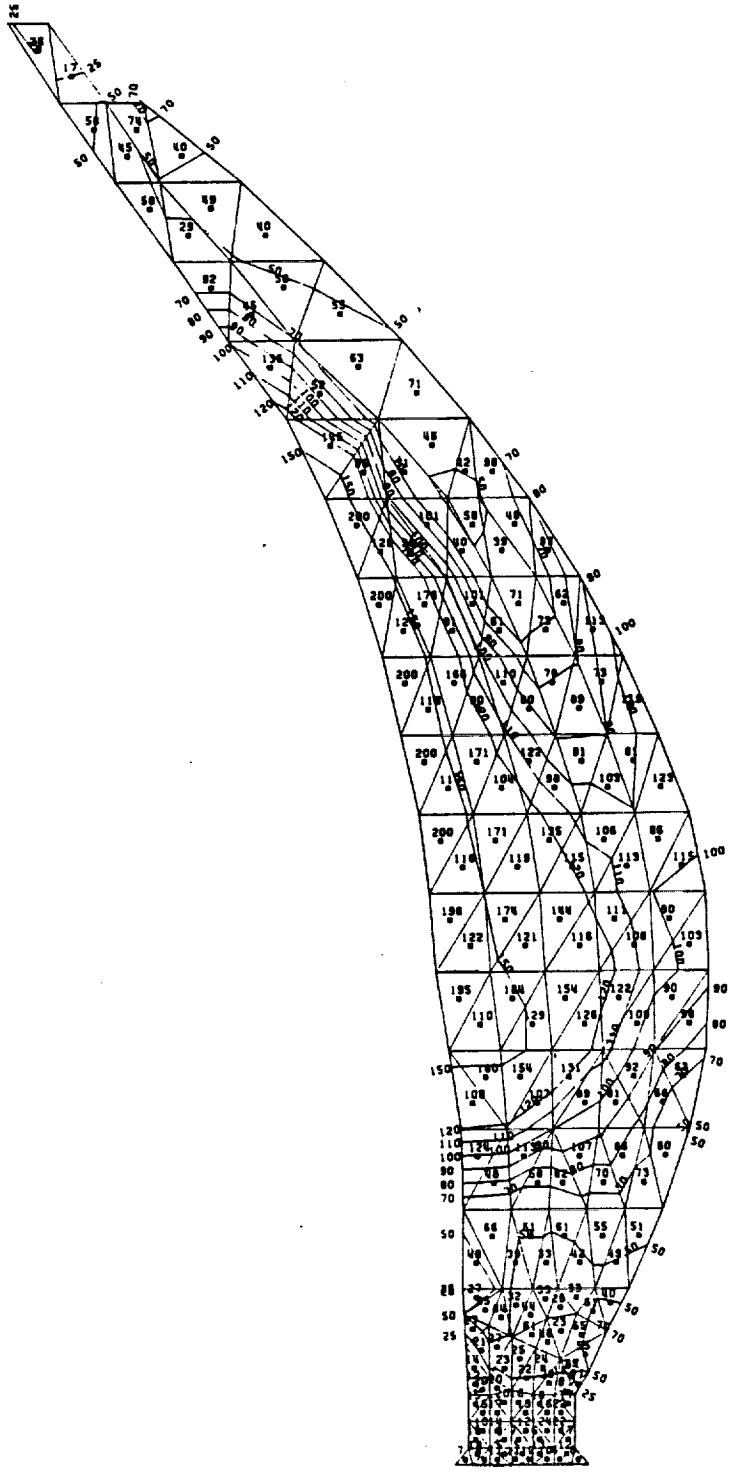

FIGURE C-27.

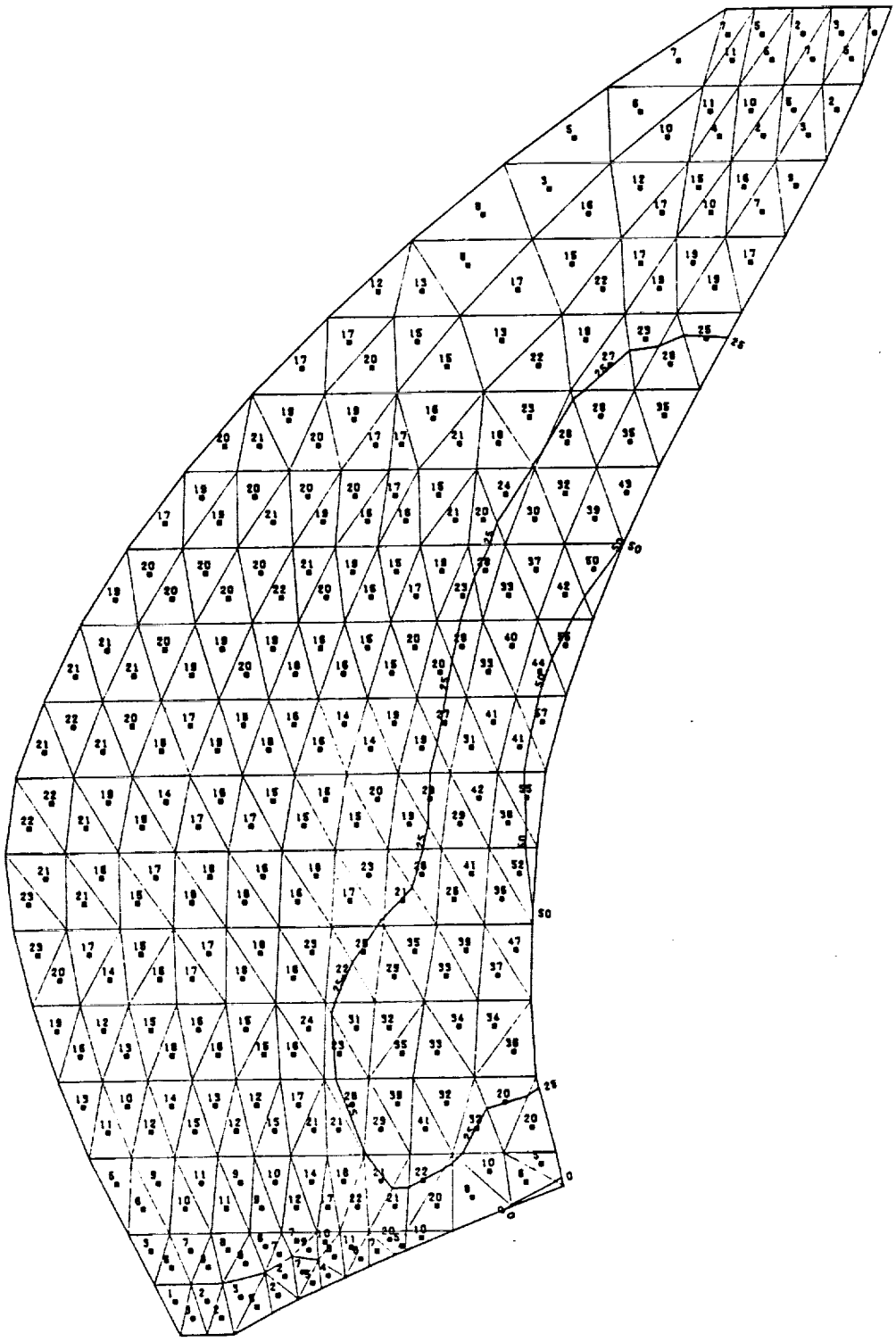

FIGURE C-28

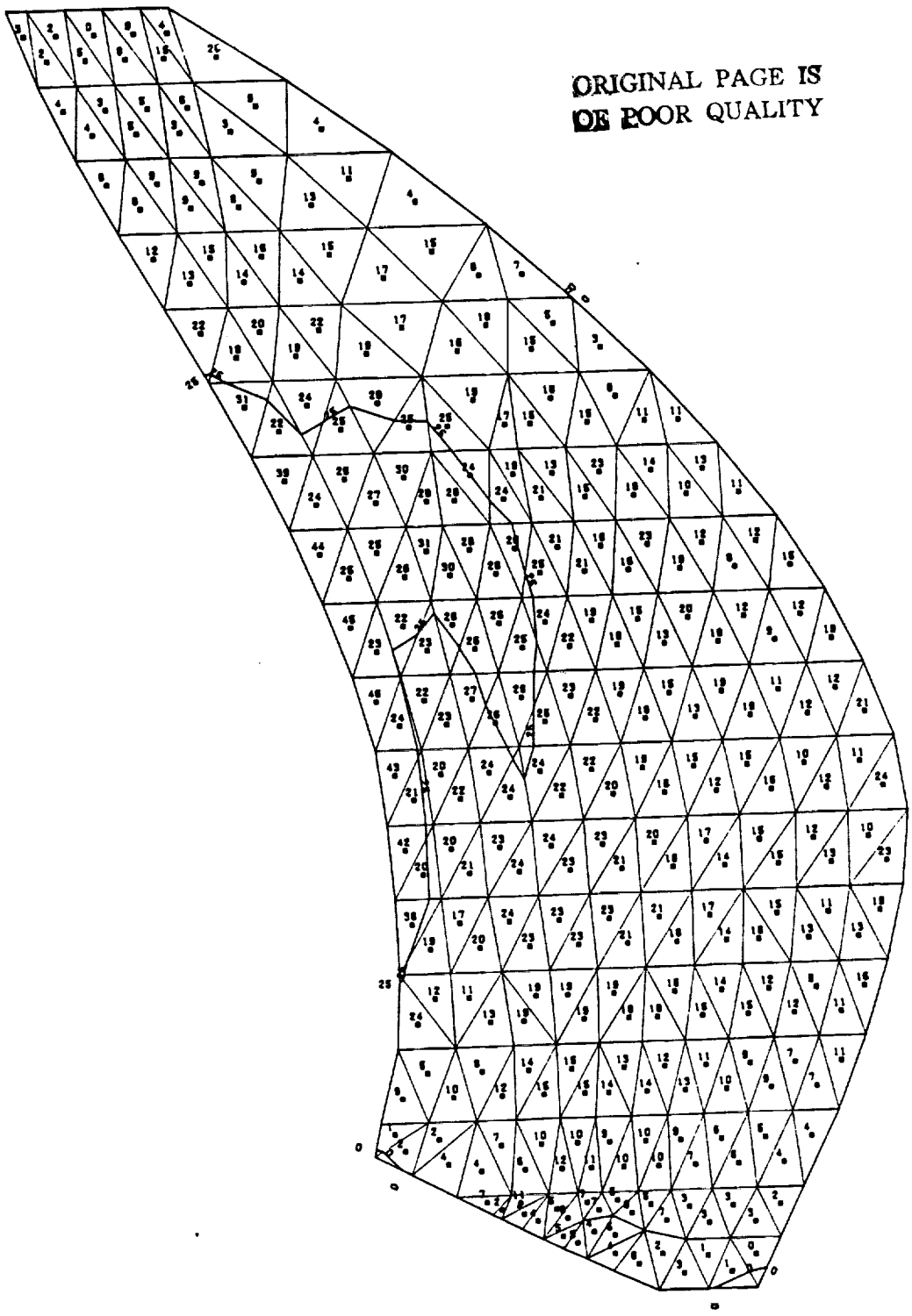

ORIGINAL PAGE IS
OF POOR QUALITY

FIGURE C-29

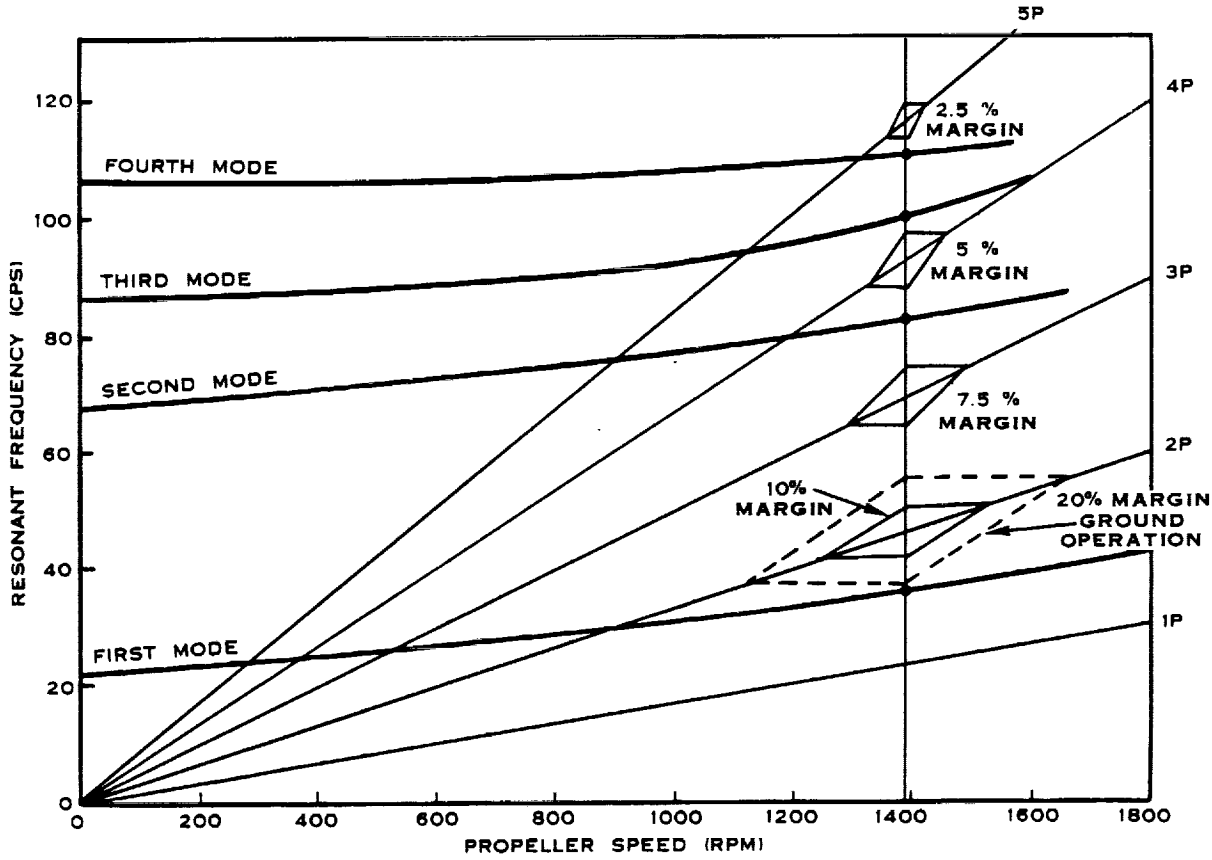
5P
4P
3P
2P
1P
2.5 %
MARGIN
5 %
MARGIN
7.5 %
MARGIN
10%
MARGIN
20% MARGIN
GROUND
OPERATION
FOURTH MODE
THIRD MODE
SECOND MODE
FIRST MODE
RESONANT FREQUENCY (CPS)
PROPELLER SPEED (RPM)
0
20
40
60
80
100
120
0
200
400
600
800
1000
1200
1400
1600
1800

FIGURE C-30

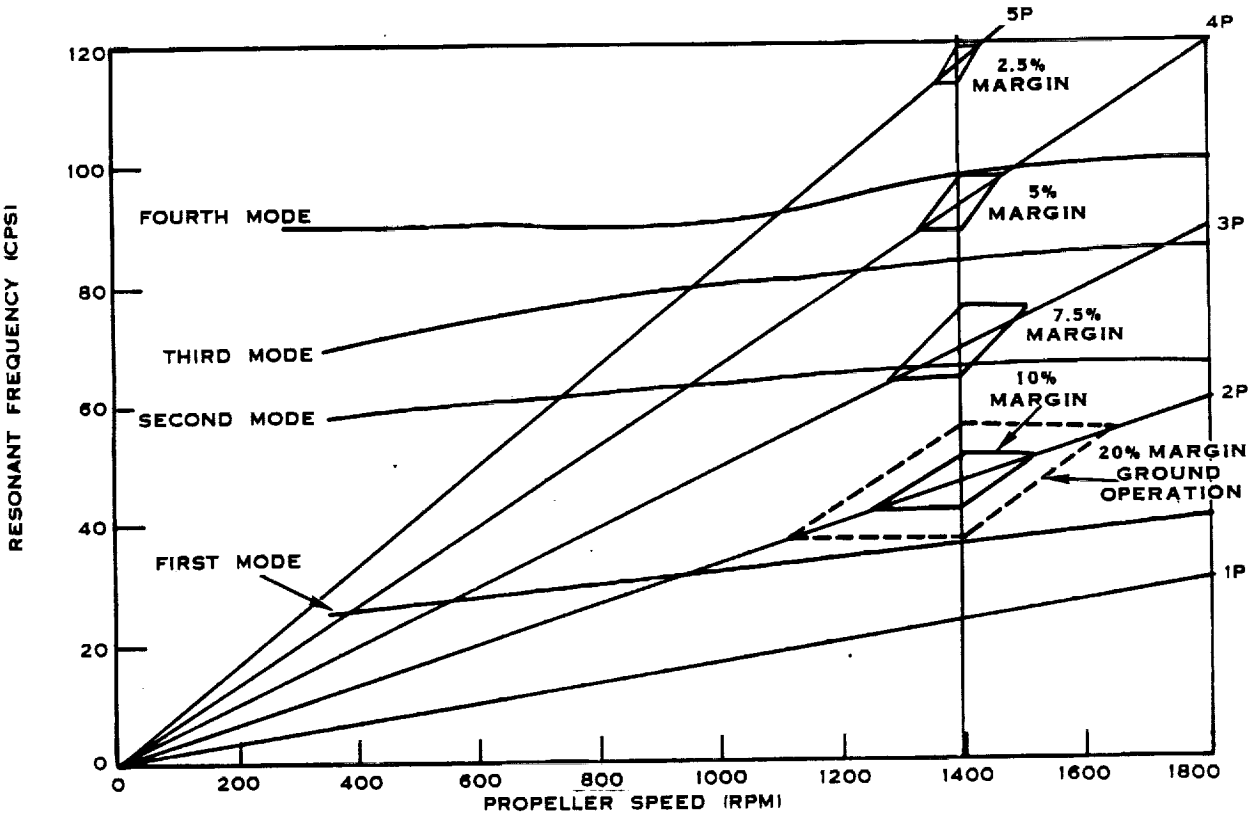
RESONANT FREQUENCY (CPS)
120
100
80
60
40
20
0
0
200
400
600
800
1000
1200
1400
1600
1800
PROPELLER SPEED (RPM)
FOURTH MODE
THIRD MODE
SECOND MODE
FIRST MODE
5P
4P
3P
2P
1P
2.5% MARGIN
5% MARGIN
7.5% MARGIN
10% MARGIN
20% MARGIN
GROUND OPERATION

FIGURE C-31.

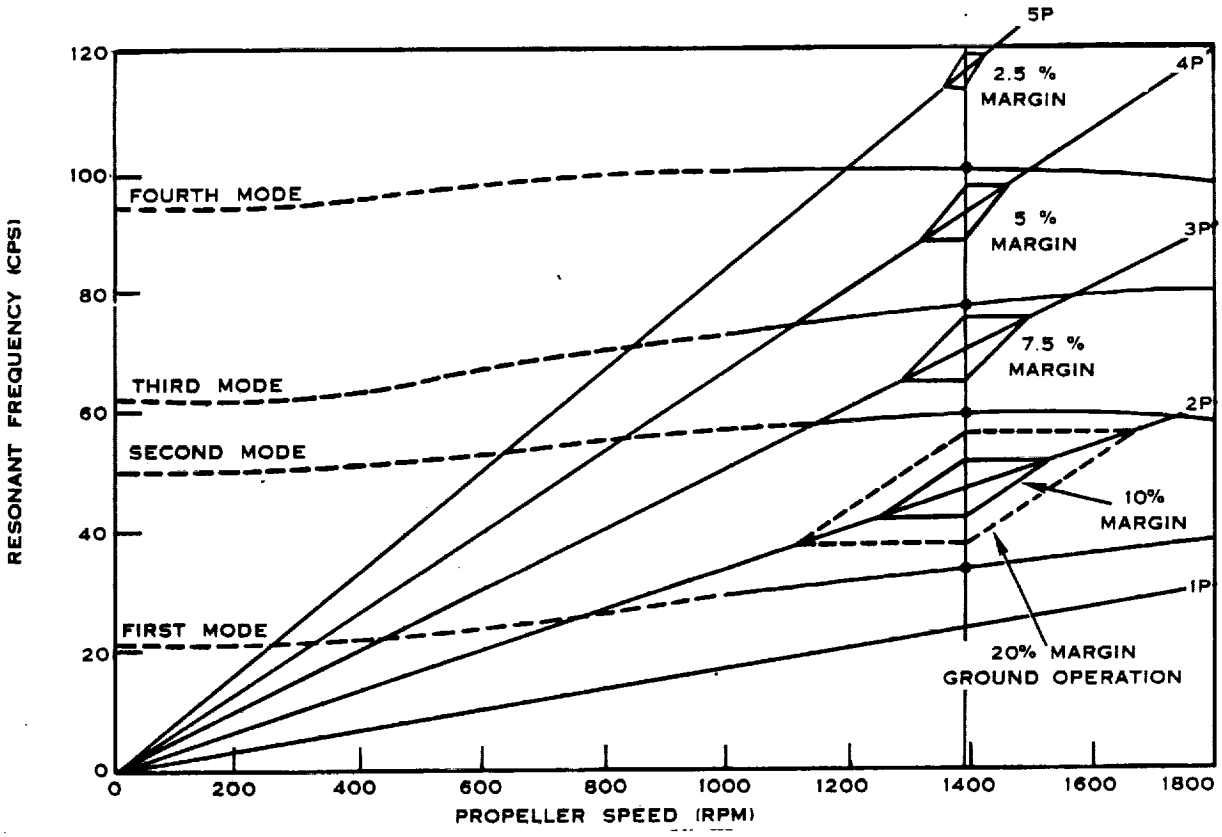
RESONANT FREQUENCY (CPS)
120
100
80
60
40
20
0
FOURTH MODE
THIRD MODE
SECOND MODE
FIRST MODE
5P
4P
3P
2P
1P
2.5 %
MARGIN
5 %
MARGIN
7.5 %
MARGIN
10%
MARGIN
20% MARGIN
GROUND OPERATION
0
200
400
600
800
1000
1200
1400
1600
1800
PROPELLER SPEED (RPM)

FIGURE C-32

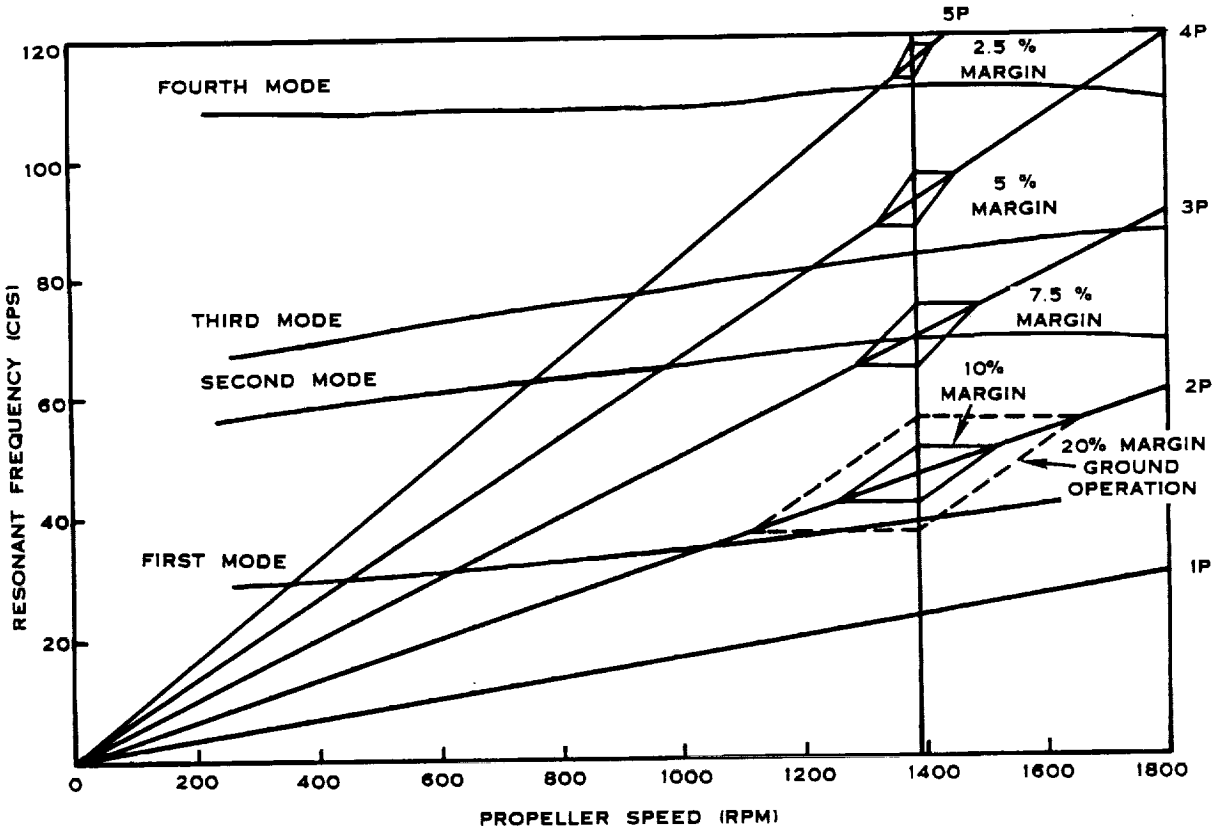
5P
4P
2.5 %
MARGIN
FOURTH MODE
5 %
MARGIN
3P
7.5 %
MARGIN
THIRD MODE
SECOND MODE
10%
MARGIN
2P
20% MARGIN
GROUND
OPERATION
FIRST MODE
1P
RESONANT FREQUENCY (CPS)
120
100
80
60
40
20
0
200
400
600
800
1000
1200
1400
1600
1800
PROPELLER SPEED (RPM)

FIGURE C-33.

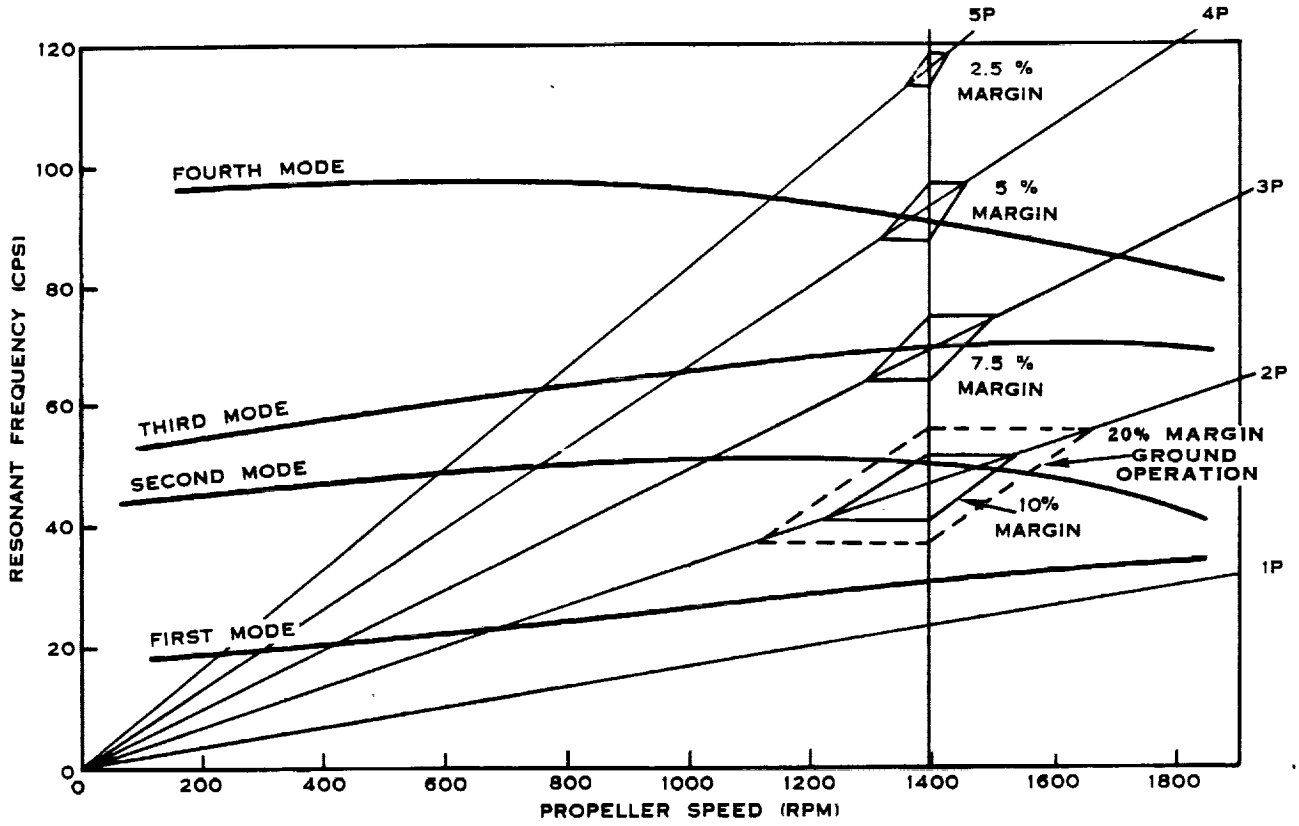
5P
4P
120
2.5 %
MARGIN
100
FOURTH MODE
5 %
MARGIN
3P
80
7.5 %
MARGIN
60
THIRD MODE
2P
20% MARGIN
GROUND
OPERATION
SECOND MODE
40
10%
MARGIN
1P
FIRST MODE
20
0
0
200
400
600
800
1000
1200
1400
1600
1800
RESONANT FREQUENCY (CPS)
PROPELLER SPEED (RPM)

FIGURE C-34

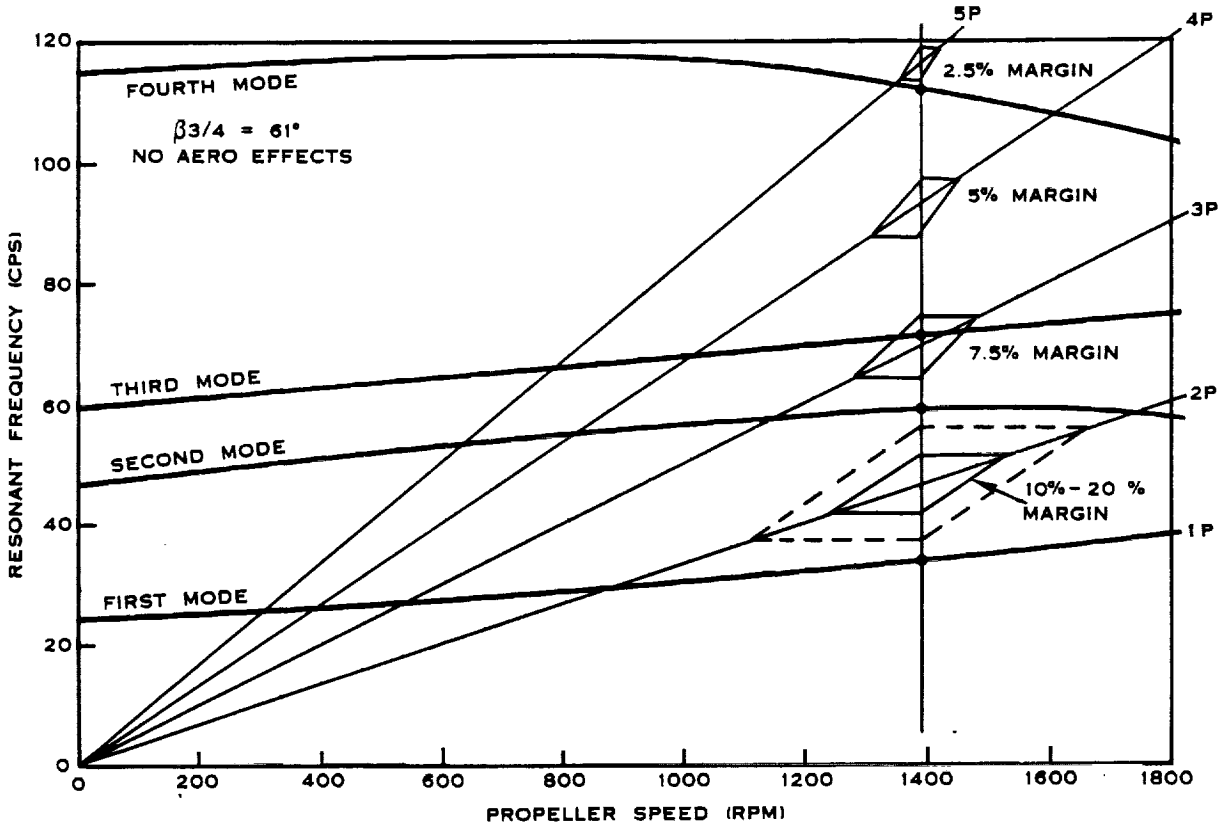
5P
4P
2.5% MARGIN
FOURTH MODE
β3/4 = 61°
NO AERO EFFECTS
5% MARGIN
3P
7.5% MARGIN
THIRD MODE
2P
SECOND MODE
10%-20 %
MARGIN
1P
FIRST MODE
RESONANT FREQUENCY (CPS)
PROPELLER SPEED (RPM)
0
20
40
60
80
100
120
0
200
400
600
800
1000
1200
1400
1600
1800

FIGURE C-35.

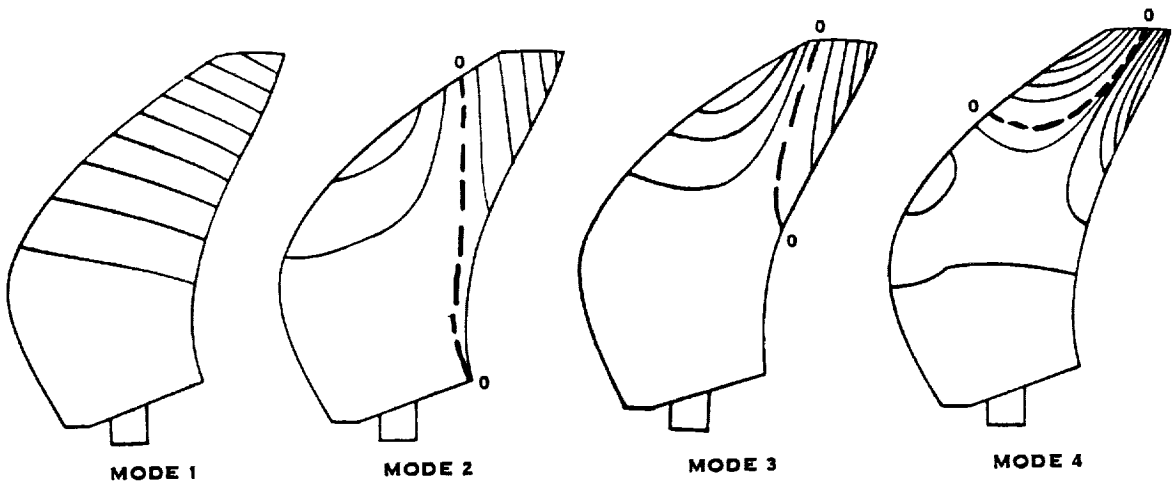

FIGURE C-36

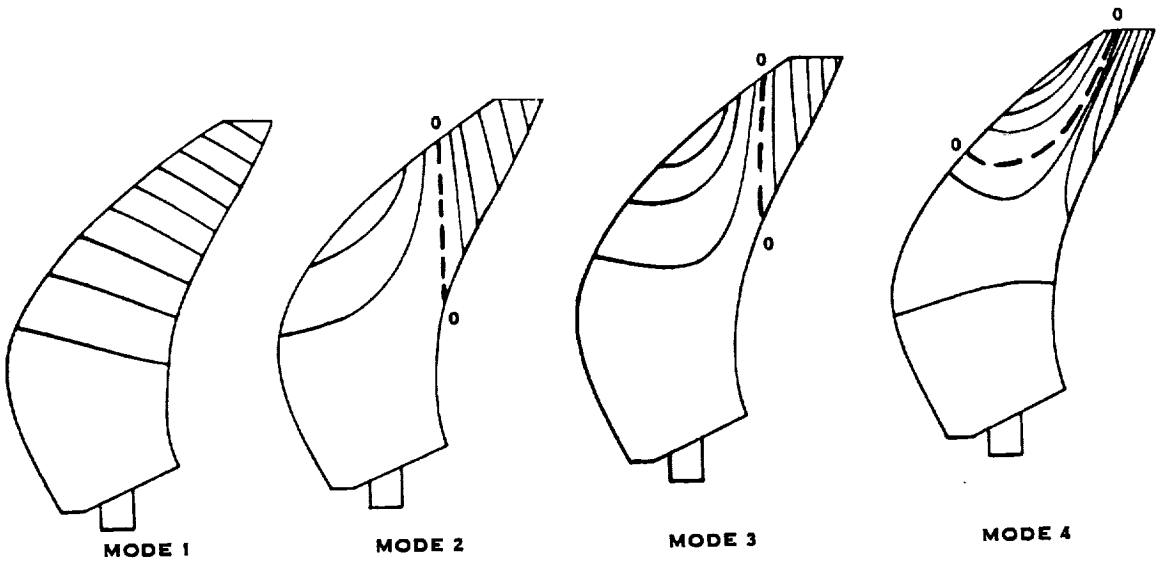

FIGURE C-37

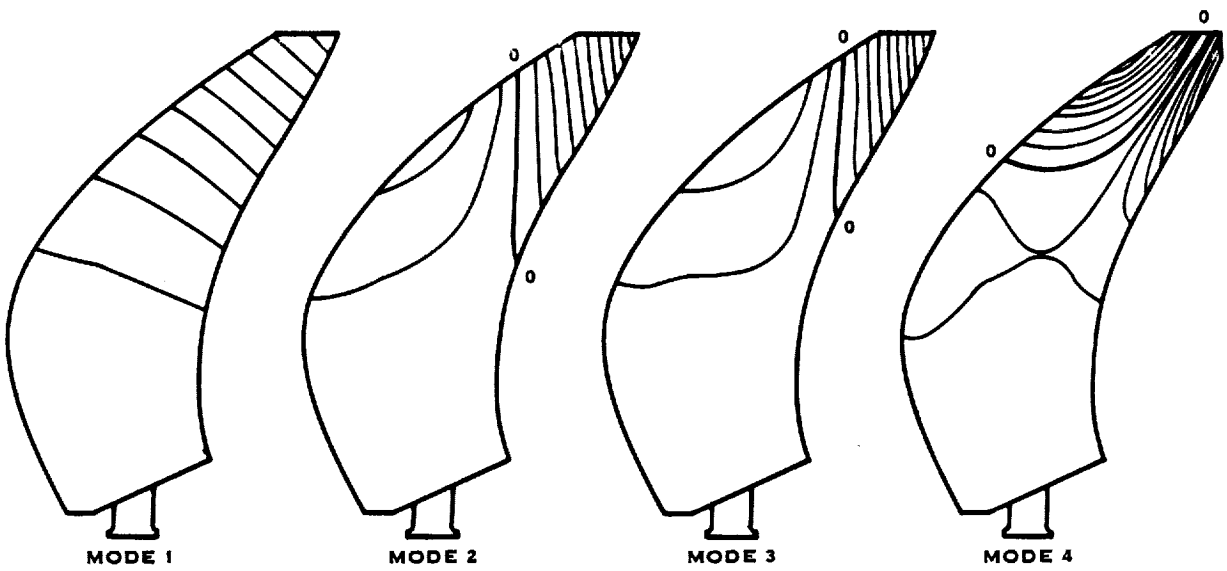

FIGURE C-38.

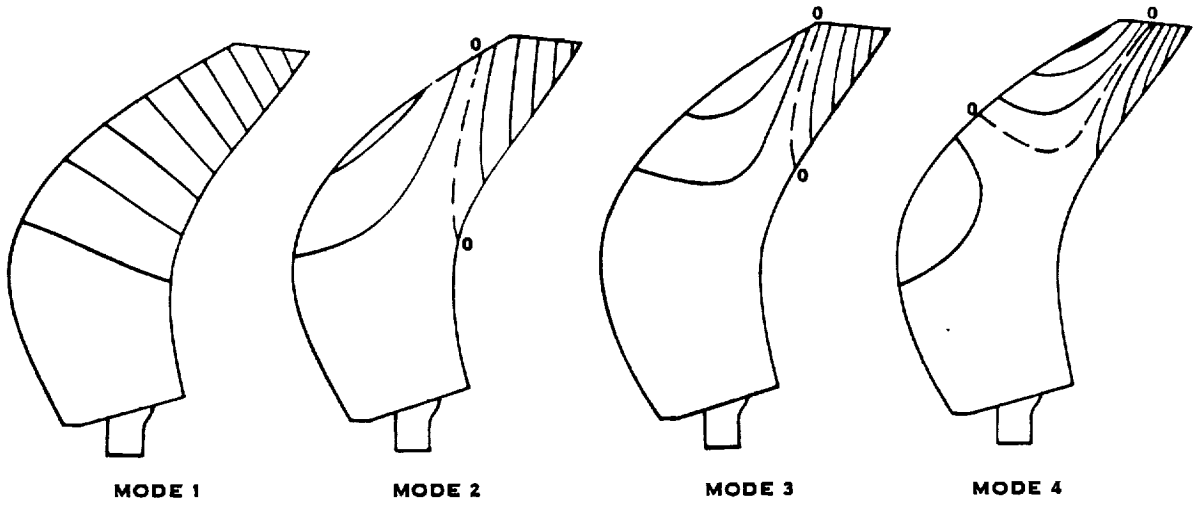

FIGURE C-39.

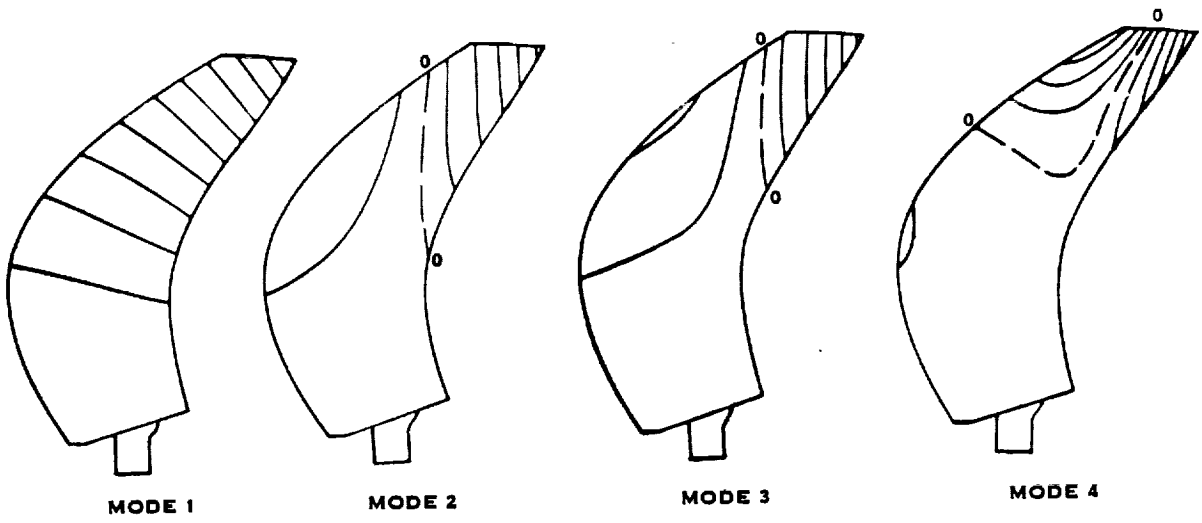

FIGURE C-40.

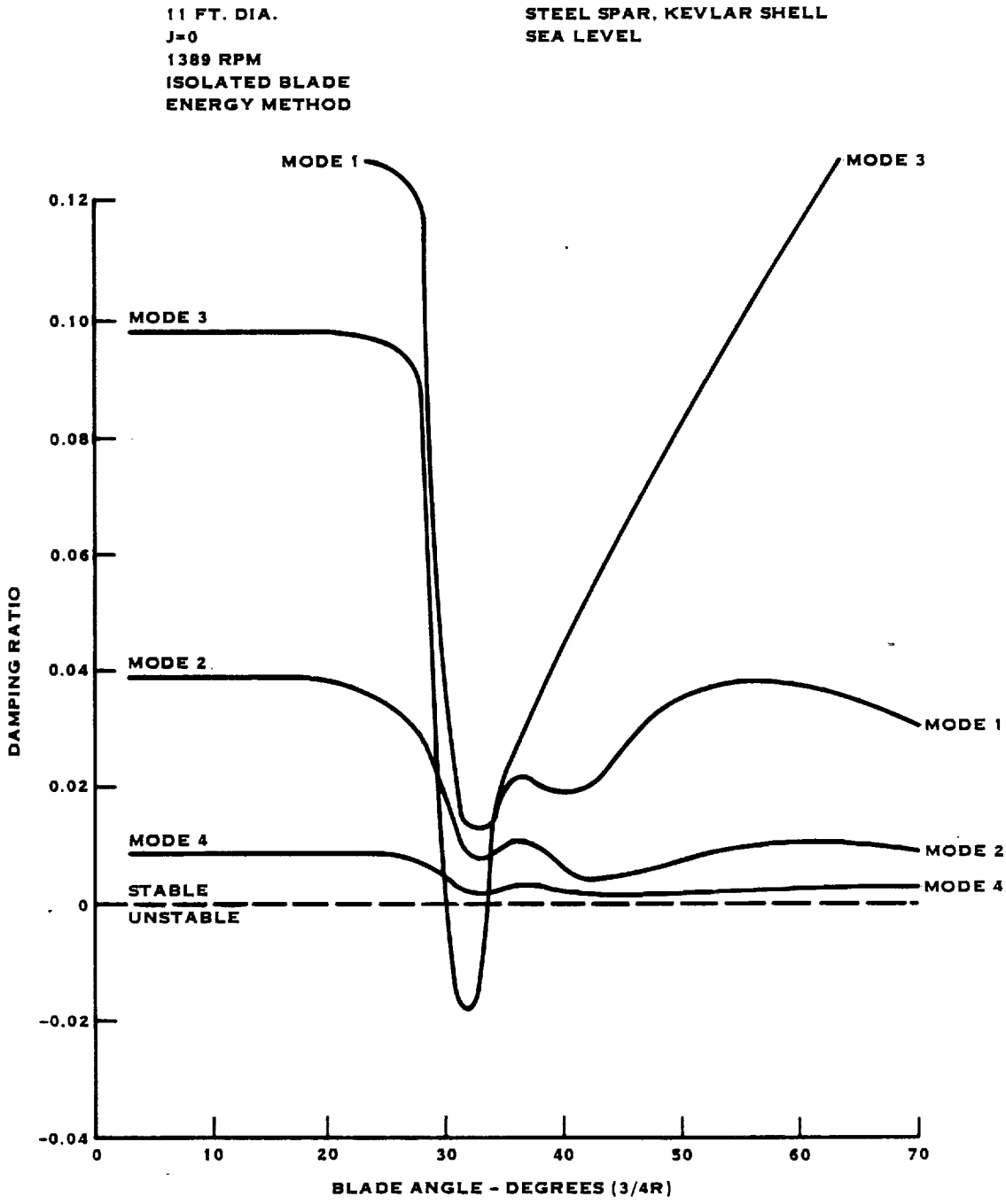

FIGURE C-41. SR-2 STALL FLUTTER DAMPING RATIO

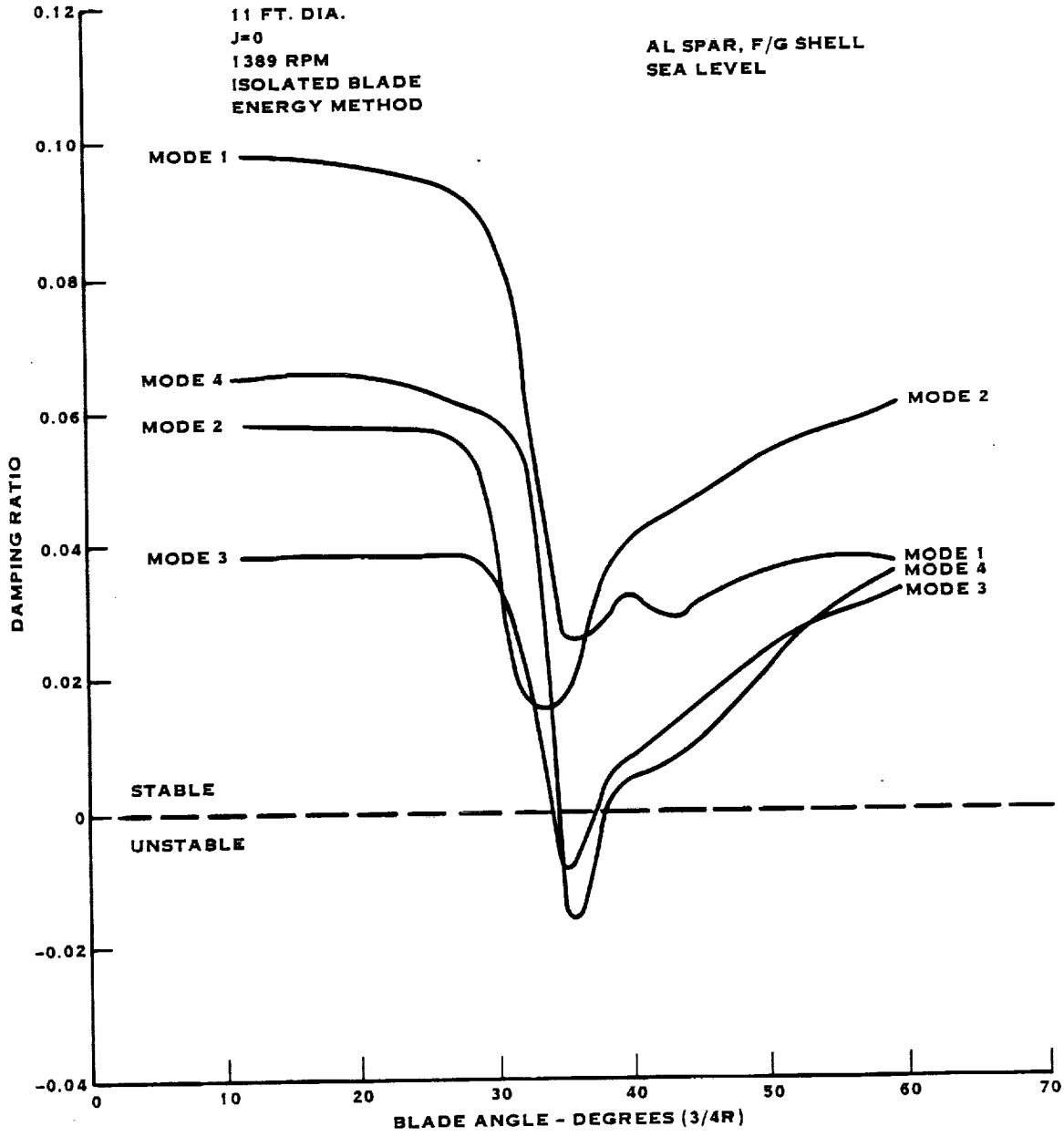

FIGURE C-42. SR-3(8) STALL FLUTTER DAMPING RATIO

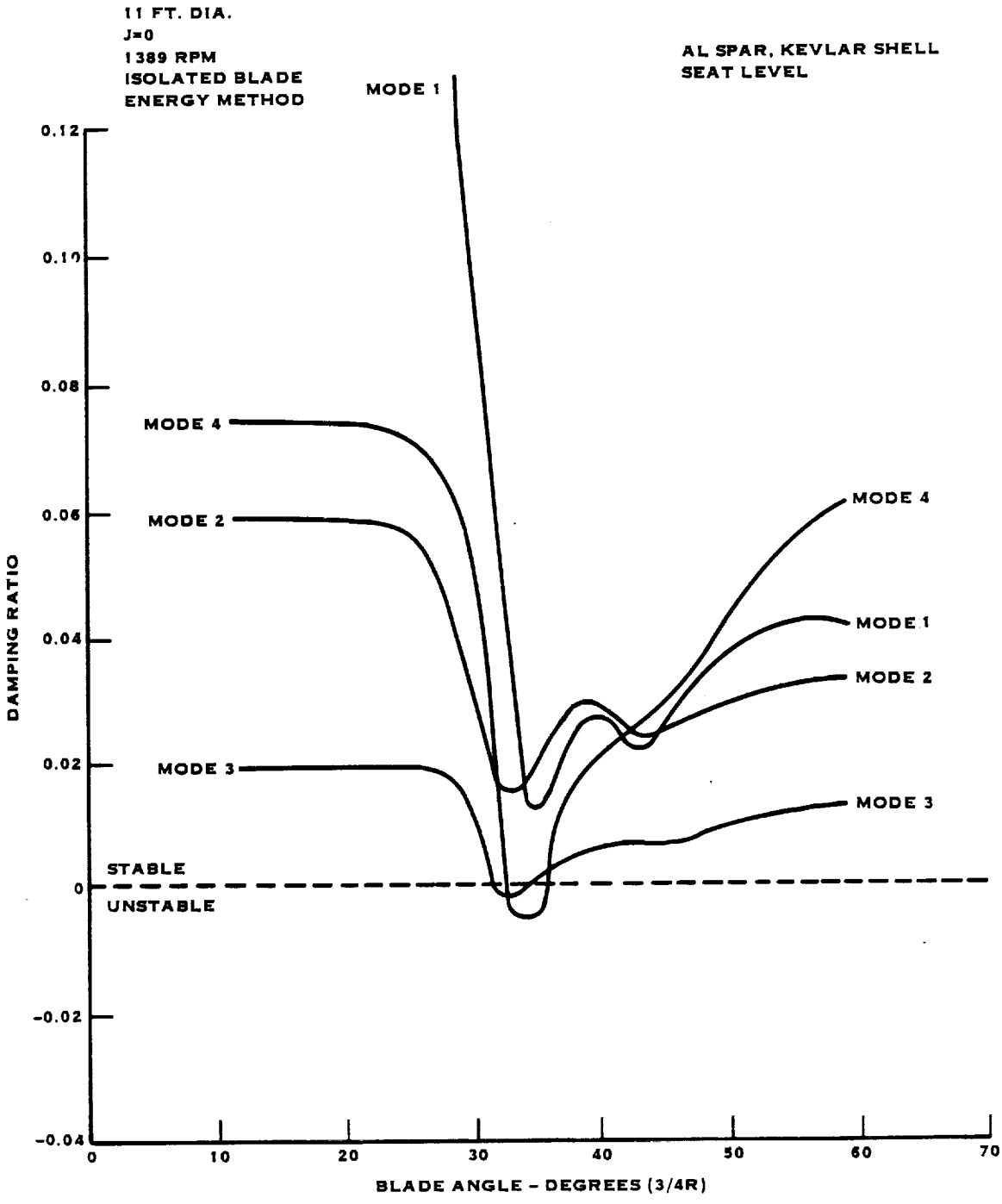

FIGURE C-43. SR-3(10) STALL FLUTTER DAMPING RATIO

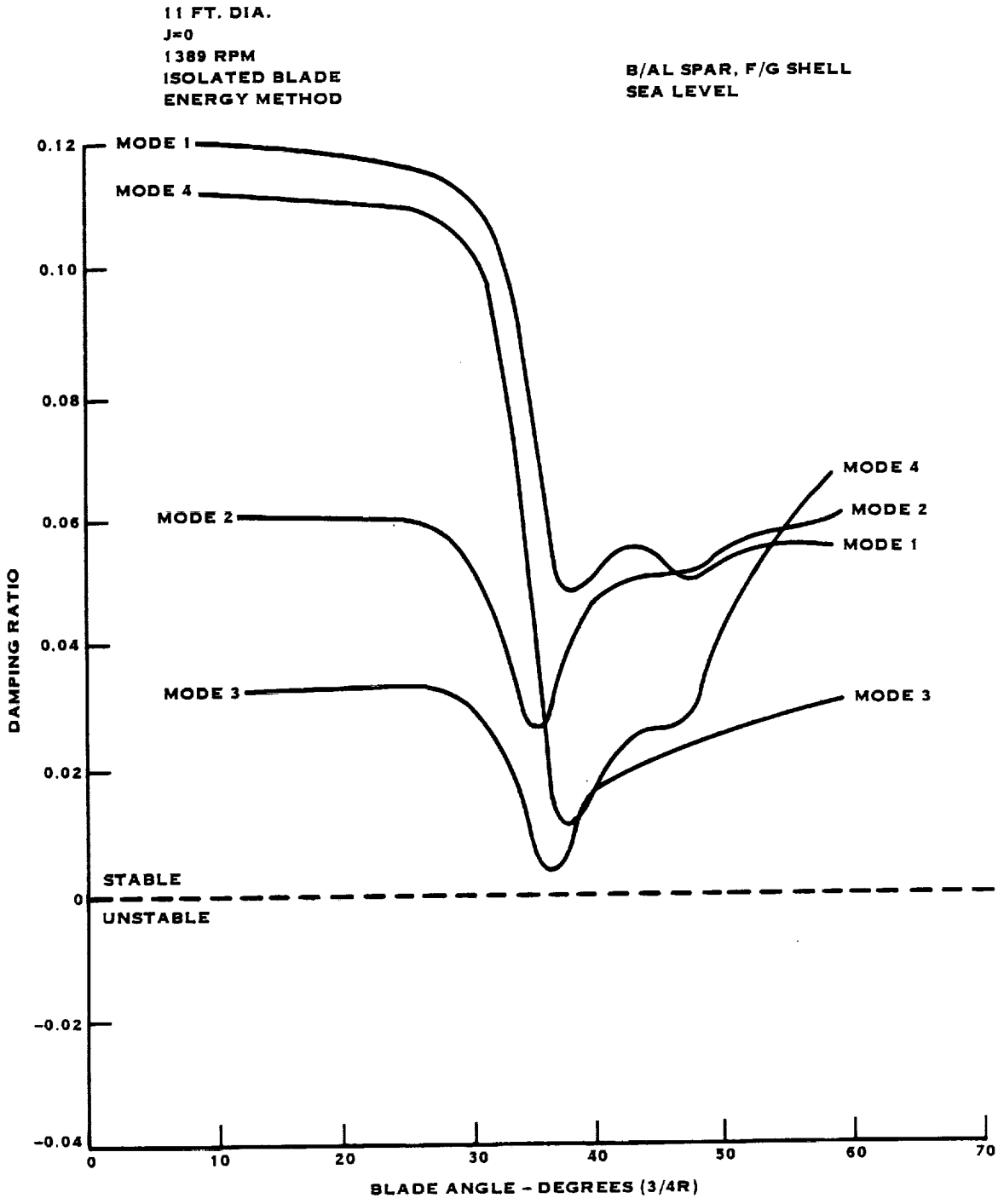

FIGURE C-44. SR-5B STALL FLUTTER DAMPING RATIO

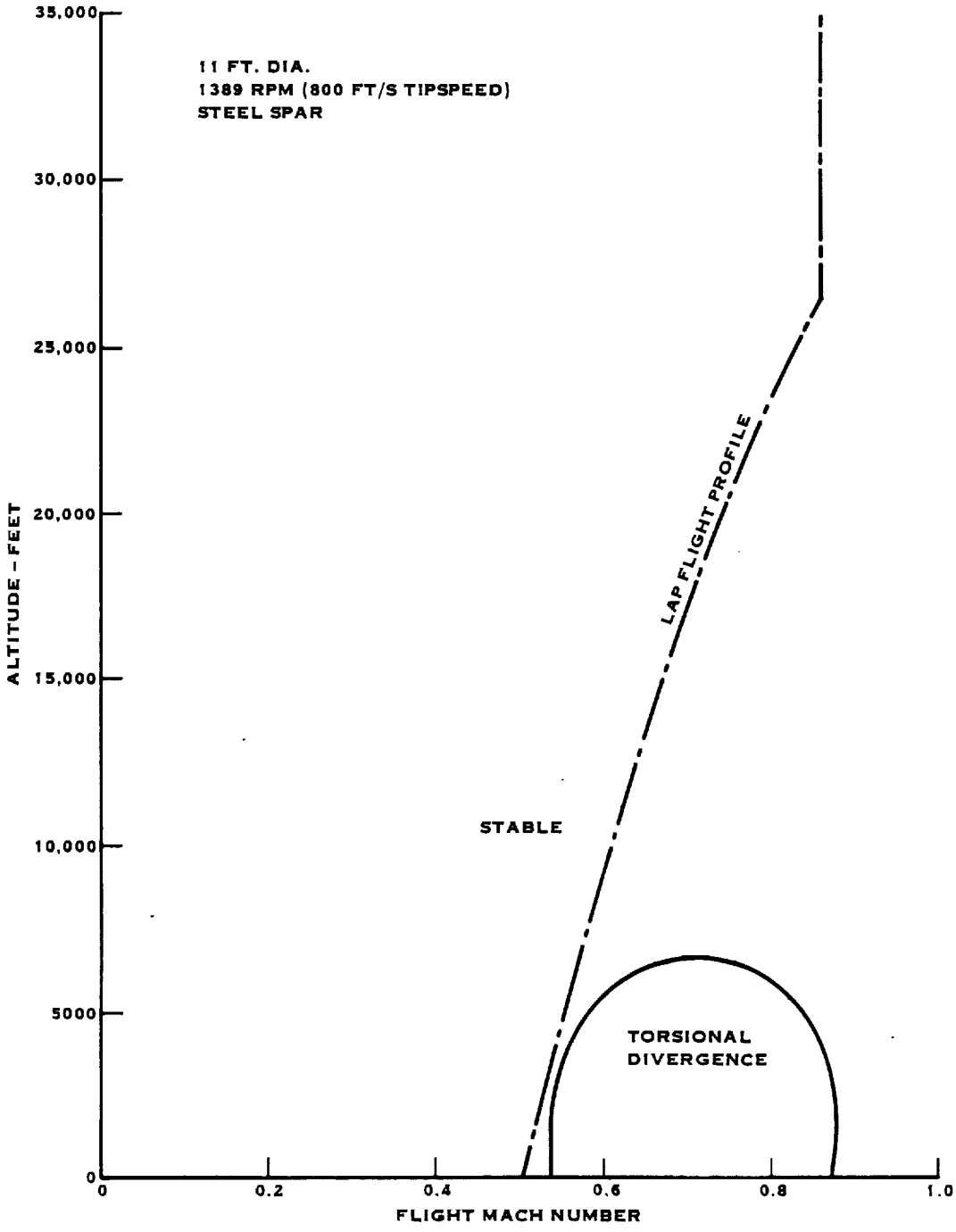

FIGURE C-45. SR-2 UNSTALLED FLUTTER STABILITY BOUNDARY

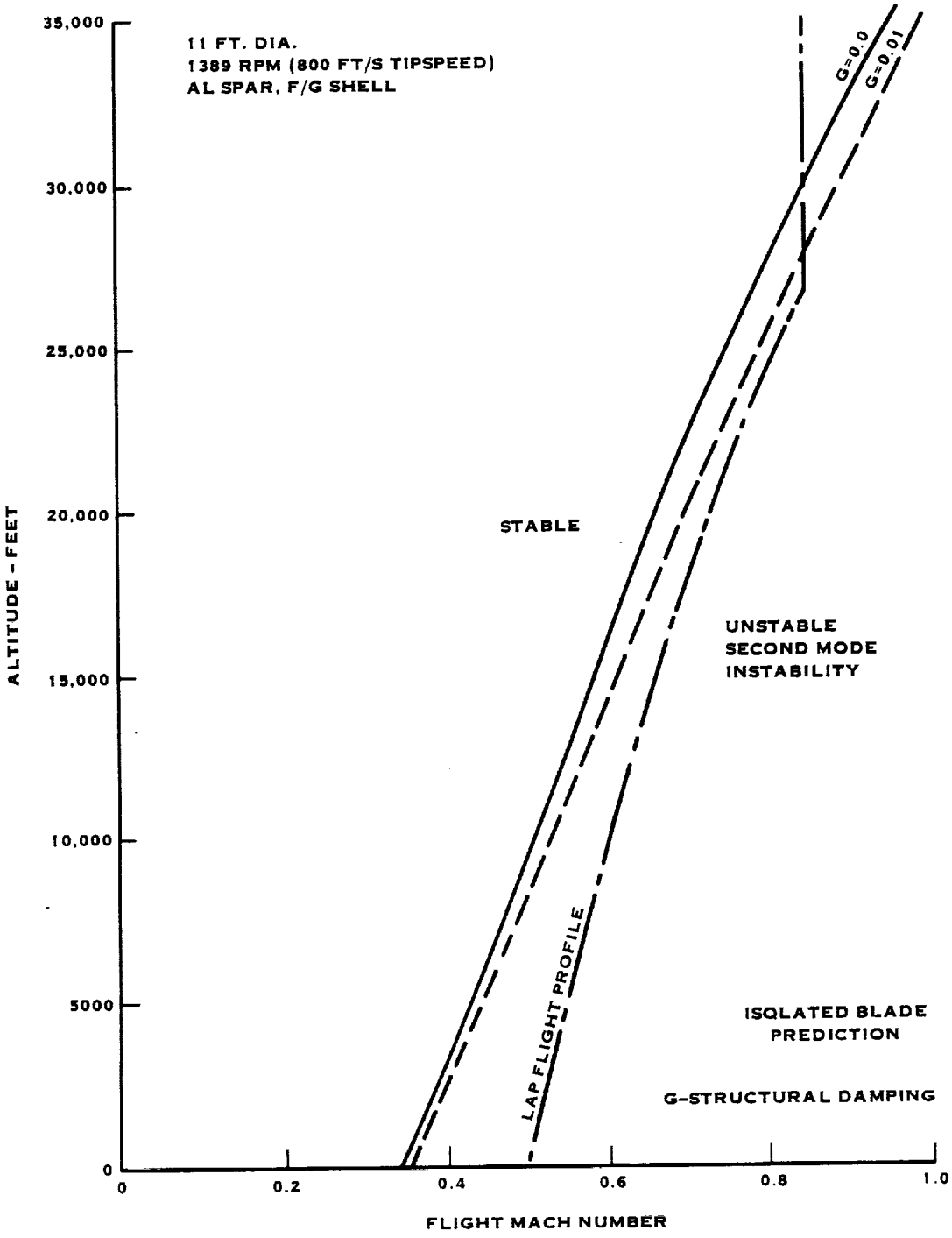

FIGURE C-46. SR-3(8) UNSTALLED FLUTTER STABILITY BOUNDARY

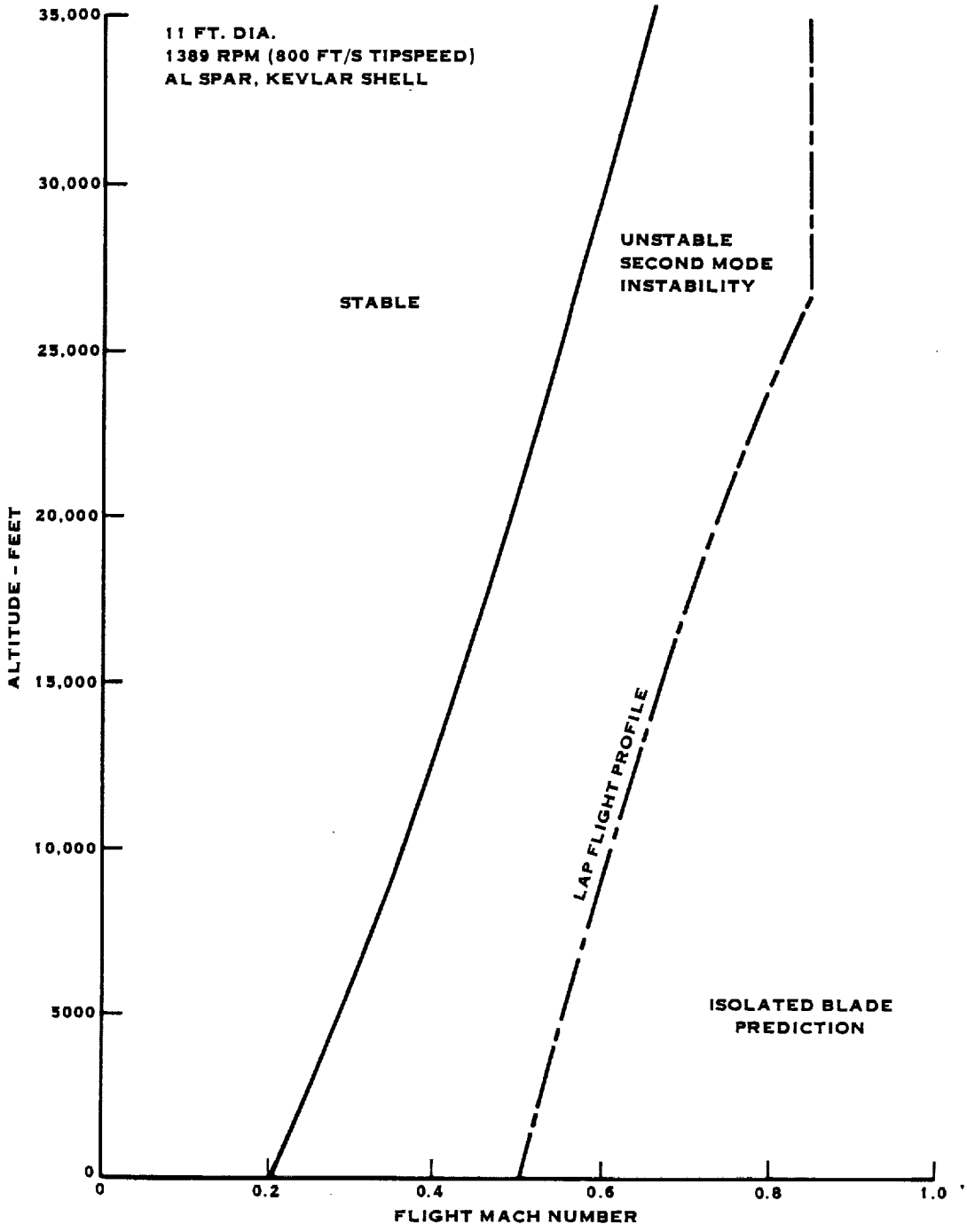

FIGURE C-47 SR-3(10) UNSTALLED FLUTTER STABILITY BOUNDARY

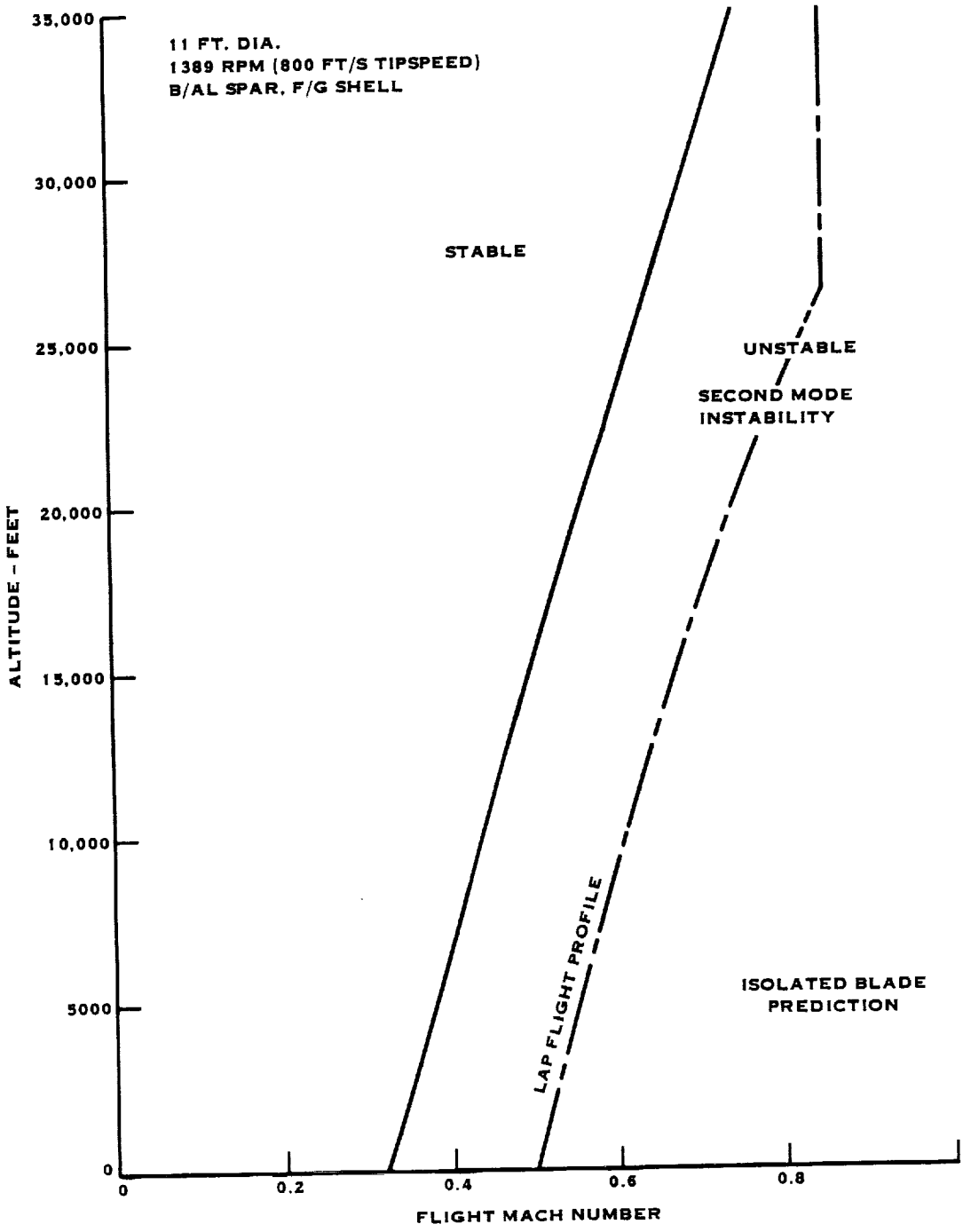

FIGURE C-48. SR-5B UNSTALLED FLUTTER STABILITY BOUNDARY

1. Report No.	2. Government Accession No.	3. Recipient's Catalog No.
CR 174992		

4. Title and Subtitle	5. Report Date
Large Scale Prop-Fan Structural Design Study Volume I - Initial Concepts	6. Performing Organization Code 73030

7. Author(s)	8. Performing Organization Report No.
L.C. Billman R.M. Ladden J.E. Turnberg C.J. Gruska D.K. Leishman	HSER 11518

9. Performing Organization Name and Address	10. Work Unit No.
Hamilton Standard Division United Technologies Corporation PO Box 1000 Windsor Locks, Connecticut 06096	11. Contract or Grant No. NAS3-22394

12. Sponsoring Agency Name and Address	13. Type of Report and Period Covered
National Aeronautics and Space Administration Washington, DC 20546	Contractor Report 14. Sponsoring Agency Code

15. Supplementary Notes

Project Manager, David A. Sagerser, Advanced Turbo Prop Project Office, NASA Lewis Research Center, Cleveland, Ohio 44135

16. Abstract

In recent years, considerable attention has been directed toward improving aircraft fuel consumption. Studies have shown that the inherent efficiency advantage that turboprop propulsion systems have demonstrated at lower cruise speeds may now be extended to the higher speeds of today's turbofan and turbojet-powered aircraft. In order to achieve this goal, new propeller designs will require features such as thin, high-speed airfoils and aerodynamic sweep, features currently found only in wing designs for high-speed aircraft.

The purpose of the effort described in Volume I of this report was to establish stuructural concepts for such advanced propeller blades, to define their structural properties, to identify any new design, analysis, or fabrication techniques which were required, and to determine the structural tradeoffs involved with several blade shapes which were selected primarily on the basis of aero/acoustic design considerations. The feasibility of fabricating and testing dynamically scaled models of these blades for aerolastic testing was also established. In addition, the preliminary design of a blade suitable for flight use in a testbed advanced turboprop was conducted and is described in Volume II.

17. Key Words (Suggested by Author(s))

Prop-Fan
Blade
Structural Design

of this information in whole or in part. Date for general release August, 1989.

19. Security Classif. (of this report)	20. Security Classif. (of this page)	21. No. of Pages	22. Price*
		124	

[redacted]

NASA-C-168 (Rev. 10-75)